Design of Human Skin Tribometer: Experimental Investigation and Empirical Modelling of Finger Pad Tribological Contact with Domiciliary Textiles and Metal Interfaces

THESIS

Submitted in the partial fulfilment of the requirement for the degree of

DOCTOR OF PHILOSOPHY

by

ASHISH KUMAR SRIVASTAVA
2017PHXF0029P

Under the Supervision of

PROF. JITENDRA SINGH RATHORE
Associate Professor
Department of Mechanical Engineering
Birla Institute of Technology & Science Pilani – 333031 Jhunjhunu (Rajasthan)

and

Co-Supervision of

PROF. SHARAD SHRIVASTAVA
Associate Professor
Department of Mechanical Engineering
Birla Institute of Technology & Science Pilani – 333031 Jhunjhunu (Rajasthan)

BITS Pilani
Pilani | Dubai | Goa | Hyderabad

BIRLA INSTITUTE OF TECHNOLOGY & SCIENCE

PILANI-333031 (RAJASTHAN), INDIA

2023

Dedicated to my father for bestowing his silent love, enduring support, and life principles on me

BIRLA INSTITUTE OF TECHNOLOGY AND SCIENCE, PILANI

CERTIFICATE

This is to certify that the thesis titled **Design of Human Skin Tribometer: Experimental Investigation and Empirical Modelling of Finger Pad Tribological Contact with Domiciliary Textiles and Metal Interfaces** submitted by **ASHISH KUMAR SRIVASTAVA** ID No **2017PHXF0029P** for award of Ph.D. of the Institute embodies original work done by him/her under my supervision.

Signature of the Supervisor:
Name in capital letters: PROF. JITENDRA SINGH RATHORE
Designation: **Associate Professor**
Date:

Signature of the Co-Supervisor:
Name in capital letters: PROF. SHARAD SHRIVASTAVA
Designation: **Associate Professor**
Date:

I offer respectful obeisance to my supervisor **Prof. Jitendra Singh Rathore** and my co-supervisor **Prof. Sharad Shrivastava**, for the guidance and support they have provided throughout the course of the thesis. Their advice and words of encouragement have always been a strong support in difficult moments.

I am immensely thankful to **Prof. V. Ramgopal Rao** (Group Vice Chancellor, BITS Pilani), **Prof. Sudhirkumar Barai** (Director, BITS-Pilani, Pilani campus). I express my gratitude to **Prof. Srinivas Krishnaswamy** (Dean, Academic Graduate Studies & Research Division); and **Prof. Sanjay Kumar Verma** (Dean, Administration), Pilani campus. I also feel thankful to **Prof. Shamik Chakraborty** (Associate Dean, Academic Graduate Studies & Research Division); BITS -Pilani, Pilani campus for his constant and official support and encouragement.

My sincere thanks to **Prof. Srikanta Routroy** (Head of the Department, Mechanical Engineering). I also pay my humble respects to **Prof. Mani Sankar Dasgupta** (Ex- Head of the Department, Mechanical Engineering. I am grateful to the entire faculty and staff of Mechanical Engineering Department for their kind support and assistance.

I thank Doctoral Research Committee (DRC); my Doctoral Advisory Committee (DAC) members; **Prof. Arun Kumar Jalan** and **Dr. Murali Palla**; who gave their precious time to provide suggestions during the progress of the research work that helped in improving the quality of this thesis.

My endless thanks to my friends **Mr. Gaurav Kumar, Dr. Vivek Tiwari, Dr. Santosh Saraswat, Dr. Shailendra Singh Pawanr, Mr. Amresh Kumar, Mr. Premsai Ragella, Mr. Rahul Ukey, Mr. Rishi Kumar, Mr. Anish Kumar, Mr. Rishi Parvanda** and **Mr. Shailendra Tripathi.**

I express immense love and gratitude to my parents, my mother **Mrs. Aradhana Srivastava and my father Mr. Vijai Kumar Srivastava** for their endless support and affection. I am

thankful to my brothers **Mr. Abhinav Kumar Srivastava** and **Mr. Abhishek Kumar Srivastava** along with my sisters-in-laws, **Mrs. Pooja Srivastava** and **Mrs. Shuchi Srivastava** who were my emotional support. My special love goes to the little ones **Aniket** and **Kiara** who did not miss a chance to put smile on my face with their ever-glittering eyes in rough phases of compilation of the thesis. Indeed, a phenomenal thank goes to my friend and wife **Mrs. Ridhi Srivastava** who has been a concreate pillar of thoughts to me.

Above all, I would like to thank God and put forward my gratitude to all those who have not been named here and have been my support during this course of research work.

Ashish Kumar Srivastava

Abstract

Bio tribology has developed as a significant discipline of tribological research with increasing demand of customisable products and need of ergonomics. Hence, the tribological concerns for the effect of relative motion between skin and the interacting materials has recently been intensified. This has raised the need for realistic experimental investigations for the frictional behaviour at skin contact interface. The aim of the current research is to develop an economic and reliable human skin tribometer to simulate the relative motion between human skin and domicillary materials. Furthermore, the experimental investigation of test materials is performed to investigate its frictional attributes with human skin. Lastly, a predictive model is provided for the coefficient of friction at human skin contact.

Chapter 1 introduces skin tribology as a subdomain of tribological research. An overview of human skin anatomy is presented. Mechanisms and measurement techniques of human skin friction are discussed based on the published literature. Further, objectives are defined for the proposed research and the methodology adopted for the same. Motivation of the present research is highlighted at the end of the chapter.

Chapter 2 provides information on the latest reported research and growth in the field through a bibliometric study. This also yields insights on the most impactful authors, affiliations, co-citation networks and author collaborations in human skin tribological research. Additionally, to further narrow down to the in- vivo experimental research, a scoping review is conducted through preferred reporting items for systematic reviews and meta-analyses (PRISMA) technique, which classified the in-vivo experimental research into four popular anatomical regions taken as site of human skin tribological investigations. Review highlights that no experimental investigations have been performed over finger pad through parallel-rotary measurement techniques. It was also concluded that no study is reported taking indian test subjects along with the indian geographical conditions.

Chapter 3 elaborates the design and development of parallel rotary type and sliding (reciprocating) type human skin tribometer. Further, validation tests are performed for the repeatability and reproducibility of rotary device. The developed rotary tribometer has higher range for normal load and sliding velocity in comparison with the designs reported in the literature. Sliding type tribometer is developed to simulate the popular technique of human friction measurement through sliding relative motion.

Chapter 4 conducts the human based survey to get the feedback for the material selection as the test samples. In-vivo experiments are performed on human test subjects on rotary and

sliding tribometers. Load range for the rotary tribometers is taken between 4 to 10 N. While for sliding tribometer normal load varies from 2 to 15 N. Sliding velocity range for rotary tribometer is 4.5 to 10.5 cm/ sec and in sliding type this ranges from 20 to 60 mm/ sec. Both the tribometers report higher coefficient of friction (COF) for wet state experiments. Also, experimental investigations conclude that the COF varies as a function of power law with normal load.

Chapter 5 provides the predictive model and optimization of COF at finger pad interface. A full factorial design of experimental runs is performed for combination at different levels of normal load, sliding velocity and skin hydration of test subjects. Response surface methodology (RSM) and Artificial neural network (ANN) techniques are used to develop the predictive model. Further, a comparative study on the predictability of the developed model through two techniques reported ANN to perform better with 5.91 % than that of RSM with 9.93 % relative error. Lastly, a minimisation of COF is performed with RSM to get the optimal values of input parameters of the developed model.

Chapter 6 includes the conclusions and future scope of the present work.

Table of Contents

CONTENTS **Page No.**

CONTENTS **Page No.**

Chapter - 1
Introduction

1.1 Skin Tribology

Tribology is the study of the frictional interaction of two contact surfaces in relative motion to each other. Tribology is studied in the purview of industrial, computational, geological, biological, space, and green processes where wear and lubrication are explored as a part of it.. In tribological studies, researchers have strong opinions over both beneficial and non - beneficial aspects of friction. Bio tribology is the subdomain of tribology that studies the friction, wear or lubrication phenomenon of the two-interacting surface one or both of which are part of a biological system. Bio tribology encapsulates multiple domains of dental, joint, skin, and oral tribology.

Skin tribology studies the tribological behaviour of skin with interacting material. Skin tribology is a multi-disciplinary field encapsulating the principles of contact mechanics, dermatology, biosciences and engineering, and material science as illustrated in Figure 1.1. Skin frictional interaction has been studied in various fields in relevance and adaptability to their particular objectives such as medicine [1]–[3], product design [4]–[7], textile development [8]–[12], and robotics [13]–[15]. The thesis presents the tribological aspects of the finger pad (tactile friction) and attributes affecting it, their range, and interaction (discussed in detail in later chapters) with the tested material samples in the Indian context.

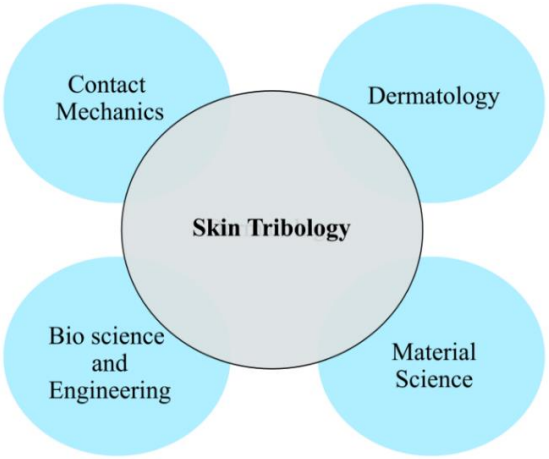

Figure 1.1 Domain interconnections in skin tribology

1.2 Human Skin Anatomy

Human skin is a complex structure that protects the body from any physical, chemical, and biological attacks from the external environment. Skin is one of the prominent tissues of the

human body and accounts for ~15 % of body weight, bears thickness between 1.5- 4 mm and has a surface area of 2 square meters [16]. Human skin helps in sensation and metabolism for the structure of the human body [17]. Skin is broadly divided into three layers: the epidermis (which acts as a protective barrier and forms new skin) is the uppermost, the dermis (grows hair, sweat generation, and supply of blood) in the middle, and hypodermis (acts as a cushion for muscles and bones) at the bottom [16] as shown in Figure 1.2. The structure and characteristics of human skin are a function of anatomical location, age, sex, and ethnicity [18] or environmental factors [19]. Human skin is highly non-linear and viscoelastic [20], [21] making its tribological investigations complex with its structure and local microclimate affecting the frictional parameters at the contact interface.

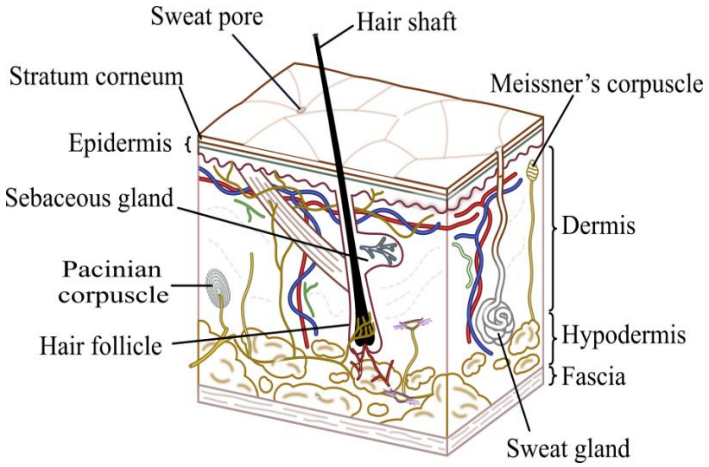

Figure 1.2 Multi-layered structure of human skin

Mostly, all the experiments for tribological explorations are performed over the human finger pad so understanding the finger pad anatomy gains importance in relevance to the current study. The anatomy of the finger pad adapted from [22] is depicted in Figure 1.3 and is used to understand its structure and further its tribological aspects in the later chapters of the thesis [23]–[25]. A finger pad is a multi-layered structure composed of epidermis, dermis, and subcutaneous tissue. Dermis the thickest layer that makes 90% of the total thickness consists of Meissner mechanoreceptors responsible for sensing fine touches. Vibration through the skin is also sensed by the Meissner mechanoreceptors while subcutis has the Pacinian mechanoreceptors that are receptors of pressure. The dermis has the sweat glands where secretion takes place depending on individual characteristics and in turn, this affects the amount of friction force needed for a particular gripping task. Finger friction is not limited to manipulation tasks but also relates to surface perception [26].

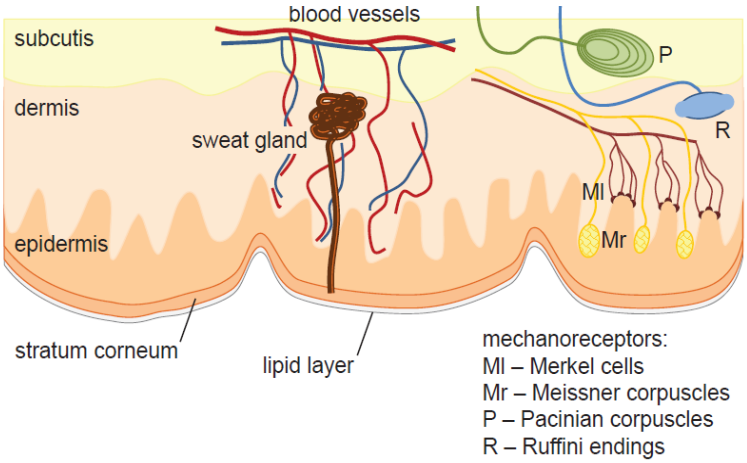

Figure 1.3 Anatomy of human finger pad (adapted from [22])

1.3 Skin Friction Mechanism

Literature reports extensive work for the investigation of skin friction by a frictionless spherical probe rotating or sliding on the skin [27]–[31] to replicate the interaction between skin and the contact material. Amonton's law defines coefficient of friction (COF) as the ratio of frictional force and the applied normal load that holds true for the tribological investigations of human skin. Researchers have tried to mimic the skin's mechanical characteristics such as viscoelasticity, toughness, and stretchability [32]–[34] to the extent of replicating the human skin in the possible areas of application. With the usage of elastomeric materials [35] and considering the mechanical attributes of human skin, the application of theoretical friction models in the tribological aspects of human skin [36] is popular. The Two-term friction model of elastomer consists of an adhesion and deformation component of the frictional force as shown in equation 1.1.

$$F_{\mu} = F_{adhesion} + F_{deformation} \quad \textbf{1.1}$$

The adhesion component is reported to have a major role while the deformation component is not that significant in relation to the friction measurements of human skin [27]. In literature multiple theoretical models viz. Hertz, Johnson–Kendall-Roberts (JKR), and Greenwood-Williamson (GW) are reported that explain contact behaviour and friction mechanisms related to the human skin [28], [37]. Hertz's theory assumes the material to be isotropic and is applicable for small deformations [37].

The adhesion component is the amount of force required to break the bonds due to adhesion between the two surfaces in contact as in equation 1.2, where τ is the interfacial shear strength and A_{real} is the actual area in contact between the two surfaces.

$$F_{adhesion} = \tau * A_{real} \quad \textbf{1.2}$$

Viscoelastic nature of skin causes work dissipation when skin is indented by a harder counter surface. The resulting deformation is compensated by the work loss due to hysteresis per unit length of sliding distance. The deformation component is evaluated by equation 1.3, where β is the viscoelastic loss fraction and a/ R is the relative indentation into the skin.

$$F_{deformation} = \frac{3}{16} * \beta * \frac{a}{R} * F \qquad \textbf{1.3}$$

1.4 Skin Friction Measurement Techniques

Human skin friction has been studied by various researchers widely about its mechanical attributes. Broadly, [38] encapsulated the methods used for the development of equipment for measuring human skin. Human skin tribological investigations have been studied under two broad domains: First, ex-vivo or in-vitro, and second in-vivo. The thesis progresses with the second classification (in-vivo) based on the type of motion between the two materials: rotary, sliding (reciprocating), or moving skin [39]. Prominent experimental studies and tribometers used in the investigation of human skin tribological aspects and their measurement have been discussed in Chapters 2 and 3 in a detailed manner.

1.5 Methodology

Following are the research methodology adopted for the development of the thesis:

- Bibliometric analysis followed by a scoping review is performed, aiming at in-vivo experimentations in human skin tribology. Bibliometric analysis is a descriptive overview of the domain experts, collaborations, journals, and the timeline. In the scoping review, content analysis is performed to chronologically arrange the in-vivo experiments performed in the domain of human skin tribology.
- Design, development, and fabrication of parallel rotary type (PTT) and sliding type tribometer (STT) for human skin friction measurement is done. In the PTT tribometer, rotary probes of countersurface materials are developed for friction measurement with human skin. While STT measures the finger pad friction by making sliding contact with a moving countersurface attached to the force plate as a sheet.
- Experimental investigations and analysis of the friction measurements of the test materials (as counter surface) with a finger pad are performed. In PTT experimental investigations are performed for two textiles, two polymeric materials, one acrylic, and four metal test samples. STT experiments are performed for acrylic, mica, wood, and 4 metal test samples

- Modelling and optimization of frictional parameters for minimizing the COF value between the steel probe and finger pad are carried out. The predictive model is developed using response surface methodology (RSM) and artificial neural network (ANN). Further, comparisons were made for the predictability of COF as a response variable between the two models.

1.6 Motivation

The thesis contributes to the pertinent knowledge on human skin tribology for researchers, product designers, and end users. The bibliographic study presented, is one of its kind in the domain of human skin tribology, which will help budding researchers to identify newer research areas and enhance collaboration network with existing experts working in the field. All 4 popular anatomical regions that have been identified through literature are used as the site of tribological investigations in the in-vivo tribological explorations of human skin.

Tribometers are developed based on the two most common nature of relative motion between skin and equipment; namely rotary and sliding. The rotary and sliding are customized as parallel rotary-type and sliding type respectively. The purpose of designing a parallel rotary-type tribometer is two-fold, primarily having the benefits of both portable and bench-top design to achieve, higher versatility and less variability in the COF measurements. Secondly, as discussed in previous sections with multiple application areas of skin friction investigations, making an economical, easy to develop, and foremost customizable tribometer is highly required. A reciprocating tribometer is fabricated to investigate the coupling of two measurement principles (sliding probe and moving skin) discussed in chapter 4. Experiments have been conducted both in a ‘dry’ and ‘wet’ state. All the experimental results reported can be normalized for COF value considering other micro and macro parameters such as the nature of contact, texture, and environment.

The developed models for the COF between finger pad and steel probe can be replicated with other materials. Similarly, optimal values of input parameters could be obtained for the minimization, or targeted value of COF as per the requirement (precision or power grip) based on the product features and application area.

References

[1] S. Yusuf *et al.*, "Microclimate and development of pressure ulcers and superficial skin changes," *Int. Wound J.*, vol. 12, no. 1, pp. 40–46, 2015, doi: 10.1111/iwj.12048.

[2] M. Woodhouse, P. R. Worsley, D. Voegeli, L. Schoonhoven, and D. L. Bader, "How consistent and effective are current repositioning strategies for pressure ulcer prevention?," *Appl. Nurs. Res.*, vol. 48, no. May, pp. 58–62, 2019, doi: 10.1016/j.apnr.2019.05.013.

[3] M. Lindberg, B. Skytt, and M. Lindberg, "Continued wearing of gloves: a risk behaviour in patient care," *Infect. Prev. Pract.*, vol. 2, no. 4, p. 100091, 2020, doi: 10.1016/j.infpip.2020.100091.

[4] D. Gueorguiev, S. Bochereau, A. Mouraux, V. Hayward, and J. L. Thonnard, "Touch uses frictional cues to discriminate flat materials," *Sci. Rep.*, vol. 6, no. May, pp. 1–7, 2016, doi: 10.1038/srep25553.

[5] A. Abdouni, R. Vargiolu, and H. Zahouani, "Impact of finger biophysical properties on touch gestures and tactile perception: Aging and gender effects," *Sci. Rep.*, vol. 8, no. 1, pp. 1–13, 2018, doi: 10.1038/s41598-018-30677-2.

[6] C. J. Boyle, D. Carpanen, T. Pandelani, C. A. Higgins, M. A. Masen, and S. D. Masouros, "Lateral pressure equalisation as a principle for designing support surfaces to prevent deep tissue pressure ulcers," *PLoS One*, vol. 15, no. 1, pp. 1–19, 2020, doi: 10.1371/journal.pone.0227064.

[7] C. Basdogan, F. Giraud, V. Levesque, and S. Choi, "A Review of Surface Haptics: Enabling Tactile Effects on Touch Surfaces," *IEEE Trans. Haptics*, vol. 13, no. 3, pp. 450–470, 2020, doi: 10.1109/TOH.2020.2990712.

[8] L. C. Gerhardt, A. Lenz, N. D. Spencer, T. Münzer, and S. Derler, "Skin-textile friction and skin elasticity in young and aged persons," *Ski. Res. Technol.*, vol. 15, no. 3, pp. 288–298, 2009, doi: 10.1111/j.1600-0846.2009.00363.x.

[9] S. Derler, U. Schrade, and L. C. Gerhardt, "Tribology of human skin and mechanical skin equivalents in contact with textiles," *Wear*, vol. 263, no. 7-12 SPEC. ISS., pp. 1112–1116, 2007, doi: 10.1016/j.wear.2006.11.031.

[10] A. Ramalho, P. Szekeres, and E. Fernandes, "Friction and tactile perception of textile fabrics," *Tribol. Int.*, vol. 63, pp. 29–33, 2013, doi: 10.1016/j.triboint.2012.08.018.

[11] J. Lyu, N. Özgün, D. J. Kondziela, and R. Bennewitz, "Role of Hair Coverage and Sweating for Textile Friction on the Forearm," *Tribol. Lett.*, vol. 68, no. 4, pp. 1–9, 2020, doi: 10.1007/s11249-020-01341-6.

[12] R. Baby, K. Mathur, and E. DenHartog, “Skin-textiles friction: importance and prospects in skin comfort and in healthcare in prevention of skin injuries,” *J. Text. Inst.*, vol. 112, no. 9, pp. 1514–1530, 2021, doi: 10.1080/00405000.2020.1827582.

[13] A. J. Spiers, B. Calli, and A. M. Dollar, “Variable-Friction Finger Surfaces to Enable Within-Hand Manipulation via Gripping and Sliding,” *IEEE Robot. Autom. Lett.*, vol. 3, no. 4, pp. 4116–4123, 2018, doi: 10.1109/LRA.2018.2856398.

[14] C. Shultz, M. Peshkin, and J. E. Colgate, “The application of tactile, audible, and ultrasonic forces to human fingertips using broadband electroadhesion,” *IEEE Trans. Haptics*, vol. 11, no. 2, pp. 279–290, 2018, doi: 10.1109/TOH.2018.2793867.

[15] M. Strohmayr, “Artificial Skin in Robotics,” pp. 15–24, 2012.

[16] P. Humbert, F. Ferial, P. Agache, and H. I. Maibach, *Agache ’ s Measuring the Skin*. 2004.

[17] T. Burns, S. Breathnach, N. Cox, and C. Griffiths, *Rook’s Textbook of Dermatology, 4 Volume Set*, vol. 1. John Wiley \& Sons, 2010.

[18] S. Mac-Mary *et al.*, “Assessment of cumulative exposure to UVA through the study of asymmetrical facial skin aging.,” *Clin. Interv. Aging*, vol. 5, pp. 277–284, Sep. 2010, [Online]. Available: https://pubmed.ncbi.nlm.nih.gov/20924436.

[19] F. Fanian *et al.*, “Efficacy of micronutrient supplementation on skin aging and seasonal variation: A randomized, placebo-controlled, double-blind study,” *Clin. Interv. Aging*, vol. 8, pp. 1527–1537, 2013, doi: 10.2147/CIA.S43976.

[20] M. Xing, N. Pan, W. Zhong, and H. Maibach, “Skin friction blistering: Computer model,” *Ski. Res. Technol.*, vol. 13, no. 3, pp. 310–316, 2007, doi: 10.1111/j.1600-0846.2007.00230.x.

[21] M. A. Meyers, P. Y. Chen, A. Y. M. Lin, and Y. Seki, “Biological materials: Structure and mechanical properties,” *Prog. Mater. Sci.*, vol. 53, no. 1, pp. 1–206, Jan. 2008, doi: 10.1016/J.PMATSCI.2007.05.002.

[22] J. van Kuilenburg, *A mechanistic approach to tactile friction*. 2013.

[23] H. Tagami, “Location-related differences in structure and function of the stratum corneum with special emphasis on those of the facial skin,” *Int. J. Cosmet. Sci.*, vol. 30, no. 6, pp. 413–434, 2008, doi: 10.1111/j.1468-2494.2008.00459.x.

[24] J. Sandby-Møller, T. Poulsen, and H. C. Wulf, “Epidermal Thickness at Different Body Sites: Relationship to Age, Gender, Pigmentation, Blood Content, Skin Type and Smoking Habits,” *Acta Derm. Venereol.*, vol. 83, no. 6, pp. 410–413, 2003, doi: 10.1080/00015550310015419.

[25] E. Jacquet, J. Chambert, J. Pauchot, and P. Sandoz, “Intra- and inter-individual variability in the mechanical properties of the human skin from in vivo measurements on 20 volunteers,” *Ski. Res. Technol.*, vol. 23, no. 4, pp. 491–499, 2017, doi: 10.1111/srt.12361.

[26] X. Liu, Z. Yue, Z. Cai, D. G. Chetwynd, and S. T. Smith, “Quantifying touch-feel perception: Tribological aspects,” *Meas. Sci. Technol.*, vol. 19, no. 8, 2008, doi: 10.1088/0957-0233/19/8/084007.

[27] M. J. Adams, B. J. Briscoe, and S. A. Johnson, “Friction and lubrication of human skin,” *Tribol. Lett.*, vol. 26, no. 3, pp. 239–253, 2007, doi: 10.1007/s11249-007-9206-0.

[28] Koudine, Barquins, Anthoine, Aubert, and Lévêque, “Frictional properties of skin: Proposal of a new approach,” *Int. J. Cosmet. Sci.*, vol. 22, no. 1, pp. 11–20, 2000, doi: 10.1046/j.1467-2494.2000.00006.x.

[29] J. Asserin, H. Zahouani, P. Humbert, V. Couturaud, and D. Mougin, “Measurement of the friction coefficient of the human skin in vivo: Quantification of the cutaneous smoothness,” *Colloids Surfaces B Biointerfaces*, vol. 19, no. 1, pp. 1–12, Nov. 2000, doi: 10.1016/S0927-7765(99)00169-1.

[30] R. K. Sivamani, J. Goodman, N. V. Gitis, and H. I. Maibach, “Friction coefficient of skin in real-time,” *Ski. Res. Technol.*, vol. 9, no. 3, pp. 235–239, 2003, doi: 10.1034/j.1600-0846.2003.20361.x.

[31] W. Li, M. Kong, X. D. Liu, and Z. R. Zhou, “Tribological behavior of scar skin and prosthetic skin in vivo,” *Tribol. Int.*, vol. 41, no. 7, pp. 640–647, 2008, doi: 10.1016/j.triboint.2007.11.009.

[32] M. Vatankhah-Varnosfaderani *et al.*, “Mimicking biological stress–strain behaviour with synthetic elastomers,” *Nature*, vol. 549, no. 7673, pp. 497–501, 2017, doi: 10.1038/nature23673.

[33] J. Wu, L. H. Cai, and D. A. Weitz, “Tough Self-Healing Elastomers by Molecular Enforced Integration of Covalent and Reversible Networks,” *Adv. Mater.*, vol. 29, no. 38, 2017, doi: 10.1002/adma.201702616.

[34] H. Gotoh *et al.*, “Optically transparent, high-toughness elastomer using a polyrotaxane cross-linker as a molecular pulley,” *Sci. Adv.*, vol. 4, no. 10, 2018, doi: 10.1126/sciadv.aat7629.

[35] S. Chen *et al.*, “Mechanically and biologically skin-like elastomers for bio-integrated electronics,” *Nat. Commun.*, vol. 11, no. 1, 2020, doi: 10.1038/s41467-020-14446-2.

[36] K. P. Wilhelm, P. Elsner, E. Berardesca, and H. I. Maibach, *Bioengineering of the skin:*

Skin imaging & analysis. 2006.

[37] C. Pailler-Mattéi and H. Zahouani, “Study of adhesion forces and mechanical properties of human skin in vivo,” *J. Adhes. Sci. Technol.*, vol. 18, no. 15–16, pp. 1739–1758, 2004, doi: 10.1163/1568561042708368.

[38] M. A. Masen, N. Veijgen, and M. Klaassen, “Experimental Tribology of Human Skin,” *Stud. Mechanobiol. Tissue Eng. Biomater.*, vol. 22, pp. 281–295, 2019, doi: 10.1007/978-3-030-13279-8_10.

[39] N. K. Veijgen, E. van der Heide, and M. A. Masen, “Skin friction measurement; the development of a new device,” *Prod. Acad. Issues*, vol. 2, pp. 28 – 35, 2010, [Online]. Available: https://www.scopus.com/inward/record.uri?eid=2-s2.0-81255168901&partnerID=40&md5=a16c3251fe95e448a637ea62a51df1bd.

Chapter - 2
Literature Review

2.1 Introduction

In the previous chapter, an introduction to skin tribology and its relevance to investigating human skin friction was discussed. In the current chapter, a detailed discussion, and an outline of the overall progress of research in the domain of human skin tribology through a bibliometric study is presented. Further, scoping review is performed for the in-depth literature survey in the interdisciplinary domain ascribed to its anatomy [1], mechanical characteristics [2], biological attributes, and frictional properties [3]. Human skin is highly non-linear [4], anisotropic [5], and viscoelastic [6] hence, its tribological behaviour has been studied by different researchers through rotary or sliding friction measurement devices discussed in detail in the later sections.

Depending on the anatomical region, nature of the test specimen, and objective of the study, the researchers have opted for different techniques to investigate the mechanical properties of human skin. The three most popular testing techniques to measure the mechanical properties of human skin reported in the literature are indentation [7]–[11], suction [12], and optical coherence tomography (OCT) [13].

Micro and macro attributes affecting the human skin frictional behaviour are shown in Figure 2.1. Micro attributes are hard to measure, quantify and report at a single point in time, while the macro parameters have high variance, visible impact and ease in quantification. Another classification of attributes affecting human skin friction is intrinsic (related to subject characteristics) and extrinsic (any attributes other than the subject characteristics). Micro attributes affecting the friction of human skin are the ridges between the fingerprint in the case of the finger pad and sole, sweat secretion characteristics [14], [15], hair on the skin [16], sebum [17], relative humidity [18]–[20], temperature [18], and skin hydration [21]–[23].

Macro attributes affecting the friction of human skin are normal load [24]–[27], sliding velocity [28]–[30], surface roughness [22], [26], [31], [32], textures [33]–[35], skin conditions and the physical attributes of the material in contact. Few researchers have studied anatomical region [36]–[38], gender [39], [40], ethnicity [41], and age [21], [42] as the macro attributes affecting the tribology of human skin. Since skin alters its mechanical properties [43] at different body

regions, it is a must to highlight the correlation between the intrinsic and extrinsic attributes for a better understanding of the factors affecting the human skin tribology [20], [44]–[47].

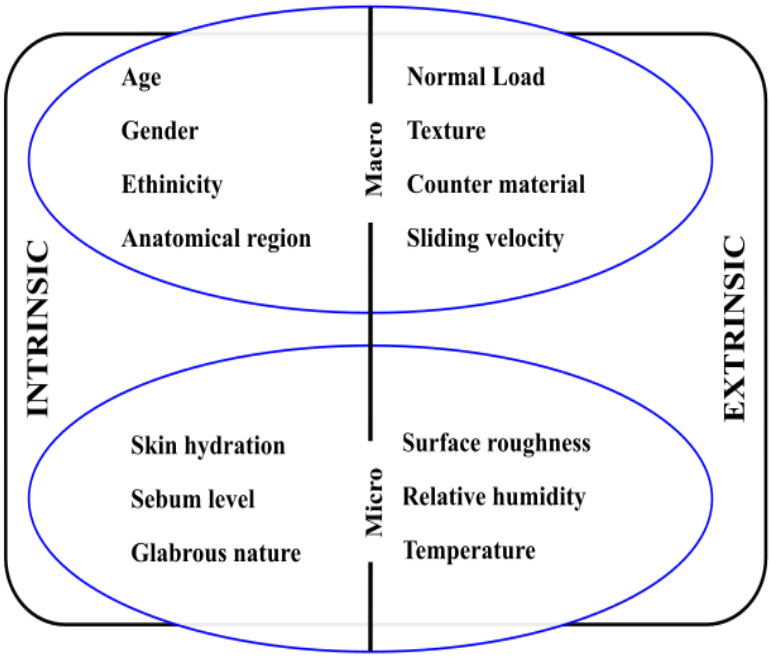

Figure 2.1 Attributes of human skin friction based on two classifications: subject-based (Intrinsic and Extrinsic) and scale-based (Micro and Macro)

Various researchers in the domain of bio tribology have presented highly informative review studies for human skin frictional interaction and its behaviour [2], [3], [48]–[53]. This chapter presents a literature review compiled in four sections. Section 2.2 presents the global level bibliometric overview for the domain of human skin tribology based on a literature survey. Section 2.3 further narrows down the literature survey through a scoping review to segregate the in-vivo experimental investigations to align with the defined objectives of the current research work. Section 2.4 highlights the research gaps identified through the literature review. Last section 2.5 summaries chapter 2.

2.2 Bibliometric Overview

Bibliometrics is a popular method to identify the research clusters in a structured fashion, to analyze and explore the trends, themes, and future research within the field embarked on the interest of investigators. The bibliometric analysis presents a general layout of the reported studies based on parameters like Total global citations (TGC) and Total local citations (TLC). TGC is a measure of the number of citations by all studies indexed in the database. TLC refers to the number of citations of studies in an extracted database. The application of bibliometric studies has been extended to various disciplines like healthcare [54], entrepreneurship [55],

dentistry [56], hospitality [57], and manufacturing [58]. No attempt for bibliometric analysis in the domain of human skin tribological studies is yet reported.

2.2.1 Data extraction and corpus creation

An exhaustive literature survey was conducted in a scientific approach through two databases namely Web of Science (WoS) and Scopus. The search operation is performed through basic keywords, to segregate the data as enumerated in Table 2.1.

Table 2.1 Keywords used, and number of documents retrieved for initial search process

Keyword	Number of documents	
	Scopus	**Web of Science**
"Human skin tribology"	2701	174
"Human skin" AND "Friction"	3225	244
"Human skin" AND "Skin Tribology"	101	21
"Human skin" AND "Friction Measurement"	222	10
"Human skin" AND "Pressure ulcers"	3185	82
"Human skin" AND "Skin temperature"	5497	273
"Human skin" AND "Skin roughness"	608	33
"Human skin" AND "Skin hydration"	3026	216
"Human skin" AND "Sliding velocity"	52	6

The search query was performed till the last week of February 2022. The same set of keywords was used for data extraction from both Scopus and WoS databases. The search pattern used generated a wide range of keywords, spread over various subjects and fields. The early analysis concluded, the need for target-oriented document extraction. A string shown as 2.1 is designed for the search criteria limiting the large range of data scattered over different disciplines. String takes the input of all the popular keywords from the literature arranged in the form of set *A, B,* and *C* as shown in Table 2.2.

A customized string is defined using Boolean operators for data extraction as:

$$((" A_1 " OR " A_2 " OR ... " A_n) AND (" B_1 " OR " B_2 " OR ... " B_n) AND (" C_1 " OR " C_2 " OR ... " C_n) \quad \textbf{2.1}$$

Table 2.2 Keywords for search optimization

Field of study (A)	**Parameters/ Factors (B)**	**Anatomical region/ Contact surface (C)**
Tribology	Pressure ulcers	Human skin
Human skin tribology	Skin mechanical	Skin
Human skin friction	properties	Fingertip/ Fingertip
Skin tribology	Indentation	Finger pad/ Finger pad
Bio-tribology/ Bio	Skin temperature	Forearm
tribology/ Bio tribology	Skin roughness	Finger
Friction measurement	Skin hydration	Hand
Tactile perception	Sliding velocity	
Tactile friction	Normal load	
	Friction coefficient	
	Relative humidity	
	Textile	
	Woven	

Search string extracted “3956” and “190” documents from Scopus and WoS respectively. The extracted dataset generated through the above-mentioned string is elaborately shown in Table 2.3.

Table 2.3 Document distribution for Scopus and Web of Science

Scopus			**WoS**		
Document type	N	Contribution (%)	Document type	N	Contribution (%)
Articles	182	95.78	Article	2794	70.62
Proceedings Paper	22	11.57	Conference Paper	467	11.80
Review Articles	8	4.21	Review	421	10.64
-	-	-	Book Chapter	146	3.6
-	-	-	Book	112	2.8
-	-	-	Letter	4	0.001
-	-	-	Note	4	0.001
-	-	-	Short Survey	3	0.00075
-	-	-	Editorial	2	0.00050
-	-	-	Conference Review	1	0.00025
-	-	-	Data Paper	1	0.00025
-	-	-	Retracted	1	0.00025

N- Number of documents extracted

Manual inspection of the retrieved documents raised the need for filtering criteria. Individual inclusion or exclusion criteria opted for both databases before extracting the bibliometric data for further analysis as shown in Table 2.4. Review articles from both databases are excluded to

avoid any sort of biasness to the citation data to a particular article. In Scopus, to limit the extracted data in the nearest periphery to the domain of human skin tribology engineering and material science are taken as inclusion criteria. Document type is taken as article and conference in the Scopus dataset. Books series and trend journals are excluded from the dataset.

Table 2.4 Filter criteria for data extraction

Scopus			**N**	**WoS**			**N**
Filter criteria	In	Ex		Filter criteria	In	Ex	
Year: *(Earlier than1991)*	-	✓	3919	**Document type:** Review	-	✓	182
Keywords: *Tribology; Friction coefficients/(s); Skin friction; Skin friction coefficient; Finger; Tactile perception; Shear stress; Velocity; Moisture; Bio tribology; Fabrics; Indentation; Roughness; Tactile; Coefficient of friction*	✓	-	1687	**Language:** English	✓	-	181
Subject area: *Engineering Material science*	✓	-	1307	-	-	-	-
Source type: *Final*	✓	-	1279	-	-	-	-
Language: *English*	✓	-	1190	-	-	-	-
Document type: *Article Conference*	✓	-	1122	-	-	-	-
Source type: *Book series Trade journal*	-	✓	1095	-	-	-	-

In- Inclusion criteria, **Ex-**Exclusion criteria & **N-**Number of documents extracted

Finally, the number of documents extracted for the bibliometric analysis for Scopus and WoS are 1095 and 181 respectively. Different tags like the author, affiliation, country, TGC, and TLC are retrieved for further analysis from the databases.

2.2.2 Bibliometric analysis

Bibliometric analysis works on two indicators namely, performance analysis and science mapping. Performance analysis deals with descriptive statistics such as citation, author, organization country, and keyword data. Science mapping nucleates around the development

of relationships between research constituents. An R-tool [59] is used for data analysis and science mapping. The author, organization, and country-wise collaboration network are presented using a Louvain clustering algorithm proposed by [60]. The advantage of the Louvain algorithm over other clustering algorithms is its quality and less time in determining the community network. A three-field plot based on the Sankey diagram is plotted which visualizes how keywords, countries, and authors are interrelated. These databases are used for most of the quantitative analyses. For network mapping and visualization, only the WoS database is used to keep the study succinct.

The study analyzed the published articles in the discipline of human skin tribology published from 1992 to 2021. Scopus reviewed 1095 documents from 401 sources by 2977 authors with an average of 6.77 citations per document. While WoS reviewed 181 documents from 58 sources by 505 authors. Table 2.5 shows the document types from Scopus and WoS. Scopus reports 51 (4.65%) and WoS 5 (2.7%) single-authored documents.

Table 2.5 Documents type extracted from Scopus and Web of Science

Scopus		**WoS**	
Type of Document		Type of Document	
Article	921	Article	181
Conference paper	174	Proceeding papers	22

A. Research growth

It has been a long now; the friction of human skin is been studied with the limited availability of information on attributes and testing methods. Human skin tribology has developed as a domain of multidisciplinary research. Figure 2.2 shows the year-wise publication data of research articles in Scopus and WoS. A steep rise in the number of publications post-year 2005 complements the trend of citation per year data depicted in Figure 2.3. The highest number of publications (NP) and total citations (TC) is in the year 2018 for both Scopus and WoS. Both these indexes highlight the production of articles in the field of human skin tribology in the last two decades.

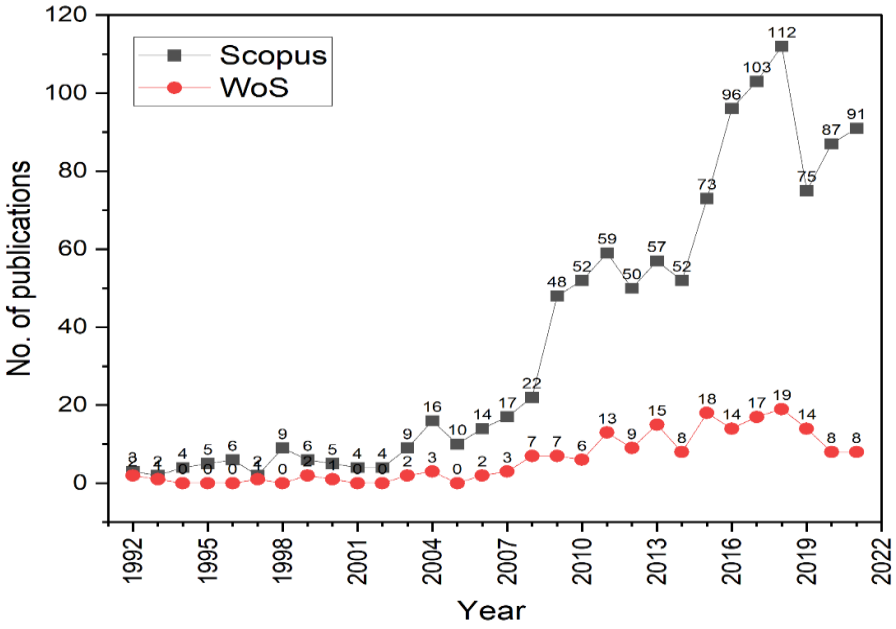

Figure 2.2 Number of publications (NP)

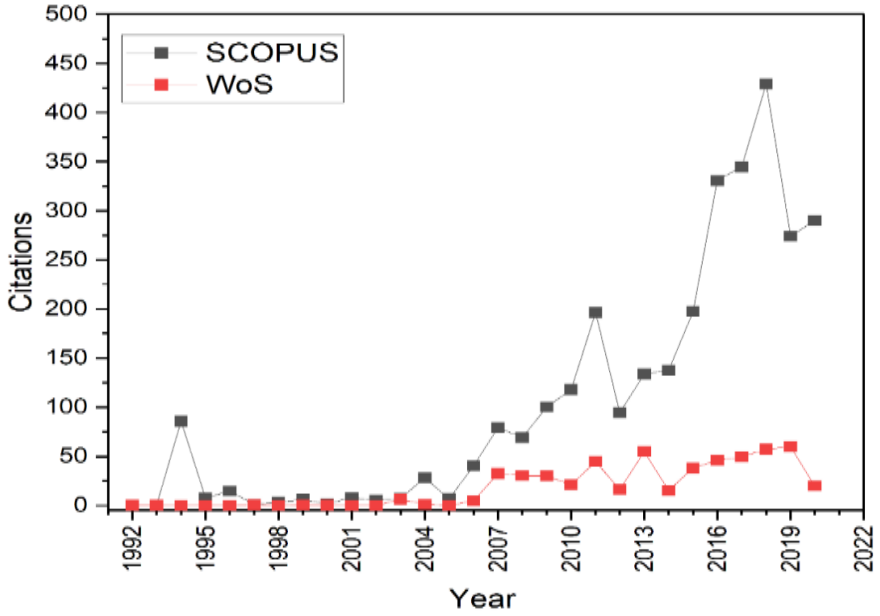

Figure 2.3 Total citation (TC) per year for Scopus and WoS

B. Most impactful and cited authors

This refers to the highly cited and referred authors extracted from both Scopus and WoS based on H-index. The h-index is defined as an author-level measuring index for the scholarly contribution to a particular domain of research. The top 10 most impactful authors are reported in Table 2.6 in the field of human skin tribology. In both the data bases Derler, S. is at the top having total citations of 992 and 531 in Scopus and WoS respectively. In Scopus, Derler S. is followed by Van Der Heide, E., Rossi, R. M., Bueno M. A., Lewis, R. and Carre, M. J. with

18, 14, 20, 16, and 13 publications respectively. Li, W., Zahouani, H., Masen, M. A., and Zeng, X have at least 10 publications.

Table 2.6 Top 10 most impactful authors

Scopus				Web of Science			
Author	h-index	TC	NP	Author	h-index	TC	NP
Derler, S.	17	992	20	Derler, S.	11	531	12
Van Der Heide, E.	12	329	18	Van Der Heide, E.	8	216	10
Rossi, R. M.	11	289	14	Masen, M. A.	7	190	7
Bueno, M. A.	10	380	20	Bueno, M. A.	6	100	7
Lewis, R.	10	387	16	Gerhardt, L. C.	6	632	6
Carre, M. J.	9	330	13	Rossi, R. M.	6	136	7
Li, W.	9	143	11	Chen, S.	5	72	6
Zahouani, H.	9	664	13	Rotaru, G. M.	5	112	6
Masen, M. A.	8	272	10	Rutland, M. W.	5	217	5
Zeng, X.	8	166	11	Skedung, L.	5	217	5

The author's collaborative network drawn from the WoS database is presented in Figure 2.4. A network having 50 nodes is drawn through the Louvain algorithm having an association method for the normalization. Each node represents the author, and the edges indicate the co-authorship relation. The blue cluster represents 8 authors, and the pink cluster and light red cluster with 6 authors each represent the significant and impactful author collaboration network. Purple, green, yellow, and aquamarine represent 4, 3, 3, and 3 authors respectively. The other 4 clusters represent a weak collaboration having two authors each. The network represents a scope to improve the collaboration network among the authors.

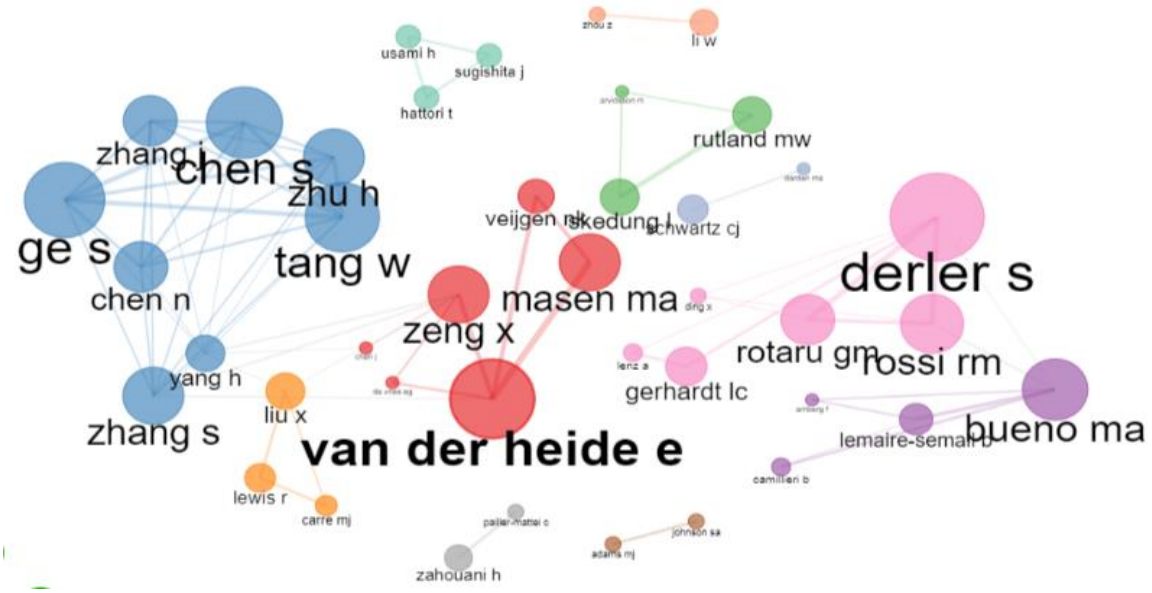

Figure 2.4 Author's collaboration network

The co-citation analysis of the authors is shown in Figure 2.5. Co-citation mapping represents the two authors cited simultaneously. 3 clusters are shown that are widely co-cited. This represents the intellectual contribution made by the authors to the research domain. The size of the circle represents the higher number of times the author is co-cited.

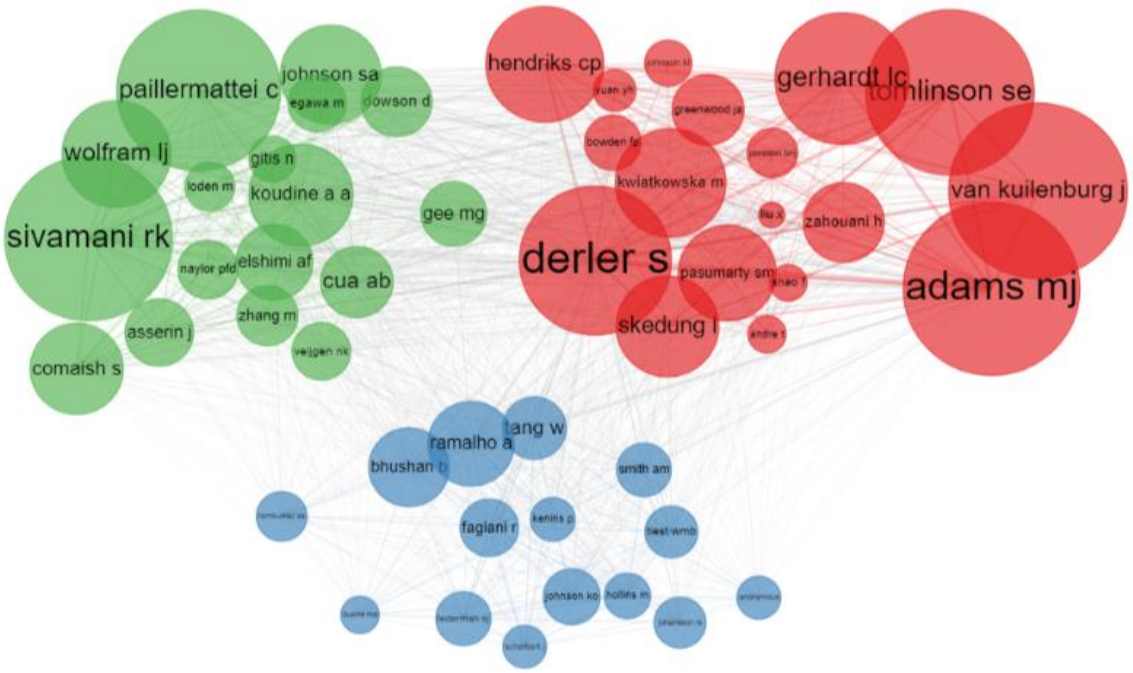

Figure 2.5 Co-citation network of the authors

C. Influential organizations

From both databases, the top 10 organizations are listed in Table 2.7 for the institute-wise analysis. Donghua university with 29 publications and the University of Twente with 26 publications from Scopus and WoS database are the foremost in the domain. Other institutions that are common to both databases are Tsinghua University, University of Twente, University of Sheffield, University of Southampton, and Swiss Federal Laboratories.

Table 2.7 Top 10 most influential organizations

Scopus		**WoS**	
Affiliations	NP	Affiliations	NP
Donghua University	29	University of Twente	26
Tsinghua University	27	China University Min and Technology	15
University Of Twente	26	University Haute Alsace	14
University Of Sheffield	21	University of Sheffield	12
Southwest Jiaotong University	19	University of Lyon	11
Tohoku University	17	Swiss Federal Laboratories for Materials Science and Technology	10
University Of Southampton	16	University of Southampton	10

Lanzhou Institute of Chemical Physics	15	Swiss Fed Labs Mat Testing and Research	8
Swiss Federal Laboratories for Materials Science and Technology	15	Tsinghua University	8

The organization plays a vital role in terms of collaboration based on available research facilities, flexibility in operation, and a degree of openness. The affiliation and collaboration network shown in Figure 2.6 represents the collaboration network amongst the most influential organizations working in the domain of human skin tribology. The red cluster with 5 organizations represents the heaviest and most influential collaboration among the organizations. The Blue and green cluster represents 7 and 5 organizations respectively. Purple, brown, pink, and yellow clusters represent the binary collaboration between the organizations.

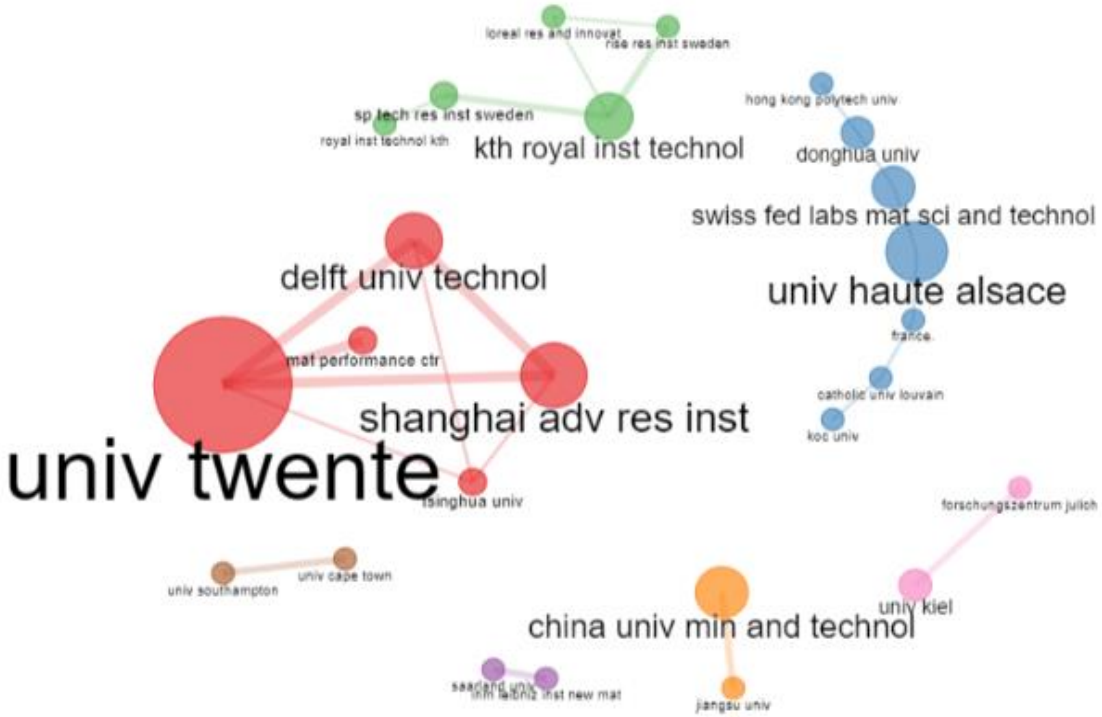

Figure 2.6 Collaboration network for most influential affiliations

D. Most preferred journal

This section discusses the journals from both databases that have widely been preferred by the authors to document and publish their contribution to the discipline. The top 10 journals have been ranked as per the total citation separately by both the databases as shown in Table 2.8.

In both the databases Tribology International is at the top with 81 and 32 publications from Scopus and WoS respectively. In Scopus, it is followed by Wear (51), Tribology Letters (44),

Proceedings of the Institution of Mechanical Engineers, Part J: Journal of Engineering Tribology (24), Journal of the Mechanical Behaviour of Biomedical Materials (22), and Surface and Coatings Technology (19). Journals listed between 7 to 10 in terms of a number of publications have total citations of more than 250, increasing the credibility of journals for referencing purposes.

In WoS, Tribology letters report the highest citation number of 875, followed by Tribology International (642), Wear (358), Journal of the Royal Society Interface (344), Skin Research and Technology (269), and Journal of the Mechanical Behaviour of Biomedical Materials (119).

Table 2.8 Top 10 most preferred journal

Scopus			**WoS**		
Source	NP	TC	Source	NP	TC
Tribology International	81	1646	Tribology International	32	642
Wear	51	1591	Tribology Letters	25	875
Tribology Letters	44	1395	Proceedings of the Institution of Mechanical Engineers Part J-Journal of Engineering Tribology	13	170
Proceedings of the Institution of Mechanical Engineers, Part J: Journal of Engineering Tribology	24	339	Wear	10	358
Journal of the Mechanical behaviour of Biomedical Materials	22	300	Skin Research and Technology	6	269
Surface and Coatings Technology	19	571	Journal of the Mechanical behaviour of Biomedical Materials	6	119
Textile Research Journal	19	362	Journal of the Royal Society Interface	5	344
Journal Of Fluid Mechanics	17	554	IEE Transactions on Haptics	4	28
ACS Applied Materials and Interfaces	15	421	Scientific Reports	4	164
Langmuir	14	256	Sensors	4	36

NP-Number of publications, TC- Total citation

E. Country-wise analysis

Country-wise total citation data is shown in Table 2.9 from the extracted data and sorted based on total citations. In Scopus, the United states of America (USA) reports the highest TC of

4519 and average article citation (AAC) of 36.74, followed by China (2467), the United Kingdom (UK) (2012), France (1844), and so on. Italy reports TC of 390 against AAC of 16.25.

In WoS, Switzerland tops the list with 803 total citations, which is less than the top 6 countries in the listing of the Scopus database. Switzerland reports the highest AAC value of 57.4 toppings the list is sorted based on total citations. It is followed by the UK (687), USA (475), Netherlands (432), China (417), and so on.

Figure 2.7 depicts the total citation (TC) on the (left y-axis) vs country data and average article citation (right y-axis) vs country. Belgium has the highest proportionate average citations per article.

Table 2.9 Top 5 Country wise total citation data

Scopus			**WoS**		
Country	TC	AAC	Country	TC	AAC
USA	4519	36.74	Switzerland	803	57.4
China	2467	11.53	UK	687	40.4
UK	2012	26.47	USA	475	18.3
France	1844	29.74	Netherlands	432	24
Switzerland	908	41.27	China	417	10.7

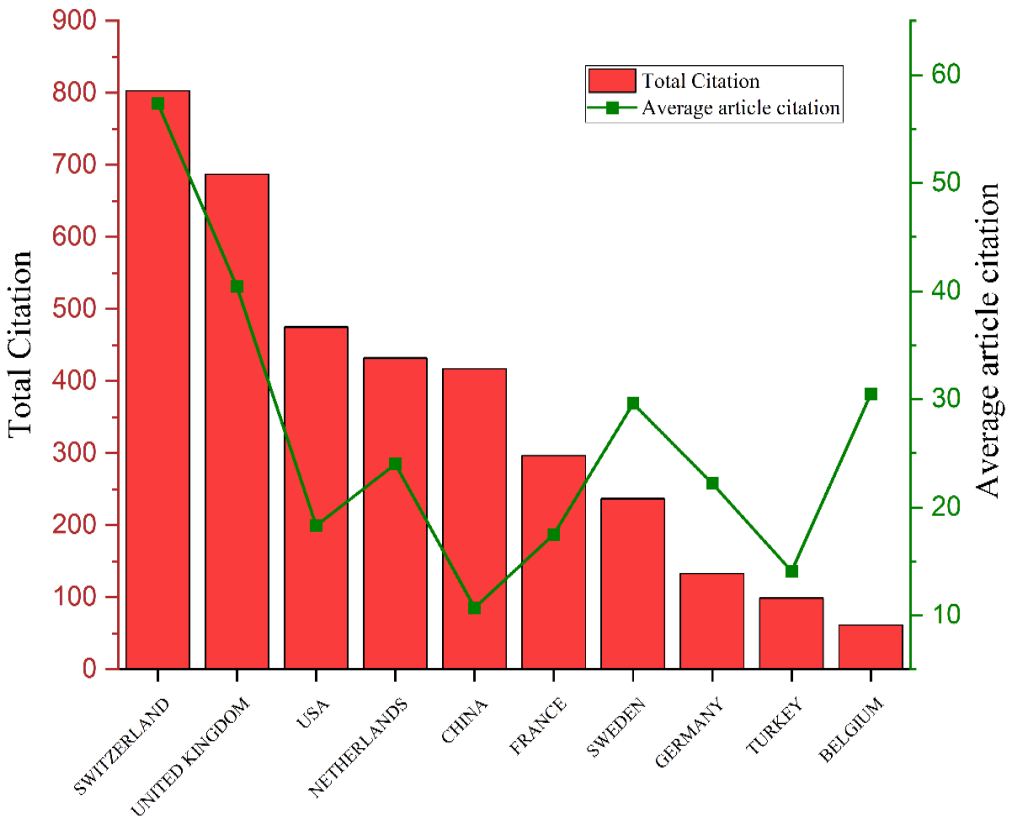

Figure 2.7 Total citation and average article citation per country as per WoS database

F. Most influential articles

A ranking of the most influential and highly referred articles is shown in Table 2.10 sorted by TGC and TLC. The top 3 articles in TC ranking [61], [62], and [63] are common to both TGC and TLC rankings. Other highly influential and cited articles in the domain of human skin tribology are [64], [36], [65], [47], [66] and [33].

Table 2.10 Ranking of top 20 articles sorted by TGC and TLC

Rank	Sorted based on TGC		Sorted based TLC	
	Article	TGC	Article	TLC
1	[61]	247	[61]	61
2	[62]	202	[63]	44
3	[63]	155	[36]	39
4	[64]	140	[62]	35
5	[36]	108	[65]	31
6	[65]	100	[47]	29
7	[67]	88	[67]	24
8	[68]	88	[66]	23
9	[47]	87	[69]	17
10	[21]	71	[33]	15
11	[66]	65	[70]	15
12	[71]	65	[72]	13
13	[69]	63	[73]	13
14	[74]	61	[75]	11
15	[76]	61	[21]	10
16	[9]	53	[77]	10
17	[78]	53	[79]	9
18	[80]	52	[81]	9
19	[82]	51	[83]	9
20	[84]	45	[9]	8

G. World collaboration network

The world collaboration network highlights the intensity and volume of the collaboration between countries all around the world. Table 2.11 compiles the top 10 collaborating countries from Scopus and WoS databases. In Scopus maximum number of collaborations is of China with the United Kingdom (14) and the USA (12). Followed by USA-France (12), France-Switzerland (11), France-Italy (10), and so on. While WoS database highlights the collaboration network of China-Netherlands (3), China-United Kingdom (2), China-USA (2), and so on. China tops the list in both databases for collaborative publications in the domain of human skin friction. Figure 2.8 shows the worldwide collaborative network for the WoS database.

Table 2.11 World collaboration network

Scopus			WoS		
From	**To**	**F**	**From**	**To**	**F**
China	United Kingdom	14	China	Netherlands	3
China	USA	12	China	United Kingdom	2
USA	France	12	China	USA	2
France	Switzerland	11	France	Italy	2
France	Italy	10	France	Sweden	2
China	Netherlands	9	Netherlands	Poland	2
United Kingdom	Germany	8	Netherlands	United Kingdom	2
United Kingdom	Netherlands	8	Switzerland	France	2
China	Hong Kong	7	United Kingdom	South Africa	2
United Kingdom	Italy	7	USA	United Kingdom	2
China	Canada	6	Belgium	Canada	1
Japan	Germany	6	China	Japan	1
China	Japan	5	China	Singapore	1
Pakistan	Saudi Arabia	5	China	Spain	1
Portugal	Brazil	5	China	Switzerland	1
United Kingdom	Australia	5	France	Belgium	1
United Kingdom	South Africa	5	France	Canada	1
USA	Canada	5	Germany	Italy	1
USA	Germany	5	Germany	Spain	1
USA	Japan	5	Ireland	Serbia	1
China	Italy	4	Italy	Ireland	1
China	Singapore	4	Italy	Serbia	1
Netherlands	Belgium	4	Netherlands	Spain	1
Netherlands	Poland	4	South Africa	Poland	1
Romania	Iraq	4	Sweden	Finland	1
Romania	Malaysia	4	Switzerland	Germany	1
United Kingdom	Singapore	4	Switzerland	Sweden	1
USA	Sweden	4	Turkey	Belgium	1
China	Australia	3	United Kingdom	Germany	1
China	Belgium	3	United Kingdom	Japan	1

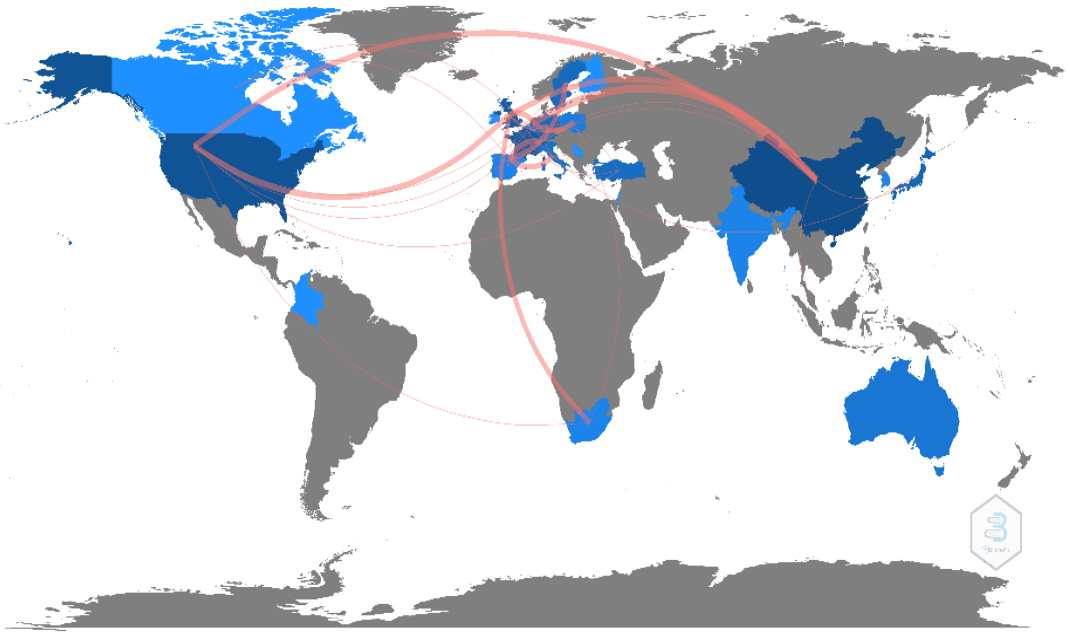

Figure 2.8 World collaboration network

H. Three-field plot

An interconnection between countries (left), author (center), and popular keywords (right) in the domain of human skin tribology is shown in Figure 2.9 depicting a three-field plot. Switzerland and China top the list in terms of publications. Followed by Netherlands, France, and United Kingdom. It is worth noticing that combined European region countries working in the domain. Derler S., Van der heide E., Zeng X., and Rutland, M.W are highly cited authors. The right of the three-field plot shows the most popular keywords in the literature, Friction, skin tribology, tactile perception, bio tribology, and skin friction to name a few.

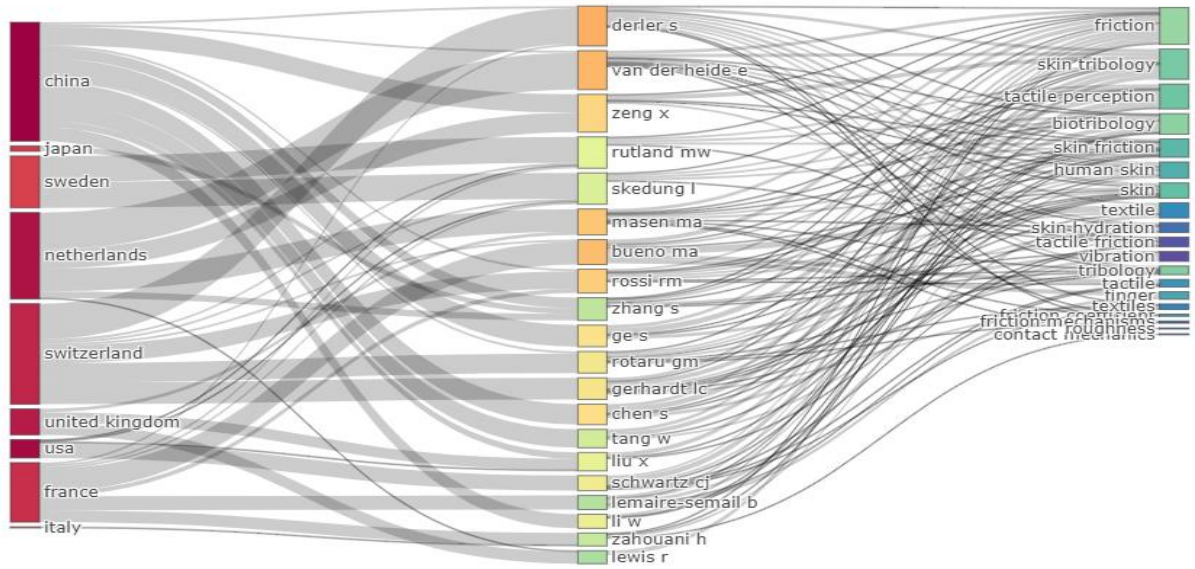

Figure 2.9 Three field plot

2.3 Scoping Review through the Preferred Reporting Items for Systematic Reviews and Meta-analyses (PRISMA) Technique

The bibliometric study reported in the previous section presented the descriptive analysis in the field of human skin tribology. Further, the dataset of the bibliometric analysis was narrowed down through a scoping review incorporating the *in-vivo* experimental investigations. Scoping review is performed by making use of preferred reporting items for systematic reviews and meta-analyses (PRISMA) technique as shown in Figure 2.10.

(*a*) *Declaration of the research question*

In-vivo experimental studies are available for assessing the frictional behaviour of human skin: both quantitative and qualitative evaluation.

(*b*) *Search for literature*

A literature search was conducted across two widely popular databases namely Scopus and web of science with different keywords like finger friction, skin tribology, tactile, haptics, texture, fingertip, and finger pad. Then inclusion criteria were adopted for relevant articles related to the research question.

(*c*) *Criteria for inclusion of literature*

All the attributes affecting human skin friction are included. Criteria may be as listed:

- Articles post the year 2000.
- *In-vivo* experimental techniques related to human skin friction only.
- Articles available in English language only.

(*d*) *Information extraction and analysis.*

- Included studies are chronologically arranged in a tabular format and divided into four different anatomical regions. Tabular data chronologically presents the crux of included studies highlighting:
- Year of publication.
- Subject attributes (age & gender).
- Equipment used.
- Variation of coefficient of friction (COF) with the parameters considered in the study.
- Contacting material.
- Key findings.

(*e*) *Selection of experimental research for further classification*

An extensive literature survey comprises of bibliometric study and its analysis with a scoping review to sort out the in-vivo experimental studies. The studies are classified into four anatomical regions as discussed in the later part of this section. The studies conducted from 2000 to 2020 are arranged in chronological order and discussed highlighting the aim, experimental techniques, counter surface material, tools, and conclusions drawn among researchers and scientists.

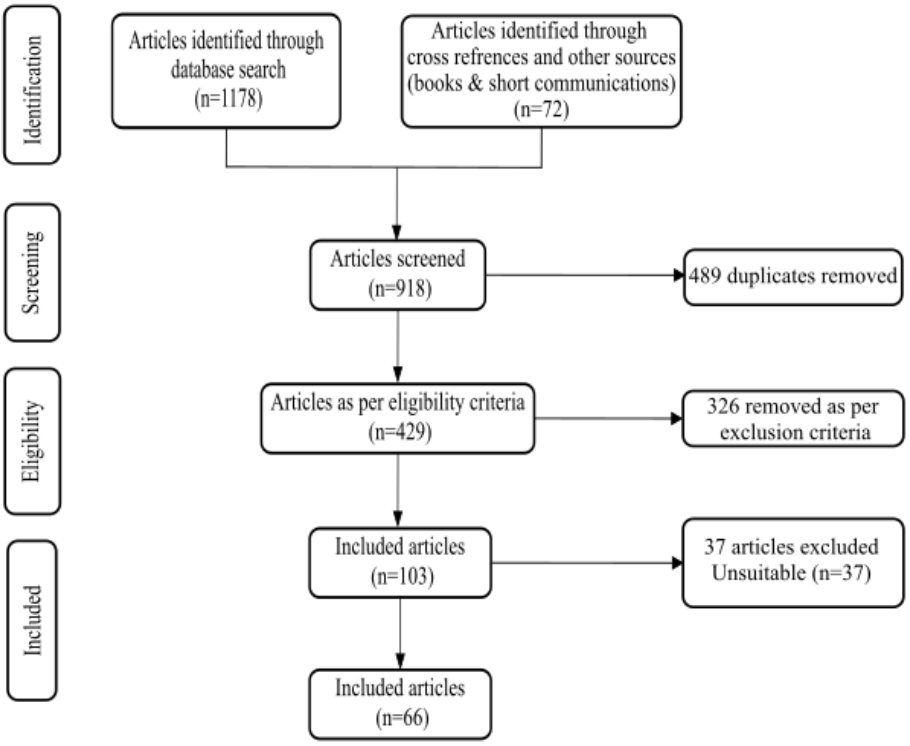

Figure 2.10 PRISMA flow diagram for the scoping review

Researchers have used different methods for the determination of skins tribological or mechanical properties such as indentation test [10], [24], [85], [86], friction test [14], [19], [22], [41], [46], [61], [62], [87], [88] and acoustic emission test [32]. An experimental study involves two components: (i) experimental setup and (ii) post-processing analysis of test results. Sample preparation, friction measurement, and data acquisition constitute the part of experimental design. Similarly, the interdisciplinary nature of the current research for the post-processing of test results needs multi-domain expertise ranging from material characterization to dermatology, statistics, and tribology. Human skin frictional study involves two materials one being human skin and counter material.

In-vivo experimental studies are classified as fingertip, finger pad, forearm, and other regions based on the anatomical region after scoping literature survey as shown in Figure 2.11. Since maximum researchers have opted for fingertip and finger pad as the anatomical sites of

experimental investigations having a share of 22% and 36% respectively. Therefore, the finger pad is taken as the site of experimental investigation for the current work. Figure 2.12 is drawn to highlight the permutations of various materials taken as test samples along with the anatomical region in the experimental investigations reported between the year 2000-2020. In vivo, experimental studies classified in four anatomical regions are discussed in the following subsections.

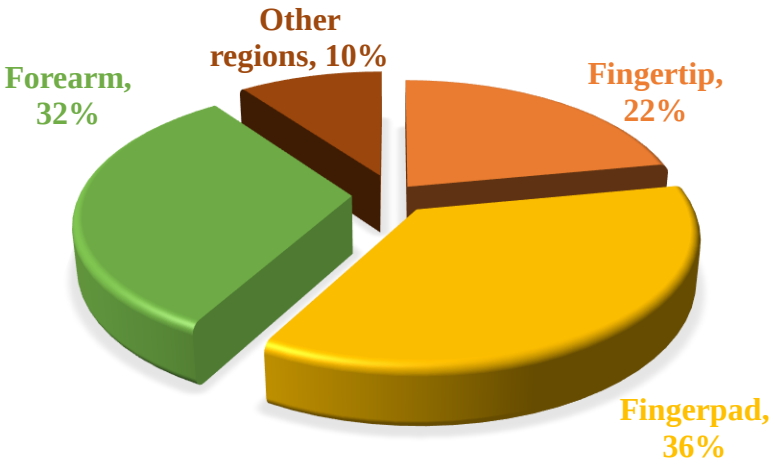

Figure 2.11 Popular anatomical regions for experimental investigation of human skin friction

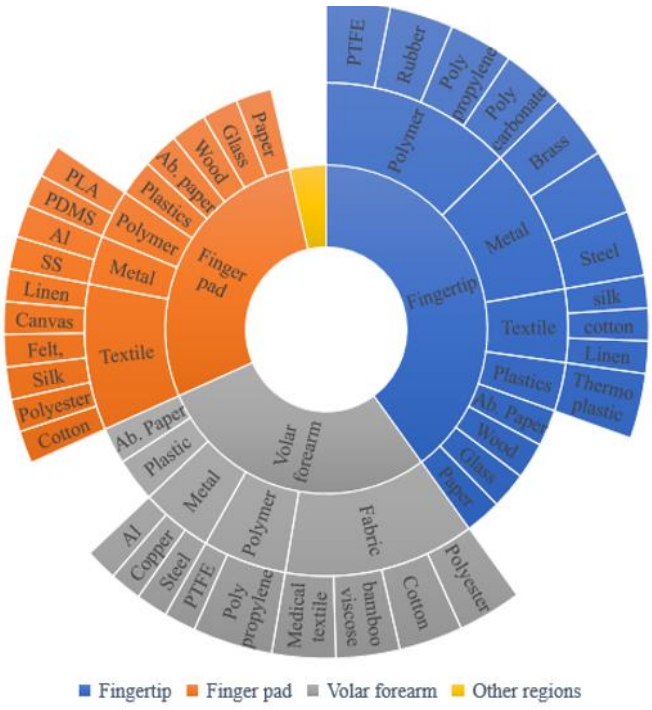

Figure 2.12 Permutation of human skin frictional study with various material

2.3.1 Fingertip

A range of literature is found exploring the fingertip as the site for human skin friction measurements. Fingertip being one of the most common interactions of human touch is widely popular among researchers. Versatility in the experimental setup and the simplicity of procedures is another reason that makes fingertip popular for human skin friction measurement studies as listed in Table 2.12.

A design of a test rig is proposed [89] to investigate the coefficient of friction (COF) while sliding the soft fabrics with human skin making use of the strain gauges arranged in x and y directions to measure the corresponding normal load and shear force.

Friction for the untreated dry finger with a reference textile attached through a transducer was investigated in [63]. The further study simulates the frictional phenomenon of textile and the artificial skin model.

Effect of normal load investigated in [90], the finger friction test rig proposed that the frictional force is linearly proportional to the applied normal force tested with 12 materials including metals, elastomers, and plastics. For a smooth surface at a normal load greater than 1N, frictional and normal forces are linearly correlated. The roughness of the finger plays a vital role when in contact with relatively low surface roughness value material.

Tribological attributes of human skin are investigated [81] and its effect on the tactile characteristics of polymer fabrics is reported by sliding a fingertip over the samples stuck to the polyethylene plate which is attached to a dynamometer. The study states that the swipe of a human finger over the three-axis dynamometer is effective for the COF measurements of fabric polymers with human skin. The study highlighted that tactile assessment was not well co-related to the COF.

Fingertip friction measurements were performed in conjunction with the manipulation tasks to study the combined effect of moisture and static COF [91]. Normal force and the shear forces were measured through an attached force transducer on the specially designed test setup. At high levels of skin moisture, COF is inversely proportional to the normal force.

Finger frictional measurements were measured through a combination of a piezoelectric force sensor and a charged amplifier for the amplification of the signal data [31]. Surface roughness and finger friction show an inverse relation.

Tribo touch setup was developed in [92] for the evaluation of frictional characteristics of wood replicas made of vinyl and polyurethane. Measurements were performed by sliding the fingers over the plate of the test setup composed of two tri-axial force sensors.

Static COF was measured in [93] with a setup very similar to that used in [91]. The only modification is the absence of a linear translating mechanism. The six-axis force and torque sensor measure the normal force and tangential force at the onset of slipping.

Tactile perception evoked by friction and vibration is investigated for various surface textures [94]. Surface recognition was performed by attaching the fabric and paper samples to the three-axis force sensor monitoring unit. The study reported the lower value of COF for the increasing value of the surface texture dimensions.

Finger friction measurements were performed for the stimulation generated due to the lateral vibrations [95]. Greater friction forces are perceived when vibrating in comparison to that of the stationery state of sliding of the finger.

A tactile discrimination study in [45] performed over by sliding fingers on the abrasive sheets with different grades reported that friction forces are highly affected by the surface topography and the edge effects of the samples used.

An electro adhesive technique is incorporated to control the friction force of the sliding fingertips. The developed device is capable of capturing the friction forces up to 6 kHz of frequency. Furthur the device's capability is demonstrated by the measurement of skin vibrations through a laser doppler vibrometer (LDV) [96].

Sliding contact of finger friction is studied with surfaces having different morphologies using high-speed cameras and the force measurement units [97] as shown in Figure 2.13.

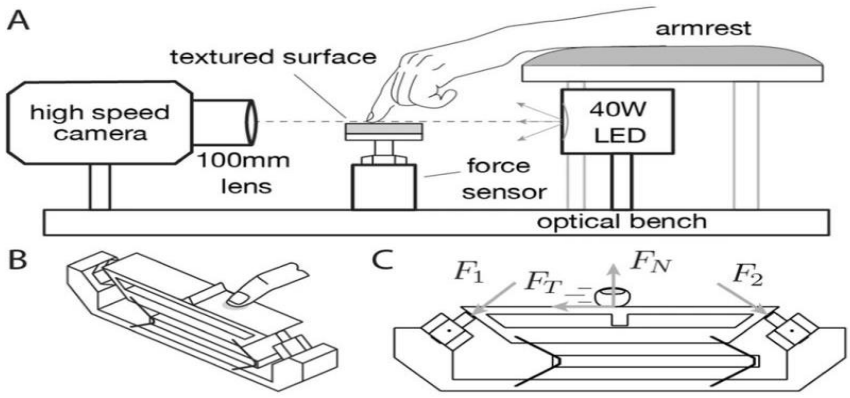

Figure 2.13 (A) Measurement system, side view (B) Isometric view of the two-axis force sensor. (C) Frontal view of the force measurement device with force decomposition [97].

Table 2.12 Experimental studies of fingertip human skin friction

Y	No. of subjects {Age}	Equipment	Variation with COF	Interacting Surface	Highlight	Ref
2005	1 M {23}	In-house developed test rig measuring force with mounted strain gauges.	μ with a finger: PC>Rubber >Steel>PE>Glass >Paper	Rubber, Thermoplastic elastomer, PE, steel, PC, glass, paper	The study has further investigated μ with steel and rubber ball	[89]
2007	6 F 6 M {24-61}	Quartz 3 axis dynamometer, Corneometer	NL ⊘ μ ↑SH: ↑ μ	Wool fabric	7 ASM frictional test was also performed	[63]
2009	1	The finger friction rig consists of two load cells, Moist sense.	Friction force for plastics (except acetal) and metal showed linear variation with normal force.	Al, SS, Brass, Nylon, HDPE, Acetal, PP, PVC, Elastomers (4).		[90]
2009	1 M	3- axis dynamometer	$\mu_{perpendicular} > \mu_{parallel}$	Polymer fabrics (14)	The amount of radially outward fabric has a high correlation to μ	[81]
2009	5 F 5 M {20-53}	Linear translation stage, 2 force sensors,	↑ NL: ↓ μ_{static}		Presents combined effects of NL and Moisture on ↑ μ_{static}	[91]
2016	10 F 8 M	Profilometer, Tribo Touch Setup, NappOmatic,	μ : Wood replica>PUR	Wood replica (vinyl), PUR	No effect of material on μ	[92]

Table 2.12 (continued...)

2016	3 F 9 M {18-60}	Manipulandum with two six-axis force and torque sensors, Corneometer	↑ NL : ↑ μ_{static}	Polyimide film	The method proposed to measure static μ for fingertip-object contact	[93]
2017	20	EEG sensing cap for tactile perception, UMT-2 Tribometer	Tactile perception is sensitive to fabric textures. ERP analysis methods are useful for studying the brain's response to skin friction.	Fabric (3), Paper (3)	μ and frictional vibration signals were measured	[94]
2011	10 F 15 M {22-29}	Test rig developed consisting of 3 component piezoelectric force sensor.	↑ NL: ↓ μ ↑R_a: ↓ μ P.C.: ↓ μ	Paper	8 Different grades of paper with different R_a	[31]
2017		3 axis force sensors	↑ friction: Vibration > sliding	Plastics	Vibrotactile stimuli	[95]
2018	11 F 12 M {>18}	3- axis force transducer	↓Grit size of texture sample: ↓ ability to differentiate the samples. Edge effects were reported for friction measurements.	Abrasive paper	Tactile discriminati on of textures	[45]
2018	15 F 20 M {20-30}	An in-house developed setup consisting of a 3 d force sensor, accelerometer, and DAQ	↑ Oscillations in friction force lower sliding speed on the finger pad. Vibration mag: Fingertip > Finger pad	Sandpaper (#600, #800)	Correlation between tactile perception and tribological properties for the human finger	[30]

Table 2.12 (continued...)

2018	1	Rotational tribometer, LDV sensor, MEMS Microphone, vibrometer	The velocity of fingertip vibration was measured through a laser.	PTFE	Electro adhesive approach developed to control friction on sliding fingertips modeling air gap as a parallel plate capacitor.	[96]
2018	2 M {29, 35}	Piezoelectric transducers, High-speed camera,	Friction force varied with relief of contact surface.	AL 6061	Contributio n of contact geometry and mechanics in friction force prediction	[97]

AL- Aluminium
ASM- Artificial skin material
DAQ- Data acquisition
EEG- Electroencephalogram
ERP- Event related potential
HDPE- High Density
LDV-Laser Doppler vibrometer
MEMS- Microelectromechanical system NL- Normal Load
Poly Ethylene
PC- Polycarbonate
PE- Polyethylene
PP- Polypropylene
PTFE- Polytetrafluoroethylene
PUR- Polyurethane
PVC-Polyvinylchloride
P.C.- Perceived Coarseness
Ra- Surface Roughness
SH- Skin Hydration
SS- Stainless steel
#- Number
µ-COF
µ-COF

2.3.2 Finger pad

Various studies have opted for the finger pad region for investigating the tribological properties of skin for tactile perception, texture discrimination, electro adhesions, human haptics, and human gripping. Studies having finger pad as site the of tribological investigation are tabulated in Table 2.13 in chronological order listing the setup, counter-surface material, variation with COF if reported, and the highlights of the study. Tribological investigations to determine the

variables influencing human skin friction used a portable device on multiple anatomical regions including finger pad [19]. The in-house developed device had the axis of rotation perpendicular to the skin and the application of normal load was controlled through the spring-based mechanism in the range of 0.5 N to 2 N. Velocity is controlled in steps of 1, 2, 5, or 10 mm/sec. COF was reported to significantly increase with age, ambient temperature, and relative humidity when the friction of human skin was tested with the aluminum sample.

A test rig to measure finger friction is developed and tests are performed over the bare finger and donned over gloves of two materials [98]. In the reciprocating motion, the study reported the use of water, increases the COF while the same amount of oil decreases the COF.

Frictional behaviour of human skin with a glass having different roughness was investigated with skin contact area measurements using pressure-sensitive films. Adhesion was found to be a predominant contributor to frictional force in the experimental investigations. Viscoelastic deformations of human skin played a relatively small role in the friction value [36].

Primitive test setup in [26] consists of the three-axis load cell for the measurement of normal and the frictional forces reported that the deformation component of skin at the micro scale has a significant role in total frictional force as per equation 2.2. Conclusions drawn were validated both for the dry and the wet state of skin, where skin softening takes place.

$$\mu \propto C_{adh}.N^{(\frac{-1}{3})} + C_{def}.N^{(\frac{1}{3})}. \qquad \textbf{2.2}$$

An attempt to study the relationship between surface texture and tactile friction reported a decrease in COF with increasing normal load [33]. Further, an influence of elastic behaviour of the uppermost skin layer was reported to affect the surface texture and COF when the effect of the former over the latter was investigated.

Stick-slip behaviour was investigated for finger sliding over the smooth glass in a wet state as a function of normal load and sliding velocity [28]. COF values reported during stick-slip were reported to be 30% lower than those for stationary sliding. All the measurements were performed by sliding over the finger on the smooth glass plate attached to the 3- component dynamometer.

A distinctive study on the frictional interaction of the topography between samples consisting of glass, plastic, and fabric was performed through a specially designed test rig [44]. The measurement setup consisted of two load cells arranged to measure normal load and the

tangential force to determine the COF at the finger pad and test sample interface. The results showed significant different in variance for the COF of the different sample surfaces tested.

The effect of roughness on vibration generated on the human finger during a friction test was investigated through a haptic tribometer [99]. The device consists of an accelerometer, normal force sensor, and a displacement system to measure vibrations generated due to rubbing of the finger pad, applied normal load, and moving the sample surface in translatory motion respectively. The study reported the combined effect of skin deformation and vibration can be used to determine their physical environment through the sense of touch.

Variations in the pressure distribution and its influence on the friction of the finger pad are attempted by sliding a human finger over the pressure-sensitive films attached to the force plate [100]. The pressure-sensitive film had a defined arithmetic average surface height of 0.91 ± 0.24 µm. The study reported a decrease in COF with an increase in the skin contact pressure that aligned with the adhesion model of friction. The distributions of the pressure during friction measurement were attributed to the low forces at the rounded profiles.

Friction and abrasion of the finger pad were investigated with abrasive papers using a tri-axial force plate [101]. The study reported that the number and volume of particles abraded varied with the grit size of abrasive papers but showed very comparable COF values. Ploughing phenomenon is of importance when considering friction mechanisms of the skin and abrasive papers.

Braille print is an efficient technique for persons dependent on the sense of touch for the source of communication. A study presents the influence of patterns and skin behaviour on COF [102]. Dot features of varying heights embossed over the paper samples were used to swipe the finger. A piezoelectric three-force dynamometer was used to measure normal and tangential forces. The study reported that the macroscale surface features contribute very nominal to the overall friction that arises from the adhesion mechanisms. The magnitude of the hysteretic deformation of the soft finger pad was dominant and thereby governed the overall mechanism.

An investigation aimed to develop a correlation between human finger perception and finger friction attributes are attempted in [29]. A specially designed tactile stimulator was mounted over the tribometer, and subjects were instructed to slide their finger over the plate maintaining a normal load of 0.5 N. Two friction conditions were obtained through vibration at two separate amplitudes. The study concluded that better friction discrimination could be made at lower values of sliding velocity.

A dermatological study aimed at measuring the friction of the index finger pad sliding over the artificial skin materials after the application of cream and lotion through a force board consists a horizontal and vertical load cells [103]. The study reported an increase in the COF values for hydrated skin due to an increased contact area between the bare skin and the skin model.

A laser-treated, stamped and cold-rolled micro-structured stainless steel sheet is used for investigation of its friction and tactile characteristics when a finger pad is slid over it [25]. For finger friction measurements a multi-axis force transducer is used that measures the normal load and tangential force with a resolution of 25 mN and 12.5 mN respectively. The study concluded that tactile friction is inversely proportional to the comfort perception obtained as part of subjective perception investigation.

Finger pad friction for the medical gloves is investigated through a setup consisting of a force plate and speaker attached to it for vibration generation [104]. Finger sliding experiments reported increased friction in dry and reduced friction in wet conditions. Results showed the perception of the vibrational frequency decreased while the gloves were donned.

Slipperiness and roughness perception as an effect of topography and friction are investigated [105]. Drawn conclusions highlight that for spatial distances below 100 µm, slipperiness is more dominant than the roughness of the surface. Differences in the friction force between participants are approximately equal to the differences measured between the different surfaces.

The study is conducted to develop a contact mechanics model and validated through the experimental data in [106]. A 10 N transducer was used to measure the loading behaviour and a glass plate as a support fixture was attached to the transducer. Gross area (A_g) and ridge contact area (A_r) as a function of load (W) as shown in equation 2.3 and 2.4 respectively is developed and is experimentally validated.

$$A_g = k_g \left[\frac{W}{1+\beta W} \right]^{\frac{2}{3}} \quad \textbf{2.3}$$

$$A_r = k_r \left[\frac{W^{5/6}}{(1+\beta W)^{1/3}} \right] \quad \textbf{2.4}$$

Where,

$\widehat{k_g}$, $\widehat{k_r}$ being the load coefficient for finger pad gross contact area and load coefficient for fingerprint ridge contact area. β , is the load coefficient for the secant modulus. An experimental study aimed to investigate the contact area between the finger pad and the flat surface is reported in [107]. Three popular methods are used for measuring the static and dynamic contact areas namely ink printing, optical coherence tomography (OCT), and digital image correlation (DIC). The setup consisted of a force plate attached to the linear reciprocating stage, a low coherence light source along with a fibre -coupler. Out of the three mentioned techniques, OCT is concluded to be the most effective method for micro- scale analysis for an improved understanding of the human skin friction phenomenon.

An experimental investigation aimed at identifying the factors that potentially affect the ability to discriminate the textured surfaces in [35] reported that the mean spacing of the profile peaks for the tested surfaces should have significant differences. It further classified that the differences in the average roughness measures and individual discrimination ability for textures are not correlated.

Gross and real imaging for the contacts under dynamic loading are examined in [108]. The study intended to develop an instrument to investigate finger contacts for tangential dynamic loading. The setup consists of a tribometer coupled with a high-speed imaging apparatus. Traction is reported to decrease at a higher rate in dry fingers in comparison to lubricated fingers.

A study was performed to determine the influence of age and gender on the biophysical properties of the human finger to evaluate touch comprehension by evaluating the adhesive force at the contact interface [40]. Adhesive forces are responsible for the increase or decrease in the contact area. Thus, affecting the tactile properties at the interface. Conclusions drawn reflect the positive correlation between age and the mean of surface roughness for men and an inverse relation for women. Tactile perception decreases with increasing age across test subjects irrespective of gender.

A frictional study aimed to compare the tactile perception between the real and the virtual textile fabrics is performed in [109]. The finger friction study highlighted the good rendering of virtual to the real fabric. Although the conclusions were made about finger-induced vibrations for the efficient discrimination of the textures for the two fabrics.

Mechanism to highlight the effect of sliding velocities that affect tactile perception by investigating the tribological properties of the finger pad is proposed in [30]. Parametric investigation of each parameter namely velocity, roughness, and the contact area are performed. An increase in sliding velocity shows an increase in vibration and a pronounced stick-slip phenomenon is observed at lower sliding velocities.

The impact of biophysical properties of fingers is investigated for the determination of aging and gender effects on tactile perception [88]. An accelerometer glued over the finger captured the vibrations and the two strain gauges attached below the surface measured the applied normal and tangential forces. The study demonstrated surface topography as a vital physical aspect of tactile perception. The better capability of tactile perception is attributed to female subjects.

A study to understand the contact mechanics between the human finger and touch screen under electro adhesion is investigated in [110]. The friction measurements are conducted through a tribometer consisting of a motor to translate at desired velocity and a force sensor as a support to the touchscreen. All the experiments were conducted in the range of 0.1 to 0.9 N normal loads and 50 mm/ sec of sliding speed. A study reported that electro adhesion causes an increase in the contact area leading to higher tangential forces.

In the purview of age and gender, tactile perception and touch anisotropy are investigated through finger size and real contact area [111]. The test setup consisted of a normal force sensor and fingerprint sensor coupled with an indentation system. Contact area as a function of the force applied is obtained. Size and real contact are considered important attributes to define the density of the mechanoreceptors available. The study concluded that the finger size and the real contact area carry vital importance in the determination of tactile perception. Further, better tactile perception is reported in the lateral direction of the finger movement.

A finger friction study was conducted with textured polymeric substances prepared through 3-D micro fabrication techniques in [34]. Investigations aimed to study the grip effect of two polymeric materials through the tribological tests were conducted by sliding finger pad on the specially fabricated counter materials with varied textures. The setup consisted of a force plate over which the materials were mounted and a normal load of up to 10 N is applied at a sliding speed of 60 ± 10 mm/sec.

An experimental investigation was conducted to determine the relationship between the roughness and physical parameters such as skin vibration, COF, and particle size [112]. A

wearable skin sensor was mounted over the finger that was sliding over the plate attached to the 6-axis force sensor. The sensor measured the vibrations generated through the skin while the force plate measured the external forces. Although no approximations could be made to establish an estimation model but highlighted the differences in the roughness ratings.

Finger pad friction measurements were conducted to develop the empirical approach for the determination of skin elasticity [27]. Different rubber textured specimens were taken as a counter surface over which a finger pad slid up to a normal load of 5 N for measuring dynamic COF and a combined analytical and numerical contact model is presented. The normal load is applied using the static weights and force is calculated through the mounted transducer. The range of normal load was 0.1 N to 5 N. The developed method is limited to the dry state contacts and textures having lateral distributions that have relatively small heights compared to stratum corneum. Figure 2.14 illustrates the experimental setup used for the study.

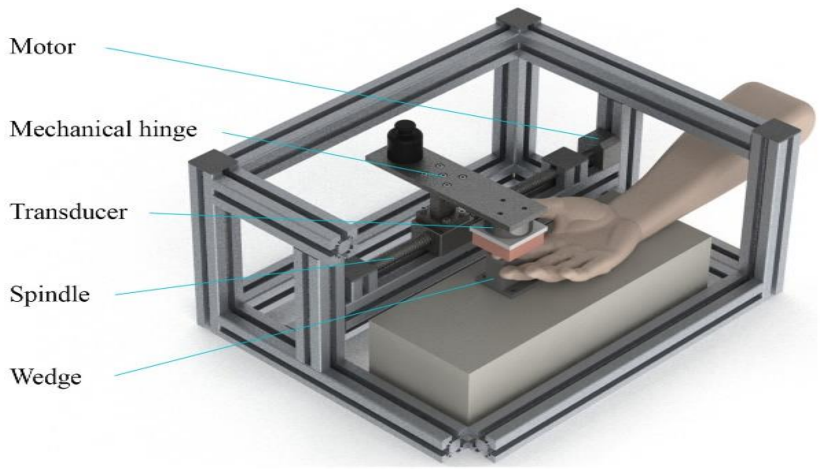

Figure 2.14 Friction measurement device [27]

The effect of material hardness on friction is studied between the finger and artificial skin [113]. The test setup consists of a normal force sensor and a single shear force sensor. Artificial skins with 7 different hardness values were used. All artificial skins were 5 mm thick and had constant roughness values. The study reported, for dry conditions when the skin model was harder than a bare finger, COF was independent of the normal load, and when artificial skin is softer than the finger COF decreased with increasing normal load. Under lubricated conditions, COF depended on normal load for softer artificial skin, and COF because of the deformation friction increases with increasing normal load for the harder (in comparison to bare skin) artificial skin.

Frictional behaviour of the human finger pad at the phalange region is evaluated for the gripping task in [114]. Experiments were performed on the reciprocating sliding contact using a UMT 2 tribometer equipped with a load sensor with a measuring range of up to 20 N, applied normal load ranging between 1 N to 2 N, and a sliding speed of 1mm/ sec was taken. Distal phalanges reported the highest elasticity, and there was a larger application of grip force. Irrespective of gender, aged persons need to apply twice the force as required for the young person. Stiffness of the finger influences the manipulating tasks and the fit of the grip. The gripping force is reported to be different for both hands (left or right).

Table 2.13 Experimental studies of fingerpad human skin friction

Y	No. of subjects {Age}	Equipment	Variation with COF	Interacting Surface	Highlight	Ref
2007	1 M {23}	The test rig contained two load cells	Dry: $\mu_{kh} > \mu_{lx} > \mu_{finger}$ Water: almost equal Oil: least for latex	Nitrile rubber Kitchen Glove, L_X	Human torque calculations are presented for gripping of bottle	[98]
2008	2 F 2 M {23-45}	Custom-built Dynamometer	Adhesion predominated resulting in ↑μ. Deformation had very little effect on μ.		The pressure-sensitive film, Normal load, Glass, Function of contact pressure	[36]
2011	1 M	Load cell	μ varies with NL ↑Roughness: μ↓	SS	Tactile friction	[26]
2012	1 M {35}	Skin Micro-Tribometer model UMT	↑NL:↓μ	Metal, Thermoplastic PUR	Surface texture, Tactile friction	[33]
2013	1 M {49}	Quartz 3 component dynamometer	↑NF:↓μ ↑SV:↓μ	Wet/ smooth glass	Stick-slip phenomena	[28]
2013	1 M {24}	In-home developed test equipment containing two load cells equipped with DAQ	Two parameters-finger friction level and variance in friction described for discrimination of surface texture	Linen, canvas, felt, silk, velvet, cotton, plastic	Linear regression analysis of the relationship performed normal load and μ	[44]

Table 2.13 (continued...)

2013	34 M 16 F {Median 28}	Revolt ST mobile device	↑Age:↑ μ ↑Temp:↑μ ↑RH:↑μ ↑Height:↓μ ↑Hair:↓μ	Al 6060	Correlation has been made with variables influencing human skin frictional behaviour	[19]
2013	1 M	Haptic tribometer, accelerometer	Roughness transferred to fingerprint is relevant to tactile perception	Abrasive papers	Vibrations in skin due to roughness	[99]
2013	2 F 1 M {-}	Force plate	The effect of Pressure distribution on μ is analyzed.	Smooth pressure-sensitive film	COF of finger pad is investigated	[100]
2015	1 M {25}	Tri-axial force plate Kistler type 9254	Micro stretches on epidermis observed. Skin particles abraded on abrasive paper.	Glass, abrasive papers	Friction mechanism, abrasion	[101]
2015	1 M	Piezo electric 3 force dynamometer	↑μ ∅ Presence of dot features. ↑ NL: μ↓ ↑ dot radius: ↑ μ	Braille dots of 0.48mm, 0.75mm, and 1.0 mm on paper	Influence of cell patterns	[102]
2016	20	Ultrasonic tactile simulator, tactile tribometer	↓ SV: ↑ FC $FC = 1 - \frac{\mu_1}{\mu_0}$	The surface of the tactile simulator	Analysis of friction b/w index finger and surface of stimulator	[29]

Table 2.13 (continued...)

2016	1	Force Board, OCT	For hydrated skin: ↑ Contact Area: ↑μ Full film Lubrication: Contact area ∅ μ	Model skin substrate (Vitro-skin)	Evaluation of moisturizing components in skin creams for effect on frictional properties.	[103]
2017	8 F 8 M {20-30}	Corneo meter, multi-axis force/torque transducer	↑ NL :↓μ	SS (5)	Textured samples prepared through different modes	[25]
2017	1 M {23}	Multi-component force plate	Dry:↑μ Wet:↓μ	Latex surgical glove	The effect of glove use on the perception of tactile vibration is explored	[104]
2017	6	Profilometer Force Board, Corneometer	Due to slipperiness, very smooth surfaces are perceived to be rougher than textured surfaces	PDMS	Effect of topography and friction on perceived roughness	[105]
2017	1 F {27}	UTM	An elastic model providing expressions for gross and ridge contact area	Glass plate	μ is independent of normal force due to surface roughness.	[106]
2017	1 F {25}	Ink printing, OCT, DIC	The contact area is dependent on NL.	Flat Surface	Measurement of contact area	[107]
2017	16 F 10 M	3- axis dynamometer, Profilometer, SEM	μ measured in two directions: aligned and transverse	Abrasive Papers	Effect of friction and Surface attributes on tactile discrimination of textured surface	[35]

Table 2.13 (continued...)

2017	-	Custom built device	The developed device is capable of recording finger dynamics with imaging features.	Flat glass prism	Finger contact under dynamic loading	[108]
2017	20 F 20 M {23-64}	Indentation device, Air blast system, Chromatic Imaging	Adhesive force: Women >Men Young's Modulus: Women> Men	Contactless indentation using wave propagation technique	Age and gender effects on Biophysical properties of finger	[40]
2018	4 F 5 M {28-57}	3- Axis load cell, accelerometer	Brain activation is similar for real and virtual twill fabrics but differences with velvet	Twill and velvet	Real and virtual textile fabrics	[109]
2018	15 F 20 M {20-30}	In-house developed setup	↑SV: ↑vibration acceleration Vibration accn: Fingertip> finger pad	Sandpaper	Correlation of tactile perception and tribological properties for a human finger	[30]
2018	20 F 20 M {23-64}	Haptic tribometer Accelerometer	Mel frequency Cepstral Coefficient algorithm is an efficient tool for surface quality via vibratory signal	Tissue, Paper, Plastics	Impact of biophysical properties on touch gestures and tactile perception: Age and gender effects	[88]
2018	-	In house setup FE-SEM	Friction depends on electrostatic attraction. Proposed a mean-field theory to analyze the effect of electro adhesion.	Touchscreen layering	Effect of electro adhesion on sliding friction	[110]

Table 2.13 (continued...)

2018	20 F 20 M	In-house developed indentation device, Fingerprint reader	↑Tactile perception for females < 40 years of age Anisotropy of mechanical properties leads to the anisotropy of TP		Static and active tactile perception	[111]
2019	12 F 18 M {18-24}	6 axis force sensors, wearable skin vibration sensor	↑roughness: ↑ skin vibration	Glass particle surface, Sandpapers	Glass particles had a high correlation with subjective roughness	[112]
2019	44 M	An in-house setup consisting multi-axis force sensor	↑ Texture: ↑Ploughing friction	PLA, PDMS	The effect of positive and negative textures is considered	[34]
2019	-	6-axis Mini 40 Transducer, Corneometer 825 M	↑NL: ↑Mean apparent pressure, ↑ Contact area,↓μ	Silicon rubber	Effect of change in contact area on frictional behaviour.	[27]
2020	1F Wet 8M 11M - Dry {20-29}	2 axial force sensors	ASM harder than finger: NL Ø μ ASM Softer than finger: ↑NL: ↓ μ	Dry and lubricated ASM	Investigated role of Material hardness on friction	[113]
2020	1 F 2 M {34-67}	Tribometer UMT 2	Distal phalange has the highest COF	SS	Friction behaviour of human skin in precision task	[114]

ASM- Artificial skin material	L_X- Latex Glove	µ-COF
Al- Aluminium	NF- Normal Force	∅- Does not effect
DAQ- Data acquisition	NL- Normal Load	
DIC- Digital Image Correlation	OCT- Optical Coherence Tomography	
FE-SEM- Finite element SEM	PDMS- Poly dimethyl siloxane	
FC –Friction Constant	PLA- Poly lactic acid	
	PUR- Polyurethane	
	RH- Relative Humidity	
	SS- Stainless steel	
	SV- Sliding Velocity	
	Temp- Temperature	
	UTM- Universal Tribometer	

2.3.3 Forearm

The forearm is one of the most widely preferred sites for the tribological investigation of the human skin because of its accessibility, limited variation in mechanical property, glabrous nature, and ease of experimentation. In-vivo experimental investigations that have been performed taking the forearm as the frictional test region are further discussed in detail. Studies taking the forearm as the site the of tribological investigation are tabulated in Table 2.14 in chronological order listing the setup, counter-surface material, variation with COF, and the highlight of the investigation.

A tribological investigation was conducted to assess the feasibility of friction and electrical properties of skin that differentiates the chemicals applied to the skin [41]. UMT series tribometer was used to perform frictional measurements. The copper probe was pressed through 20 g weight moving at a constant velocity of 0.4 mm/sec. No potential differences were reported across age, gender, and ethnicity. Glycerine and petrolatum increased COF by a similar value.

An attempt is made to relate the frictional mechanism of human skin with the acoustic attributes in [32]. The setup consists of a microphone that measures the acoustic emissions transmitted by the stratum corneum. The probe consists of sensitive acoustic sensors and is adjusted for speed, distance, and the smaller values of normal load. The study concluded acoustic emissions are correlated with the stiffness and surface roughness of the outermost layer of human skin.

In [61] the study reports the frictional phenomena of human skin for hydrophilic and hydrophobic counter surfaces in the dry and wet states. The setup consists of a balance arm attached to the fulcrum through a bearing. Tangential force is measured by two flexible strain gauges attached to a rigid beam assembly. Normal load up to 4 N is applied through the probe

with static weights. Reciprocating motion is provided by the translation stage which moves at a constant velocity of 8 mm/sec. Results highlight that the contact area and interfacial shear strength between the contact surface highly influence the frictional behaviour of skin in both dry and wet states.

Experimental investigations to evaluate the influence of normal load and sliding velocity on the tribological attributes of human skin are reported in [24]. All the measurements were performed using a micro tribometer taking a polypropylene probe. Normal load and sliding velocity varied from 0.1 to 0.9 N and 0.5 to 4.5 mm/ sec respectively. It is reported that with the increase in sliding speed, both COF and stick-slip phenomena increase.

Static friction tests are performed using a bio tribometer to characterize the human skin's mechanical properties [86]. Bio tribometer operates on low contact loads of 0.5 to 2 kPa and a normal load of 54 to 100 mN. A steel indenter with a smooth surface finish is chosen to perform the experimental over the forearm. Displacements in the vertical (z) direction control the depth of indentation. Friction tests performed to study the mechanical properties of skin reported young's modulus and shear modulus as 8.5 ± 1.74 kPa and 3.3 ± 0.8 kPa.

An in-vivo experimental investigation was performed to examine the influence of epidermal hydration on the friction of human skin when tested for textiles [62]. Experiments were performed on the forearm with hospital fabric as a counter-surface material. All the friction measurements were performed on the tri-axial force plate and the normal load varied from 14.8 ± 1.3 N, whereas the considered sliding velocity taken was 140 mm/sec. Results show that the wet COF is twice that of the dry COF. Increased skin hydration increases the COF due to higher real contact area and adhesion at the interface.

A device is developed to investigate the friction between the curved surface and non-woven textiles [23]. Curved friction measurement was performed by pulling the material trough a cross head of a tensometer having a suspended weight to it. Repeatability for the curved measurements is good in comparison with straight friction measurements. The speed of the crosshead was set to 150 mm/sec. For the curved measurements, 45º of inclination was taken from the vertical plane. Results depicted a good correlation between the static COF for dry and overhydrated skin.

A study was conducted to evaluate the skin-textile friction and elasticity of skin across different age groups [21]. Normal load ranged between 11 to 19 N and the sliding velocity was maintained at 135 mm/sec to represent a real contact interface. Conclusions were drawn that

the deformation component of friction also affects the total friction force along with the adhesion component. Low elasticity in the elderly is attributed to tissue displacements due to the frictional forces at the interface.

Friction measurement is performed with low friction textiles to prevent pressure ulcers in bedridden patients [87]. Two standard bed sheets and a newly developed bed sheet were taken as samples for friction measurement. Samples were attached to the tri-axial force plate and the normal load was randomly varied in the range of 0.15 N to 10 N. Velocity varied in the range of 50 to 150 mm/ sec. Measurements were performed both for dry and wet conditions. Results show approximately 50 % higher friction values for the standard bedsheet over the newly developed prototype bedsheet.

Aimed at dermatological compositions, a frictional study is reported on the effect of facial scrub cleansers of different sizes, amounts, and hardness on human skin [22]. Hardness is measured through a hardness tester and frictional studies are performed with a biomedical micro tribometer. A normal load of 0.2 N was taken to replicate the real face cleansing process. Increased adhesion force and COF were reported in the study. Also, it is concluded that the scrub material properties greatly affect the tribological properties of the skin.

An experimental study presents how human skin friction is related to its hydration and temperature [46]. The same portable tribometer is used for the study as described in [19]. Four different materials like stainless steel, aluminum, polyethylene, and polytetrafluorethylene are taken as materials for the friction tests. Static and dynamic COF showed a linear relationship. Results highlighted no significant relationship between sliding velocity and COF. Both skin temperature and skin hydration are reported to affect the friction of human skin.

Prosthetic devices and their ergonomic development are a vital contribution of the scientific community to persons with permanent limb injuries or amputation. Frictional behaviour of human skin with materials popularly used in prosthetic development is investigated, through a sclerometer considering factors such as probe geometry, hair on the skin, sweat, skin moisture, indentation depth, interaction velocity, and pressure on the skin in [14]. Out of the seven considered parameters, only sweat and hairy skin are concluded as the significant factors from the obtained experimental results.

Experimental investigations to compare the friction and deformation behaviour of an artificial skin model (ASM) with e real forearm are performed in [115]. Four ASM and a human volar forearm were compared for indentation and friction measurements. Friction tests were

performed with stainless steel taking a normal load of 30 mN, speed of 0.5 mm/ sec having five cycles each. For human skin, COF was reported higher in the moist state, while for ASM higher COF is reported in the dry state. ASM showed good similarity for frictional and deformation behaviour when compared to human skin.

The influence of environmental temperature and relative humidity is investigated on the friction of human skin [18]. The setup consists of an enclosed chamber to control relative humidity and temperature. A heater 60 W heater controls the temperature with an accuracy of 0.2 ºC. The relative humidity is maintained between 40% to 20% with an accuracy of 3% by inserting dry air and through an ultrasonic humidifier. A woven cotton fabric attached to the probe is reciprocated over the forearm for measuring the COF. Statistical analysis performed on the obtained experimental results highlighted the product of temperature and relative humidity has a more pronounced effect on the COF.

The same setup as discussed in [18] is used to examine the static friction response as a function of surface energy and environmental conditions in [20]. Frictional measurements are performed with varying wettability. Materials with higher wettability have increased COF when tested under high temperatures and relative humidity. Shear strength at the interface can be computed through measure COF and the real area of contact.

A study developed an artificial skin material (ASM) and investigated its frictional interaction with wound dressings [116]. UMT-Tribolab was used for all the frictional measurements. ASM was developed in a ratio of 70:30 for polydimethylsiloxane (hydrophobic) and carboxyl chitosan (hydrophobic). Although, COF for the ASM was higher compared to that of the forearm when tested against the wound dressing but the decreasing trend was the same in both cases. The use of wound dressing is suggested for the prevention of decubitus generation.

An in-depth study is performed to correlate the underlying mechanisms of skin that relate to the variation in friction behaviour between the test subjects [117]. For the analysis of underlying properties, Fourier Transform Infrared Spectroscopy (FTIR) is performed over the same skin to perform the friction measurements. The normal load applied was 0.45 N and a sliding speed of 200 µm/ sec is taken for sliding the textile specimen with a forearm. Friction shows a linear correlation with skin moisture with an acceptable R^2 value of 0.61. Further, the study concludes that the amount of lipid on the skin is insignificant for the friction at the interface.

The role of hair and sweating on the skin-textile frictional characteristics of the forearm is studied in [16] through an experimental setup as shown in Figure 2.15. The Motorized translation stage moves the probe in the x direction to achieve the reciprocating motion. Force sensors measure the normal and the shear forces at the textile forearm interface. The study concluded that the larger hair coverage had higher dry friction for cotton and lower than for polyester and the increase in friction for the wet skin affects forearms with fewer hairs and is higher for cotton material.

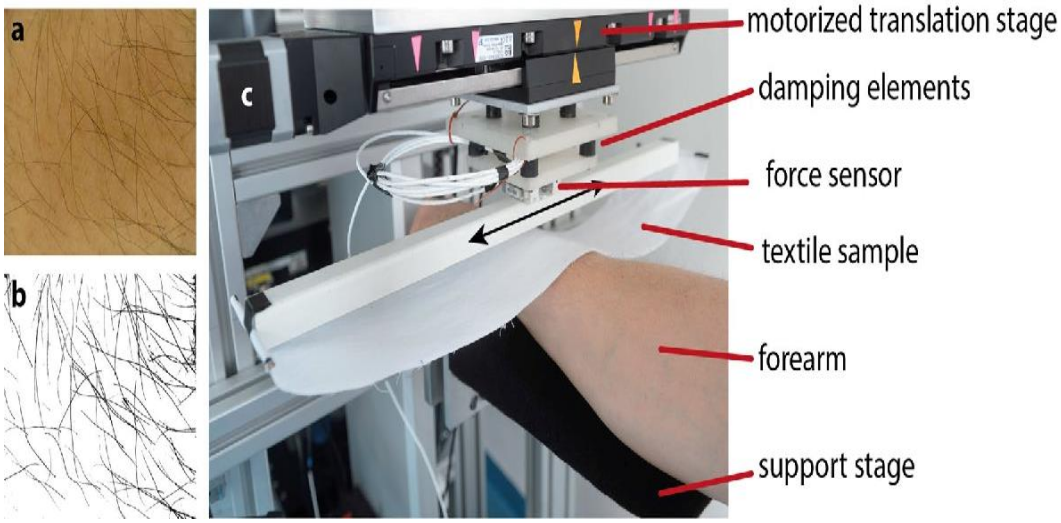

Figure 2.15 (a) Digital photograph of the contact area (b) Binary version of the photograph, the fraction of black pixels of 6.3% is taken as the hair coverage. (c) Experimental setup for the measurement of sliding friction between textiles and humans [16]

Table 2.14 Experimental studies of volar forearm human skin friction

Y	No. of subjects {Age}	Equipment	Variation with COF	Interacting Surface	Highlight	Ref
2003	30 F 29 M {-}	UMT Test setup	PVDC: ↑μ Petrolatum: ↑↑↑μ Glycerine : ↑↑↑μ	Copper cylindrical probe	The effect of Gender, ethnicity, and Age is negligible on the properties of skin	[41]
2005	15 C 15 F {-}	Acoustic Tribometer	Avg. sound level correlates with roughness and stiffness of the skin	Spherical probe	Acoustic emission is a technique to measure skin friction	[32]
2007	10 F {~30}	Skin Tribometer	↓ SC thickness: ↑μ, ↓ Stiffness	Spherical steel probe	SC does not represent the overall mechanical behavior of human skin.	[85]

Table 2.14 (continued...)

2007	1 M {-}	Tabor-Eldredge machine	Mean µ: PP>> Glass µ : Wet >>Dry	Plano-Convex glass lens, Hemispherical PP shell	Interfacial shear strength effects the frictional force	[61]
2008	4 {20-30}	UMT Micro Tribometer	↑ NL: ↑ µ ↑ SV: ↑ µ*	PP probe	Sliding velocity increases µ, deformation further increases hysteric friction.	[24]
2008	20 F {50-70}	Skin bio Tribometer	↑ NL, ↑ Age: ↓ Modulus	Spherical indentor	Dermis highly contributes to the visco-elastic characteristics of the skin	[86]
2008	11 M 11 F {23-40}	Corneometer, Cutometer, Triaxial quartz force plate	↑ SM: ↑ µ, ∅ Elasticity, Elasticity ∅ µ	Medical textile	Female skin showed greater effects of moisture	[62]
2008	5 F {18-44}	In-house developed device (using tensometer weights etc.)	COF: Hydrated> Dry	PP, Copolymer , (PP+ PE)	The device developed for both straight and curved surface friction measurement	[23]
2009	30 F 30 M {17-95}	Quartz force plate, Suction Probe,	Skin elasticity: Young>> Aged Hydration: Aged >> Young µ: Cotton>viscose>PTFE	Bamboo viscose, PTFE, 50 % Cotton, Polyester	The deformation component of friction and Shear force becomes an important parameter for old aged persons during frictional contact	[21]
2013	1 F 2 M {-}	Tri- axial Kistler force plate, CM 825 Corneometer, Xray Tomograph	µ: hb 1> hb 2 > hb 3 For dry and Wet across the subjects. Interfacial moisture and water transport: hb 1> hb 2 >hb 3	hb 1 (100% Cotton) hb 2 (50% cotton, 50% polyester) hb 3 (Synthetic fibre)	Adhesion plays a prominent role in friction mechanism of the investigated textiles.	[87]

Table 2.14 (continued...)

2013	16 F 34 M {Median 28}	Revolt ST mobile device, CM 825 Corneometer, Infrared thermometer	$\mu_{static} > \mu_{dynamic}$ for 3 different regions. $\mu_{dynamic}$: $\mu_{palmar} > \mu_{distal} > \mu_{volar}$ across the age of subjects	Al 6060 (R_a =0.45 µm)	The study has used large data set for predicting the various factors affecting human skin friction	[19]
2013	10 F 10 M {22-28}	UMT-II Micro-Tribometer, OM, SEM, video contact angle instrument	old SC Removal: ↑Hydration ↑ Adhesion force,↑ µ ↓ Ra, ↓ S Con.	Silicon Rubber	The effect of facial cleanser was analyzed at 3 locations	[22]
2013	9 F 22 M {23-56}	Revolt ST, CM 825 Corneometer,	μ_{static} and $\mu_{dynamic}$ are highly correlated µ: SST >Al > PE > PTFE	SST Al PE PTFE	$\mu_{male} < \mu_{female}$ due to higher skin hydration in females	[46]
2015	-	Instrumented Sclerometer setup	↓Sweat, ↓hair: μ_{max} ↑Sweat, ↓hair: μ_{min}	PP	Considered 7 factors that majorly affect friction at the interface of prosthetic devices	[14]
2016	1 F {29}	CETR-UMT Tribometer	µ (dry/wet): HS >> ASM	Steel ball	ASM is developed by having stiffer upper layers and soft lower layers.	[115]
2016	1 M {27}	Enclosure, reciprocating tribometer consisting of a multi-axis force transducer, confocal microscopy	↑ Humidity, Temp: ↑ static µ	Cotton fabric	Influence RH and temp on human skin friction	[18]
2017	1 M {28}	Corneometer, Enclosure, reciprocating tribometer	↑ Temp, RH: ↑Friction force	Glass, Silicon Nitride, Chrome steel, PTFE	Effect of surface energy and environment on friction force	[20]

Table 2.14 (continued...)

2019	10 F 9 M {16-38}	UST 100 series, Corneometer Derma unit SSC3, UMT- Tribo lab	ASM Developed its tribological analysis with 7 types of wound dressings	Nylon Probe	Usage of wound dressing decreases μ up to 50%	[116]
2020	15 {20-35}	FTIR Spectrometer, 6 axis transducers	↑Moisture of SC: ↑ μ	Polyester	Skin lipid attributes and friction are highly correlated	[117]
2020	15 {23-30}	SEM, 3-Axis force sensor	μ: Cotton >Polyester (dry/wet)	Cotton Polyester	Experimentation for the effect of hair and sweating on textile friction	[16]

ASM- Artificial skin material
Al- Aluminium
HS- Human skin
FTIR- Fourier-transform infrared spectroscopy
hb- Hospital Bedsheet
NL- Normal Load
PE - Polyethylene
PP- Polypropylene
PTFE- Polytetrafluoro ethylene
PVDC- Polyvinyliden e chloride
Ra- Surface Roughness
RH- Relative Humidity
SC- Stratum Corneum
S Con. –Skin Conductance
SEM- Scanning electron microscope
SM- Skin moisture
SV- Sliding Velocity
SST- Stainless steel
μ-COF
∅- Does not affect

2.3.4 Other regions

Skin is highly diverse in structure throughout the body. Various researchers have used different anatomical locations as per application needs, ease, and efficient measurements. Popular skin sites have already been discussed in the former part of the section. Other regions that are highly popular amongst researchers are the back, knee, scar, face, forehead, and calf. Researchers have investigated these anatomical regions for experimental investigations as per their application needs. Table 2.15 summarizes the studies done on these anatomical regions. A comparative investigation of the tribological behaviour of a polyethylene ball (a prosthetic socket material) with scar skin, healthy skin, and prosthetic skin is performed in [118]. All the experiments were performed on a reciprocating UMT-II micro tribometer with a normal force at 0.1, 0.7, and 0.8 N respectively. COF for all the measurements decreased with the increasing value of the normal load. Maximum COF reported is for the scarred skin followed by the highest fluctuations in the measurements. Most tolerant of the comfortless sensations is the skin wearing the prosthetic socket.

For persons with amputation use of prosthetics is a great need for their efficient day-to-day life. Prosthetics cause a sense of discomfort with the residual limb on which it is mounted. To overcome this use of socks in prosthetic devices is recommended. An in vivo friction study between the four popular prosthetic socks materials namely nylon, wool, cotton, and silk with the residual limb skin is conducted in [119]. Each fabric was cut into a specific dimension and wrapped in an acrylic probe. Five sites of 4 cm^2 were selected as test sites on the skin taken as a flat sample with a normal load of 2 N equivalent to the 39.8 kPa pressure. The study concluded that the fabric surface features and material composition affected the frictional behaviour at the interface. While sliding COF for nylon and wool socks was higher due to the coarse surface finish compared to that for cotton and silk which had fewer irritations.

A portable multi-component-based sensor is developed to investigate the friction and the tactile perception of human skin with textiles [70]. Two knitted and three plain fabrics were taken as test samples. The site of the investigation was the ventral forearm and the palmar region. Normal load varied between 0 to 1 N and sliding velocity of about 35 ± 10mm /sec for the experimentation. Friction test results for the palm were gender sensitive males had twice the COF that for the female. Wool reported the highest COF, irrespective of gender and site of friction test. Friction results and tactile perception showed a high positive correlation.

Friction measurements to evaluate the effect of pressure distributions on the human skin were performed in [100]. As discussed for the fingerpad, a similar trend of decreasing COF was observed for the knuckle replicating the thin layer over a bonny surface having sharp peaks. All the measurements were performed through a pressure-sensitive film attached to the force plate to measure the normal and the shear forces. Pressure distributions had a below 10% effect on the COF and thereby reductions in the friction value are attributed to the skin hydration or the differences in the finger positions while measurements.

The anatomical region carries the least importance while sweat significantly affects the value of COF in [15] at the interface. Figure 2.16 represents a recent work that measures the COF on trans-femoral amputees. This study uses a portable tribometer that due to its versatility, can operate on the volar forearm and other three regions of the transfemoral residual limb. The device has its axis of rotation perpendicular to the site of friction measurement.

Figure 2.16 Handheld tribometer used for the measurement of COF at the residual limb [15]

Table 2.15 Experimental study of human skin friction on the calf, scar, residual limb, etc.

Y	No. of subjects {Age}	Equipment	Variation with COF	Interacting Surface	Highlight	Ref
2005	15 C 15 F {-}	Acoustic tribometer	Avg. sound level correlates with roughness and stiffness of the skin	Spherical probe	Acoustic emission is a technique to measure skin friction	[32]
2008	8 F {24-53}	UMT-II multi specimen Micro-Tribometer	μ: Prosthetic ~ Healthy skin. Scar/ healthy skins are more sensitive than Prosthetic skins.	PE: Residual limb scar skin, Prosthetic skin, Healthy skin (in vivo)	The comfort of 3 different kinds of is skins investigated	[118]
2011	5 F 5 M {24-53}	UMT series multi-specimen Biomedical Micro-Tribometer	↓ Coarse fabric: ↑ Comfort sensation	Cotton, Nylon, Silk, Wool	The effect of fabric weave parameters, surface features, and material composition on tribological behaviour is studied	[119]

Table 2.15 (continued...)

2012	7 F 12 M {21-57}	An in-house developed device with two cantilever load cells	μ_{wool} is the highest. Palm region: $\mu_{female} < \mu_{male}$	PA, PE, silk, wool, cotton	The friction of the Palmar portion of human skin is measured	[70]
2013	2 F 1 M {-}	Force Plate	The effect of Pressure distribution on μ is analyzed.	Smooth pressure-sensitive film	COF of Knuckle portion is investigated	[100]
2020	7 F 15 M {21-88}	Handheld tribometer	Sweat at the interface is a significant attribute for μ	Scar skin: Socket internal surface, PP	COF measurements of transfemoral amputees.	[15]

PA- Polyamide PP- Polypropylene μ-COF
PE- Polyethylene

2.4 Gaps in the Existing Literature

Following crisp research gaps are identified based on the literature survey:

- **Research trends:** Lack of structured trends and growth in the research domain.
- **Lack of an engineering-based design framework:** All the attempts to develop the friction measurement device were based on the application, range of controllable attributes, and the counter material used without considering their relative importance in the measurement framework.
- **Raw material selection:** Test samples in all the investigations were randomly taken without the user-based selections.
- **Design constraints:** Need for low maintenance, cost-efficient, and a handy friction measurement device based on parallel rotary movement having repeatability, calibration, and reliability.
- **Test environment and subjects:** Lack of an attempt on the Indian population as test subjects and climatic conditions. No comparative studies on the same set of subjects for rotary and sliding friction measurements were reported.
- **Predictive model and its optimization:** Very few studies presented a predictive model for the determination of COF at finger pad with counter material and no study could be traced for the optimization of the same.

Based on the discussed literature gaps, the following objectives have been aimed in the current research:

1. An extensive literature survey based on the bibliometric methodology and PRISMA technique is addressed in Chapter 2.
2. The design and development of the tribometer for finger pad friction measurement are addressed in chapter 3.
3. Experimental investigation of finger pad frictional behaviour of human skin addressed in chapter 4.
4. Predictive model development for the COF at the material and finger pad contact interface and its optimization is addressed in chapter 5.

2.5 Organization of Thesis

The thesis is subdivided into 6 chapters. Chapter 1 introduction: presents the overall introduction on skin tribology, anatomy of human skin and finger pad, followed by skin friction mechanisms and its measurement techniques. Chapter 2 presents an extensive literature survey post-year 2000 and classifies the highly cited experimental investigations performed for the in-vivo human skin friction measurements based on popular sites of tribological investigation on the human body. Chapter 3 conducts a response-based survey for the selection of test materials across six geographical divisions of India considering the environmental effects on the tribological aspects of human skin. A parallel rotary type tribometer is developed to measure the human skin friction and validation of equipment is performed through gage repeatability and reproducibility tests (R&R) tests. Followed by the development of a sliding type tribometer. Chapter 4 reports the experimental investigations and their analysis with textile, rubber, and metal probes are performed. Experimental measurements of finger pad friction were performed through a reciprocating tribometer through a multi-axis dynamometer in contact with seven different samples including 5 metals, 1 wood, and 1 acrylic test sample. Chapter 5 presents predictive modeling COF for the finger pad and steel probe is reported using response surface methodology (RSM) and artificial neural network (ANN) technique. Finally, optimization is performed through RSM to minimize COF to get the optimal values of input parameters. Chapter 6 presents the summary of the conclusions and future scope of the present study.

2.5 Summary

1. A literature review is conducted in the domain of human skin tribology. Section 2.2 presents a bibliometric study performed over the research domain of human skin tribology. Two widely popular databases are used for the selection of articles through specialized keywords. Further, this presents a detailed citation analysis, co-citation analysis, collaboration between prominent authors and countries, and the most influential authors.
2. In section 2.3 a systematic literature review is conducted through preferred reporting items for systematic reviews and meta-analyses (PRISMA) technique for the in vivo experimental studies and classified the experimental studies based on the sites of tribological investigation of human skin.
3. Section 2.4 lists out the research gaps identified from the literature and based on those, the proposed objectives are defined for the current research that is addressed in chapters 3, chapter 4, and chapter 5.

References:

[1] P. Humbert, F. Ferial, P. Agache, and H. I. Maibach, *Agache ' s Measuring the Skin*. 2004.

[2] H. Joodaki and M. B. Panzer, "Skin mechanical properties and modeling: A review," *Proc. Inst. Mech. Eng. Part H J. Eng. Med.*, vol. 232, no. 4, pp. 323–343, 2018, doi: 10.1177/0954411918759801.

[3] Z. R. Zhou and Z. M. Jin, "Biotribology: Recent progresses and future perspectives," *Biosurface and Biotribology*, vol. 1, no. 1, pp. 3–24, 2015, doi: 10.1016/j.bsbt.2015.03.001.

[4] W. Maurel, Y. Wu, and N. M. Thalmann, *Biomechanical Models for Soft Tissue Simulation ESPRIT Basic Research Series*, vol. 15, no. 4. 1998.

[5] D. Robertson and D. Cook, "Unrealistic statistics: How average constitutive coefficients can produce non-physical results," *J. Mech. Behav. Biomed. Mater.*, vol. 40, pp. 234–239, 2014, doi: 10.1016/j.jmbbm.2014.09.006.

[6] R. G. Shah, D. DeVore, and F. H. Silver, "Biomechanical analysis of decellularized dermis and skin: Initial in vivo observations using optical cohesion tomography and vibrational analysis," *J. Biomed. Mater. Res. - Part A*, vol. 106, no. 5, pp. 1421–1427, 2018, doi: 10.1002/jbm.a.36344.

[7] W. Tang, S. Liu, H. Zhu, and S. Ge, "Microtribological and micromechanical properties of the skin stratum corneum," *Proc. Inst. Mech. Eng. Part J J. Eng. Tribol.*, vol. 226, no. 10, pp. 880–886, 2012, doi: 10.1177/1350650112450395.

[8] C. Pailler-Mattéi and H. Zahouani, "Study of adhesion forces and mechanical properties of human skin in vivo," *J. Adhes. Sci. Technol.*, vol. 18, no. 15–16, pp. 1739–1758, 2004, doi: 10.1163/1568561042708368.

[9] C. Pailler-Mattéi and H. Zahouani, "Analysis of adhesive behaviour of human skin in vivo by an indentation test," *Tribol. Int.*, vol. 39, no. 1, pp. 12–21, 2006, doi: 10.1016/j.triboint.2004.11.003.

[10] J. Jachowicz, R. Mcmullen, and D. Prettypaul, "Indentometric analysis of in vivo skin and comparison with artificial skin models," *Ski. Res. Technol.*, vol. 13, no. 3, pp. 299–309, 2007, doi: 10.1111/j.1600-0846.2007.00229.x.

[11] L. J. A. Isaza, D. Lacroix, and J. Ramírez, "Influence of indentation test factors on the mechanical response of the skin," *Univ. Sci.*, vol. 24, no. 1, pp. 49–72, 2019, doi: 10.11144/JAVERIANA.SC24-1.IOIT.

[12] A. Delalleau, G. Josse, J. M. Lagarde, H. Zahouani, and J. M. Bergheau, “A nonlinear elastic behavior to identify the mechanical parameters of human skin in vivo,” *Ski. Res. Technol.*, vol. 14, no. 2, pp. 152–164, 2008, doi: 10.1111/j.1600-0846.2007.00269.x.

[13] C. Li, G. Guan, R. Reif, Z. Huang, and R. K. Wang, “Determining elastic properties of skin by measuring surface waves from an impulse mechanical stimulus using phase-sensitive optical coherence tomography,” *J. R. Soc. Interface*, vol. 9, no. 70, pp. 831–841, 2012, doi: 10.1098/rsif.2011.0583.

[14] J. F. Ramírez, J. J. Pavón, and A. Toro, “Experimental assessment of friction coefficient between polypropylene and human skin using instrumented sclerometer,” *Proc. Inst. Mech. Eng. Part J J. Eng. Tribol.*, vol. 229, no. 3, pp. 259–265, 2015, doi: 10.1177/1350650114526579.

[15] S. C. Henao, S. Cuartas-Escobar, and J. Ramírez, “Coefficient of Friction Measurements on Transfemoral Amputees,” *Biotribology*, vol. 22, no. November 2019, p. 100126, 2020, doi: 10.1016/j.biotri.2020.100126.

[16] J. Lyu, N. Özgün, D. J. Kondziela, and R. Bennewitz, “Role of Hair Coverage and Sweating for Textile Friction on the Forearm,” *Tribol. Lett.*, vol. 68, no. 4, pp. 1–9, 2020, doi: 10.1007/s11249-020-01341-6.

[17] C. Pailler-Mattei, S. Nicoli, F. Pirot, R. Vargiolu, and H. Zahouani, “A new approach to describe the skin surface physical properties in vivo,” *Colloids Surfaces B Biointerfaces*, vol. 68, no. 2, pp. 200–206, Feb. 2009, doi: 10.1016/j.colsurfb.2008.10.005.

[18] M. Klaassen, D. J. Schipper, and M. A. Masen, “Influence of the relative humidity and the temperature on the in-vivo friction behaviour of human skin,” *Biotribology*, vol. 6, pp. 21–28, 2016, doi: 10.1016/j.biotri.2016.03.003.

[19] N. K. Veijgen, M. A. Masen, and E. van der Heide, “Variables influencing the frictional behaviour of in vivo human skin,” *J. Mech. Behav. Biomed. Mater.*, vol. 28, pp. 448–461, 2013, doi: 10.1016/j.jmbbm.2013.02.009.

[20] M. Klaassen, E. G. de Vries, and M. A. Masen, “The static friction response of non-glabrous skin as a function of surface energy and environmental conditions,” *Biotribology*, vol. 11, no. May, pp. 124–131, 2017, doi: 10.1016/j.biotri.2017.05.004.

[21] L. C. Gerhardt, A. Lenz, N. D. Spencer, T. Münzer, and S. Derler, “Skin-textile friction and skin elasticity in young and aged persons,” *Ski. Res. Technol.*, vol. 15, no. 3, pp. 288–298, 2009, doi: 10.1111/j.1600-0846.2009.00363.x.

[22] W. Li, Z. H. Zhai, Q. Pang, L. Kong, and Z. R. Zhou, “Influence of exfoliating facial cleanser on the bio-tribological properties of human skin,” *Wear*, vol. 301, no. 1–2, pp.

353–361, 2013, doi: 10.1016/j.wear.2012.11.073.

[23] A. M. Cottenden, W. K. Wong, D. J. Cottenden, and A. Farbrot, “Development and validation of a new method for measuring friction between skin and nonwoven materials,” *Proc. Inst. Mech. Eng. Part H J. Eng. Med.*, vol. 222, no. 5, pp. 791–803, 2008, doi: 10.1243/09544119JEIM313.

[24] W. Tang, S. rong Ge, H. Zhu, X. chuan Cao, and N. Li, “The Influence of Normal Load and Sliding Speed on Frictional Properties of Skin,” *J. Bionic Eng.*, vol. 5, no. 1, pp. 33–38, 2008, doi: 10.1016/S1672-6529(08)60004-9.

[25] C. Fortes, D. Version, and C. Fortes, “Finger pad friction and tactile perception of laser treated , stamped and cold rolled micro-structured stainless steel sheet surfaces,” 2017, doi: 10.1007/s40544-017-0147-9.

[26] M. A. Masen, “A systems based experimental approach to tactile friction,” *J. Mech. Behav. Biomed. Mater.*, vol. 4, no. 8, pp. 1620–1626, 2011, doi: 10.1016/j.jmbbm.2011.04.007.

[27] D. A. Sergachev, D. T. A. A. Matthews, and E. van der Heide, “An Empirical Approach for the Determination of Skin Elasticity: Finger pad Friction against Textured Surfaces,” *Biotribology*, vol. 18, no. April, p. 100097, 2019, doi: 10.1016/j.biotri.2019.100097.

[28] S. Derler and G. M. Rotaru, “Stick-slip phenomena in the friction of human skin,” *Wear*, vol. 301, no. 1–2, pp. 324–329, 2013, doi: 10.1016/j.wear.2012.11.030.

[29] W. Ben Messaoud, M. A. Bueno, and B. Lemaire-Semail, “Relation between human perceived friction and finger friction characteristics,” *Tribol. Int.*, vol. 98, pp. 261–269, 2016, doi: 10.1016/j.triboint.2016.02.031.

[30] X. Zhou *et al.*, “Correlation between tactile perception and tribological and dynamical properties for human finger under different sliding speeds,” *Tribol. Int.*, vol. 123, no. March, pp. 286–295, 2018, doi: 10.1016/j.triboint.2018.03.012.

[31] L. Skedung *et al.*, “Tactile perception: Finger friction, surface roughness and perceived coarseness,” *Tribol. Int.*, vol. 44, no. 5, pp. 505–512, 2011, doi: 10.1016/j.triboint.2010.04.010.

[32] H. Zahouani, F. Flament, R. Vargiolu, A. L. E. Bot, and A. Mavon, “Acoustic tribology of human skin,” in *Proceedings of the World Tribology Congress III - 2005*, 2005, pp. 699–700, doi: 10.1115/wtc2005-64216.

[33] J. Van Kuilenburg, M. A. Masen, M. N. W. Groenendijk, V. Bana, and E. Van Der Heide, “An experimental study on the relation between surface texture and tactile friction,” *Tribol. Int.*, vol. 48, pp. 15–21, 2012, doi: 10.1016/j.triboint.2011.06.003.

[34] L. M. Vilhena and A. Ramalho, “Friction Behavior of Human Skin Rubbing against Different Textured Polymeric Materials Obtained by a 3D Printing Microfabrication Technique,” *Tribol. Trans.*, vol. 62, no. 2, pp. 324–336, 2019, doi: 10.1080/10402004.2018.1543782.

[35] G. P. Chimata and C. J. Schwartz, “Tactile Discrimination of Randomly Textured Surfaces: Effect of Friction and Surface Parameters,” *Biotribology*, vol. 11, no. October 2016, pp. 102–109, 2017, doi: 10.1016/j.biotri.2017.01.004.

[36] S. Derler, L. C. Gerhardt, A. Lenz, E. Bertaux, and M. Hadad, “Friction of human skin against smooth and rough glass as a function of the contact pressure,” *Tribol. Int.*, vol. 42, no. 11–12, pp. 1565–1574, 2009, doi: 10.1016/j.triboint.2008.11.009.

[37] M. Zhang and A. F. T. Mak, “In vivo friction properties of human skin,” *Prosthet. Orthot. Int.*, vol. 23, no. 2, pp. 135–141, 1999, doi: 10.3109/03093649909071625.

[38] Y. H. Zhu, S. P. Song, W. Luo, P. M. Elias, and M. Q. Man, “Characterization of skin friction coefficient, and relationship to stratum corneum hydration in a normal chinese population,” *Skin Pharmacol. Physiol.*, vol. 24, no. 2, pp. 81–86, 2011, doi: 10.1159/000321993.

[39] A. B. Cua, K. P. Wilhelm, and H. I. Maibach, “Skin surface lipid and skin friction: relation to age, sex and anatomical region.,” *Skin Pharmacol.*, vol. 8, no. 5, pp. 246–251, 1995, doi: 10.1159/000211354.

[40] A. Abdouni, M. Djaghloul, C. Thieulin, R. Vargiolu, C. Pailler-Mattei, and H. Zahouani, “Biophysical properties of the human finger for touch comprehension: Influences of ageing and gender,” *R. Soc. Open Sci.*, vol. 4, no. 8, 2017, doi: 10.1098/rsos.170321.

[41] R. K. Sivamani, G. C. Wu, N. V. Gitis, and H. I. Maibach, “Tribological testing of skin products: Gender, age, and ethnicity on the volar forearm,” *Ski. Res. Technol.*, vol. 9, no. 4, pp. 299–305, Nov. 2003, doi: 10.1034/j.1600-0846.2003.00034.x.

[42] M. Egawa, M. Oguri, T. Hirao, M. Takahashi, and M. Miyakawa, “The evaluation of skin friction using a frictional feel analyzer,” *Ski. Res. Technol.*, vol. 8, no. 1, pp. 41–51, Feb. 2002, doi: 10.1034/j.1600-0846.2002.080107.x.

[43] A. B. Cua, K. P. Wilhelm, and H. I. Maibach, “Elastic properties of human skin: relation to age, sex, and anatomical region,” *Arch. Dermatol. Res.*, vol. 282, no. 5, pp. 283–288, 1990, doi: 10.1007/BF00375720.

[44] M. S. Kim, I. Y. Kim, Y. K. Park, and Y. Z. Lee, “The friction measurement between finger skin and material surfaces,” *Wear*, vol. 301, no. 1–2, pp. 338–342, 2013, doi: 10.1016/j.wear.2012.12.036.

[45] G. P. Chimata and C. J. Schwartz, “Investigation of the Role of Diminishing Surface Area on Friction-Based Tactile Discrimination of Textures,” *Biotribology*, vol. 15, no. June, pp. 1–8, 2018, doi: 10.1016/j.biotri.2018.07.001.

[46] N. K. Veijgen, M. A. Masen, and E. Van Der Heide, “Relating friction on the human skin to the hydration and temperature of the skin,” *Tribol. Lett.*, vol. 49, no. 1, pp. 251–262, 2013, doi: 10.1007/s11249-012-0062-1.

[47] C. P. Hendriks and S. E. Franklin, “Influence of surface roughness, material and climate conditions on the friction of human skin,” *Tribol. Lett.*, vol. 37, no. 2, pp. 361–373, 2010, doi: 10.1007/s11249-009-9530-7.

[48] S. Derler and L. C. Gerhardt, “Tribology of skin: Review and analysis of experimental results for the friction coefficient of human skin,” *Tribol. Lett.*, vol. 45, no. 1, pp. 1–27, 2012, doi: 10.1007/s11249-011-9854-y.

[49] N. Gitis and R. Sivamani, “Tribometrology of skin,” *Tribol. Trans.*, vol. 47, no. 4, pp. 461–469, 2004, doi: 10.1080/05698190490493355.

[50] A. K. Dabrowska *et al.*, “Materials used to simulate physical properties of human skin,” *Ski. Res. Technol.*, vol. 22, no. 1, pp. 3–14, 2016, doi: 10.1111/srt.12235.

[51] S. Zhang *et al.*, “Selection of micro-fabrication techniques on stainless steel sheet for skin friction,” *Friction*, vol. 4, no. 2, pp. 89–104, 2016, doi: 10.1007/s40544-016-0115-9.

[52] A. I. Vakis *et al.*, “Modeling and simulation in tribology across scales: An overview,” *Tribol. Int.*, vol. 125, no. February, pp. 169–199, 2018, doi: 10.1016/j.triboint.2018.02.005.

[53] Y. Meng, J. Xu, Z. Jin, B. Prakash, and Y. Hu, *A review of recent advances in tribology*, vol. 8, no. 2. 2020.

[54] Y. Wei and Z. Jiang, “The evolution and future of diabetic kidney disease research: a bibliometric analysis,” *BMC Nephrol.*, vol. 22, no. 1, pp. 1–16, 2021, doi: 10.1186/s12882-021-02369-z.

[55] Z. Xu, X. Wang, X. Wang, and M. Skare, “A comprehensive bibliometric analysis of entrepreneurship and crisis literature published from 1984 to 2020,” *J. Bus. Res.*, vol. 135, pp. 304–318, 2021, doi: https://doi.org/10.1016/j.jbusres.2021.06.051.

[56] F. H. Liu, C. H. Yu, and Y. C. Chang, “Bibliometric analysis of articles published in journal of dental sciences from 2009 to 2020,” *J. Dent. Sci.*, no. xxxx, 2021, doi: 10.1016/j.jds.2021.08.002.

[57] H. Kim and K. K. F. So, “Two decades of customer experience research in hospitality

and tourism: A bibliometric analysis and thematic content analysis," *Int. J. Hosp. Manag.*, vol. 100, no. July 2021, p. 103082, 2022, doi: 10.1016/j.ijhm.2021.103082.

[58] Y. Bhatt, K. Ghuman, and A. Dhir, "Sustainable manufacturing. Bibliometrics and content analysis," *J. Clean. Prod.*, vol. 260, p. 120988, 2020, doi: 10.1016/j.jclepro.2020.120988.

[59] M. Aria and C. Cuccurullo, "bibliometrix: An R-tool for comprehensive science mapping analysis," *J. Informetr.*, vol. 11, no. 4, pp. 959–975, 2017, doi: 10.1016/j.joi.2017.08.007.

[60] V. D. Blondel, J. L. Guillaume, R. Lambiotte, and E. Lefebvre, "Fast unfolding of communities in large networks," *J. Stat. Mech. Theory Exp.*, vol. 2008, no. 10, 2008, doi: 10.1088/1742-5468/2008/10/P10008.

[61] M. J. Adams, B. J. Briscoe, and S. A. Johnson, "Friction and lubrication of human skin," *Tribol. Lett.*, vol. 26, no. 3, pp. 239–253, 2007, doi: 10.1007/s11249-007-9206-0.

[62] L. C. Gerhardt, V. Strässle, A. Lenz, N. D. Spencer, and S. Derler, "Influence of epidermal hydration on the friction of human skin against textiles," *J. R. Soc. Interface*, vol. 5, no. 28, pp. 1317–1328, 2008, doi: 10.1098/rsif.2008.0034.

[63] S. Derler, U. Schrade, and L. C. Gerhardt, "Tribology of human skin and mechanical skin equivalents in contact with textiles," *Wear*, vol. 263, no. 7-12 SPEC. ISS., pp. 1112–1116, 2007, doi: 10.1016/j.wear.2006.11.031.

[64] L. Skedung, M. Arvidsson, J. Y. Chung, C. M. Stafford, B. Berglund, and M. W. Rutland, "Feeling small: Exploring the tactile perception limits," *Sci. Rep.*, vol. 3, 2013, doi: 10.1038/srep02617.

[65] R. K. Sivamani, J. Goodman, N. V. Gitis, and H. I. Maibach, "Friction coefficient of skin in real-time," *Ski. Res. Technol.*, vol. 9, no. 3, pp. 235–239, 2003, doi: 10.1034/j.1600-0846.2003.20361.x.

[66] S. E. Tomlinson, R. Lewis, X. Liu, C. Texier, and M. J. Carré, "Understanding the friction mechanisms between the human finger and flat contacting surfaces in moist conditions," *Tribol. Lett.*, vol. 41, no. 1, pp. 283–294, 2011, doi: 10.1007/s11249-010-9709-y.

[67] S. M. Pasumarty, S. A. Johnson, S. A. Watson, and M. J. Adams, "Friction of the human finger pad: Influence of moisture, occlusion and velocity," *Tribol. Lett.*, vol. 44, no. 2, pp. 117–137, 2011, doi: 10.1007/s11249-011-9828-0.

[68] X. Guo, Y. Huang, X. Cai, C. Liu, and P. Liu, "Capacitive wearable tactile sensor based on smart textile substrate with carbon black /silicone rubber composite dielectric," *Meas.*

Sci. Technol., vol. 27, no. 4, 2016, doi: 10.1088/0957-0233/27/4/045105.

[69] L. C. Gerhardt, N. Mattle, G. U. Schrade, N. D. Spencer, and S. Derler, "Study of skin-fabric interactions of relevance to decubitus: Friction and contact-pressure measurements," *Ski. Res. Technol.*, vol. 14, no. 1, pp. 77–88, 2008, doi: 10.1111/j.1600-0846.2007.00264.x.

[70] A. Ramalho, P. Szekeres, and E. Fernandes, "Friction and tactile perception of textile fabrics," *Tribol. Int.*, vol. 63, pp. 29–33, 2013, doi: 10.1016/j.triboint.2012.08.018.

[71] R. A. Berthé, G. Westhoff, H. Bleckmann, and S. N. Gorb, "Surface structure and frictional properties of the skin of the Amazon tree boa Corallus hortulanus (Squamata, Boidae)," *J. Comp. Physiol. A Neuroethol. Sensory, Neural, Behav. Physiol.*, vol. 195, no. 3, pp. 311–318, 2009, doi: 10.1007/s00359-008-0408-1.

[72] L. Skedung *et al.*, "Finger friction measurements on coated and uncoated printing papers," *Tribol. Lett.*, vol. 37, no. 2, pp. 389–399, 2010, doi: 10.1007/s11249-009-9538-z.

[73] R. Fagiani, F. Massi, E. Chatelet, J. P. Costes, and Y. Berthier, "Contact of a finger on rigid surfaces and textiles: Friction coefficient and induced vibrations," *Tribol. Lett.*, vol. 48, no. 2, pp. 145–158, 2012, doi: 10.1007/s11249-012-0010-0.

[74] T. André, V. Lévesque, V. Hayward, P. Lefèvre, and J. L. Thonnard, "Effect of skin hydration on the dynamics of fingertip gripping contact," *Journal of the Royal Society Interface*, vol. 8, no. 64. pp. 1574–1583, 2011, doi: 10.1098/rsif.2011.0086.

[75] I. M. Koç and C. Aksu, "Tactile sensing of constructional differences in fabrics with a polymeric finger tip," *Tribol. Int.*, vol. 59, pp. 339–349, 2013, doi: 10.1016/j.triboint.2012.04.021.

[76] E. D. Bonnevie, V. J. Baro, L. Wang, and D. L. Burris, "In situ studies of cartilage microtribology: Roles of speed and contact area," *Tribol. Lett.*, vol. 41, no. 1, pp. 83–95, 2011, doi: 10.1007/s11249-010-9687-0.

[77] P. H. Cornuault, L. Carpentier, M. A. Bueno, J. M. Cote, and G. Monteil, "Influence of physico-chemical, mechanical and morphological finger pad properties on the frictional distinction of sticky/ slippery surfaces," *Journal of the Royal Society Interface*, vol. 12, no. 110. 2015, doi: 10.1098/rsif.2015.0495.

[78] J. M. Coles, J. J. Blum, G. D. Jay, E. M. Darling, F. Guilak, and S. Zauscher, "In situ friction measurement on murine cartilage by atomic force microscopy," *J. Biomech.*, vol. 41, no. 3, pp. 541–548, 2008, doi: 10.1016/j.jbiomech.2007.10.013.

[79] X. Liu, Z. Yue, Z. Cai, D. G. Chetwynd, and S. T. Smith, "Quantifying touch-feel

perception: Tribological aspects," *Meas. Sci. Technol.*, vol. 19, no. 8, 2008, doi: 10.1088/0957-0233/19/8/084007.

[80] T. H. C. Childs and B. Henson, "Human tactile perception of screen-printed surfaces: Self-report and contact mechanics experiments," *Proc. Inst. Mech. Eng. Part J J. Eng. Tribol.*, vol. 221, no. 3, pp. 427–441, 2007, doi: 10.1243/13506501JET217.

[81] M. A. Darden and C. J. Schwartz, "Investigation of skin tribology and its effects on the tactile attributes of polymer fabrics," *Wear*, vol. 267, no. 5–8, pp. 1289–1294, 2009, doi: 10.1016/j.wear.2008.12.041.

[82] J. Van Kuilenburg, M. A. Masen, and E. Van Der Heide, "Contact modelling of human skin: What value to use for the modulus of elasticity?," *Proc. Inst. Mech. Eng. Part J J. Eng. Tribol.*, vol. 227, no. 4, pp. 349–361, 2013, doi: 10.1177/1350650112463307.

[83] S. Derler, R. Huber, H. P. Feuz, and M. Hadad, "Influence of surface microstructure on the sliding friction of plantar skin against hard substrates," *Wear*, vol. 267, no. 5–8, pp. 1281–1288, 2009, doi: 10.1016/j.wear.2008.12.053.

[84] O. S. Dinç, C. M. Ettles, S. J. Calabrese, and H. A. Scarton, "Some parameters affecting tactile friction," *J. Tribol.*, vol. 113, no. 3, pp. 512–517, 1991, doi: 10.1115/1.2920653.

[85] C. Pailler-Mattei, S. Pavan, R. Vargiolu, F. Pirot, F. Falson, and H. Zahouani, "Contribution of stratum corneum in determining bio-tribological properties of the human skin," *Wear*, vol. 263, no. 7-12 SPEC. ISS., pp. 1038–1043, 2007, doi: 10.1016/j.wear.2007.01.128.

[86] H. Zahouani, C. Pailler-Mattei, B. Sohm, R. Vargiolu, V. Cenizo, and R. Debret, "Characterization of the mechanical properties of a dermal equivalent compared with human skin in vivo by indentation and static friction tests," *Ski. Res. Technol.*, vol. 15, no. 1, pp. 68–76, 2009, doi: 10.1111/j.1600-0846.2008.00329.x.

[87] G. M. Rotaru *et al.*, "Friction between human skin and medical textiles for decubitus prevention," in *Tribology International*, 2013, vol. 65, pp. 91–96, doi: 10.1016/j.triboint.2013.02.005.

[88] A. Abdouni, R. Vargiolu, and H. Zahouani, "Impact of finger biophysical properties on touch gestures and tactile perception: Aging and gender effects," *Sci. Rep.*, vol. 8, no. 1, pp. 1–13, 2018, doi: 10.1038/s41598-018-30677-2.

[89] M. G. Gee, P. Tomlins, A. Calver, R. H. Darling, and M. Rides, "A new friction measurement system for the frictional component of touch," *Wear*, vol. 259, no. 7–12, pp. 1437–1442, 2005, doi: 10.1016/j.wear.2005.02.053.

[90] S. E. Tomlinson, R. Lewis, and M. J. Carré, "The effect of normal force and roughness

on friction in human finger contact," *Wear*, vol. 267, no. 5–8, pp. 1311–1318, 2009, doi: 10.1016/j.wear.2008.12.084.

[91] T. André, P. Lefèvre, and J. L. Thonnard, "A continuous measure of fingertip friction during precision grip," *J. Neurosci. Methods*, vol. 179, no. 2, pp. 224–229, 2009, doi: 10.1016/j.jneumeth.2009.01.031.

[92] J. D. Ndengue *et al.*, "Tactile Perception and Friction-Induced Vibrations: Discrimination of Similarly Patterned Wood-Like Surfaces," *IEEE Trans. Haptics*, vol. 10, no. 3, pp. 409–417, 2017, doi: 10.1109/TOH.2016.2643662.

[93] A. Barrea, D. C. Bulens, P. Lefevre, and J. L. Thonnard, "Simple and Reliable Method to Estimate the Fingertip Static Coefficient of Friction in Precision Grip," *IEEE Trans. Haptics*, vol. 9, no. 4, pp. 492–498, 2016, doi: 10.1109/TOH.2016.2609921.

[94] S. Chen and S. Ge, "Experimental research on the tactile perception from fingertip skin friction," *Wear*, vol. 376–377, pp. 305–314, 2017, doi: 10.1016/j.wear.2016.11.014.

[95] A. Imaizumi, S. Okamoto, and Y. Yamada, "Friction perception resulting from laterally vibrotactile stimuli," *ROBOMECH J.*, vol. 4, no. 1, 2017, doi: 10.1186/s40648-017-0080-8.

[96] C. Shultz, M. Peshkin, and J. E. Colgate, "The application of tactile, audible, and ultrasonic forces to human fingertips using broadband electroadhesion," *IEEE Trans. Haptics*, vol. 11, no. 2, pp. 279–290, 2018, doi: 10.1109/TOH.2018.2793867.

[97] M. Janko, M. Wiertlewski, and Y. Visell, "Contact geometry and mechanics predict friction forces during tactile surface exploration," *Sci. Rep.*, no. March, pp. 1–10, 2018, doi: 10.1038/s41598-018-23150-7.

[98] R. Lewis, C. Menardi, A. Yoxall, and J. Langley, "Finger friction: Grip and opening packaging," *Wear*, vol. 263, no. 7-12 SPEC. ISS., pp. 1124–1132, 2007, doi: 10.1016/j.wear.2006.12.024.

[99] H. Zahouani, S. Mezghani, R. Vargiolu, T. Hoc, and M. El Mansori, "Effect of roughness on vibration of human finger during a friction test," *Wear*, vol. 301, no. 1–2, pp. 343–352, 2013, doi: 10.1016/j.wear.2012.11.028.

[100] S. Derler, J. Süess, A. Rao, and G. M. Rotaru, "Influence of variations in the pressure distribution on the friction of the finger pad," *Tribol. Int.*, vol. 63, pp. 14–20, 2013, doi: 10.1016/j.triboint.2012.03.001.

[101] S. Derler, M. Preiswerk, G. M. Rotaru, J. P. Kaiser, and R. M. Rossi, "Friction mechanisms and abrasion of the human finger pad in contact with rough surfaces," *Tribol. Int.*, vol. 89, pp. 119–127, 2015, doi: 10.1016/j.triboint.2014.12.023.

[102] M. A. Darden and C. J. Schwartz, “Skin tribology phenomena associated with reading braille print: The influence of cell patterns and skin behavior on coefficient of friction,” *Wear*, vol. 332–333, pp. 734–741, 2015, doi: 10.1016/j.wear.2014.12.053.

[103] L. Skedung, I. Buraczewska-Norin, N. Dawood, M. W. Rutland, and L. Ringstad, “Tactile friction of topical formulations,” *Ski. Res. Technol.*, vol. 22, no. 1, pp. 46–54, 2016, doi: 10.1111/srt.12227.

[104] M. J. Carré, S. K. Tan, P. T. Mylon, and R. Lewis, “Influence of medical gloves on fingerpad friction and feel,” *Wear*, vol. 376–377, pp. 324–328, 2017, doi: 10.1016/j.wear.2017.01.077.

[105] M. Arvidsson, L. Ringstad, L. Skedung, K. Duvefelt, and M. W. Rutland, “Feeling fine - the effect of topography and friction on perceived roughness and slipperiness,” *Biotribology*, vol. 11, no. May, pp. 92–101, 2017, doi: 10.1016/j.biotri.2017.01.002.

[106] B. M. Dzidek, M. J. Adams, J. W. Andrews, Z. Zhang, and S. A. Johnson, “Contact mechanics of the human finger pad under compressive loads,” *J. R. Soc. Interface*, vol. 14, no. 127, 2017, doi: 10.1098/rsif.2016.0935.

[107] X. Liu, M. J. Carré, Q. Zhang, Z. Lu, S. J. Matcher, and R. Lewis, “Measuring contact area in a sliding human finger-pad contact,” *Ski. Res. Technol.*, vol. 24, no. 1, pp. 31–44, 2018, doi: 10.1111/srt.12387.

[108] S. Bochereau, B. Dzidek, M. Adams, and V. Hayward, “Characterizing and imaging gross and real finger contacts under dynamic loading,” *IEEE Trans. Haptics*, vol. 10, no. 4, pp. 456–466, 2017, doi: 10.1109/TOH.2017.2686849.

[109] B. Camillieri, M. A. Bueno, M. Fabre, B. Juan, B. Lemaire-Semail, and L. Mouchnino, “From finger friction and induced vibrations to brain activation: Tactile comparison between real and virtual textile fabrics,” *Tribol. Int.*, vol. 126, no. March, pp. 283–296, 2018, doi: 10.1016/j.triboint.2018.05.031.

[110] M. Ayyildiz, M. Scaraggi, O. Sirin, C. Basdogan, and B. N. J. Persson, “Contact mechanics between the human finger and a touchscreen under electroadhesion,” *Proc. Natl. Acad. Sci. U. S. A.*, vol. 115, no. 50, pp. 12668–12673, 2018, doi: 10.1073/pnas.1811750115.

[111] A. Abdouni, G. Moreau, R. Vargiolu, and H. Zahouani, “Static and active tactile perception and touch anisotropy: aging and gender effect,” *Sci. Rep.*, vol. 8, no. 1, pp. 1–11, 2018, doi: 10.1038/s41598-018-32724-4.

[112] M. Natsume, Y. Tanaka, and A. M. L. Kappers, “Individual differences in cognitive processing for roughness rating of fine and coarse textures,” *PLoS One*, vol. 14, no. 1,

pp. 1–16, 2019, doi: 10.1371/journal.pone.0211407.

[113] K. Inoue, S. Okamoto, Y. Akiyama, and Y. Yamada, “Effect of Material Hardness on Friction between a Bare Finger and Dry and Lubricated Artificial Skin,” *IEEE Trans. Haptics*, vol. 13, no. 1, pp. 123–129, 2020, doi: 10.1109/TOH.2020.2966704.

[114] V. Carlescu, C. M. Oprişan, G. Ianuş, and D. N. Olaru, “Evaluation of friction behaviour on human finger skin considering precision grip task,” *IOP Conf. Ser. Mater. Sci. Eng.*, vol. 997, no. 1, 2020, doi: 10.1088/1757-899X/997/1/012007.

[115] M. Nachman and S. E. Franklin, “Artificial Skin Model simulating dry and moist in vivo human skin friction and deformation behaviour,” *Tribol. Int.*, vol. 97, pp. 431–439, 2016, doi: 10.1016/j.triboint.2016.01.043.

[116] J. Chen, H. Yang, J. Li, J. Chen, Y. Zhang, and X. Zeng, “The development of an artificial skin model and its frictional interaction with wound dressings,” *J. Mech. Behav. Biomed. Mater.*, vol. 94, no. January, pp. 308–316, 2019, doi: 10.1016/j.jmbbm.2019.03.013.

[117] M. Klaassen, E. G. De Vries, and M. A. Masen, “Interpersonal differences in the friction response of skin relate to FTIR measures for skin lipids and hydration,” *Colloids Surfaces B Biointerfaces*, vol. 189, no. June 2018, p. 110883, 2020, doi: 10.1016/j.colsurfb.2020.110883.

[118] W. Li, M. Kong, X. D. Liu, and Z. R. Zhou, “Tribological behavior of scar skin and prosthetic skin in vivo,” *Tribol. Int.*, vol. 41, no. 7, pp. 640–647, 2008, doi: 10.1016/j.triboint.2007.11.009.

[119] W. Li, X. D. Liu, Z. B. Cai, J. Zheng, and Z. R. Zhou, “Effect of prosthetic socks on the frictional properties of residual limb skin,” *Wear*, vol. 271, no. 11–12, pp. 2804–2811, 2011, doi: 10.1016/j.wear.2011.05.032.

Chapter - 3
Design, Development and Fabrication of Human Skin Tribometer

3.1 Introduction

In the previous chapter, comprehensive literature review has been presented for human skin friction measurement. Human skin friction behaviour has been reviewed in the context of environmental conditions, effect of micro and macro parameters and the nature of contact surface. Measurement technique highly influences the coefficient of friction (COF) for the human skin contact. Surface roughness of the material needs to be specifically mentioned to provide information on the contact between human skin and counter surface at the microscopic level. Higher number of test subjects increase the reliability and acceptability of the experimental results [1]. Since, the measurement of tribological aspects of human skin depend on multiple parameters (as discussed in chapter 2 section 2.1), it is important to replicate the test and contact conditions for specific application.

Tribometer designs for most of the in- vivo experimental investigations reported so far, can be classified broadly as rotary type and reciprocating (sliding) type tribometers. In the literature friction measuring devices are classified based on the application and the anatomical region being investigated. Based on portability tribometers range from small handheld devices having high flexibility, constrained variation in parameters and low reliability to the fixed setups that have higher reliability, less dynamic in operations but high repeatability of results.

Chapter 3 is further divided in three sections. Section 3.2 presents the design and development of parallel rotary type tribometer (RTT) while, section 3.3 presents the development of reciprocating (sliding) type tribometer (STT). Both the designs proposed here measure the frictional interaction of human skin (finger pad) at the macro scale but differ in relative motion with the human skin within each other. Section 3.4 provides the summary of chapter 3.

3.2 Design of Rotary Type Tribometer (RTT)

The tribometer features to control and measure the external macro mechanical parameters affecting the human skin friction with a material-in-contact such as normal load, sliding velocity and customisable contact surface properties.

Most of the portable tribometers for human skin friction measurement reported in literature are rotary type [2]–[6]. In rotary tribometers, friction force is calculated through the measurement

of torque of the motor that is required to maintain a constant angular velocity [3]. Different designs proposed by researchers had constraints attached to them with reference to efficient friction measurement such as uncontrolled [5], constant [7], and low range variation [4], [6], [8] of normal load and sliding velocity. Most of the rotary type tribometers have axis of rotation perpendicular to the skin surface which are further discussed in detail.

In 1973, comaish et al. [7] developed a Newcastle friction meter (handheld) as shown in Figure 3.1, with a rechargeable battery for the power supply. The developed instrument is highly portable and versatile but lacks in variation of normal load and speed. It operates with a constant load and speed to minimise variation based on the application of test parameters. Velocity between the contact was also not constant and increased from inside to outside over the contact area. No provision for recording of friction data was available. A counter-balance and support are provided through anti-friction bearings to all the moving parts.

Figure 3.1 Newcastle friction meter [7]

A study using a rotary type skin friction meter is reported for frictional force measurement of skin as shown in Figure 3.2 [3]. It employs a D.C. motor attached, to vary the speed and a spring balance to monitor the normal load. The applied normal load is assumed constant (probe weight), if and only if the relative position of the rotary probe to the base plate is kept constant. Friction force is measured through the torque generated by the motor when probe rests on the skin.

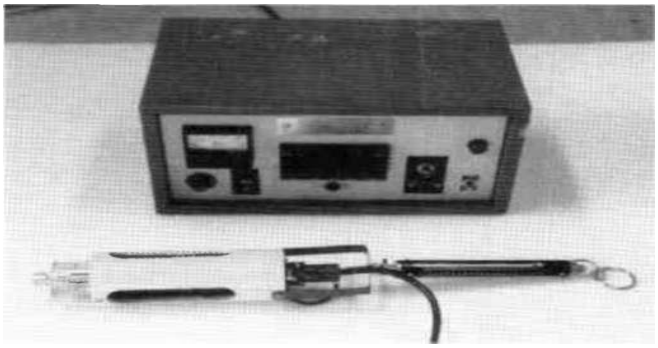

Figure 3.2 Skin friction meter [3]

A customised friction measurement device is developed [4] as shown in Figure 3.3. An arrangement of normal load application is made through loading a probe ring with linear elastic spring which is controlled by adjusting its length from 1 to 5 N. Support rings are provided around the probe to evenly distribute the pressure at the contact and shear stress on the ring. Tangential force is measured through a transducer attached to the DC motor. Velocity can be controlled in the precise range of 0.5 to 500 mm/sec.

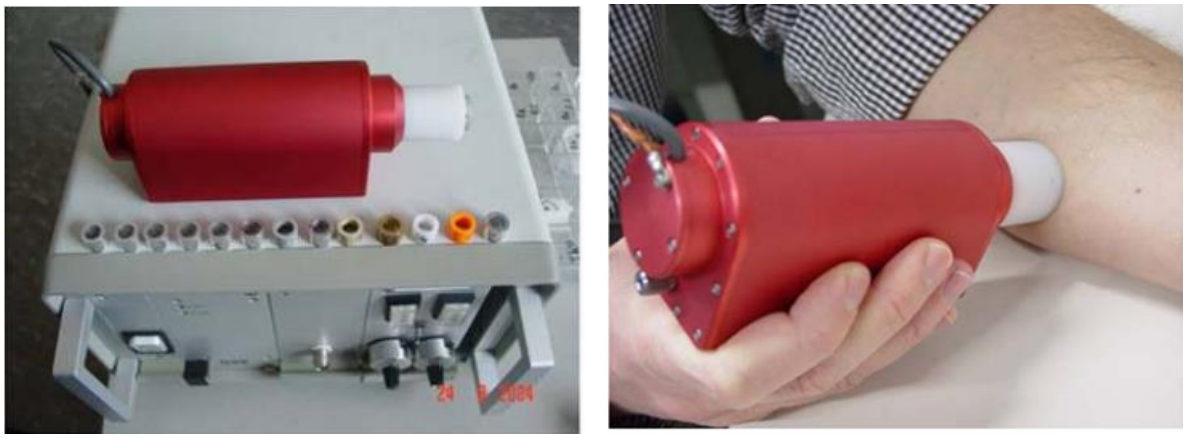

(a) (b)

Figure 3.3 Custom-built rotating ring apparatus and application to the skin of the forearm and the cheek [4]

A wireless friction measurement device with a spring based normal load actuation system is developed by veijgen et al. [8] as shown in Figure 3.4. The device operates on low normal load in the range of 0.5 to 2 N and four pre-programmed velocities of 1, 2, 5 or 10 mm/ sec. Normal load and tangential forces are measured through the piezoresistive sensors attached to it. Data is sampled at the frequency of 2.5 kHz and has an internal storage of 7 GB. Device takes 8 seconds to get stabilized, hence the standard friction measurement time is 20 seconds.

Figure 3.4 Portable handheld device [8]

To overcome the above discussed drawbacks, we have developed a customised tribometer as shown in Figure 3.5. The developed tribometer for the effective measurement of the skin interface friction has the following merits:

(1) Higher range for normal load and sliding velocity variation for the test requirements.

(2) Bench top design, to keep the variations to be minimum due to interfaces with the test subjects, since it is a contact-based study.

(3) Subject controlled normal load, to keep the operator-subject interface exchange minimum.

(4) Low-cost, confined portability and ease of use make this design to feature for range of materials in the measurement of human skin friction.

3.2.1 Description of device

The developed tribometer is commercially viable and versatile in operations. The required strength is provided through its structure, which is fabricated with raw wood. To keep the device versatile, counter material surface in contact with human skin is made up as probe that captures the skin-material tribological interaction. The other mechanical attributes affecting tribological phenomena of human skin with material in contact viz. roughness, hardness, hydration is proposed to be separately investigated, controlled, and parametrically reported in conjunction with the measured COF.

Figure 3.5 (a) and (b) depicts the developed tribometer and its components as: **A:** Weight plate: To activate the load cells. **B:** Rigid Support: To transfer the forces directly to the load cells. **C:** Load cell: Two 10 kg (measurement of 0 to 25 N of normal load) highly sensitive ($\pm$1 gm) load cells are mounted on the wooden frame. **D:** Probe: Probe is made up of counter surface material having diameter of 57 mm. **E:** Motor: A 12-volt D.C. motor (to achieve desired range of angular velocity) is mounted on the rigid support to generate the rotary motion of the probe. **F:** Wooden Frame: This serves as the basic support structure of the device mountings. **G:** Control board: It is the mechano-electronic interface that transmits data to the attached micro secure digital card. **H:** Platform: To give support to the human test subject.

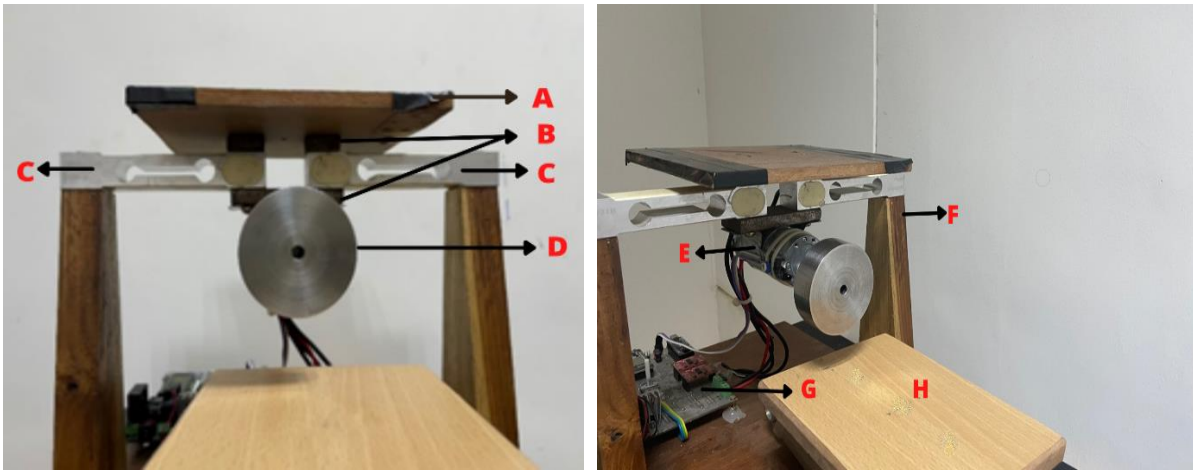

(a) **(b)**

Figure 3.5 Developed parallel rotary type human skin tribometer (a) Front view and (b) Isometric view

3.2.2 Working principle

The applicability of Amonton's law is stressed on the relevance of other factors such as contact area, surface conditions, velocity, lubricants and geometric orientation to affect the friction between the constituting bodies [9]. Till date, no concrete agreement has been drawn among the tribologists for the pertinency of Amonton's law of friction. Here, the tribometer development is based on Amonton's law that describes the coefficient of friction between two surfaces as the ratio of the tangential force generated to the normal load applied as in equation 3.1. If the counter surface material is so compressible that it cannot be given a shape of the probe, then it is mounted on the base probe to avoid any wrinkles, occlusions, and deformations on the surface.

$$COF = \frac{F_T}{F_N} \qquad \textbf{3.1}$$

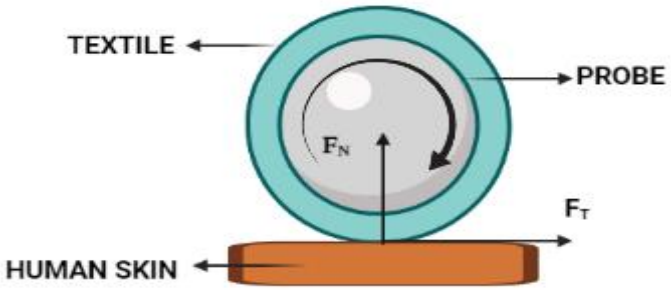

Figure 3.6 Schematic representation of forces acting at the human skin contact

Friction force is defined as the force generated to restrict the relative motion between the two interfacing surfaces. Figure 3.6 depicts the normal force (F_N) acting and tangential force (F_T)

generated due to the resistance offered by the probe to the human skin due to the rotating motion at the contact interface.

3.2.3 Force measurement system

A. Normal load measurement

The current equipment measures the normal load as a difference between the applied force through a static weight 'W' and the combined residual readings of both the load cells L_1 and L_2 shown in equation 3.2. Residual force readings acting at L_1 and L_2 are F_1 and F_2 respectively.

$$F_N = W - (F_1 + F_2) \quad \textbf{3.2}$$

Subject keeps the finger pad on the lifting platform pushing the finger downwards to avoid any unintentional contact. As the platform is lifted upwards finger pad applies force on the probe material. The force is transferred through a rigid support to the load cell as shown in Figure 3.7. For the in vivo friction measurements, it becomes totally inevitable to rule out human based measurement errors. To minimise the measurement errors and control the variations device is equipped with set of two load cells and an externally lifted resting platform respectively. Every device has its shortcomings, the current equipment lacks in portability and needs to educate the subject with the operating procedures to reduce the measurement flaws.

Working of a load cell:

Load cell works on the principle of Wheatstone bridge. Wheatstone bridge changes its voltage output with change in resistance on the application of the load. For the no load condition, there is no deformation in the cell. This is the balanced condition of the bridge circuit, and the output voltage of the load cell is zero. When a load is applied change in resistance is witnessed causing an imbalance in the circuits resulting in an output voltage.

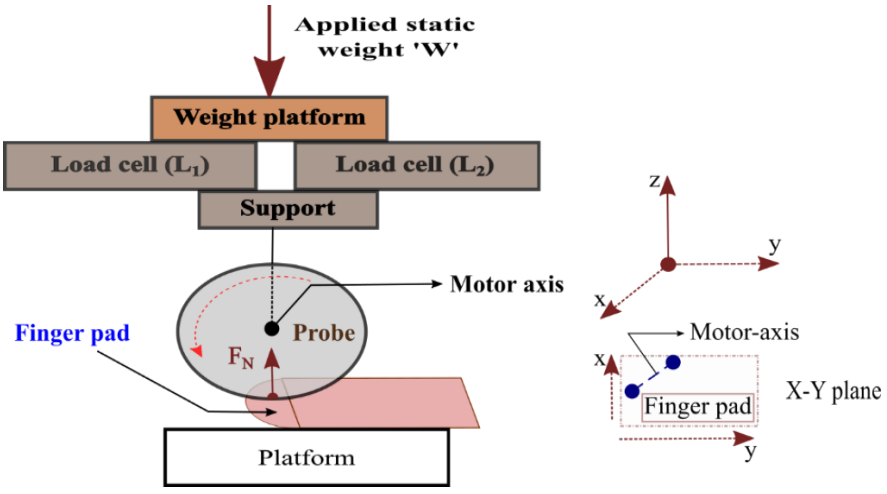

Figure 3.7 Schematic representation for the measurement of normal force

B. Tangential force measurement

In the Amonton's third law with increase in tangential velocity there is an increase in the COF value at a constant normal load. Shearing that tends to rotate the probe at the contact interface is caused by the tangential force (or, shearing force). Tangential force in the current device is measured in relation to the current consumed and the torque at the contact interface.

In a D.C. motor at constant voltage (V)

$$Current(i) \propto Torque\ (\tau)$$

Relationship of tangential force and electrical current consumption can be understood as follows:

Step 1:

At multiple voltages current consumption in no load and load conditions were measured.

The force acting at the lowest portion of the probe while rotating was measured through an external digital weigh scale as depicted in Figure 3.8.

Step 2:

A plot was developed for six set of values for V and I following the ohm's law. An analogous relation of voltage current and resistance was developed using ohm's law and the equation of straight line (y= mx+c).

Step 3:

Different values of slopes m_1, m_2 …m_6 for resistances and that for intercept c_1, c_2, ….c_6 were calculated for the proposed dc motor. A special written code is developed to calculate COF as an output, taking the instantaneous normal force and tangential force. A schematic representation of tangential force measurement is shown in Figure 3.9.

Figure 3.8 Mechanical measurement of tangential force through weigh scale

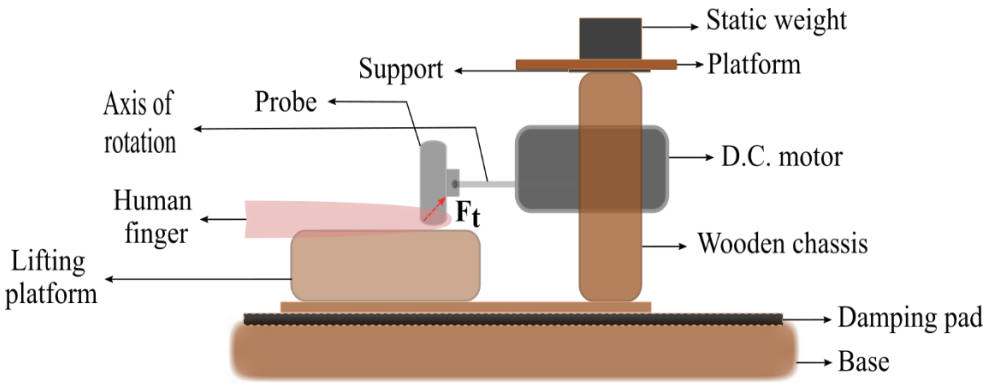

Figure 3.9 Schematic representation for the measurement of tangential force (Side view)

3.2.4 Validation of equipment

Gage repeatability & reproducibility tests:

Gage repeatability and reproducibility (R&R) study is the popular technique of measurement system analysis (MSA). Gage R&R tests are performed to measure any bias associated within or outside the measurement system. Minitab© statistical package developed by Pennsylvania state university is used to perform R&R study and analyse the results. Table 3.1 presents the ANOVA results obtained through gage R&R study for components variance.

Table 3.1 (A) shows the two-Way ANOVA analysis representing the p-values for the parts, operators, and part-operator interaction (with a significance level of $\alpha = 0.05$). Table 3.1 (B) and Table 3.1 (C) shows the total Gage R&R statistic for the component's variance and the gage evaluation respectively. Figure 3.10 illustrated the gage R&R report for the COF.

The crossed gage R&R study is opted for the validation of the device because of the following reasons:

a) It quantifies the inherent variability in the system.

b) The test is widely used for the validation of systems having non-destructive testing measurements.

The gage R&R statistic from the component variance should satisfy following criterion to be acceptable:

1) Range of percentage contribution in components of variation for the total gage R&R as per the standards [10] are :

- Less than 1%- Measurement system is acceptable.
- 1% to 9%- Measurement system is acceptable (depending on application, cost, and other factors).
- More than 9%- Measurement system cannot be accepted and should be improved.

2) The total gage R&R statistic for the gage evaluation to be acceptable, should satisfy following criterion:

- Less than 10%- Measurement system is acceptable.
- Between 10% to 30%- Measurement system is acceptable (depending on application, cost, and other factors).
- More than 30%- Measurement system cannot be accepted and should be improved.

Table 3.1 ANOVA Gage R&R results

(A) Gage R&R Study - ANOVA Method Two-Way ANOVA Table with Interaction

Source	**DF**	**SS**	**MS**	**F**	**P**
Parts	7	11.77	1.68	140.76	0.000
Operators	2	0.082	0.04	3.43	0.061
Parts * Operators	14	0.16	0.01	1.95	0.044
Repeatability	48	0.29	0.006		
Total	71	12.32			

α to remove interaction term = 0.05

(B) Gage R&R Variance Components

Source	**Var Comp**	**% Contribution (of Var Comp)**
Total Gage R&R	0.009	4.76
Repeatability	0.006	3.14
Reproducibility	0.003	1.62
Operators	0.0012	0.62
Operators*Parts	0.0019	1.00
Part-To-Part	0.18562	95.24
Total Variation	0.19490	100.00

(C) Gage Evaluation

Source	Std Dev (SD)	Study Var (6 × SD)	Study Var (%SV)
Total Gage R&R	0.096345	0.57807	21.82
Repeatability	0.078289	0.46973	17.73
Reproducibility	0.056154	0.33692	12.72
Operators	0.034811	0.20887	7.89
Operators*Parts	0.044061	0.26437	9.98
Part-To-Part	0.430839	2.58503	97.59
Total Variation	0.441480	2.64888	100.00

Number of Distinct Categories = 6

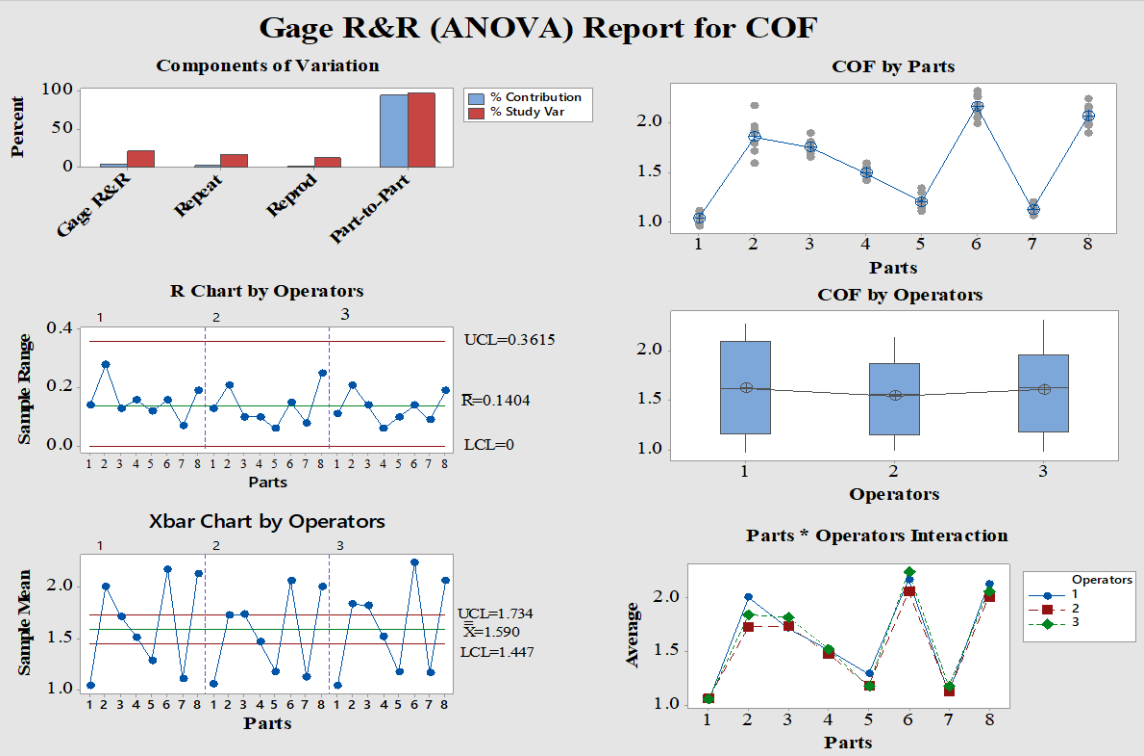

Figure 3.10 Gage R&R report for the device validation

3.3 Design of Sliding Type Tribometer (STT)

This section discusses about the development and fabrication of sliding type human skin tribometer. In the literature, the reported STT's are distinguished based on motion actuation, relative motion, mechanism type, application of normal load, variation in sliding velocity, mounting of contact material, finger - contact angle variation and measuring of shear forces etc. Human skin friction is affected by multiple intrinsic and extrinsic parameters as reported

in chapter 2 section 2.1. Two vital parameters affecting the human skin friction at the macro level namely, normal load and shear force are crucial for the designing of human skin measurement device.

In 1991, Dinc et al.[11] introduced the force transducer for the friction measurement of the sliding tactile contact between human finger and the countersurface. The setup design as shown in Figure 3.11 (a) consists of piezo-electric force transducer that gives force to all the three components (x, y, z) for any force applied. Countersurface was attached with an adhesive to the upper link of the device. Procedures were conducted on three normal loads (100-150, 300-400 and 1000-2000 gm) and three sliding velocities (0.6, 2, and 6 cm/s). Five common materials (Plexiglass, Nylon 66, Teflon, Polycarbonate and Phenolic) with different surface roughness and at different relative humidity were used for the measurement of tactile friction.

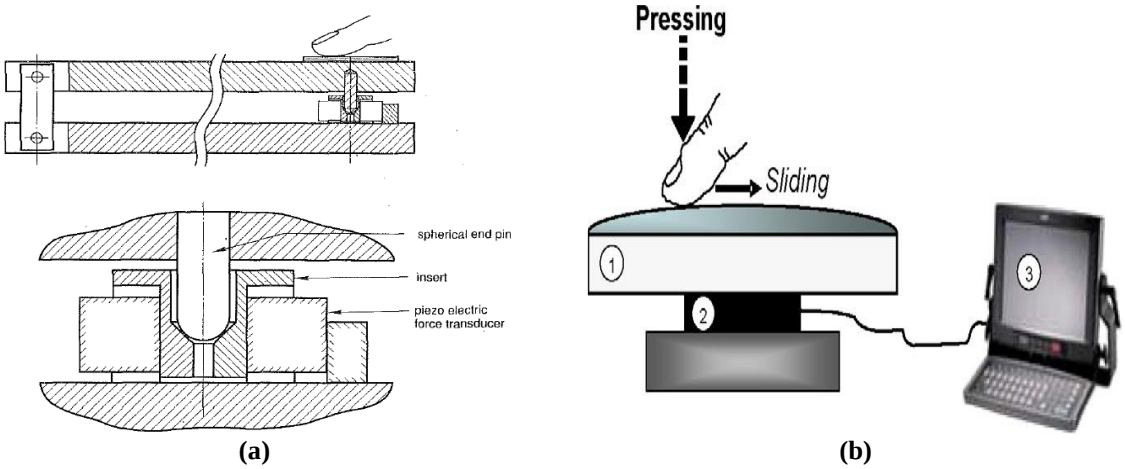

Figure 3.11 (a) Apparatus for the measurement of tactile friction [11], (b) Schematic view of the experimental test equipment. (1) Spherical glass surface, (2) Multiaxial force sensor, (3) Treatment and acquisition unit [12]

In 2007, Ramalho et al. [12] designed an equipment for the frictional force measurement of sliding finger on the glass surface as depicted in Figure 3.11 (b). Multiaxial load cell and an amplifying unit is attached for the measurement of normal and tangential forces. Defined loading range for the equipment is 0 to 70 N. For the testing purpose loading and sliding rate were taken as 60 ± 20 N/ s and 40 ± 10 mm/ s. Similar setups as in [12] where load application is controlled and actuated by subjects have been developed by Carre et al.[13], Derler et al. [14], and Kuilenburg et al. [15]. Seo and Armstrong [16] have used very similar test setup differentiating in the load application through the use of dead weights.

In 2017, Camillieri and Bueno [17] designed a tactile reciprocating tribometers as shown in Figure 3.12 for investigating tribological behaviour of textile. Oscillatory motion is controlled

by a servo -controller to which the fabric is mounted. Pulse data recorder is incorporated for the data-acquisition. A three-axis load cell is attached for the force measurement in the three orthogonal axes. An adjustable gutter is provided to hold the subject's arm for the efficient friction measurement.

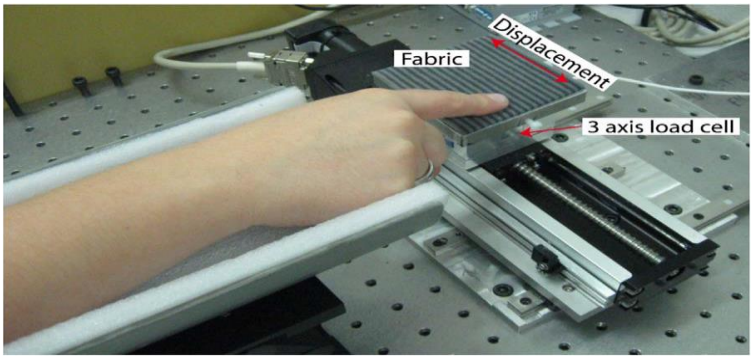

Figure 3.12 Tactile tribometer for friction measurement [**17**]

In 2017, Zhang et al. [18] designed an experimental test setup to determine the finger friction characteristics. A 2-D strain gauge sensor with a resolution of 0.005 N and a range of 0-100 N was used to measure the normal and the frictional forces. Finger bracket and a loading device is attached to control normal load and contact angle as shown in Figure 3.13. Test sample is fixed on the force sensor which in turn is driven by a servo motor. Data is recorded at a sampling frequency of 200 Hz through the linked data acquisition device.

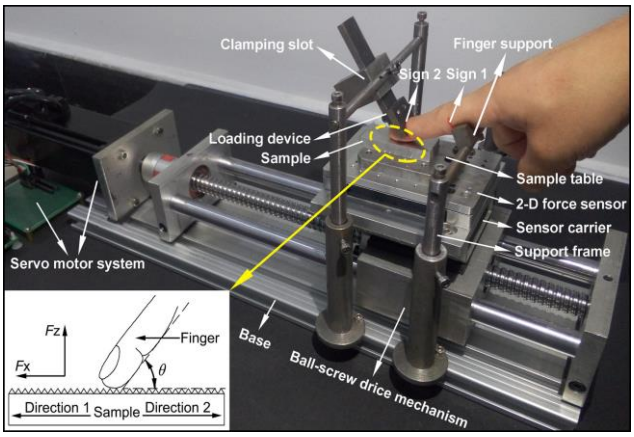

Figure 3.13 Schematic of in-house developed experimental setup [18]

Sergachev et al. [19] adapted the setup depicted in Figure 3.14 by Klaassen et al. [20] for the finger pad friction measurements. 6-axis force transducer of 100 Hz sampling frequency is mounted, and the load is applied through the static weights. Samples were attached to the load cell through bolted attachment of polymethyl methacrylate (PMMA) plate over which the samples were glued.

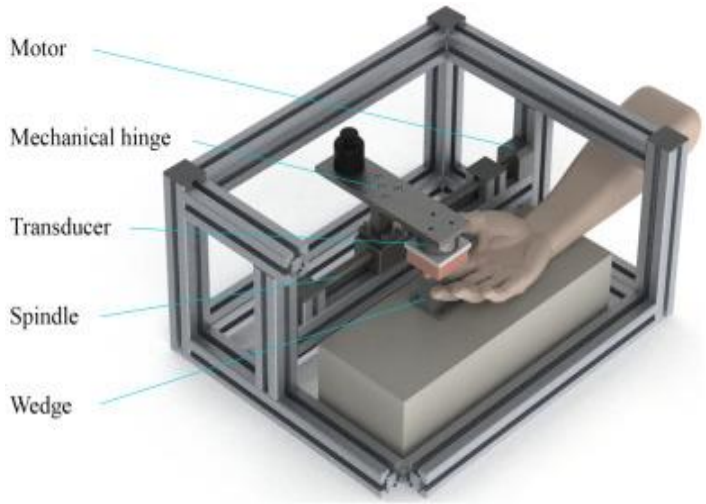

Figure 3.14 Schematic representation of the test setup used for the friction [20]

3.3.1 Description of device

A schematic of reciprocating tribometer is shown in Figure 3.15 (a). Human skin friction measurement setup consists of **A:** Power source, **B:** Computer system, **C:** Data acquisition device (DAQ), **D:** Induction motor (to reciprocate the linear stage mechanism), **E:** Limit switch (to break the circuit), **F:** Contactor (to switch an electrical power circuit for reversing the direction), Variable frequency drive (VFD-to control the speed of the linear stage) and a linear stage mechanism. Exploded view for the linear stage is as shown in Figure 3.15 (b).

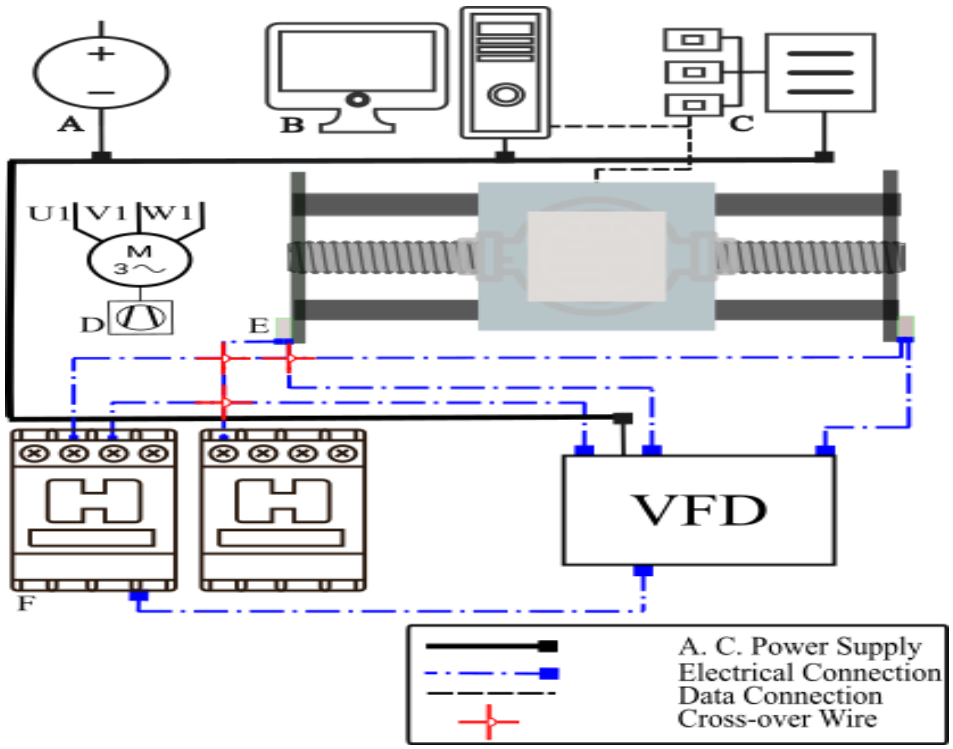

(a)

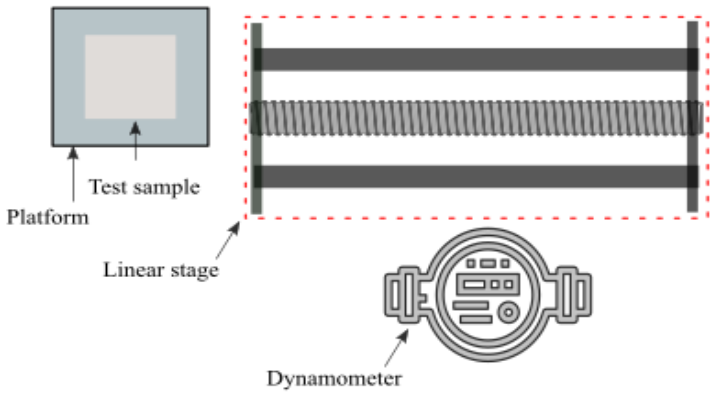

(b)

Figure 3.15 (a) Experimental setup for reciprocating type human skin tribometer, (b) Exploded view of linear stage mechanism

3.3.2 Working principle

A subject controlled normal load is applied on the test sample attached over the dynamometer as depicted in Figure 3.16 (a). Dynamometer gives the forces in the three orthogonal directions in x, y and z axis. Speed of the geared induction motor can be controlled through an attached VFD that in turn controls the reciprocating motion of the linear stage. Two contactors attached to the limit switches at both the ends of the linear stage mechanism switches on and off the electrical circuit. Subject is provided with a stand support to make a constant angle of 30 to 45 degrees as shown in Figure 3.16 (b) to limit the variation in the contact during the measurements. Applied normal load is easily visible in the attached display unit for the convenience of the subject.

(a)

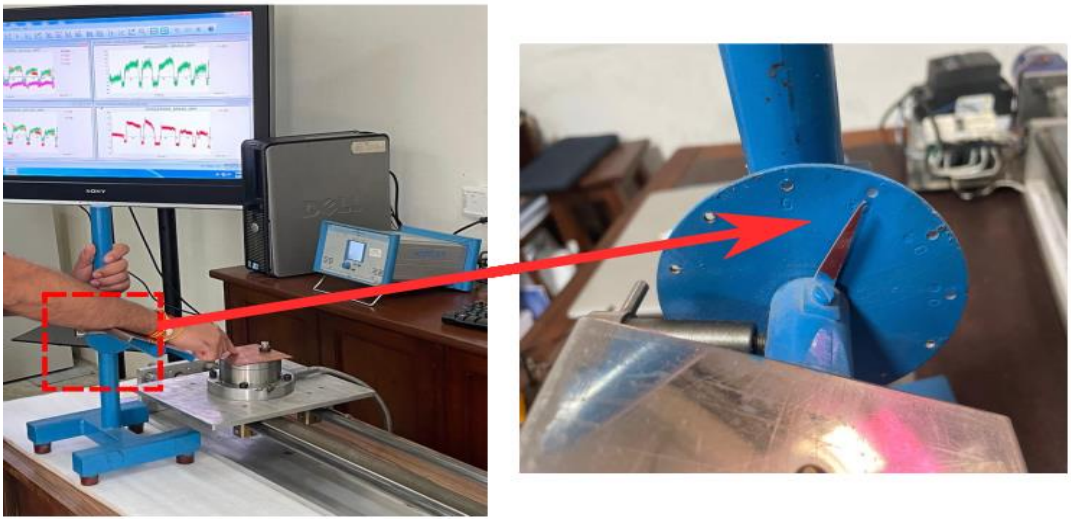

(b)

Figure 3.16 (a) Experimental test setup for sliding type tribometer (b) Measurement of finger pad friction

3.3.3 Components of sliding type tribometer

A. Induction motor

To operate the linear stage mechanism, an induction motor as shown in Figure 3.17 rated at (40 W, 230/415 VAC, 3Phase, 1440 RPM) by revolution technologies is used. A gearbox is coupled to achieve the minimum speed requirement in the application of human skin frictional measurement. The rotational speed of motor is controlled in terms of VFD frequency equivalent to 20,30,40,50 and 60 Hz.

Figure 3.17 Phase 40-Watt Induction Motor

B. Variable frequency drive (VFD)

VFD's are also known as AC Drives which is used to control the rotational speed of the AC Motors. Variable frequency drive unit is connected to the motor electrical supply. Frequency of the electricity being supplied to the motor can be controlled, that in turn controls the rotation

of the motor. VFD twice converts the voltage. Initially, it converts the AC to DC using diode and then cleans the DC using the capacitors finally converting back to AC through transistors. This design incorporates VFD002EL21W-1 manufactured by Delta 0.25 HP VFD with a frequency range of 0.1 to 400 Hz. VFD connected in the frictional measurement setup is depicted in Figure 3.18.

Figure 3.18 0.25 HP Variable frequency drive

C. Contactor

A Contactor is shown in Figure 3.19 is used for switching on or off an electric circuit. This is similar to a relay for high range electrical current. Contactors are selected based on their application. This setup consists of a contactor of model LC1D09 by Schneider Electric (SE). Two contactors are attached to the two limit switches at each end of the linear stage.

Figure 3.19 Contactor switch

D. Limit switch

Limit switches are the electromechanical device that operates through an application of a mechanical force. It is used to limit the travel of a moving object. The limit switches are electrically connected to the electrical switches. This is mostly used where the application needs to restrict the motion to make or break the connection through an electrical current. Here, 15 Ampere limit switch is shown in Figure 3.20 is attached at both the ends to break the current flow. So that the platform on the linear stage reverses the direction of motion.

Figure 3.20 Limit switch

E. Linear stage mechanism

Linear stage mechanism as shown in Figure 3.21 is developed to convert the rotary motion generated by the induction motor to the reciprocatory motion. The ends of the linear stage limit switches are connected to limit the travel of the platform within the frame. Structure is made of stainless steel and the inner travel distance is 115 cm. Two solid cylindrical rods at both the lateral ends are attached to support the platform. At the centre a helical screw rod is mounted through a mechanical attachment to the platform.

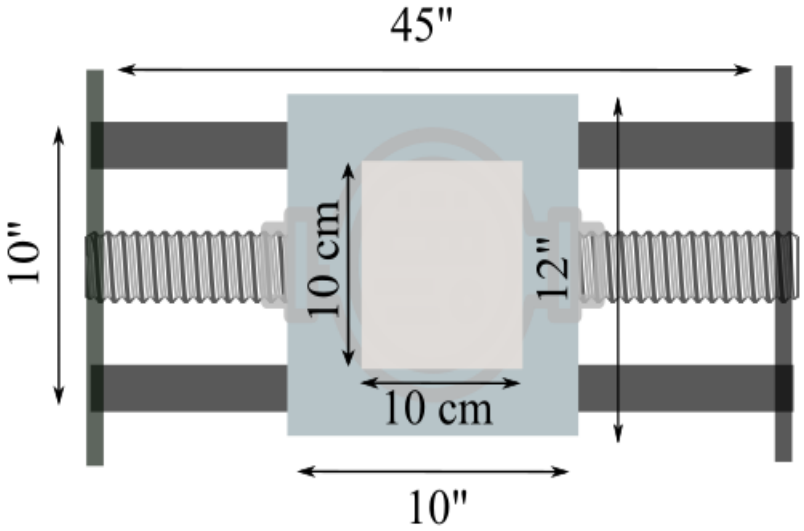

Figure 3.21 Linear stage mechanism (not to scale)

F. Dynamometer

In literature, various multi axis force plate or load cells are used to measure the normal and tangential forces for the human skin friction measurement [13], [14], [21], [22]. For the measurement of normal load and tangential force a well calibrated multi axis dynamometer Kistler 9272 shown in Figure 3.22 is mounted on the platform through bolts over the linear stage. The device can measure three orthogonal forces in x (F_X), y (F_Y), and z (F_Z) direction along with a moment around z axis. It is coupled with a high impedance connection cable 16677A5. Measuring range for F_X and F_Y is -5 to 5 kN while for F_Z its -200 to 200 kN. It is further attached to a data acquisition system with a sampling frequency of 1000 Hertz and an amplifier that stores the data in the system for analysis at a later stage.

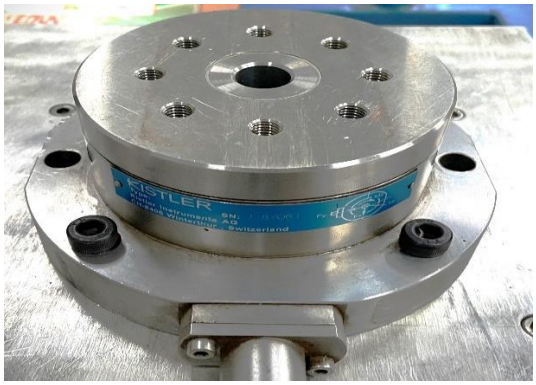

Figure 3.22 Dynamometer (Kistler 9272)

3.4 Summary

1. Section 3.1 Discusses the friction measurement techniques for the human skin classifying them into rotary and sliding type of human skin tribometer.
2. Section 3.2 provides insights on the series of developments in the rotary type of tribometers. Later in the section development, working and validation of the parallel rotary type human skin tribometer is discussed in detail.
3. Section 3.3 presents the sliding type of tribometers available in the literature. Further, discussion is presented for the development of sliding type human skin tribometer.

References

[1] S. Derler and L. C. Gerhardt, "Tribology of skin: Review and analysis of experimental results for the friction coefficient of human skin," *Tribol. Lett.*, vol. 45, no. 1, pp. 1–27, 2012, doi: 10.1007/s11249-011-9854-y.

[2] A. F. El-Shimi, "In vivo skin friction measurements," *J. Soc. Cosmet. Chem.*, vol. 51, no. February, pp. 37–51, 1977.

[3] M. Zhang and A. F. T. Mak, "In vivo friction properties of human skin," *Prosthet. Orthot. Int.*, vol. 23, no. 2, pp. 135–141, 1999, doi: 10.3109/03093649909071625.

[4] C. P. Hendriks and S. E. Franklin, "Influence of surface roughness, material and climate conditions on the friction of human skin," *Tribol. Lett.*, vol. 37, no. 2, pp. 361–373, 2010, doi: 10.1007/s11249-009-9530-7.

[5] A. B. Cua, K. P. Wilhelm, and H. I. Maibach, "Frictional properties of human skin: Relation to age, sex and anatomical region, stratum corneum hydration and transepidermal water loss," *Br. J. Dermatol.*, vol. 123, no. 4, pp. 473–479, 1990, doi: 10.1111/j.1365-2133.1990.tb01452.x.

[6] S. C. Henao, S. Cuartas-Escobar, and J. Ramírez, "Redesign and validation of a handheld tribometer to determine the coefficient of friction between the prosthesis and the residual limb of people with a transfemoral amputation," *Biotribology*, vol. 21, no. August 2019, p. 100118, 2020, doi: 10.1016/j.biotri.2020.100118.

[7] J. S. COMAISH, P. R. H. HARBOROW, and D. A. HOFMAN, "A hand-held friction meter," *Br. J. Dermatol.*, vol. 89, no. 1, pp. 33–35, 1973, doi: 10.1111/j.1365-2133.1973.tb01914.x.

[8] N. K. Veijgen, M. A. Masen, and E. Van Der Heide, "A novel approach to measuring the frictional behaviour of human skin in vivo," *Tribol. Int.*, vol. 54, pp. 38–41, 2012, doi: 10.1016/j.triboint.2012.05.022.

[9] R. M. McKeon and C. S. Gillmor, *Coulomb and the Evolution of Physics and Engineering in Eighteenth-Century France*, vol. 14, no. 2. Princeton University Press, 1973.

[10] M. Down, F. Czubak, G. Gruska, S. Stahley, and D. Benham, "Measurement Systems Analysis Reference Manual," *Automot. Ind. Action Gr.*, 2010.

[11] O. S. Dinç, C. M. Ettles, S. J. Calabrese, and H. A. Scarton, "Some parameters affecting tactile friction," *J. Tribol.*, vol. 113, no. 3, pp. 512–517, 1991, doi: 10.1115/1.2920653.

[12] A. Ramalho, C. L. Silva, A. A. C. C. Pais, and J. J. S. Sousa, "In vivo friction study of

human skin: Influence of moisturizers on different anatomical sites," *Wear*, vol. 263, no. 7-12 SPEC. ISS., pp. 1044–1049, 2007, doi: 10.1016/j.wear.2006.11.051.

[13] M. J. Carré, S. K. Tan, P. T. Mylon, and R. Lewis, "Influence of medical gloves on fingerpad friction and feel," *Wear*, vol. 376–377, pp. 324–328, 2017, doi: 10.1016/j.wear.2017.01.077.

[14] S. Derler, L. C. Gerhardt, A. Lenz, E. Bertaux, and M. Hadad, "Friction of human skin against smooth and rough glass as a function of the contact pressure," *Tribol. Int.*, vol. 42, no. 11–12, pp. 1565–1574, 2009, doi: 10.1016/j.triboint.2008.11.009.

[15] J. Van Kuilenburg, M. A. Masen, and E. Van Der Heide, "The role of the skin microrelief in the contact behaviour of human skin: Contact between the human finger and regular surface textures," *Tribol. Int.*, vol. 65, pp. 81–90, 2013, doi: 10.1016/j.triboint.2012.11.024.

[16] N. J. Seo and T. J. Armstrong, "Friction coefficients in a longitudinal direction between the finger pad and selected materials for different normal forces and curvatures," *Ergonomics*, vol. 52, no. 5. pp. 609–616, 2009, doi: 10.1080/00140130802471595.

[17] B. Camillieri and M. A. Bueno, "Artificial finger design for investigating the tactile friction of textile surfaces," *Tribol. Int.*, vol. 109, no. September 2016, pp. 274–284, 2017, doi: 10.1016/j.triboint.2016.12.013.

[18] M. Zhang, J. L. Mo, J. Y. Xu, X. Zhang, D. W. Wang, and Z. R. Zhou, "The Effect of Changing Fingerprinting Directions on Finger Friction," *Tribol. Lett.*, vol. 65, no. 2, pp. 1–9, 2017, doi: 10.1007/s11249-017-0843-7.

[19] D. A. Sergachev, D. T. A. Matthews, and E. van der Heide, "An Empirical Approach for the Determination of Skin Elasticity: Finger pad Friction against Textured Surfaces," *Biotribology*, vol. 18, no. April, p. 100097, 2019, doi: 10.1016/j.biotri.2019.100097.

[20] M. Klaassen, D. J. Schipper, and M. A. Masen, "Influence of the relative humidity and the temperature on the in-vivo friction behaviour of human skin," *Biotribology*, vol. 6, pp. 21–28, 2016, doi: 10.1016/j.biotri.2016.03.003.

[21] M. A. Masen, "A systems based experimental approach to tactile friction," *J. Mech. Behav. Biomed. Mater.*, vol. 4, no. 8, pp. 1620–1626, 2011, doi: 10.1016/j.jmbbm.2011.04.007.

[22] M. S. Kim, I. Y. Kim, Y. K. Park, and Y. Z. Lee, "The friction measurement between finger skin and material surfaces," *Wear*, vol. 301, no. 1–2, pp. 338–342, 2013, doi: 10.1016/j.wear.2012.12.036.

Chapter - 4
Experimental Investigations and Analysis for Parallel-Rotary Type and Sliding Type Human Skin Tribometer

4.1 Introduction

In the previous chapter, a parallel rotary and reciprocating type human skin tribometer was designed and fabricated for the measurement of human skin frictional parameters. This chapter consists of the experimental procedures, results, and analysis of the coefficient of friction values obtained through the respective tribometers.

There are multiple studies available in the literature for the frictional attributes of human skin. These studies are classified based on anatomical region, countersurface material, characteristic property being investigated, type of measuring technique, range of normal load, and application specific tribological research such as that for textile, gripping, medicine, and product design. One of the objective of the current research is to experimentally investigate the tribological behaviour of human skin through in-house developed parallel rotary and reciprocating tribometers. Experimental investigations are carried on finger pad taking three constraints namely (i) Subjects should represent the Indian diaspora, (ii) Experiments should be conducted to majorly represent Indian climatic conditions and (iii) normal load and sliding velocities taken should practically replicate the precision and power grips mostly vital in importance for the designing of assistive devices for elderly users.

Experiments were conducted in the time of year that suitably represented the temperature and humidity range as per data of The Indian Society of Heating, Refrigerating, and Air Conditioning Engineers (ISHRAE). The Indian climatic divisions as per the Koppen classification are divided in six zones namely, Montane, Humid subtropical, Tropical wet and dry, Tropical wet, Semi-arid and Arid.

Table 4.1 presents the data for the maximum, minimum and mean range of temperature and relative humidity (RH). Mean range of temperature for “humid subtropical”, “tropical wet and dry”, “tropical wet”, “semi-arid” and “arid” is 25.6 degree celsius and that of RH is 70 % .Therefore experiments are performed at 25 ± 2 and 60 ± 10% to replicate the climatic conditions of over 80% of Indian population. Human skin greatly affects the perception and cognitive behaviour of an individual.

Table 4.1 Max, min & mean values of temperature and relative humidity

Climatic Zone	Temp (°C)			RH (%)		
	Max	Min	Mean	Max	Min	Mean
Montane	35.1	-4.5	15.3	100	4	52
Humid Subtropical	40.8	5.5	23.8	99	13.9	70.3
Tropical wet and dry	41.5	12.1	26.7	99.1	13.4	77.9
Tropical wet	35.6	19.4	27	99.3	20	78.8
Semi-arid	40.8	5.5	23.8	99.4	13.9	70.7
Arid	44.8	5.6	27	99.3	4.1	50

Human skin friction has been studied by various researchers through different lenses as in medicine [1]–[4], sports [5]–[7], materials [8]–[10], cosmetics [11]–[14], and textiles [15]–[19]. Skin friction is one of the most common factors for the blisters of skin [20], [21]. For the product design, shear forces generated at the interface of contact should well be optimised to have both the comfort and convenience of an individual. For example, in the designing of the assistive devices for an elderly person, the reduced cognitive abilities at old age are compensated by the application of higher gripping force [22], that may result into shear at the contact interface due to generation of higher frictional forces. Sports equipment designs are highly influenced by the nature, microclimate and ergonomics of the sportsperson [5]. Researchers have worked on the evaluation and development of materials that tend to optimise the perception, feel and grips of human skin as per the domain of application [23]–[26]. Tribological tests pertaining to the personal care products are performed to be in assent of the cosmetological standards [7], [11], [27], [28]. Another focus domain for the measurement of frictional attribute of human skin is its interaction with textiles. Number of studies have been performed to investigate the tribological interaction of various anatomical regions of human skin with textile materials [29]–[31]. No literature could be traced for the frictional study on the Indian subjects and environment coupled together. In the present work, tribological study is conveniently conducted with in the Indian climatic conditions taking subjects from the Indian anthropometric domain.

Human skin friction is influenced by multiple intrinsic and extrinsic parameters as discussed in detail in chapter 2 section 2.1. Intrinsic factors constitute those attributes which are related to the subject characteristics such as skin hydration, glabrous nature, age, gender, ethnicity, and anatomical region. Extrinsic parameters constitute of normal load, sliding velocity, climate, contact material, texture, relative humidity, and temperature. Both these combined have

another classification based on size namely macro and micro. Glabrous nature [32], textures [33]–[35], relative humidity [36]–[38], temperature [36] and hydration [39]–[41] are labelled as micro attributes while, normal load [42]–[45], sliding velocity [46]–[48], and surface roughness [40], [44], [49], [50] are considered macro parameters [51].

Further, the chapter is divided in four sections. Section 4.2 presents the method of test material selection. Section 4.3 reports the experimental results obtained through parallel rotary type tribometer (RTT) while, section 4.4 reports and discusses the results obtained through sliding type tribometer (STT). Section 4.5 summaries chapter 4.

4.2 Test Material Selection

It is concluded from the literature that the experimental investigations have been performed on variety of metal, textile, polymers, wood, plastics etc. For the selection of materials as a non-metal test sample a survey was conducted for popular choices of material.

Survey was conducted (Questionnaire in Appendix I) both in offline and online modes consisting through convenience sampling such as student, staff, friends, and family. E- mail communication was sent to the participants along with a short description about the objective of the study. Total of 832 (247 offline) and (585 online) participants were approached. Overall, 685 responses were received which represents 82.33 % response rate. 179 responses were removed due to unnamed and unfinished survey. Final sample size came to 506 ,demographic data has been included in the appendix. Majority of responses were from age category 18- 30 years old (56.3%) with representation of 327 (64.6%) males and 179 (35.4%) females. Survey was conducted with in the six Indian physiographic regions with responses from central highlands (16.8%), coastal plains (eastern & western) (14.8%), great plains (41.5%), islands: Andaman & Nico bar (2.2%), northern mountains (5.9%), peninsular plateau (16.8%). As per the job affiliation most representation is from the administrative/ managerial/ teaching (52.6%), hospital/ medical staff (6.3%), housemaker (6.7%), software engineers/ bankers (20.4%), sports (1.2 %) and student (11.3%).

Three major takeaways from the responses are as follows:

- Most preferred textile for apparel design at the workplace:

Table 4.2 shows the across the job profiles other than sports, most preferred outfit for work is cotton more than double to that of denim and other.

Table 4.2 Fabric choices for different job profiles

		Fabric			Total
		Cotton	Denim	Other	
Job	Administrative or managerial or teaching	165	46	55	266
	Hospital or medical staff	17	9	6	32
	Housemaker	14	10	10	34
	Software engineers or banker	43	31	29	103
	Sports	1	3	2	6
	Student	41	7	17	65
Total		**281**	**106**	**119**	**506**

- Most preferred choice for the grip material:

Respondents were requested to rate on the scale of 0 (low) to 5 (high) as shown in Table 4.3 the most preferred material for the development of grips mostly used in rackets. Handles, tools etc. Maximum rating of is given to rubber followed by plastic, wood, enamel coated wood, and steel.

Table 4.3 Responses for choice of grip material

	Rubber	Plastic	Steel	Wood	Coated
1	10	37	57	**67**	45
2	27	98	**145**	95	103
3	52	155	**159**	148	151
4	**167**	147	99	131	143
5	**250**	69	46	65	64

- Preferred material for the cell phone case

Pie chart in Figure 4.1 shows the maximum responses opted for polymer (274), followed by plastic (92), fabric (76)and others (64) out of 506 as the material for the development of mobile case for the better grip.

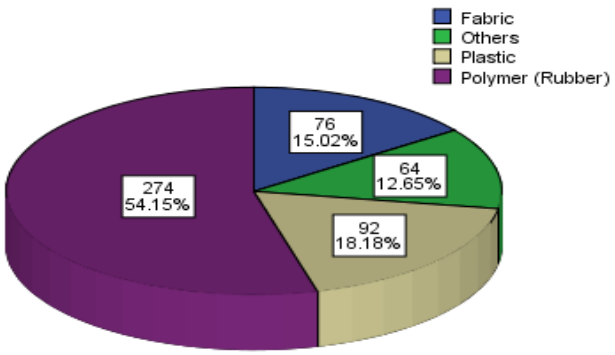

Figure 4.1 Popular material choices for mobile phone case

4.3 Experimental Investigations of COF with Parallel-RTT

Chapter 2 presented thorough the available literature the in vivo experimental investigations that have been performed in the domain of human skin tribology. This section presents the experimental results and its analysis obtained through the parallel-rotary type human skin tribometer. Fabrication of equipment and its validation has been discussed elaborately in the previous chapter.

Rotary tribometers mostly use the probe or a rotating wheel that is pressed on the human skin surface with a defined load. Major difficulty obtained through these devices was of repeatability and reproducibility [52] that have been reduced through the validation of the device through gauge R & R tests. The two most common methods used for the application of normal loads was dead weights and the spring mechanism that arguably gave incorrect readings of normal load at an instant around 30-70% of the real value. Since human skin has non-flat surface, normal load results in the source of variation due to valleys and crests in the human skin. Human skin tribological testing has been performed with different materials such as aluminium [37], [53], [54], steel [43], [44], [53], Brass [53], plastic [33], [55], [56], glass [46], [55], [57]–[59],polymer [4], [53], [55], [60], paper [49], [61], [62] and textile [61], [63], [64]. Based on literature and the survey conducted current study investigates the tribological interaction of human finger pad with two textiles (cotton and wool), two polymeric materials (latex and rubber) as non-metallic and aluminium, brass, copper, and stainless steel as metallic countersurface material.

4.3.1 Methodology

After the initialization of device, calibration starts automatically. Make sure there is no weight at the top plate. A known weight '*W*' is put on the platform and is manually fed using the user input buttons and the resultant is calculated as per the specially written program in the open-source software of the microcontroller. Resultant readings at the two load cells are F_1 and F_2 for load cell L_1 and L_2 respectively. The normal force acting on the roller would be:

$$F_N = W - (F_1 - F_2) \quad \textbf{4.1}$$

Rotate the speed knob on the control unit to set the desired linear velocity at the point of contact. Put the second surface (finger pad) on the base. When the desired value of normal force (3N) and sliding velocity is set to 4.5 cm/ sec is achieved, subject is advised to apply force on the base platform through the finger to restrict unwarranted touching with the probe.

4.3.2 Fabric and polymeric test material

Rotary tribometers reported in literature performed experiments over forearm [65], [66] , leg [66], scars [67], cheek [68] abdomen [69] and finger pad [37]. Most of the studies having textile and rubber [4], [18], [32], [36], [63], [70] as the countersurface material have used reciprocating (sliding) type tribometers for the friction measurement. This is the first attempt to investigate the friction behaviour of textile and rubber using a rotary type of tribometer on the finger pad skin. As discussed in chapter 3 measurement technique greatly affects the COF values at the contact interface which is evident from the available literature. Various attempts in varied range of normal load, sliding velocity, dry and wet state have been reported in the previous studies.

A. Test subjects

All the experiments were conducted at the constant speed of 4.5 ± 0.5 cm/s. Normal load is varied from 3 N to 12 N to replicate the precision and power grip [71] among subjects of all ages. Since these were the validation tests that are reported here, subjects are referred to as operators. 29-year-old female and 25- & 32-years old males of Indian origin were taken as operators for the tests. Participant selected was briefed about the test protocols and target of study, and the written consent was obtained. All the tests performed on the human test subject were as per the Helsinki declaration.

The experiments for the non- metallic materials were subsequently conducted to validate the gage repeatability and reproducibility (R& R) tests of the developed tribometer.

B. Test material description

Probes of counter surface material namely acrylic, aluminium, brass, copper, and steel are made as per the dimensions shown below in Figure 4.2.

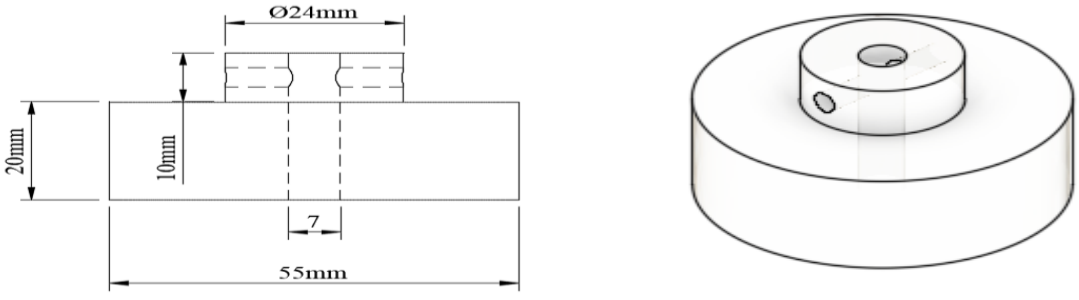

(a) **(b)**

Figure 4.2 Schematic of probe used as test sample

Textile whose frictional behaviour with human skin is to be investigated is mounted on the probe (any one of the metallic probe) with the help of industrial adhesive and rubber fasteners from back as shown in Figure 4.3 . Test material is so well mounted on the probe, it is assumed that there is no relative motion between the textile and the probe. Properties of material being tested is summarised in Table 4.4

Figure 4.3 Wool mounted over the cyllindrical probe

Table 4.4 Properties of the test samples

Material	Warp	Weft	Weight of material ('dry' state)
Cotton	34	33	475 gm/ m^2
Latex	-	-	6 gm/ glove
Rubber	-	-	0.25gm /glove
Knitted wool	-	47	311 gm/m^2

Table 4.5 Material used as parts in gage R & R study

Part Number	Description
1	Cotton-dry
2	Cotton-wet
3	Knitted wool- dry
4	Knitted wool- wet
5	Latex- dry
6	Latex- wet
7	Rubber- dry
8	Rubber- wet

C. Protocol

(1) All tests performed are *in-vivo*. Each subject performs three trials of measurement for each combination of material on the finger pad interface.

(2) As gage R&R study requires random trials to avoid any biasness due to human interaction, a random trial sheet is generated for the combination of the parts, trial, and operators.

(3) Initial readings are taken only for part number 1 ,3, 5 and 7 (as described in Table 4.5) for all three trials and each operator to keep the 'dry' state intact.

(4) 'Wet' behaviour for part 2, 4, 6, and 8 is replicated by dropping 10 µl of ionized water/ cm^2 [16] on the area of investigation. Deionized water is an accurate way to simulate sweating in friction measurement experiments. Minimum time of 1 hour is kept for the measurements to maintain the same wetness behaviour across the trials for the same material.

(5) For the trials to be unbiased and calculations easy, a constant load of 3 N is maintained for 15 seconds in each trial.

(6) All tests were performed at an ambient temperature of 25 ± 2 °C and relative humidity of 55 ± 10 %.

D. Experimental results and discussion

Figure 4.4 represents the trial 1 (of validation) measurements of subjects S1, S2 and S3 in both dry and wet conditions for cotton, latex, rubber, and knitted wool. Pronounce effect on COF for the 'wet' state is obtained for all the tested materials as shown in Figure 4.4 (a)-(d). It is observed that the COF values decrease with increase in load. In Figure 4.4 (a) – (d), COF decreases with increasing normal load in accordance with the literature [72], except for knitted wool.

Figure 4.4 (a) illustrates COF values in 'wet' state approximately twice to that of 'dry' state. This is attributed to viscoelastic nature of human skin, normal load and contact area [73]. Wet state causes an increase in the effective contact area, enhancing the adhesion component and thereby increasing the friction at the interface as shown in Figure 4.3 (a) , (b) and (c).

Figure 4.4 (b) and (c) depicts the behaviour of two polymeric materials latex and rubber. Continuous decrease in COF values with increasing normal load is observed. A sudden change in the 'dry' state COF values for operator 1 between the normal load of 9 and 12 N, may be attributed to the micro parameters such as finger ridges, skin elasticity and contact indentation which is out of scope for the current study.

Figure 4.4 (d) shows COF values for knitted wool in dry state more than of the wet state. In dry state knitted wool undergoes a relative sliding over the skin without any lubrication. Besides less lubrication orientation and hairy yarns contribute to the increase in COF. For the 'wet' state with increase in normal load, water squeezes out making a very thin layer at the interface resulting almost constant COF.

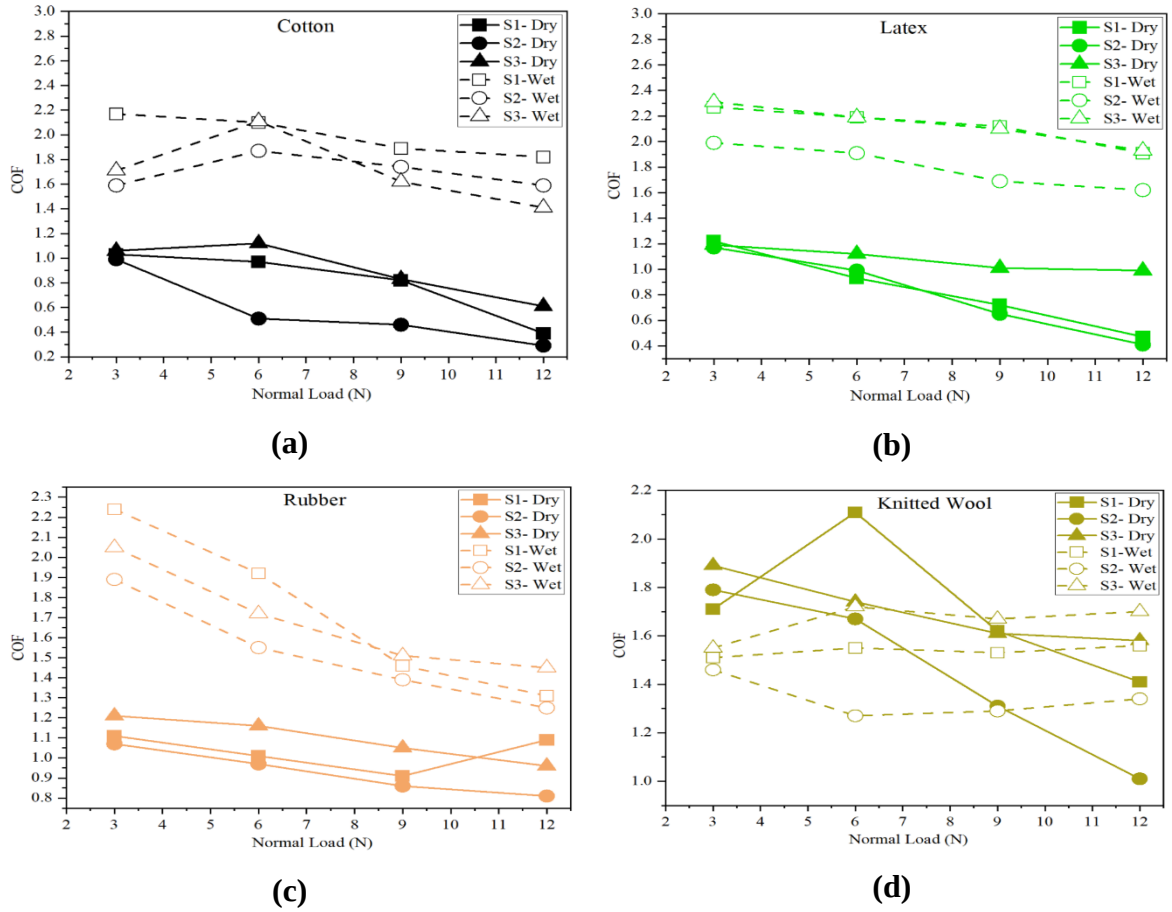

Figure 4.4 Plot of COF vs normal load for (a) Cotton, (b) Latex, (c) Rubber and (d) Knitted wool

4.3.3 Metallic and plastic test samples

Human skin friction measurements with metallic or plastic as a countersurface test material is studied by various researchers through rotary type tribometers. An experimental investigation is conducted for identifying the factors affecting human skin frictional behaviour [37]. The study takes aluminium cylinder as the countersurface material. COF ranged between 0.73 to 3.86. Experiments were conducted on ventral and dorsal forearm as well. Out of the three tested anatomical regions finger pad reported the maximum COF irrespective of the age of test subjects.

Study for the friction measurement of human skin taking palm of hand as site of investigation, reported the mean COF of 0.42 ± 0.14, 0.61 ± 0.21, and 0.46 ± 0.15 respectively for aluminium, pelite, and silicone [66]. Experiments were conducted at normal load of 25 to 100 N and rotational speed of 25 to 62.5 RPM. The plot shows a consistent decreasing trend of COF with increasing normal load in Figure 4.5. COF was reported to have a directly proportional relationship with rotation speed.

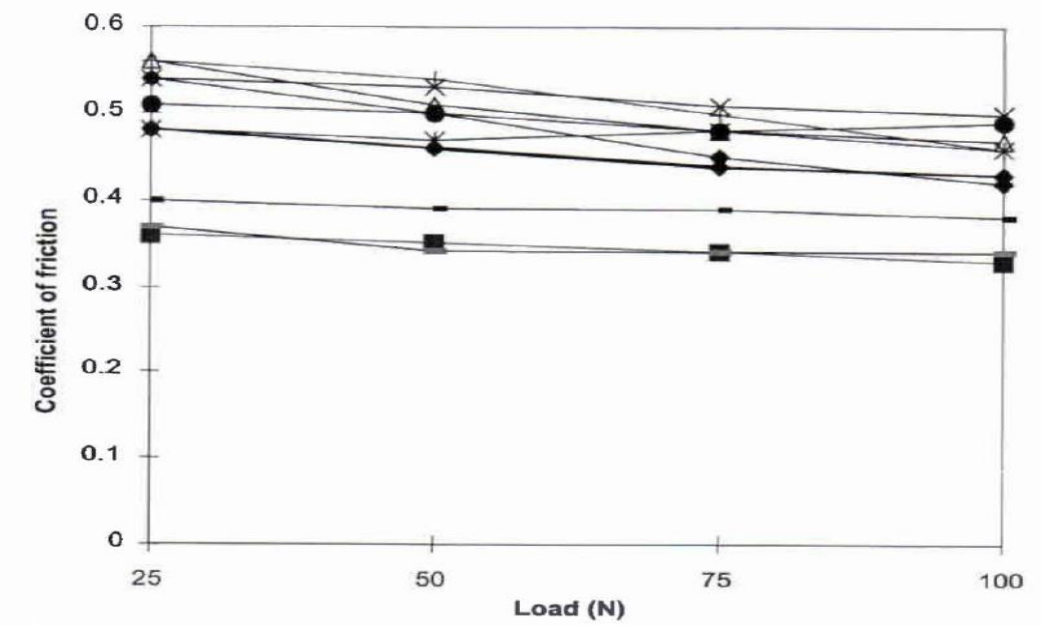

Figure 4.5 Change in friction with normal load [66]

A. Test subjects

All the experiments were conducted at different normal loads and sliding velocities. Normal load is varied from 4 N to 10 N with a step of 2 N well within the validated range of the developed tribometer. Sliding velocity was varied in the range of 4.5 cm/ sec to 10.5 cm/ sec with a step of 2 cm/ sec. Four test subjects 30, 32, 25-year-old-male and 29-year-old female of Indian origin were taken as subject 1, subject 2, subject 3, and subject 4 respectively. Skin hydration measured at the site of investigation was 34, 37, 21 and 40 (A.U.) for subject 1, 2, 3 and 4 respectively. Participant selected was briefed about the test protocols and target of study, and the written consent was obtained. All the tests performed on the human test subject were as per the Helsinki declaration.

B. Test material description

Probes of counter surface material namely acrylic, aluminium, brass, copper, and steel are made as per the dimensions shown in Figure 4.2. Conventional lathe was used for acrylic, all other

metallic probes were made through computer numerical control (CNC) facility at the central workshop of BITS Pilani as shown in Figure 4.6. Surface roughness parameters such as R_a (Roughness average), R_q (Root mean square roughness), R_z (Mean roughness depth), R_p (Maximum peak height of the roughness profile), R_v (Maximum valley depth of the roughness profile), R_{sk} (Core roughness depth), and R_{ku} (Sharpness of profile peaks), are tabulated in Table 4.6.

Table 4.6 Surface roughness parameters for the test probes

Parameter → Probe ↓	Ra (µm)	Rq (µm)	Rz (µm)	Rp (µm)	Rv (µm)	Rsk (µm)	Rku (µm)
Acrylic	2.05	3.45	12.27	5.15	10.35	-0.685	3.18
Aluminium	3.15	4.14	24.67	6.36	17.31	-1.22	4.58
Brass	2.173	2.72	15.15	7.41	7.738	-0.06	16.19
Copper	0.94	1.40	8.33	1.20	7.12	-3.08	2.94
Steel	1.53	1.88	8.66	3.13	5.53	-0.39	2.87

Probes were tested for the roundness and the cylindricity through ROUNDTEST RA-1600 (Mitutoyo) and the details of measurement are listed in Table 4.7 below.

Table 4.7 Roundness and cylindricity of the test probes

Probe	Roundness (µm)	Cylindricity (µm)
Acrylic	10.58	12.28
Aluminium	11.68	13.52
Brass	12.21	14.94
Copper	10.81	16.73
Steel	15.69	15.09

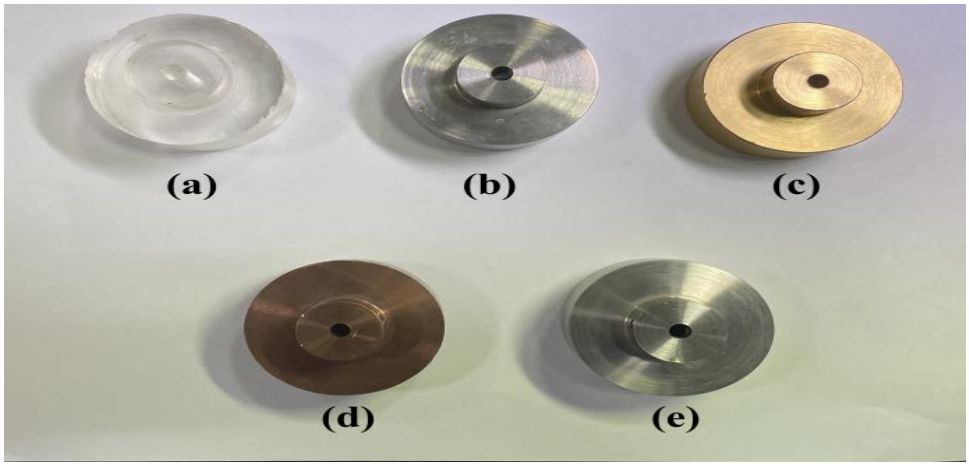

Figure 4.6 Probes used as counter surface material (a) acrylic, (b) aluminium, (c) brass, (d) copper and (e) stainless steel

C. Experimental results and discussion

Variation of normal load with sliding velocity for all materials investigated here, is in strong agreement with the literature that suggests with increasing normal load COF decreases with few exceptions as discussed in detail in the later part of this section. The plot for dry and wet keeping all other factors such as velocity, load and subject shows higher COF values for wet state than that for the dry state which again, is potentially valid as per the literature [51]. The variations that are seen in the COF values are mainly due to the individual differences in the moisture at the asperity level [73]. The decrement in the COF values with increasing normal load agrees to the adhesion friction model.

Following sections would discuss the variations of COF with normal load for the five materials tested here namely acrylic, aluminium, brass, copper, and steel.

I. Acrylic:

Figure 4.7 (a)-(d), present variation of COF at finger pad with the applied normal load for subject 1, 2, 3 and 4 respectively for acrylic. Experimental investigation reported COF values of 2.16 to 6.12 in the dry state and 3.19 to 7.41 for the wet state. In Figure 4.7 (a) For subject 1, a gentle gradient decrease in COF at normal load of 6, 8 and 10 N for 6.5 cm/ sec velocity is attributed to the stick-slip phenomenon observed at the interface. In wet state average highest COF of 5.88 is obtained at sliding velocity of 10.5 cm/ sec compared to 4.67 of that in the dry state. In Figure 4.7 (b) at 8 N normal load for 6.5 cm/ sec, dry COF is 0.61 % lower from the average COF while that for the wet state it is increased by 3.79 % through the average value of all subjects. For the wet state after 4 N normal load, COF becomes constant due to non-varying contact area. Across all subjects Figure 4.7 (c) distinguishes the COF variation with normal for

wet and dry state of subject 3. Wet state COF is varied between 4.33 to 7.41 while the dry state COF ranges from 3.66 to 6.11. Figure 4.7 (d) shows the highest COF of 6.06 at 6 N and 10.5 cm/ sec when compared to the average in the dry state.

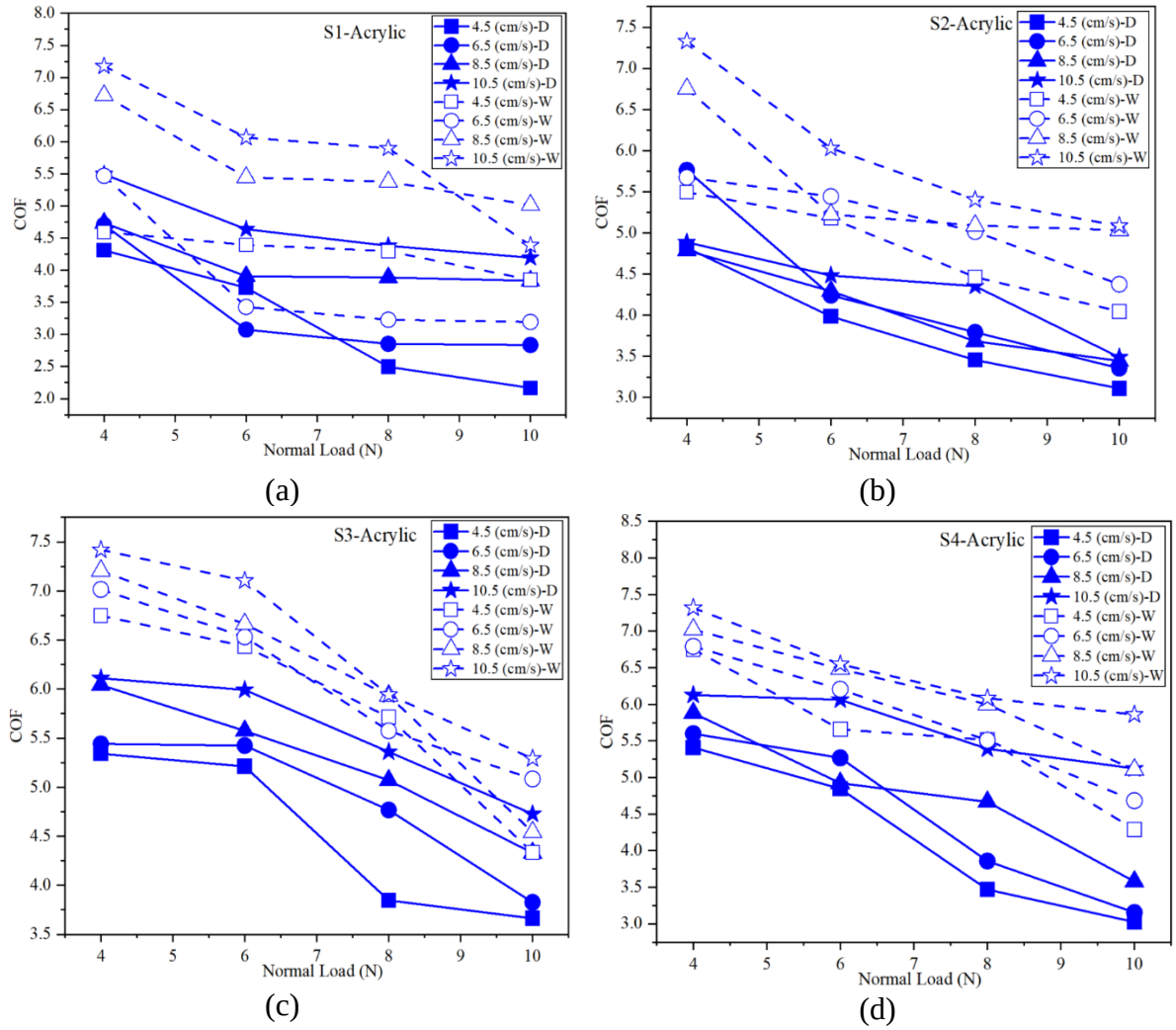

Figure 4.7 Plot for variation of COF with normal load for acrylic (a) subject 1, (b) subject 2, (c) subject 3 and (d) subject 4

II. Aluminium:

Figure 4.8 (a) - (d), present variation of COF at finger pad with the applied normal load for subject 1, 2, 3 and 4 respectively for aluminium. Experimental investigation reported COF values of 2.27 to 8.36 in the dry state and 2.95 to 8.75 for the wet state. In Figure 4.8 (a) at the intermediate velocities of 6.5 cm/ sec and 8.5 cm/ sec steep gradient change is observed at 6 N with 9.3 % and 8 N with 0.85 % decrease in COF from the average value. Figure 4.8 (b) shows at higher velocity of 10.5 cm/ sec and low normal load of 4 N very fewer difference in the COF of 0.18 in the dry state. This may be because of the incomplete contact at the interface that

increases with the increasing normal load. In Figure 4.8 (c) minimum COF is obtained for the speed of 6.5 cm/ sec and 10 N normal load in the dry state. Maximum COF of 8.75 is obtained at 10.5 cm/ sec speed and 4 N normal load highlighting that the wet contact area decreases with increasing normal load due to water splashing. Figure 4.8 (d) highlights maximum average decrease of 30.72 % in COF value at 6.5 cm/ sec and 10 N normal load in comparision to other corresponding average COF values due to gender-based subjectivities.

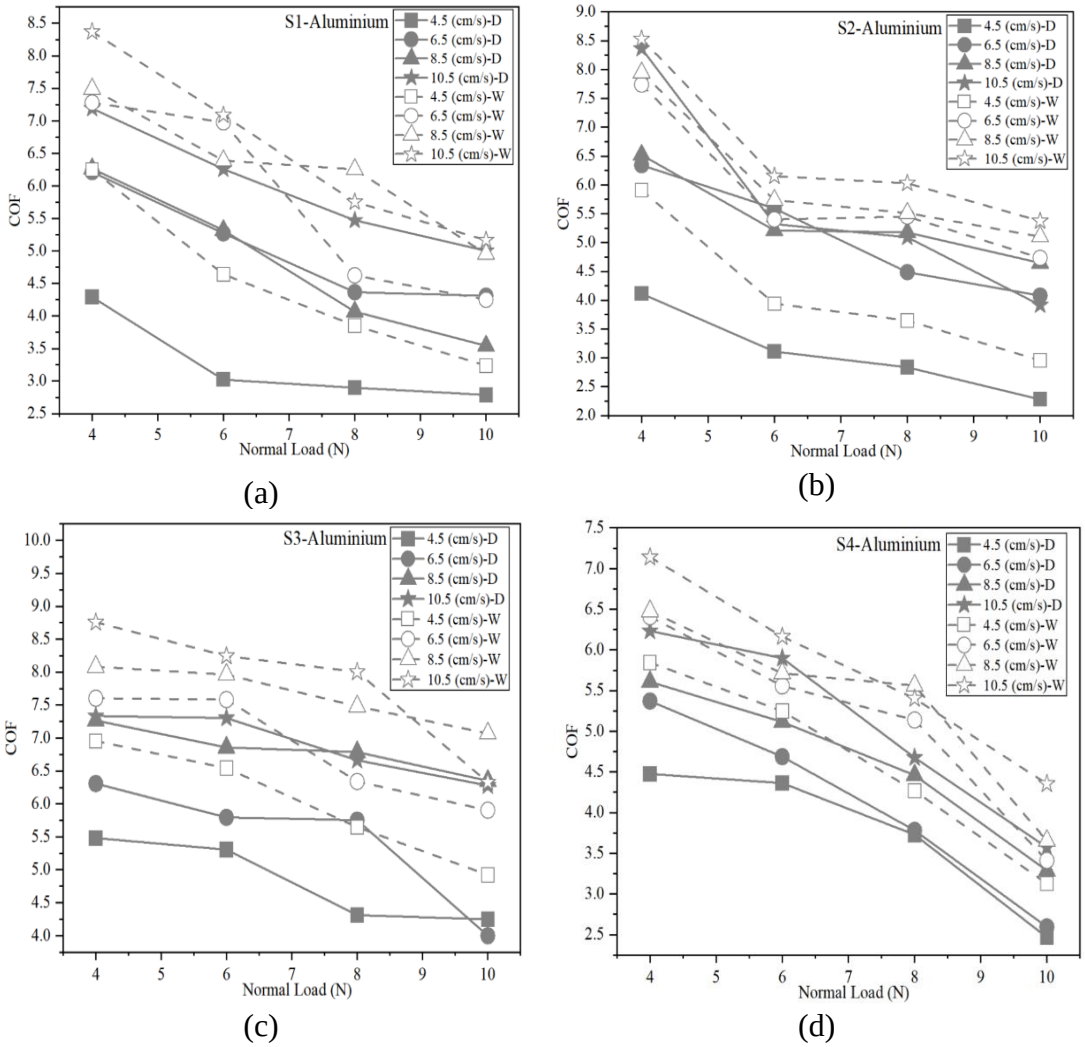

Figure 4.8 Plot for variation of COF with normal load for aluminium (a) subject 1, (b) subject 2, (c) subject 3 and (d) subject 4

III. Brass:

Figure 4.9 (a) – (d), presents variation of COF at finger pad with the applied normal load for subject 1, 2, 3 and 4 respectively for brass. Experimental investigations reported COF values of 0.99 to 4.08 in the dry state and 1.43 to 5.65 for the wet state. As discussed in earlier sections, wet contact generates higher shear forces compared to that in the dry state due to increased

contact area. Figure 4.9 (a) shows the prominent decrease in COF values across the data points of investigation. In wet state for 6.5 cm/ sec very little variation of 0.04 is observed at 6 N and 8 N. At 8 N, COF varies approximately in the range of 0.50 from 10.5, 8.5 and 6.5 cm/ sec. Figure 4.9 (b) and (c) shows the neat variation of COF with normal load both in dry and wet state. Figure 4.9 (d) shows the sudden change in gradient between 6 N and 8 N 8.5 cm/ sec dry state sliding due to the sudden breakage of the interfacial shear bonds developed at the interface to the viscoelastic nature of the human finger pad which generates the local deformations consequently affecting the epidermis- the soft upper layer of skin.

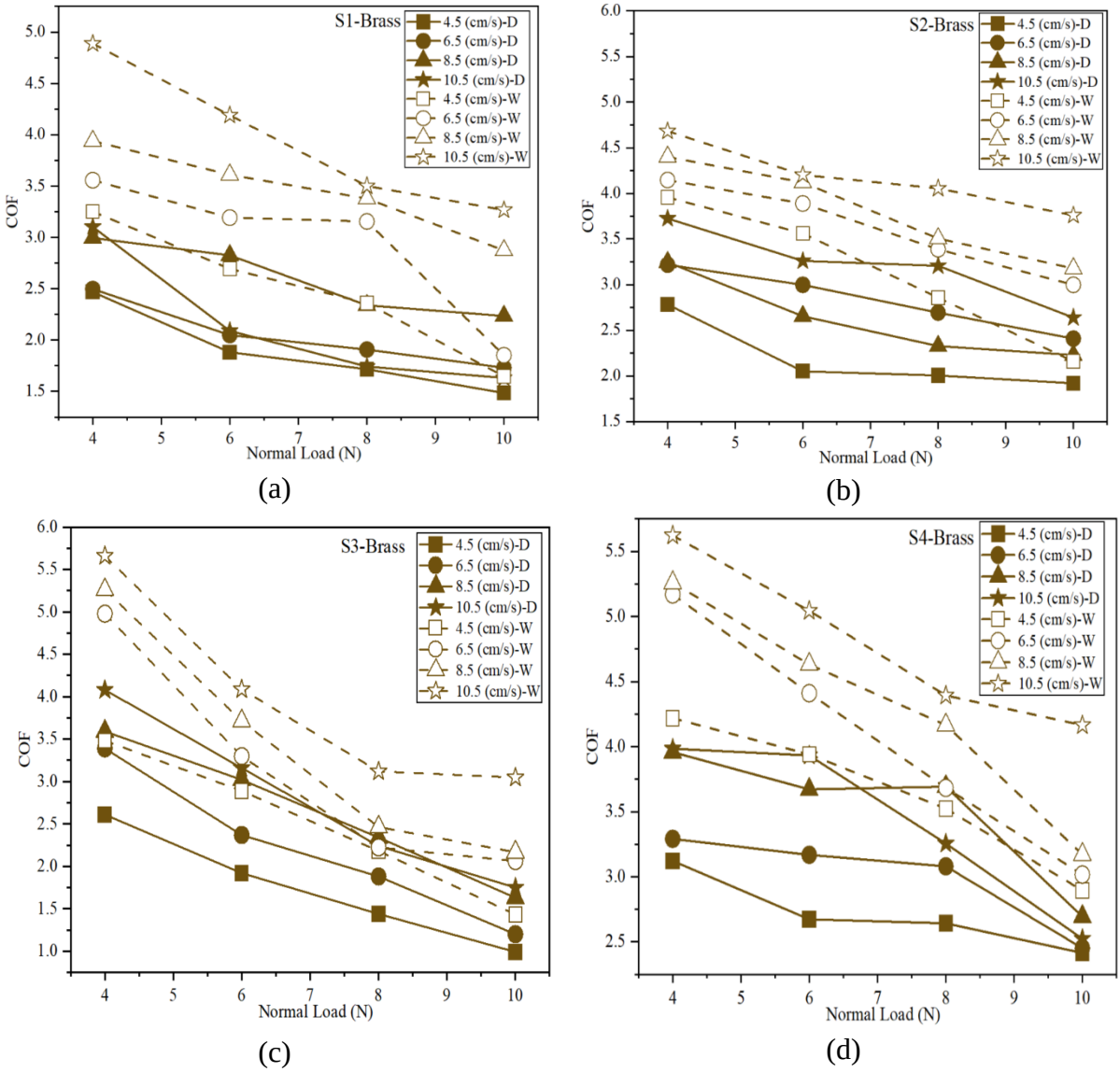

Figure 4.9 Plot for variation of COF with normal load for brass (a) subject 1, (b) subject 2, (c) subject 3 and (d) subject 4

IV. Copper:

Figure 4.10 (a) – (d), presents variation of COF at finger pad with the applied normal load for subject 1, 2, 3 and 4 respectively for copper. Figure 4.10 (a) Plot for 6.5 cm/ sec in wet state shows the effect of sliding velocity in the mid-range normal load on the COF at the interface. Obtained variation might be associated with the stick slip phenomenon at the contact interface. In Figure 4.10 (b) at 10 N in the wet state COF varies in the range of 2.20 ± 0.20 across all speeds highlighting the tribologically saturated state: in terms of load, speed, and lubrication. In Figure 4.10 (c) with increasing loads a steep decrease in the COF values for the plot of 10.5 cm/ sec in dry state is attributed to the high slipping at the contact interface with reduced friction. Saturated contact area is obtained in the wet at 6 N load for the variation plot of higher velocities as shown in Figure 4.10 (d).

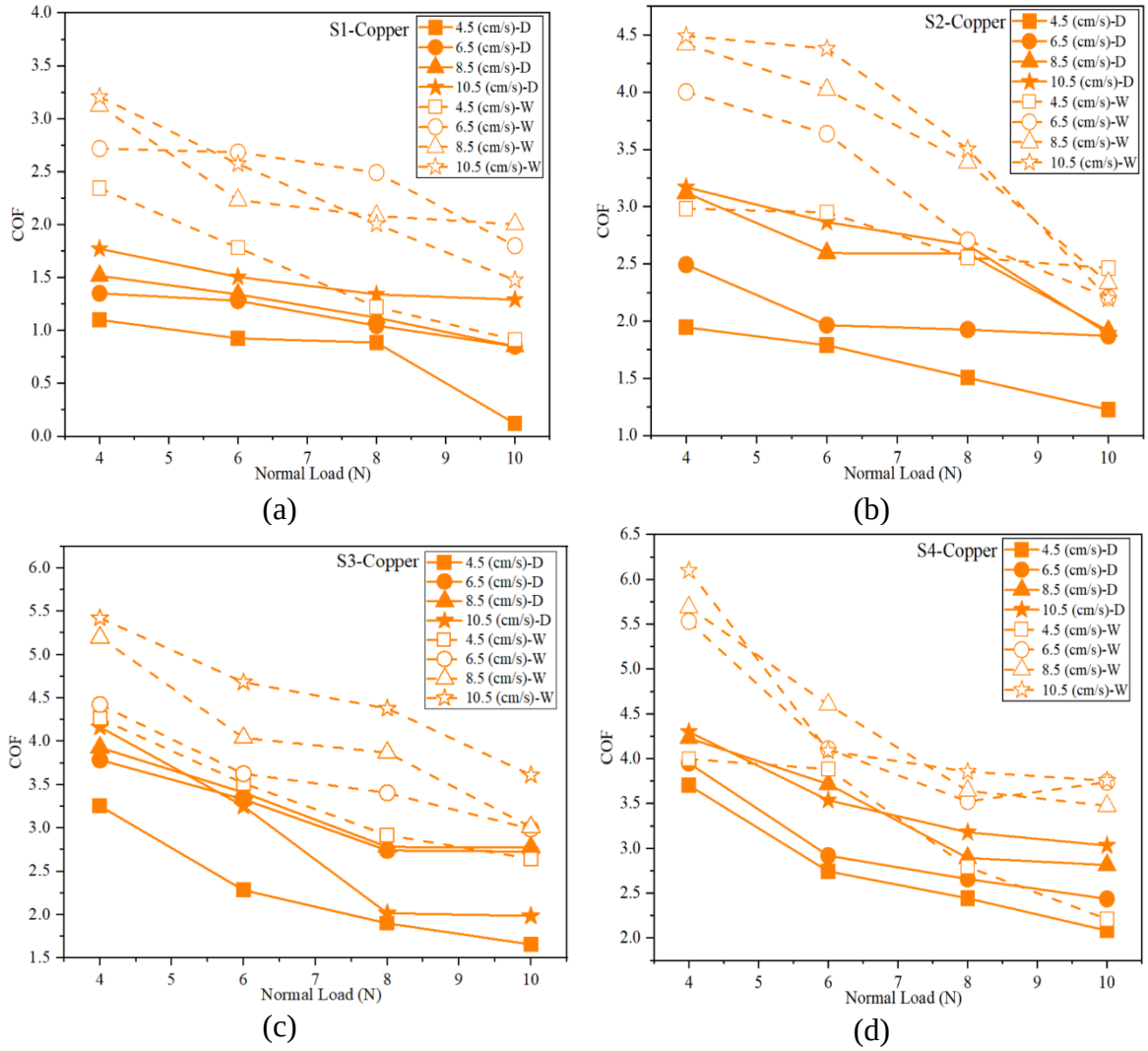

Figure 4.10 Plot for variation of COF with normal load for copper (a) subject 1, (b) subject 2, (c) subject 3 and (d) subject 4

V. Stainless steel:

Figure 4.11 (a) – (d) presents the plot for the variation of COF of steel with normal load for subject 1, subject 2, subject 3 and subject 4. COF varied between 1.62 to 6.72 for the dry state and 2.20 to 8.05 for the wet state. Figure 4.11 (a) and (b) shows the inconsistent variation across different sliding velocities for the wet state which might be due to the partial contact obtained when the steel probe rolls over the finger pad. Since real time data is recorded it is very difficult to distinguish from the tribological perspective for the COF value. Figure 4.11 (c) shows the sudden increase in COF at 10 N for 8.5 cm/ sec sliding velocity in dry state. In dry state the deformation component becomes more pronounce then the adhesion component of friction. In Figure 4.11 (d) Wet state plot at 8 N shows negligible variation at all higher speeds of 6.5, 8.5, and 10.5 cm/ sec highlighting a point of saturation for the frictional contact at the interface.

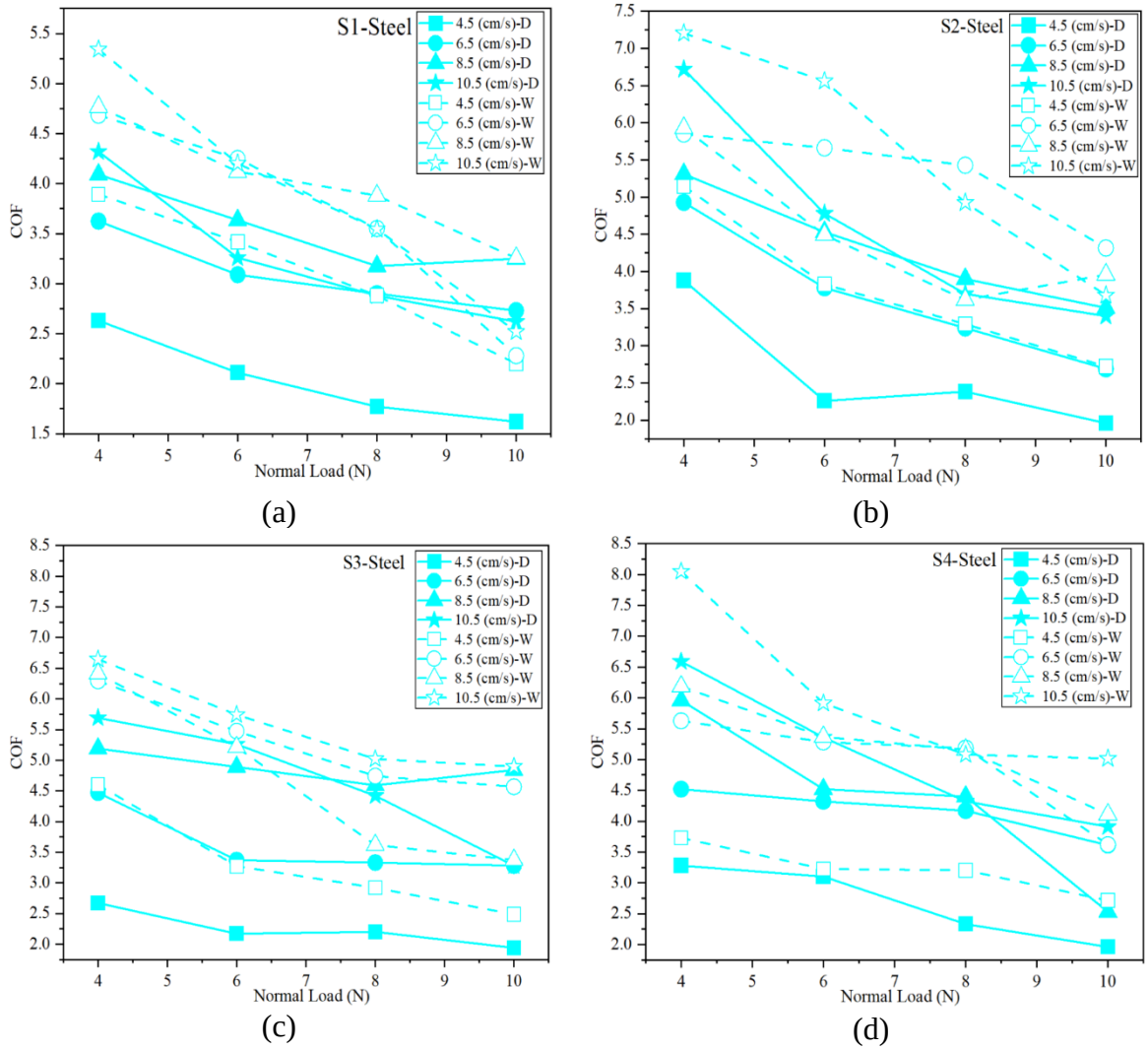

Figure 4.11 Plot for variation of COF with normal load for steel (a) subject 1, (b) subject 2, (c) subject 3 and (d) subject 4

The above sub-section discusses the material wise dependence of COF on normal load and sliding velocities on the four test subjects both in dry and wet conditions. To make the results more conclusive, the COF behaviour for subject 1 for all the five materials, at varying sliding velocity and at 4 N minimum and 10 N maximum normal load in dry and wet state is discussed. Furthur, the COF behaviour for subject 1 for all five materials, at varying normal loads and at 4.5 cm/ sec minimum and 10.5 cm/ sec maximum sliding velocity in dry and wet is plotted. Also the comparative analysis for dry and wet state is done for all 4 subjects for the acrylic material at maximum and minimum sliding velocities.

D. Detailed discussion on friction behaviour across subjects and test materials

Experimental investigations were performed with five material test probes for the measurement of human skin friction. Wet state COF is reported to be higher than the dry state COF across all the materials tested. This is attributed to the increase in contact area in the wet state that in turn results in increased friction values. In dry state a partial contact is established that neglects the finger ridges and capillary. Presence of water develops a full contact resulting in higher adhesion phenomena thereby increasing the COF at the interface [18], [39].

All the materials tested show the consistent increase in the COF values both for the dry and wet state with increasing velocity [42], [74], [75]. Friction coefficient is the ratio between the friction and the normal force irrespective of the normal load as per the Amonton's first law.

Although because of the non- linear nature, and skin being viscoelastic, adhesion friction is the predominant mechanism, at higher loads and roughness deformation component should not be ignored [76]. At certain normal loads, deviation of sliding velocity from this trend is observed which is related to the subjectivities associated with the test environment and volunteers. Still, the exact physical mechanisms that lead to increase in friction are unexplored in true essence, because of the micro scale contact attributes that affect the surface properties [51]. Energy dissipation through internal damping occurs because of the deformation and relaxation cycle [77], [78].

Figure 4.12 (a) and (b) depict the variation of COF for subject 1 at minimum normal load 4 N and maximum load of 10 N at multiple sliding velocities for all the five materials. Wet state Aluminium shows the maximum COF. This is attributed to the surface roughness of the probe as tabulated in Table 4.6. For rough surfaces with increasing surface roughness an increase in COF is observed [79]. R_a surface roughness parameters do not contain any information for the

size, shape, or density but only the statistical parameters describing the height of the profile. Increasing skin friction with probe roughness follows the theory of Moore for elastomers. Theory suggests that COF increases with increasing roughness amplitude [80].

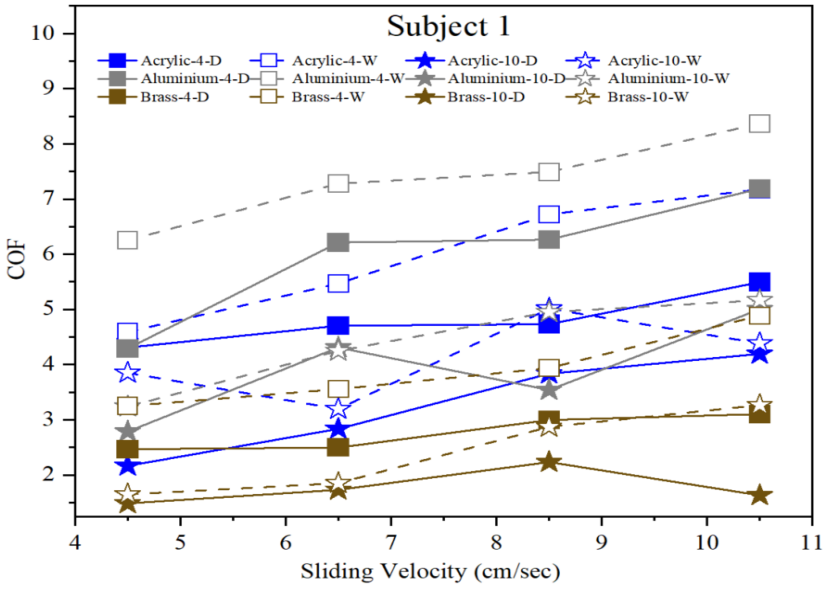

(a)

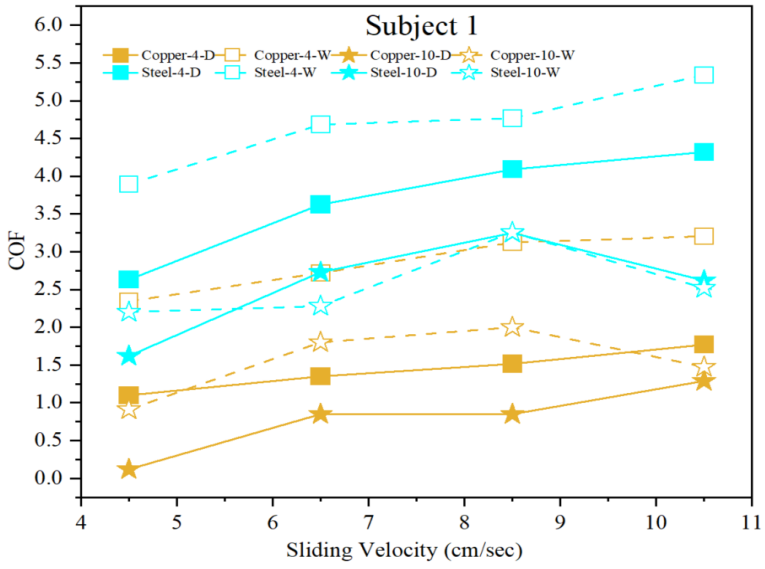

(b)

Figure 4.12 Plot for variation of COF for subject 1 with sliding velocity at 4 and 10 N of normal load in dry and wet state for (a) acrylic, aluminium & brass and (b) steel and copper

Figure 4.13 (a) and (b) depicts the variation of COF for subject 1 at minimum velocity of 4.5 cm/ sec and maximum velocity of 10.5 cm/ sec at multiple normal loads for all the five materials. In majority, with increasing normal load, a neat trend of decreasing COF is observed that is in alignment with the reported literature. Variation in size of decrease in COF depends on the range of normal load, counter surface material and nature of interface [46], [81], [82]. Since the deformation term is usually less pronounce than the adhesion component in friction measurement, it varies with the skin condition [63]. Another reason for decrease in COF with normal load increase is the flattening of contact surface under high compression and increasing the contact area. Strong dependence of the COF is reported because of the normal adhesion at the contact. Current study assumes that the real contact area varies in proportion to the contact area being measured. Viscous forces not measured here affect the COF at the interface due to the intrinsic characteristics of skin.

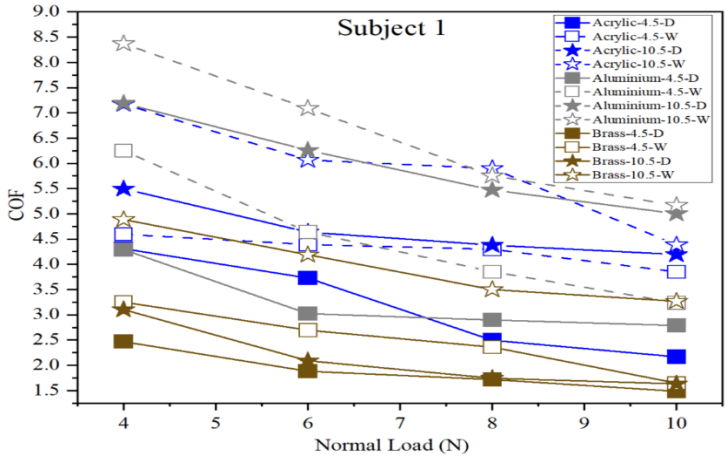

(a)

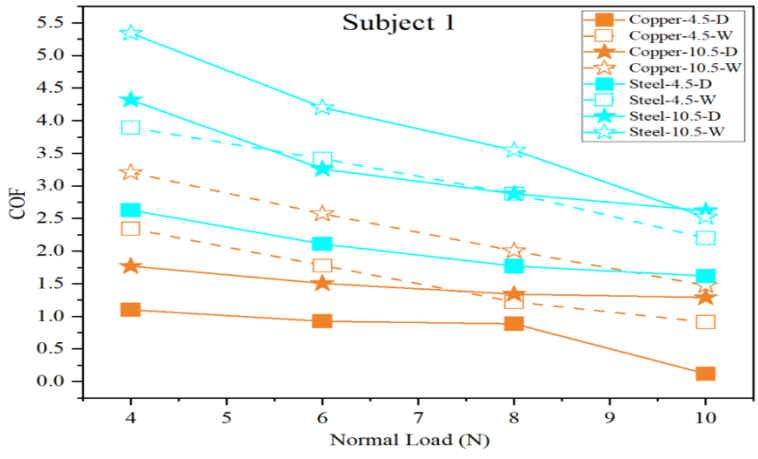

(b)

Figure 4.13 Plot for variation of COF for subject 1 with normal load at 4.5 and 10.5 cm/ sec of sliding velocity in dry and wet state for (a) acrylic, aluminium & brass and (b) steel and copper

Figure 4.14 (a) and (b) represents the plot of COF with normal load of all four subjects both in dry and wet state for acrylic. Plot highlights the higher COF values for subject 3 and subject 4 at both 4.5 cm/ sec and 10.5 cm/ sec sliding velocites. Higher wet state COF values have been elaborately discussed in the previous sections. Higher COF for high sliding velocity and low normal loads is very clearly evident from the plot below. Although studies [18], [68], [69], [83] report the high correlation between COF and the skin hydration and few studies have developed various relationships such as Linear[18], [69], Power-law [68] , exponential [83] and bell shaped [84], [85] for the two physical parameters. This study does not comprehensively comments about the relation of COF with the hydration of the test subjects across the test materials.

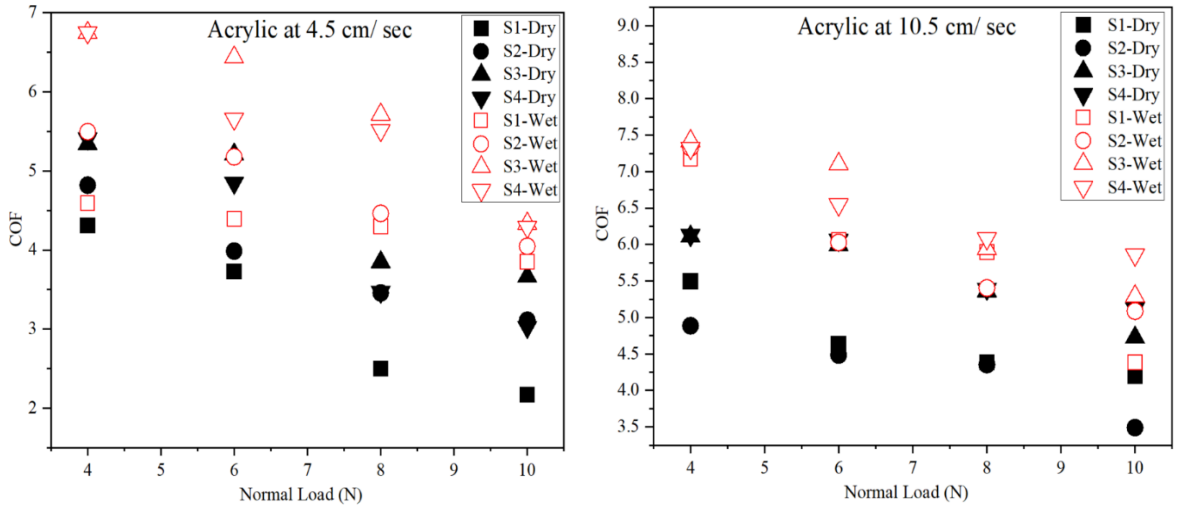

(a) **(b)**

Figure 4.14 Plot for variation of COF with normal load in dry and wet state for all 4 subjects (a) at 4.5 cm/ sec sliding velocity and (b) 10.5 cm/ sec sliding velocity

The common empirical approach to express measurement data for the friction force F is in the form of $F = k.N^n$, where K corresponds to the COF at unit normal load. Hence the COF as a function of normal load is given by $\mu(N) = k.N^{n-1}$ [86]. To relate this friction measurement data to the friction mechanism a linear regression is performed. As shown in Figure 4.15 (a) and (b) depicting a power law fit for the COF versus normal load plot for subject 1 at 4.5 cm/ sec of sliding velocity for dry and wet states respectively. Value of exponent n range from 0.20-0.82 which is well in accordance with the mean value of 0.68 reported in a previous studies [84], [87] except for copper. For the acrylic material in wet state, fit is almost a straight line. Normal load values taken for the current study were well in the range of previous studies for

comparative analogy of the regression fit. Deviation of copper from the mean value is attributed to its smooth surface finish and high real contact area in the friction measurement.

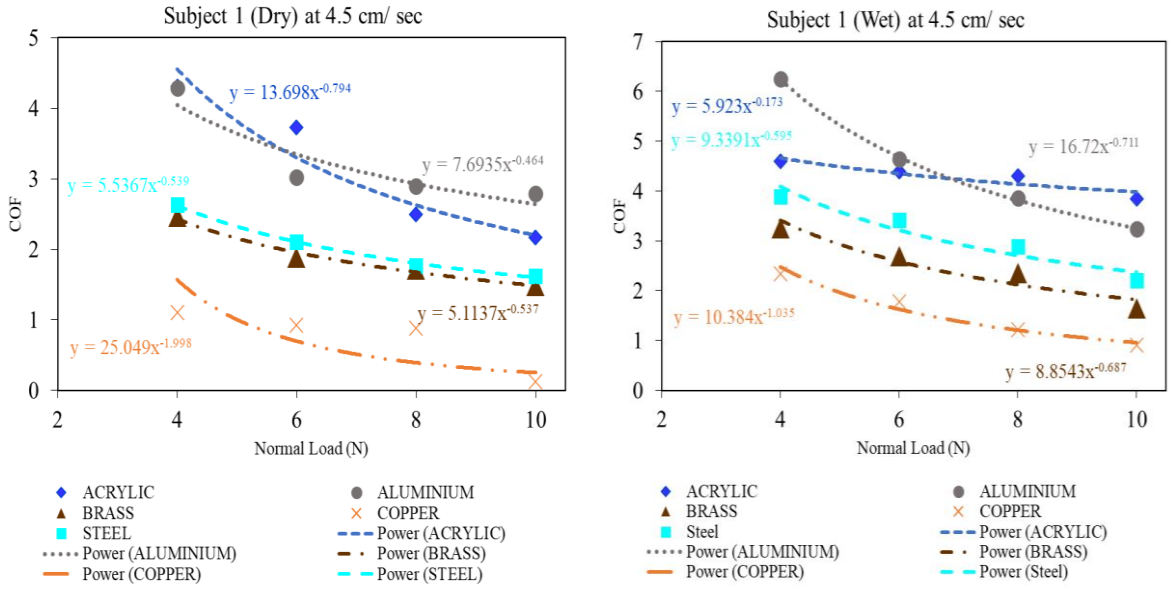

(a) **(b)**

Figure 4.15 Power law fit for the COF versus normal load plot for subject 1 at 4.5 cm/ sec of sliding velocity in (a) dry and (b) wet state

4.4 Experimental Investigations of COF with STT

This section presents the experimental results and its analysis obtained through the reciprocating (sliding) type human skin tribometer. Study [88] presents the measurement principles for skin friction shown in Figure 4.16 below.

(a) Rotating probe (b) Sliding probe (c) Moving skin

Figure 4.16 Various contact configuration for human skin tribological measurements adopted from [88]

Measurement principles shown above have their own robustness and technical or operational flaws associated to them. In Figure 4.16 (c) skin is moved over to the stationery sample.

An attempt to highlight the contribution of micro- scale forces in the total friction force for both the dry and wet skin is done in [44]. Study reported, when the asperities are too high or

positioned closed to each other valleys are not filled and hence only the partial contact occurs as shown in Figure 4.17.

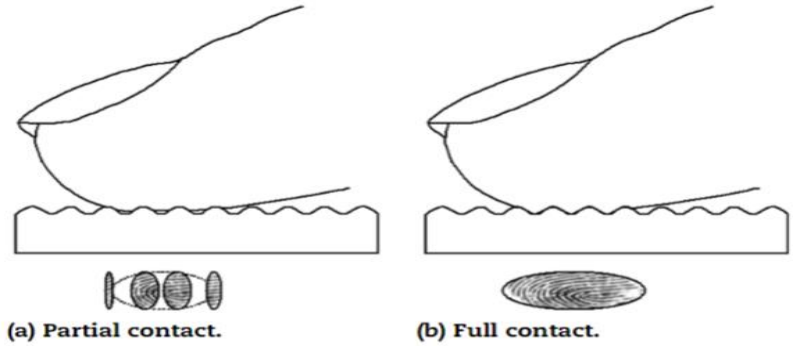

Figure 4.17 Represntation of dependance of contact on micro geometry and loading conditions [**44**]

An experimental study reports the complex relationship between COF with normal load and moisture contents. Variation of COF with normal load as shown in Figure 4.18 at a particular moisture condition is a function of power law [84].

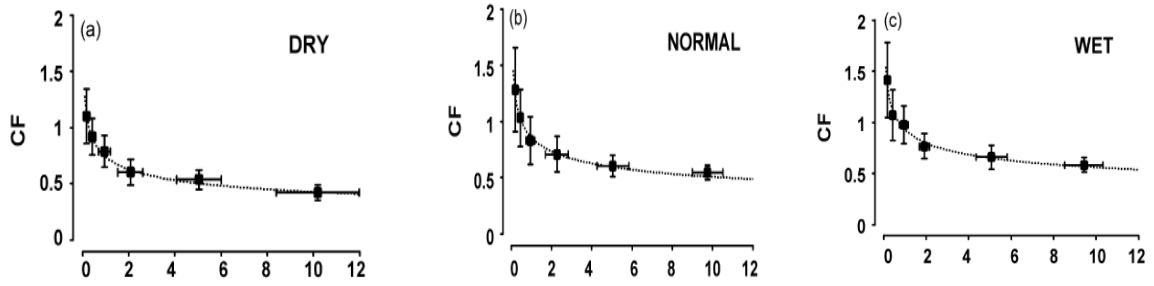

(a) (b) (c)

Figure 4.18 Relationship between coefficient of friction (COF) and normal load [**84**]

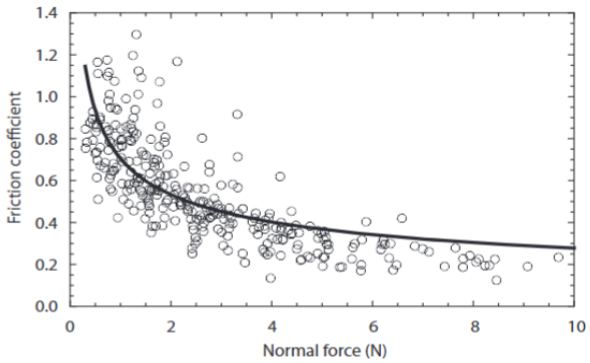

Figure 4.19 Friction coefficient of the finger pad sliding in wet state [**46**]

An investigation to study the stick-slip behaviour of index finger sliding in wet state on rough and smooth glass as a function of normal load and sliding velocity is attempted. A change of

more than ± 25% in amplitude of COF from mean value is reported [46]. Two major reasons for deviation were attributed to the substantial variations in friction force during stick-slip and variations in the application of normal load by the test subjects. A decreasing trend of COF with normal load is obtained in the range of 0 to 10 N shown in Figure 4.19.

Study presents the influence of variations in pressure distribution on the friction of the finger pad [73]. Analytical results show that the pressure distribution affects the COF. In turn, its influence cannot be separated with those factors such as variations in the skin hydration or the finger positions in the measurements. Figure 4.20 (a), (b), and (c) below depict the effect of low normal force variation on the friction force, COF and contact area respectively.

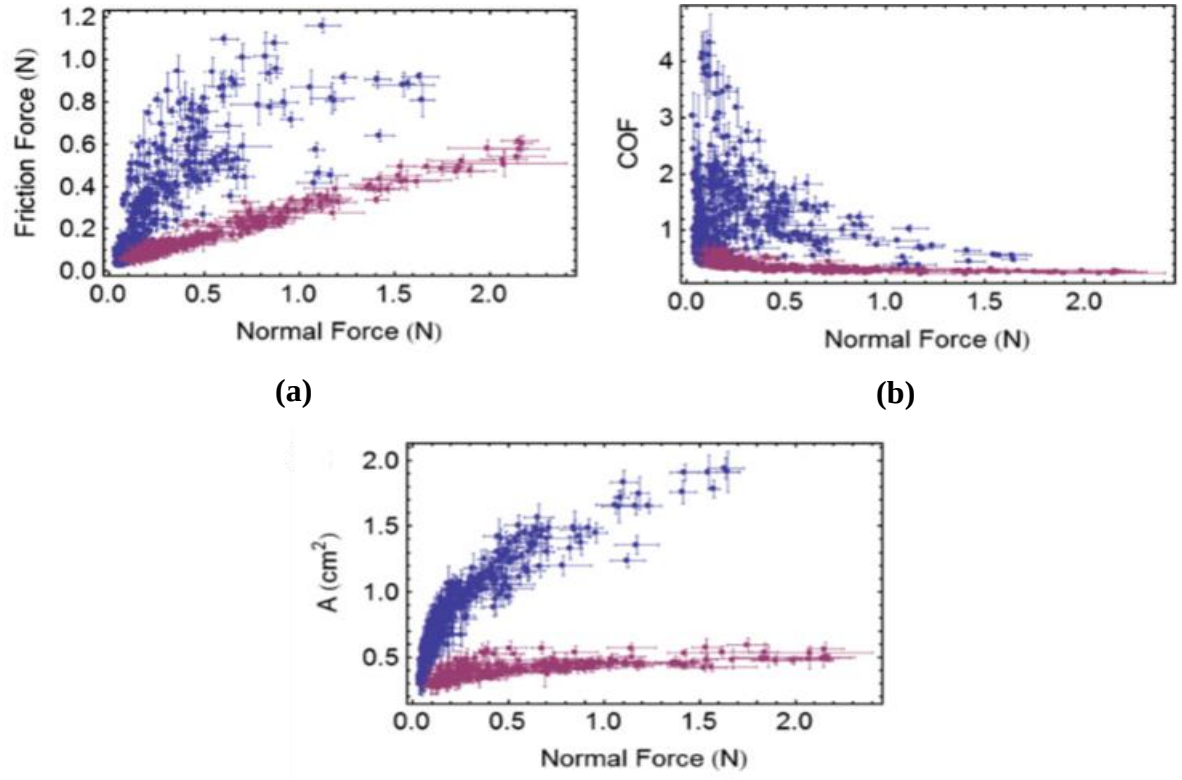

(a) **(b)**

(c)

Figure 4.20 Variation of nnormal load with (a) friction force, (b) COF, and contact area [73]

In current study the motion is given to the test sample beneath the skin, and finger pad friction is measured (although other limb areas can also be investigated). Experiments are performed as per the protocols discussed in the later part of the sub section.

A. Test subjects

All the experiments were conducted at different normal loads and sliding velocities. Normal load is varied from 2 N to 15 N at all points. Sliding velocity was varied in the range of 20 mm/

sec to 60 mm/ sec with a step of 10 mm/ sec. Six test subjects 30, 31, 32, 33, 35-year-old-male and 30-year-old female of Indian origin were taken as subject 1, subject 2, subject 4, subject 5, subject 6 and subject 3 respectively. Participant selected was briefed about the test protocols and target of study, and the written consent was obtained. All the tests performed on the human test subject were as per the Helsinki declaration and the ethics committee of the institute.

B. Test material description

Plates (10 *10 cm) for the counter surface material namely acrylic, aluminium, brass, copper, sun mica (referred as mica), steel and wood were fabricated as shown in Figure 4.21. Surface of the counter material was precisely polished and treated for any unevenness. Samples were prepared at the central workshop facility of BITS Pilani. Surface roughness parameters such as R_a (Roughness average), R_q (Root mean square roughness), R_z (Mean roughness depth), R_p (Maximum peak height of the roughness profile), R_v (Maximum valley depth of the roughness profile), R_{sk} (Core roughness depth), and R_{ku} (Sharpness of profile peaks), are tabulated in Table 4.8.

(a) (b)

Figure 4.21 Fabricated plates used as test material (a) Acrylic and (b) Wood

Table 4.8 Roughness parameters for the fabricated plates used as the test sample for tribological testing

Parameter → Material ↓	Ra (µm)	Rq (µm)	Rz (µm)	Rp (µm)	Rv (µm)	Rsk (µm)	Rku (µm)
Acrylic	0.56	0.67	2.27	1.53	0.74	-0.97	1.99
Aluminium	2.34	3.00	15.41	5.65	9.76	-0.77	3.69
Brass	0.36	0.51	3.33	1.37	1.95	-0.51	6.46
Copper	2.00	2.67	16.27	5.53	10.74	-0.97	5.25

Steel	1.34	1.43	12.68	3.39	7.41	-0.45	2.25
Sun mica	0.42	0.51	0.96	1.80	0.67	-0.58	0.85
Wood	6.34	8.5	56.84	21.37	35.47	-0.82	5.27

C. Protocol

(1) Test sample is mounted over the force plate with a ½ inch screw and a washer to fasten the counter surface to the force plate, to restrict any relative motion between them (force plate and material).

(2) Once the subject is acclimatised and briefed about the procedure, linear drive is set to 20 mm/ sec for one complete reciprocation of the linear drive. With completion of each cycle speed is increased by a step of 10 mm/ sec up to 60 mm/ sec.

(3) All performed tests performed are of *in-vivo* nature. Subject applies and controls the normal load through a screen attached to the measurement unit. A support fixture is provided to maintain a contact angle of 30 - 45 degrees between finger pad and contact material.

(4) Normal force (F_Z) and tangential force (shear force- F_X) are deduced as per Figure 4.22. F_Y is assumed to not take part in the shear force generation as no separate motion exists in the Y direction (along the DAQ cable) as in Figure 4.22 (c).

(5) Data acquisition system generates a .csv file at the frequency of 10 kHz for each sliding velocity.

(6) A specially written macro-enabled program separates the data for normal load and shear forces (both the direction) in the range of 2 N to 15 N with a step of 1 N to calculate the coefficient of friction value as the ratio of F_X / F_Z at sliding velocities of 20, 30, 40, 50 and 60 mm/ sec.

(7) All tests were performed at an ambient temperature of 25 ± 2 °C and relative humidity of 55 ± 10 %.

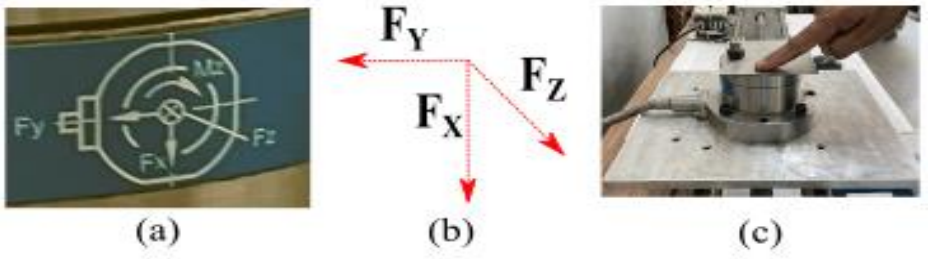

Figure 4.22 Force measurement through kistler force measurement sytem. (a) Force directions as mentioned over kistler force plate, (b) Force direction described as per the

DAQ cable as mentioned over force plate and (c) Real finger orientation at the experimental setup

D. Experimental results and discussion

This section discusses the coefficient of friction (COF) variation with normal load for the reciprocating tribometer. Experimental investigations were performed on 6 subjects and 7 materials over the range of sliding velocities from 20 mm/ sec to 60 mm/ sec with a step of 10 mm/ sec. To keep the results succinct and efficient, graphical representation of COF plots for maximum and minimum velocities are only shown in Figure 4.23 to Figure 4.28. The behaviour of COF with normal load at different velocities are in strong agreement with the reported literature [51]. The following sub-sections discusses subject wise variation of COF with normal load at different velocities on different materials:

I. Subject 1:

Figure 4.23 (a)–(g) shows the variation of COF with normal load at maximum velocity of 60 mm/ sec and minimum velocity of 20 mm/ sec for acrylic, aluminium, brass, copper, sun mica, steel, and wood materials respectively. The consistent decrease in the COF with increasing normal load is observed for all the seven test materials in both dry and wet state. The decrease in COF at higher load is due to the decrease in relative contribution of adhesion. It is also observed that COF increases with increase in sliding velocity, because of increase in surface temperature which in turn increases the contact area and therefore the amount of adhesive friction. The COF is found to be higher in wet state than dry state for all the materials at a particular speed. Also, it is observed that the difference in COF value between dry and wet state is more at low loads and with the increase in load this difference tends to decrease. This might be due to higher effect of shear component in comparison to normal component at low loads in wet state than in dry state. At higher loads the normal component of force dominates, and the deformation component also increases which in turn reduces the contact area and hence reduces the friction. In all the materials sudden rise in COF around 4 to 5 N load is observed which may be because of the complete interaction with skin ridges and surface irregularities at these loads. Thereafter, similar trend of decreasing COF with increasing loads were observed. At higher loads COF is found independent of normal loads, only steel material shows the exception which might be due to error in measurements.

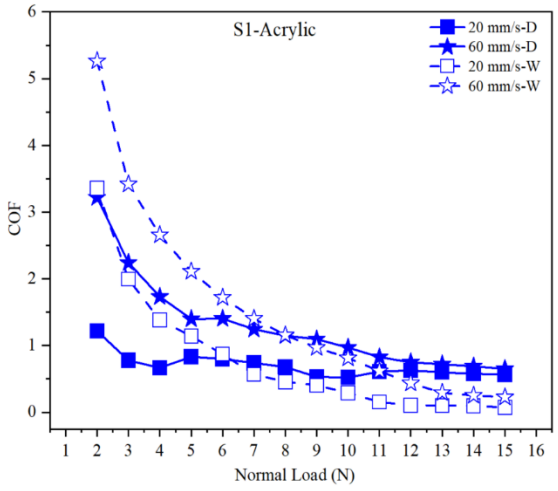
S1-Acrylic
20 mm/s-D
60 mm/s-D
20 mm/s-W
60 mm/s-W
COF
Normal Load (N)

(a)

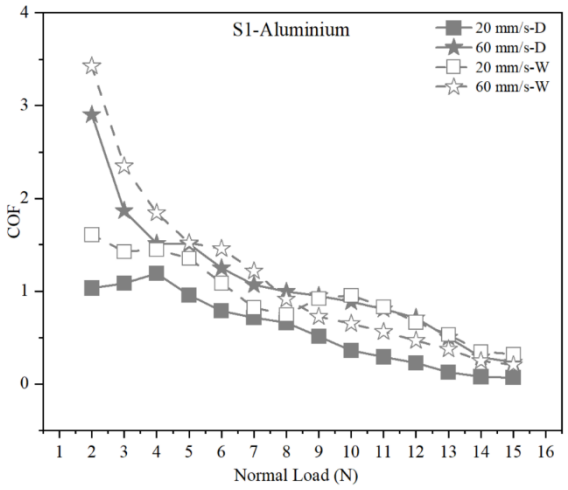
S1-Aluminium
20 mm/s-D
60 mm/s-D
20 mm/s-W
60 mm/s-W
COF
Normal Load (N)

(b)

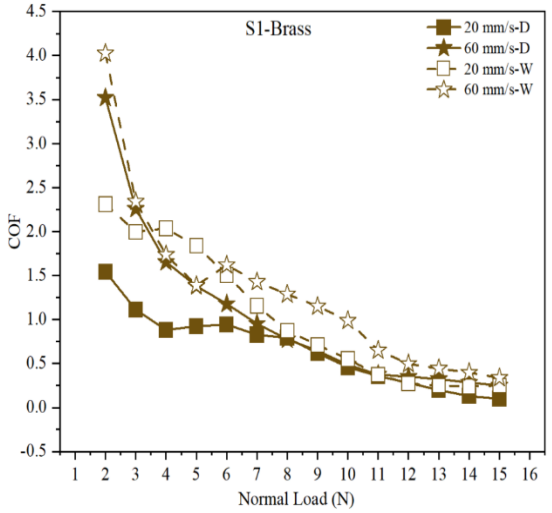
S1-Brass
20 mm/s-D
60 mm/s-D
20 mm/s-W
60 mm/s-W
COF
Normal Load (N)

(c)

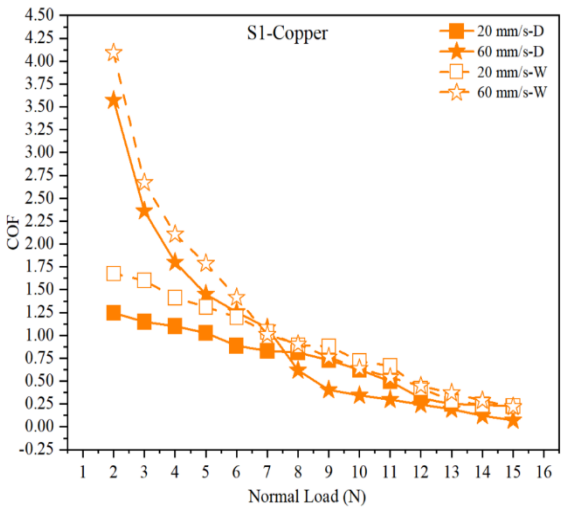
S1-Copper
20 mm/s-D
60 mm/s-D
20 mm/s-W
60 mm/s-W
COF
Normal Load (N)

(d)

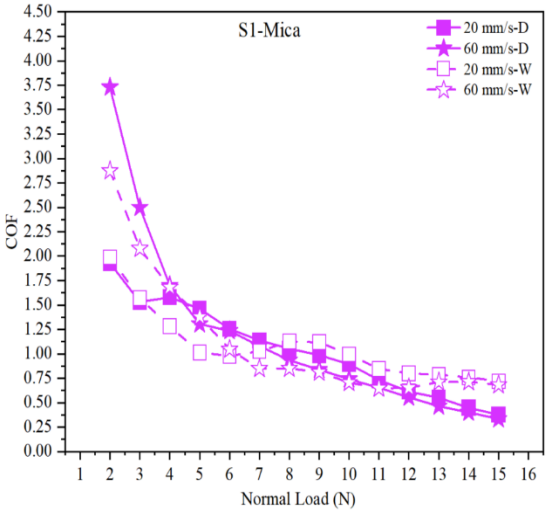
S1-Mica
20 mm/s-D
60 mm/s-D
20 mm/s-W
60 mm/s-W
COF
Normal Load (N)

(e)

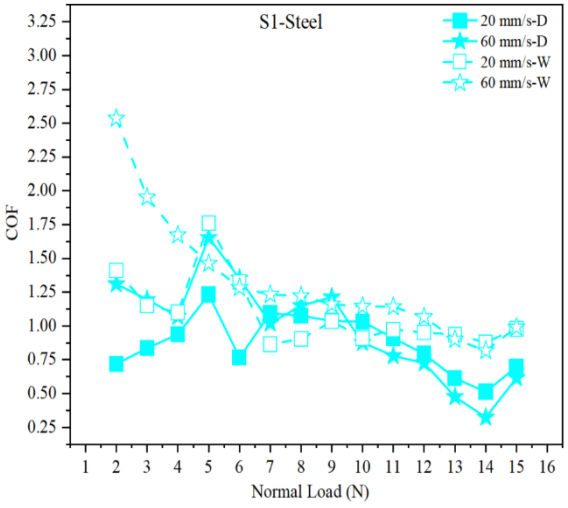
S1-Steel
20 mm/s-D
60 mm/s-D
20 mm/s-W
60 mm/s-W
COF
Normal Load (N)

(f)

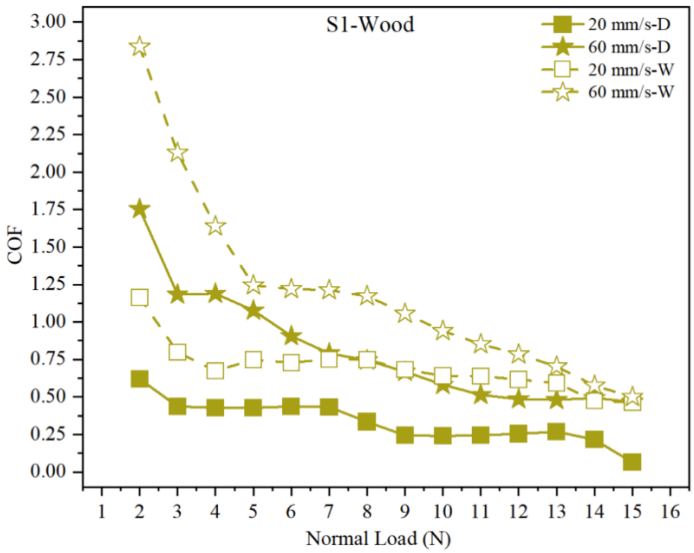

(g)

Figure 4.23 Plot for the variation of COF with normal load for subject 1 (a) acrylic, (b) aluminium, (c) brass, (d) copper, (e) mica, (f) steel and (g) wood

II. Subject 2:

Figure 4.24 (a)-(g) shows the plot for COF vs normal load for acrylic, aluminium, brass, copper, sun mica, steel, and wood respectively. Very similar trends are observed for a particular material over the range of subjects as for subject 1.The abrupt results were seen at 20 mm/ sec in dry state for acrylic for this subject, which shown increase in COF with normal loads. There is no adequate justification for this except that this might be improper contact pressure between the skin and materials. In wet state measurements, higher shear forces are generated as evident with the higher COF values. Here also, it is observed that at low loads, COF in wet conditions is much greater than dry skin at same load condition and with the increase in load this difference tends to decrease. This might be due to dominance of normal load at higher load which increases the deformation of skin and hence reducing the contact area, thereby reducing the friction. At higher loads COF is found to be independent of normal loads and to some extent on sliding velocity in both dry and wet conditions with few exceptions which might be due to experimentation error.

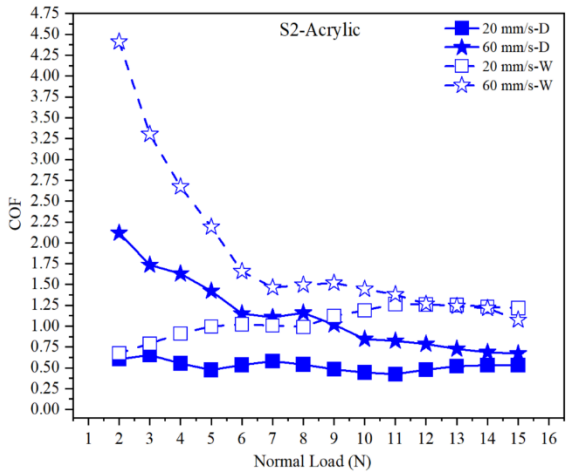
S2-Acrylic
20 mm/s-D
60 mm/s-D
20 mm/s-W
60 mm/s-W
COF
Normal Load (N)

(a)

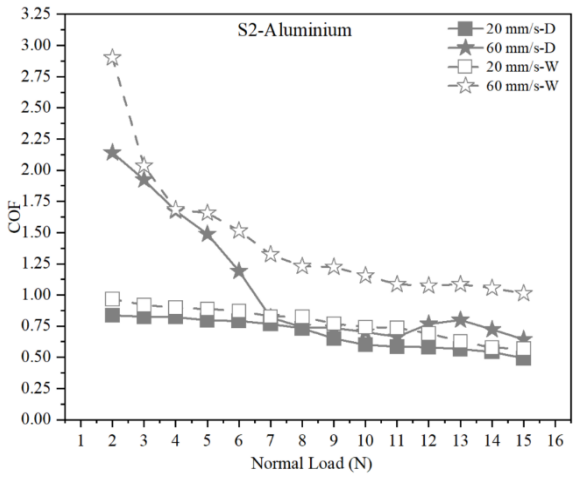
S2-Aluminium
20 mm/s-D
60 mm/s-D
20 mm/s-W
60 mm/s-W
COF
Normal Load (N)

(b)

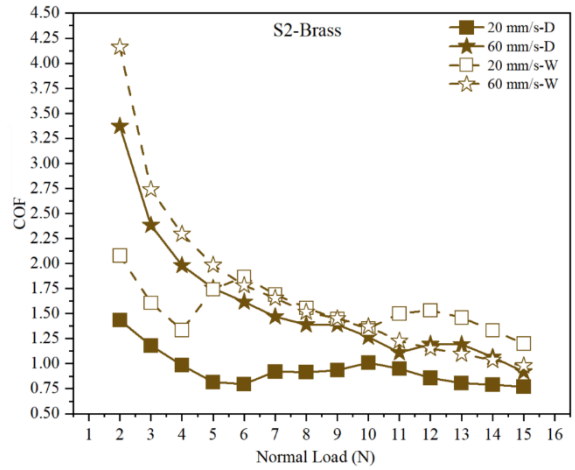
S2-Brass
20 mm/s-D
60 mm/s-D
20 mm/s-W
60 mm/s-W
COF
Normal Load (N)

(c)

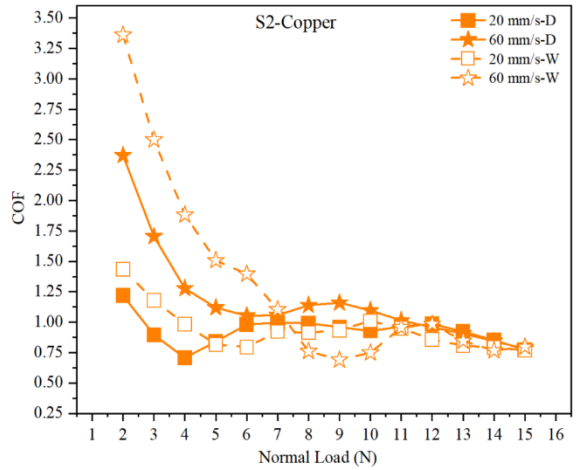
S2-Copper
20 mm/s-D
60 mm/s-D
20 mm/s-W
60 mm/s-W
COF
Normal Load (N)

(d)

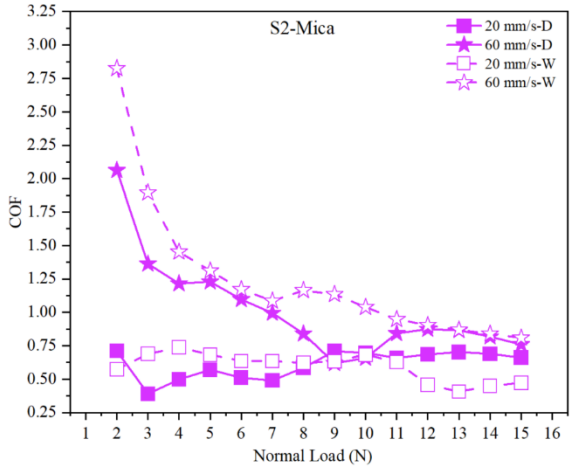
S2-Mica
20 mm/s-D
60 mm/s-D
20 mm/s-W
60 mm/s-W
COF
Normal Load (N)

(e)

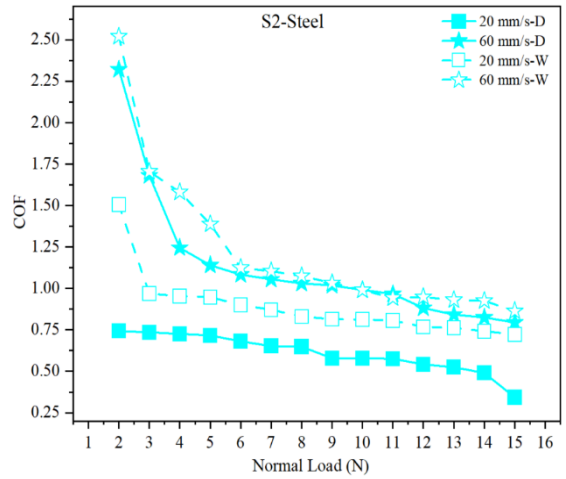
S2-Steel
20 mm/s-D
60 mm/s-D
20 mm/s-W
60 mm/s-W
COF
Normal Load (N)

(f)

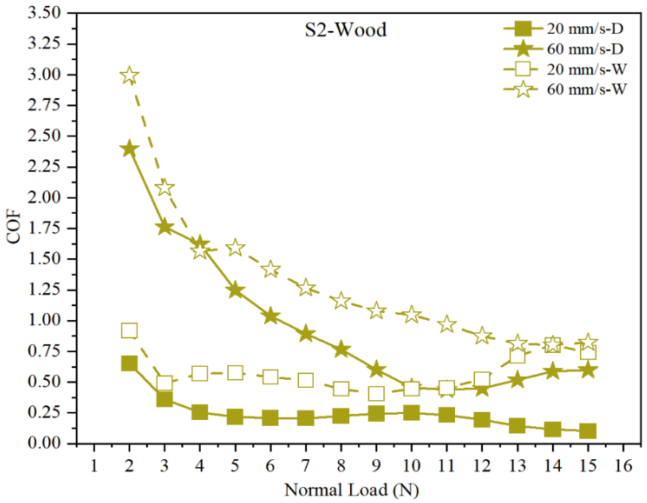

(g)

Figure 4.24 Plot for the variation of COF with normal load for subject 2 (a) acrylic, (b) aluminium, (c) brass, (d) copper, (e) mica, (f) steel and (g) wood

III. Subject 3:

Figure 4.25 (a)-(g) shows the plot for COF vs normal load for acrylic, aluminium, brass, copper, sun mica, steel, and wood respectively for subject 3. Figure 4.25 (a) shows an abrupt increase in COF at normal load greater than 6 N for both the sliding velocity of 60 mm/ sec and 20 mm/ sec. Contact at the interface between the ridges of finger and the material surface creates an interfacial bond that resists the motion, tending to increase the COF at the contact. Pronounce COF values are obtained for the wet state in comparison to the dry state across all materials because of the higher adhesion component of the frictional force. At load range between 6 to 8 N, COF is found independent of normal loads and to some extent on sliding velocity in both dry and wet conditions Since subject 3 is a female subject, gender-based effect cannot be ruled out on the frictional behaviour across the test materials. The same trend was seen in earlier subject at much higher loads.

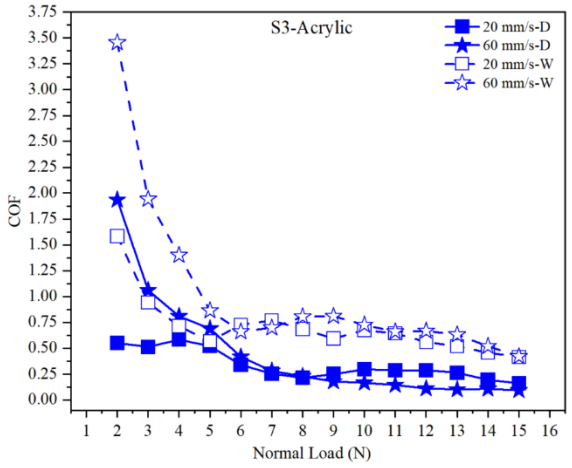
S3-Acrylic
20 mm/s-D
60 mm/s-D
20 mm/s-W
60 mm/s-W
COF
Normal Load (N)

(a)

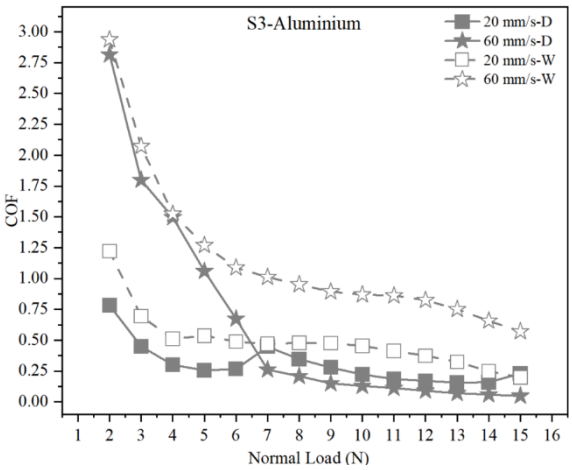
S3-Aluminium
20 mm/s-D
60 mm/s-D
20 mm/s-W
60 mm/s-W
COF
Normal Load (N)

(b)

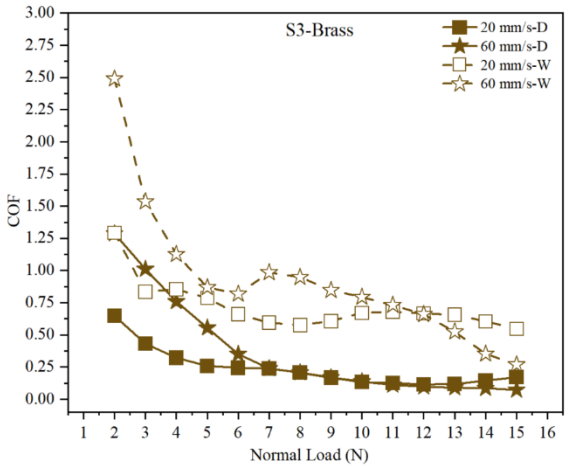
S3-Brass
20 mm/s-D
60 mm/s-D
20 mm/s-W
60 mm/s-W
COF
Normal Load (N)

(c)

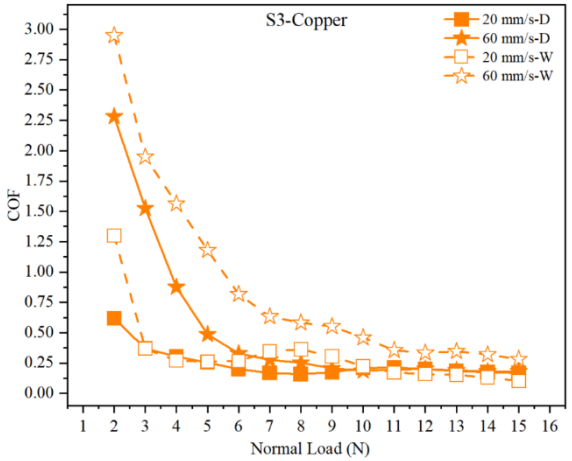
S3-Copper
20 mm/s-D
60 mm/s-D
20 mm/s-W
60 mm/s-W
COF
Normal Load (N)

(d)

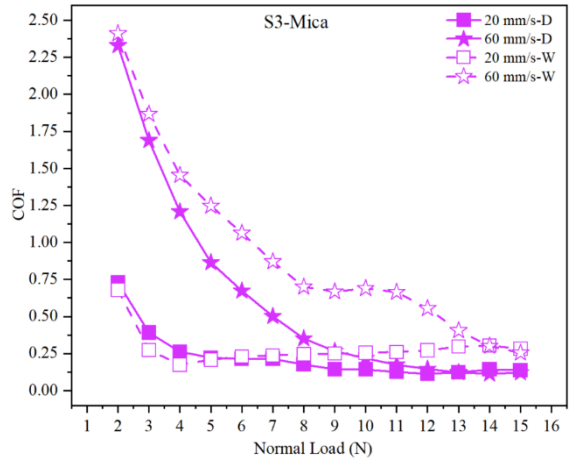
S3-Mica
20 mm/s-D
60 mm/s-D
20 mm/s-W
60 mm/s-W
COF
Normal Load (N)

(e)

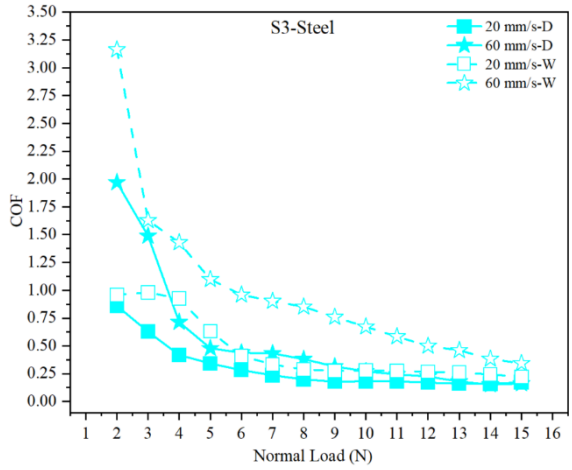
S3-Steel
20 mm/s-D
60 mm/s-D
20 mm/s-W
60 mm/s-W
COF
Normal Load (N)

(f)

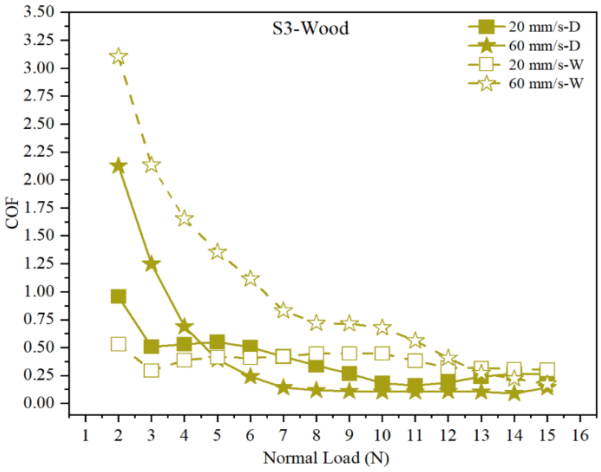

(g)

Figure 4.25 Plot for the variation of COF with normal load for subject 3 (a) acrylic, (b) aluminium, (c) brass, (d) copper, (e) mica, (f) steel and (g) wood

IV. Subject 4:

Figure 4.26 (a)-(g) shows the plot for COF vs normal load for acrylic, aluminium, brass, copper, sun mica, steel, and wood respectively for subject 4. Here also the same trend of increase in COF is seen at low loads. This is due to creation of interfacial bond due to contact at the interface between the ridges of finger and the acrylic surface. The COF becomes independent of normal load at higher load and the effect of sliding velocity also diminishes at these loads.

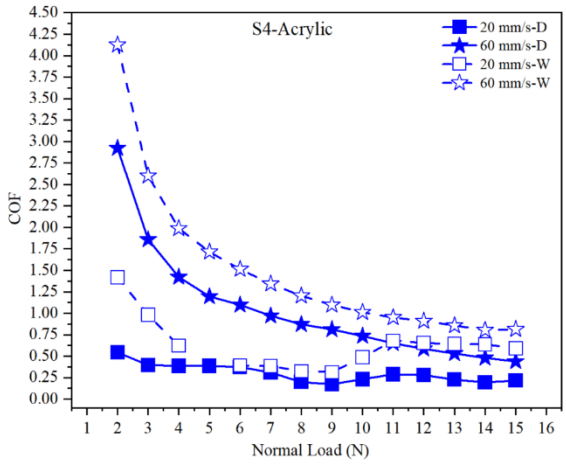

(a)

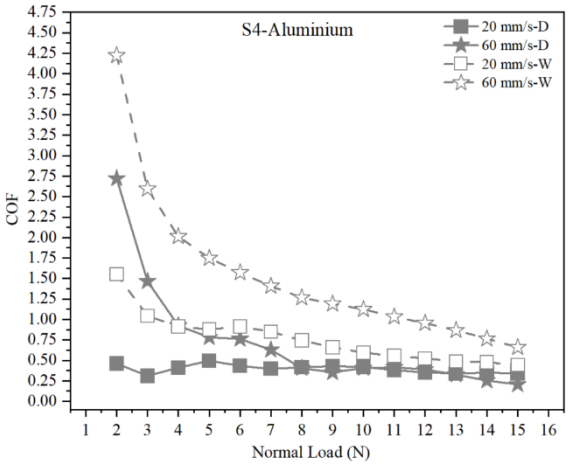

(b)

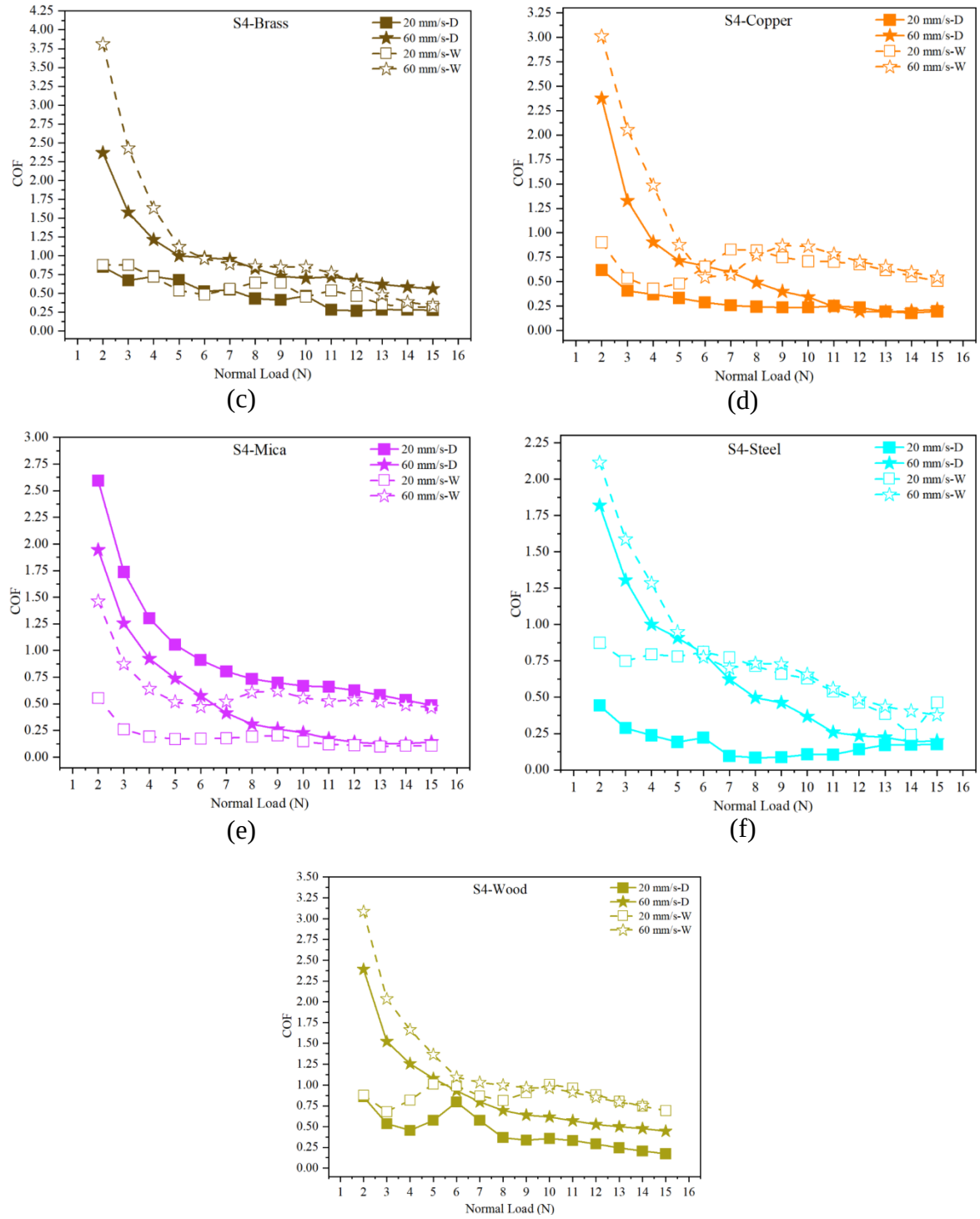

Figure 4.26 Plot for the variation of COF with normal load for subject 4 (a) acrylic, (b) aluminium, (c) brass, (d) copper, (e) mica, (f) steel and (g) wood

V. Subject 5 and Subject 6:

Figure 4.27 (a)-(g) and Fig. 4.28 (a)-(g), shows the plot for COF vs normal load for acrylic, aluminium, brass, copper, sun mica, steel, and wood respectively for subject 5 and 6. Here also the abrupt behaviour is seen around normal load range of 4 to 6 N in both dry and wet

conditions. This is surely due to contact between surface characteristics of materials and ridges of finger. The COF becomes independent of normal load at higher load and the effect of sliding velocity also decreases at these loads. The increase in COF in wet conditions in comparison to dry conditions is due to liquid bridging between the ridges of skin and the contacting surface. This bridging effect cause increase in friction due to shear force set up.

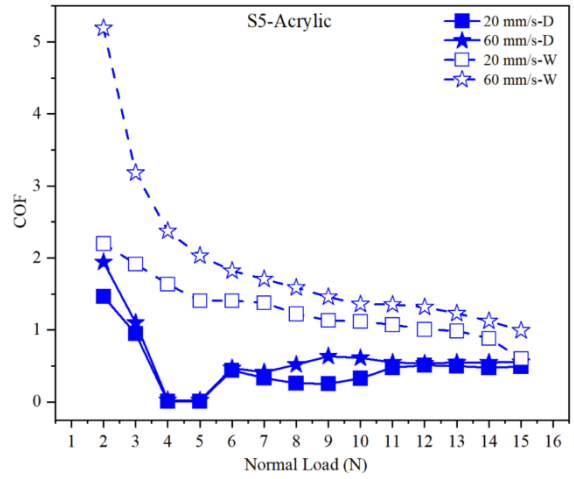

(a)

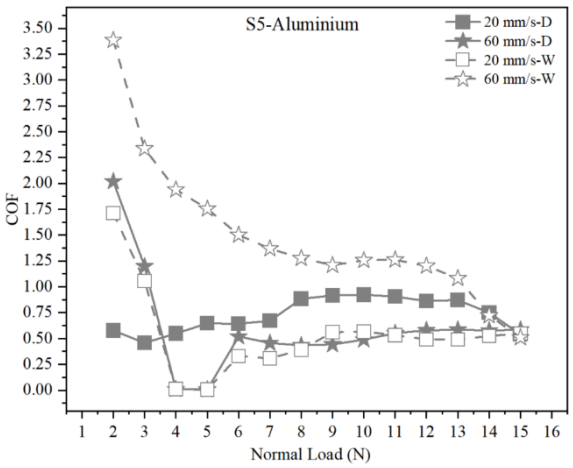

(b)

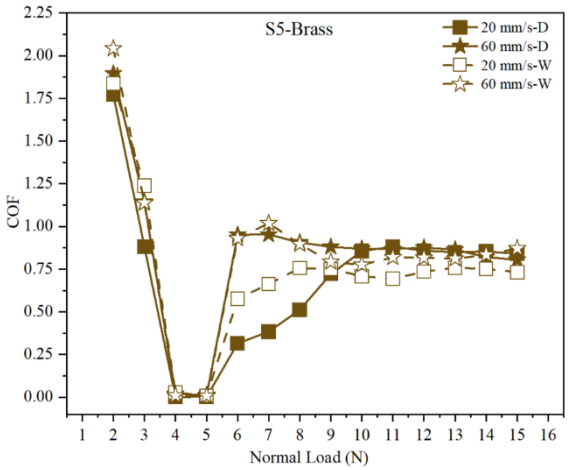

(c)

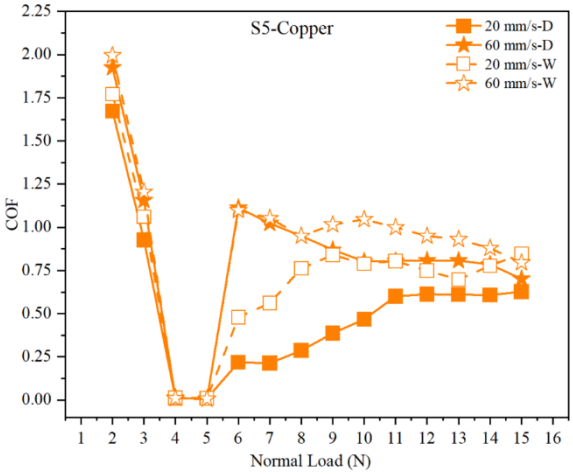

(d)

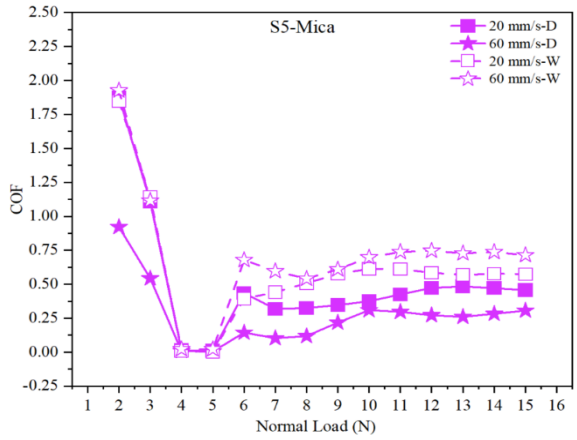

(e)

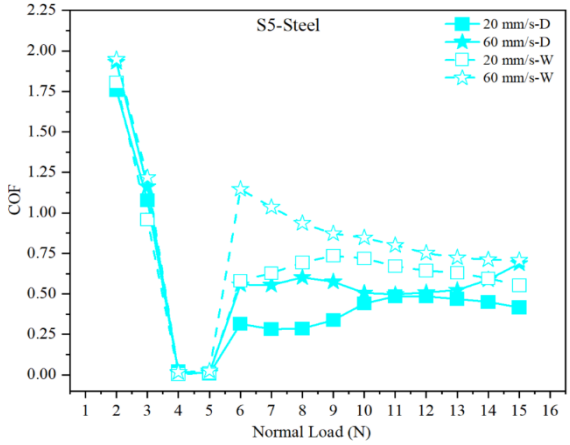

(f)

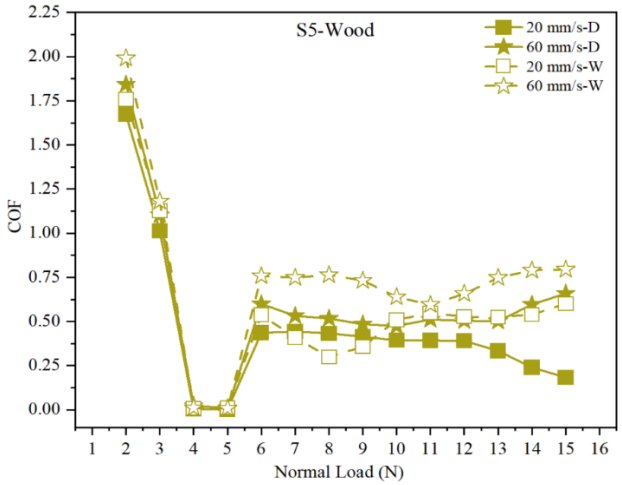

(g)

Figure 4.27 Plot for the variation of COF with normal load for subject 5 (a) acrylic, (b) aluminium, (c) brass, (d) copper, (e) mica, (f) steel and (g) wood

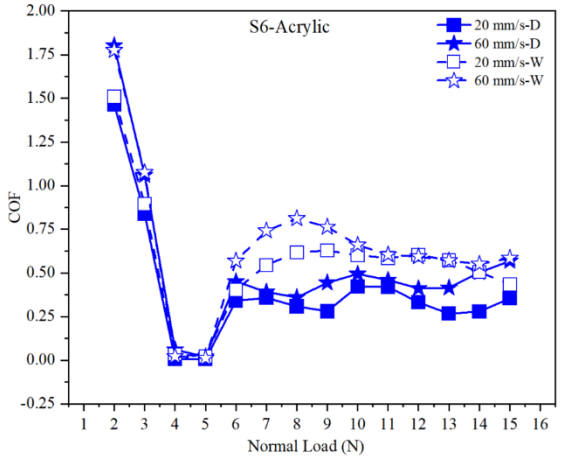

(a)

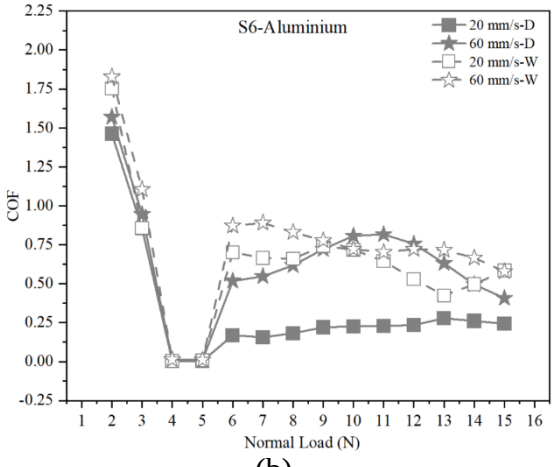

(b)

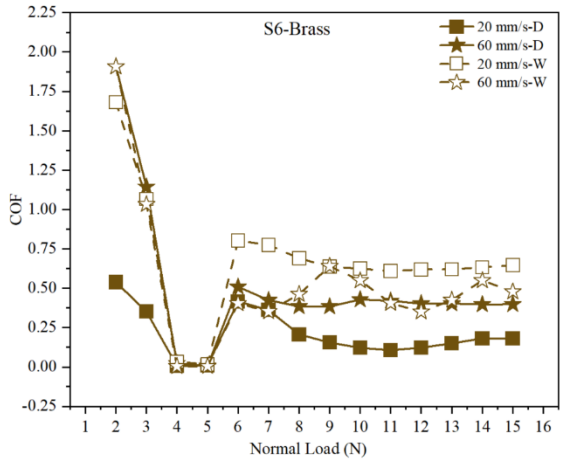

(c)

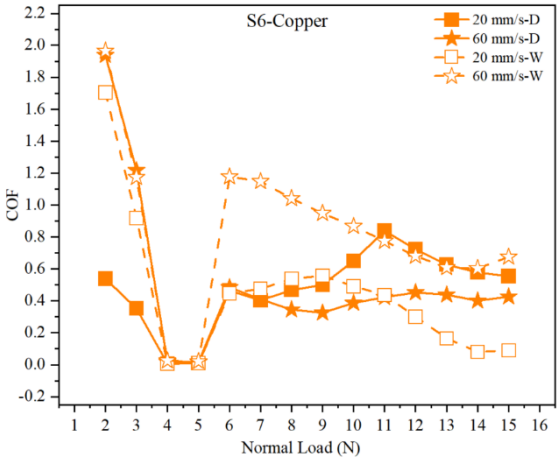

(d)

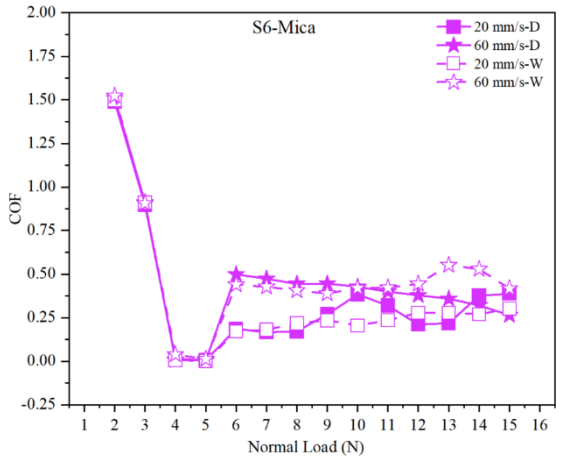

(e)

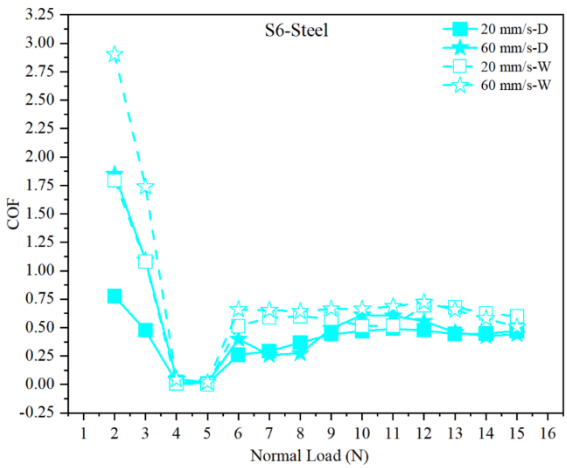

(f)

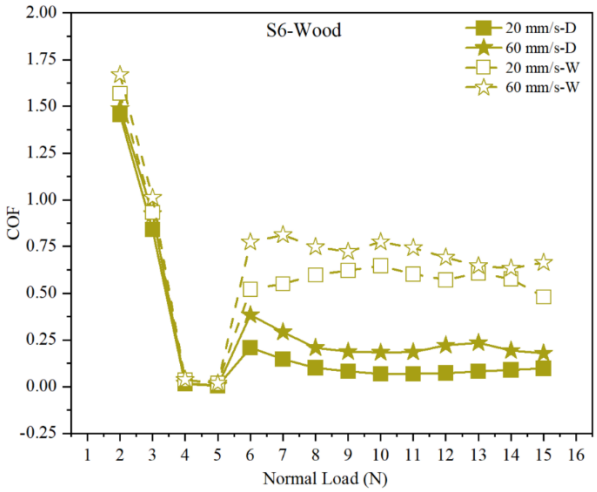

(g)

Figure 4.28 Plot for the variation of COF with normal load for subject 6 (a) acrylic, (b) aluminium, (c) brass, (d) copper, (e) mica, (f) steel and (g) wood

The above section discusses the dependence of COF values on normal loads and sliding velocities subjectwise on different materials seperately in dry and wet conditions. To make the results more conclusive, the COF behaviour on different materials and velocities is analysed on a particular subject. Also, the comparative analysis is done amongst the subjects for acrylic at maximum and minimum sliding velocities.

E. Detailed discussion on friction behaviour across subjects and test materials

As discussed in the previous sections, COF is the ratio of tangential to the normal force acting at the interface as per the Amonton's law. However, adhesion friction is the dominant friction but the viscoelastic nature of human skin leads to non-linear deformation. At higher roughness and load range, deformation component comes into existence which should also be considered [44] but is out of the scope for the current research explorations. Touch friction is complicated and is influenced by multiple factors such as, skin condition, surface properties, test conditions and surface material. Figure 4.29 (a) and (b) shows the variation of COF with normal load for subject 1 in dry state for all material at 20 mm/ sec and 60 mm/ sec. A consistent decrease in COF is observed having pronounce effect of normal load on the COF. With increasing normal load decrease in COF is in strong agreement to the available literature. Range of decrease in COF depends on multiple parameters such as normal load, counter surface material and nature of interface [46], [81], [82]. Since the deformation term is usually less pronounce than the adhesion component in friction measurement, it varies with the skin condition [63]. As discussed previously, decrease in COF with increasing normal load is due to the flattening of the contact surface under high compression and increasing the contact area. Sudden change in trend is observed for steel at low normal loads up to 9 N with little variation in the range of 0.5 to 1.5 N for both the sliding velocities.

Similar varition for the wet state is shown in Figure 4.29 (c) and (d) for the wet state. Pronounce COF range is observed in wet state for all the materials when compared to the dry state. Higher sliding velocities depict higher COF values when compared to dry state, keeping all other parameters constant. Maximum COF is depicted by acrlyic at 60 mm/ sec, while average minimum is that for wood. Acrylic shows the highest COF because of increased contact area due to the smooth surface finish having R_a of 0.67, thereby the increased adhesion component that increases the friction component. Being a layered material having the high absorption, absorbs the water at higher loads thereby decreasing the COF at the contact interface.

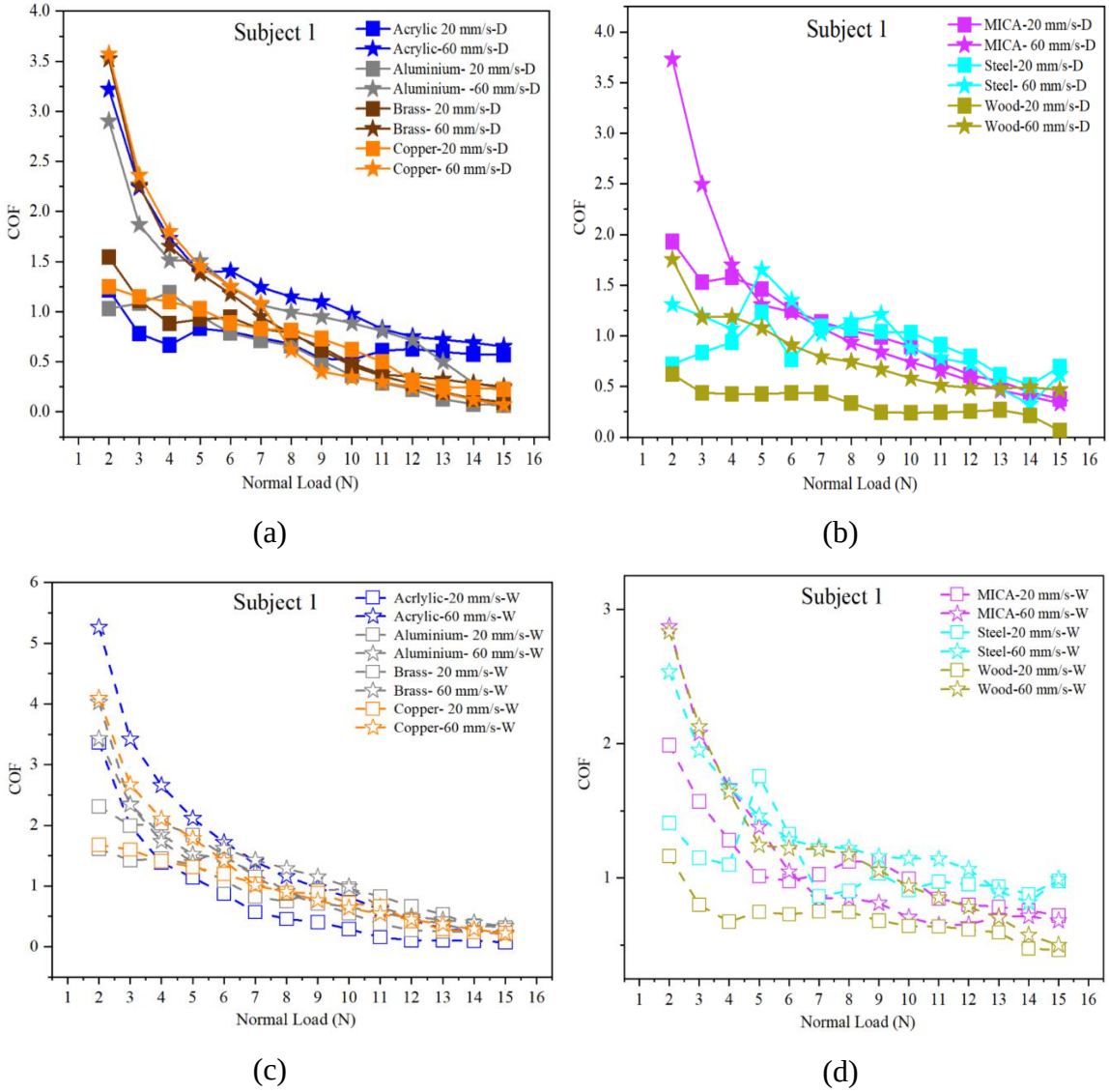

Figure 4.29 Plot for the variation of COF with normal load for subject 1 (a), (b) in dry state and (c), (d) in wet state at 20 and 60 mm/ sec velocity

Figure 4.30 (a) and (b) shows the COF variation of subject 1 for all materials both in dry and wet state at minimum speed of 20 mm/ sec. The dependence of COF with normal load is given by $\mu(N) = k.N^{n-1}$ [86]. To relate this friction measurement data to the friction mechanism a linear regression is performed. As shown in Figure 4.30 (a) value of exponent n range from 0.20-0.82 which is well in accordance with the mean value of 0.68 reported in previous studies [84], [87] for dry state. Figure 4.30 (b) shows the fit for the plot of COF versus normal load in wet state. In wet state exponent n varies between -0.013 for brass to 0.77 for steel. Deviation of acrylic, brass, and mica from the mean value is attributed to its smooth surface finish, texture, and plasticization effect in the linear movement of the finger pad for the friction measurement.

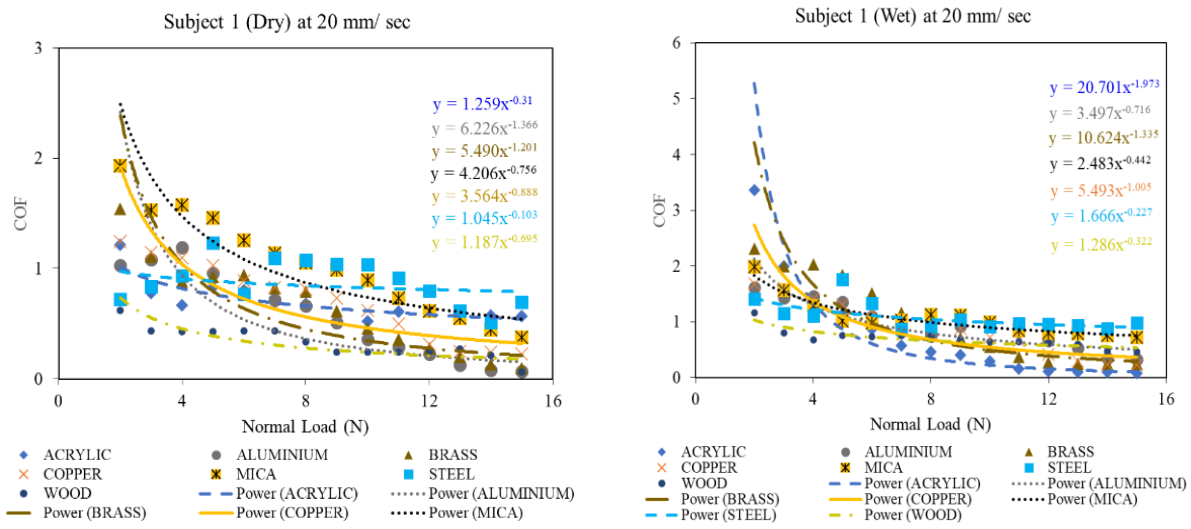

Figure 4.30 Power law fit of COF with varying normal load in (a) dry sate (b) wet state for subject 1 at 20 mm/ sec velocity

Figure 4.31 (a) and (b) represent variation of COF with normal load for acrylic at 20 mm/ sec and 60 mm/ sec both in dry and wet state for comparitive study of COF across six subjects. It is evident from the figures below, that overall COF decreases with increasing normal load while it increases with increasing sliding velocity in accordance to the previously reported studies. Range of COF variation is higher at 60 cm/ sec sliding velocity state from 0.25 to 5.25 while that for 20 mm/ sec velocity the upper range of COF is 2.25 except that for subject 1 in wet state. Figure 4.31 depict the lowest average range of COF of 0.50 and 0.68 for subject 6 in dry and wet state while subject 2 has the highest average COF of 1.15 and 1.45 in dry and wet state respectively across all materials.

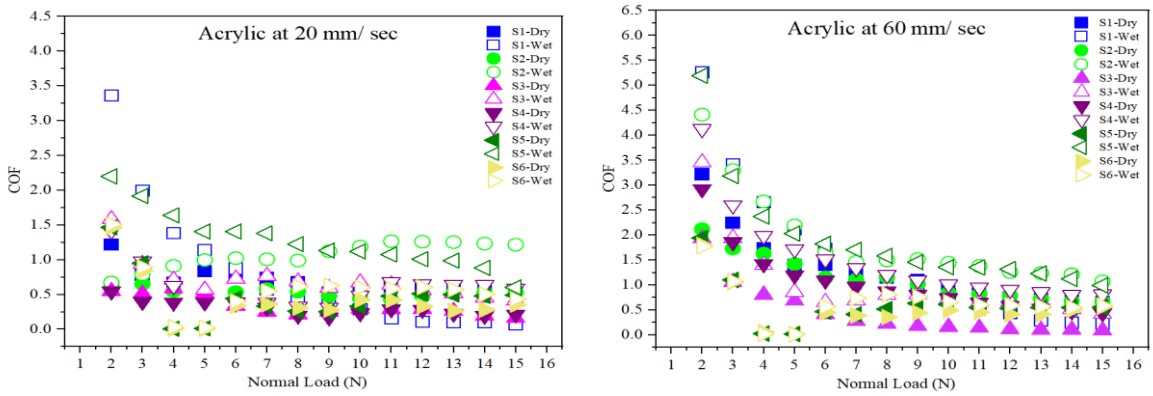

(a) (b)

Figure 4.31 Variation of COF at acrylic finger pad interface with normal load for six subjects in dry and wet state at velocity of (a) 20 mm/ sec and (b) 60 mm/ sec

4.5 Summary

This chapter discusses the experimental investigations that have been performed using the rotary type and sliding type tribometers.

Section 4.1 presents the introduction for the factors that affect the COF at human skin interface for experiments performed with the rotary and sliding type tribometers.

Section 4.2 discusses the feedback for the survey conducted to select the test sample materials.

Section 4.3 reports the experimental results performed through rotary tribometer with the textile and metal samples. Prominence decrease in COF with normal loads across the test materials is observed. Sliding velocity increases the friction component thereby increasing the COF.

Section 4.4 presents the experimental investigation of seven test materials for COF at the finger pad interface in the velocity range of 20 mm/ sec to 60 mm/ sec. Normal load is varied from 2 to 15 N. Maximum COF is reported for the acrylic material.

References

[1] L. A. De Wert, D. L. Bader, C. W. J. Oomens, L. Schoonhoven, M. Poeze, and N. D. Bouvy, "A new method to evaluate the effects of shear on the skin," *Wound Repair Regen.*, vol. 23, no. 6, pp. 885–890, 2015, doi: 10.1111/wrr.12368.

[2] J. F. J. Soetens, P. R. Worsley, J. M. Herniman, G. J. Langley, D. L. Bader, and C. W. J. Oomens, "The expression of anaerobic metabolites in sweat and sebum from human skin subjected to intermittent and continuous mechanical loading," *J. Tissue Viability*, vol. 28, no. 4, pp. 186–193, 2019, doi: 10.1016/j.jtv.2019.10.001.

[3] W. A. Traa, M. C. van Turnhout, J. L. Nelissen, G. J. Strijkers, D. L. Bader, and C. W. J. Oomens, "There is an individual tolerance to mechanical loading in compression induced deep tissue injury," *Clin. Biomech.*, vol. 63, no. October 2018, pp. 153–160, 2019, doi: 10.1016/j.clinbiomech.2019.02.015.

[4] M. J. Carré, S. K. Tan, P. T. Mylon, and R. Lewis, "Influence of medical gloves on fingerpad friction and feel," *Wear*, vol. 376–377, pp. 324–328, 2017, doi: 10.1016/j.wear.2017.01.077.

[5] R. Lewis, M. J. Carré, and S. E. Tomlinson, "Skin friction at the interface between hands and sports equipment," *Procedia Eng.*, vol. 72, no. December 2014, pp. 611–617, 2014, doi: 10.1016/j.proeng.2014.06.064.

[6] O. Troynikov, E. Ashayeri, and F. K. Fuss, "Tribological evaluation of sportswear with negative fit worn next to skin," *Proc. Inst. Mech. Eng. Part J J. Eng. Tribol.*, vol. 226, no. 7, pp. 588–597, 2012, doi: 10.1177/1350650111425876.

[7] C. C. Zouboulis *et al.*, "A novel approach to measuring the frictional behaviour of human skin in vivo," *Tribol. Int.*, vol. 11, no. 1, pp. 38–41, 2017, doi: 10.1016/j.triboint.2012.05.022.

[8] I. M. Koç and C. Aksu, "Tactile sensing of constructional differences in fabrics with a polymeric finger tip," *Tribol. Int.*, vol. 59, pp. 339–349, 2013, doi: 10.1016/j.triboint.2012.04.021.

[9] J. Chen, H. Yang, J. Li, J. Chen, Y. Zhang, and X. Zeng, "The development of an artificial skin model and its frictional interaction with wound dressings," *J. Mech. Behav. Biomed. Mater.*, vol. 94, no. January, pp. 308–316, 2019, doi: 10.1016/j.jmbbm.2019.03.013.

[10] M. Nachman and S. E. Franklin, "Artificial Skin Model simulating dry and moist in vivo

human skin friction and deformation behaviour," *Tribol. Int.*, vol. 97, pp. 431–439, 2016, doi: 10.1016/j.triboint.2016.01.043.

[11] L. Skedung, I. Buraczewska-Norin, N. Dawood, M. W. Rutland, and L. Ringstad, "Tactile friction of topical formulations," *Ski. Res. Technol.*, vol. 22, no. 1, pp. 46–54, 2016, doi: 10.1111/srt.12227.

[12] S. Ding and B. Bhushan, "Tactile perception of skin and skin cream by friction induced vibrations," *J. Colloid Interface Sci.*, vol. 481, pp. 131–143, 2016, doi: 10.1016/j.jcis.2016.07.034.

[13] B. Bhushan, S. Chen, and S. Ge, "Friction and durability of virgin and damaged skin with and without skin cream treatment using atomic force microscopy," *Beilstein J. Nanotechnol.*, vol. 3, no. 1, pp. 731–746, 2012, doi: 10.3762/bjnano.3.83.

[14] A. Ramalho, C. L. Silva, A. A. C. C. Pais, and J. J. S. Sousa, "In vivo friction study of human skin: Influence of moisturizers on different anatomical sites," *Wear*, vol. 263, no. 7-12 SPEC. ISS., pp. 1044–1049, 2007, doi: 10.1016/j.wear.2006.11.051.

[15] W. Zhong, M. M. Q. Xing, N. Pan, and H. I. Maibach, "Textiles and human skin, microclimate, cutaneous reactions: An overview," *Cutan. Ocul. Toxicol.*, vol. 25, no. 1, pp. 23–39, 2006, doi: 10.1080/15569520500536600.

[16] G. M. Rotaru *et al.*, "Friction between human skin and medical textiles for decubitus prevention," in *Tribology International*, 2013, vol. 65, pp. 91–96, doi: 10.1016/j.triboint.2013.02.005.

[17] L. Meredith, J. Brown, and E. Clarke, "Relationship between skin abrasion injuries and clothing material characteristics in motorcycle crashes," *Biotribology*, vol. 3, pp. 20–26, 2015, doi: 10.1016/j.biotri.2015.09.007.

[18] L. C. Gerhardt, V. Strässle, A. Lenz, N. D. Spencer, and S. Derler, "Influence of epidermal hydration on the friction of human skin against textiles," *J. R. Soc. Interface*, vol. 5, no. 28, pp. 1317–1328, 2008, doi: 10.1098/rsif.2008.0034.

[19] R. Baby, K. Mathur, and E. DenHartog, "Skin-textiles friction: importance and prospects in skin comfort and in healthcare in prevention of skin injuries," *J. Text. Inst.*, vol. 112, no. 9, pp. 1514–1530, 2021, doi: 10.1080/00405000.2020.1827582.

[20] G. Limbert *et al.*, "Biotribology of the ageing skin—Why we should care," *Biotribology*, vol. 17, no. February, pp. 75–90, 2019, doi: 10.1016/j.biotri.2019.03.001.

[21] M. Woodhouse, P. R. Worsley, D. Voegeli, L. Schoonhoven, and D. L. Bader, "How consistent and effective are current repositioning strategies for pressure ulcer

prevention?," *Appl. Nurs. Res.*, vol. 48, no. May, pp. 58–62, 2019, doi: 10.1016/j.apnr.2019.05.013.

[22] S. E. Tomlinson, R. Lewis, and M. J. Carré, "Review of the frictional properties of finger-object contact when gripping," *Proc. Inst. Mech. Eng. Part J J. Eng. Tribol.*, vol. 221, no. 8, pp. 841–850, 2007, doi: 10.1243/13506501JET313.

[23] S. Derler, A. Rao, P. Ballistreri, R. Huber, A. Scheel-Sailer, and R. M. Rossi, "Medical textiles with low friction for decubitus prevention," *Tribol. Int.*, vol. 46, no. 1, pp. 208–214, 2012, doi: 10.1016/j.triboint.2011.03.011.

[24] M. Belhadjamor, S. Belghith, S. Mezlini, and M. El Mansori, "Effect of the surface texturing scale on the self-clean function: Correlation between mechanical response and wetting behavior," *Tribol. Int.*, vol. 111, no. December 2016, pp. 91–99, 2017, doi: 10.1016/j.triboint.2017.03.005.

[25] M. J. Adams *et al.*, "Finger pad friction and its role in grip and touch," *Journal of the Royal Society Interface*, vol. 10, no. 80. 2013, doi: 10.1098/rsif.2012.0467.

[26] D. M. O'Meara and R. M. Smith, "Static friction properties between human palmar skin and five grabrail materials," *Ergonomics*, vol. 44, no. 11, pp. 973–988, 2001, doi: 10.1080/00140130110074882.

[27] M. F. Leyva-Mendivil, J. Lengiewicz, A. Page, N. W. Bressloff, and G. Limbert, "Skin Microstructure is a Key Contributor to Its Friction Behaviour," *Tribol. Lett.*, vol. 65, no. 1, pp. 1–17, 2017, doi: 10.1007/s11249-016-0794-4.

[28] B. Bhushan, G. Wei, and P. Haddad, "Friction and wear studies of human hair and skin," *Wear*, vol. 259, no. 7–12, pp. 1012–1021, 2005, doi: 10.1016/j.wear.2004.12.026.

[29] C. Guignier, B. Camillieri, M. Schmid, R. M. Rossi, and M. A. Bueno, "E-Knitted textile with polymer optical fibers for friction and pressure monitoring in socks," *Sensors (Switzerland)*, vol. 19, no. 13, pp. 31–33, 2019, doi: 10.3390/s19133011.

[30] W. Li, X. D. Liu, Z. B. Cai, J. Zheng, and Z. R. Zhou, "Effect of prosthetic socks on the frictional properties of residual limb skin," *Wear*, vol. 271, no. 11–12, pp. 2804–2811, 2011, doi: 10.1016/j.wear.2011.05.032.

[31] M. Lindberg, B. Skytt, and M. Lindberg, "Continued wearing of gloves: a risk behaviour in patient care," *Infect. Prev. Pract.*, vol. 2, no. 4, p. 100091, 2020, doi: 10.1016/j.infpip.2020.100091.

[32] J. Lyu, N. Özgün, D. J. Kondziela, and R. Bennewitz, "Role of Hair Coverage and Sweating for Textile Friction on the Forearm," *Tribol. Lett.*, vol. 68, no. 4, pp. 1–9, 2020,

doi: 10.1007/s11249-020-01341-6.

[33] J. Van Kuilenburg, M. A. Masen, M. N. W. Groenendijk, V. Bana, and E. Van Der Heide, “An experimental study on the relation between surface texture and tactile friction,” *Tribol. Int.*, vol. 48, pp. 15–21, 2012, doi: 10.1016/j.triboint.2011.06.003.

[34] L. M. Vilhena and A. Ramalho, “Friction Behavior of Human Skin Rubbing against Different Textured Polymeric Materials Obtained by a 3D Printing Microfabrication Technique,” *Tribol. Trans.*, vol. 62, no. 2, pp. 324–336, 2019, doi: 10.1080/10402004.2018.1543782.

[35] G. P. Chimata and C. J. Schwartz, “Tactile Discrimination of Randomly Textured Surfaces: Effect of Friction and Surface Parameters,” *Biotribology*, vol. 11, no. October 2016, pp. 102–109, 2017, doi: 10.1016/j.biotri.2017.01.004.

[36] M. Klaassen, D. J. Schipper, and M. A. Masen, “Influence of the relative humidity and the temperature on the in-vivo friction behaviour of human skin,” *Biotribology*, vol. 6, pp. 21–28, 2016, doi: 10.1016/j.biotri.2016.03.003.

[37] N. K. Veijgen, M. A. Masen, and E. van der Heide, “Variables influencing the frictional behaviour of in vivo human skin,” *J. Mech. Behav. Biomed. Mater.*, vol. 28, pp. 448–461, 2013, doi: 10.1016/j.jmbbm.2013.02.009.

[38] M. Klaassen, E. G. de Vries, and M. A. Masen, “The static friction response of non-glabrous skin as a function of surface energy and environmental conditions,” *Biotribology*, vol. 11, no. May, pp. 124–131, 2017, doi: 10.1016/j.biotri.2017.05.004.

[39] L. C. Gerhardt, A. Lenz, N. D. Spencer, T. Münzer, and S. Derler, “Skin-textile friction and skin elasticity in young and aged persons,” *Ski. Res. Technol.*, vol. 15, no. 3, pp. 288–298, 2009, doi: 10.1111/j.1600-0846.2009.00363.x.

[40] W. Li, Z. H. Zhai, Q. Pang, L. Kong, and Z. R. Zhou, “Influence of exfoliating facial cleanser on the bio-tribological properties of human skin,” *Wear*, vol. 301, no. 1–2, pp. 353–361, 2013, doi: 10.1016/j.wear.2012.11.073.

[41] A. M. Cottenden, W. K. Wong, D. J. Cottenden, and A. Farbrot, “Development and validation of a new method for measuring friction between skin and nonwoven materials,” *Proc. Inst. Mech. Eng. Part H J. Eng. Med.*, vol. 222, no. 5, pp. 791–803, 2008, doi: 10.1243/09544119JEIM313.

[42] W. Tang, S. rong Ge, H. Zhu, X. chuan Cao, and N. Li, “The Influence of Normal Load and Sliding Speed on Frictional Properties of Skin,” *J. Bionic Eng.*, vol. 5, no. 1, pp. 33–38, 2008, doi: 10.1016/S1672-6529(08)60004-9.

[43] C. Fortes, D. Version, and C. Fortes, “Finger pad friction and tactile perception of laser treated , stamped and cold rolled micro-structured stainless steel sheet surfaces,” 2017, doi: 10.1007/s40544-017-0147-9.

[44] M. A. Masen, “A systems based experimental approach to tactile friction,” *J. Mech. Behav. Biomed. Mater.*, vol. 4, no. 8, pp. 1620–1626, 2011, doi: 10.1016/j.jmbbm.2011.04.007.

[45] D. A. Sergachev, D. T. A. A. Matthews, and E. van der Heide, “An Empirical Approach for the Determination of Skin Elasticity: Finger pad Friction against Textured Surfaces,” *Biotribology*, vol. 18, no. April, p. 100097, 2019, doi: 10.1016/j.biotri.2019.100097.

[46] S. Derler and G. M. Rotaru, “Stick-slip phenomena in the friction of human skin,” *Wear*, vol. 301, no. 1–2, pp. 324–329, 2013, doi: 10.1016/j.wear.2012.11.030.

[47] W. Ben Messaoud, M. A. Bueno, and B. Lemaire-Semail, “Relation between human perceived friction and finger friction characteristics,” *Tribol. Int.*, vol. 98, pp. 261–269, 2016, doi: 10.1016/j.triboint.2016.02.031.

[48] X. Zhou *et al.*, “Correlation between tactile perception and tribological and dynamical properties for human finger under different sliding speeds,” *Tribol. Int.*, vol. 123, no. March, pp. 286–295, 2018, doi: 10.1016/j.triboint.2018.03.012.

[49] L. Skedung *et al.*, “Tactile perception: Finger friction, surface roughness and perceived coarseness,” *Tribol. Int.*, vol. 44, no. 5, pp. 505–512, 2011, doi: 10.1016/j.triboint.2010.04.010.

[50] A. Tribology and O. F. Human, “WTC2005-64216,” pp. 7–8, 2017.

[51] S. Derler and L. C. Gerhardt, “Tribology of skin: Review and analysis of experimental results for the friction coefficient of human skin,” *Tribol. Lett.*, vol. 45, no. 1, pp. 1–27, 2012, doi: 10.1007/s11249-011-9854-y.

[52] N. Gitis and R. Sivamani, “Tribometrology of skin,” *Tribol. Trans.*, vol. 47, no. 4, pp. 461–469, 2004, doi: 10.1080/05698190490493355.

[53] S. E. Tomlinson, R. Lewis, and M. J. Carré, “The effect of normal force and roughness on friction in human finger contact,” *Wear*, vol. 267, no. 5–8, pp. 1311–1318, 2009, doi: 10.1016/j.wear.2008.12.084.

[54] M. Janko, M. Wiertlewski, and Y. Visell, “Contact geometry and mechanics predict friction forces during tactile surface exploration,” *Sci. Rep.*, no. March, pp. 1–10, 2018, doi: 10.1038/s41598-018-23150-7.

[55] M. G. Gee, P. Tomlins, A. Calver, R. H. Darling, and M. Rides, “A new friction

measurement system for the frictional component of touch," *Wear*, vol. 259, no. 7–12, pp. 1437–1442, 2005, doi: 10.1016/j.wear.2005.02.053.

[56] A. Imaizumi, S. Okamoto, and Y. Yamada, "Friction perception resulting from laterally vibrotactile stimuli," *ROBOMECH J.*, vol. 4, no. 1, 2017, doi: 10.1186/s40648-017-0080-8.

[57] S. Derler, M. Preiswerk, G. M. Rotaru, J. P. Kaiser, and R. M. Rossi, "Friction mechanisms and abrasion of the human finger pad in contact with rough surfaces," *Tribol. Int.*, vol. 89, pp. 119–127, 2015, doi: 10.1016/j.triboint.2014.12.023.

[58] B. M. Dzidek, M. J. Adams, J. W. Andrews, Z. Zhang, and S. A. Johnson, "Contact mechanics of the human finger pad under compressive loads," *J. R. Soc. Interface*, vol. 14, no. 127, 2017, doi: 10.1098/rsif.2016.0935.

[59] S. Bochereau, B. Dzidek, M. Adams, and V. Hayward, "Characterizing and imaging gross and real finger contacts under dynamic loading," *IEEE Trans. Haptics*, vol. 10, no. 4, pp. 456–466, 2017, doi: 10.1109/TOH.2017.2686849.

[60] R. Lewis, C. Menardi, A. Yoxall, and J. Langley, "Finger friction: Grip and opening packaging," *Wear*, vol. 263, no. 7-12 SPEC. ISS., pp. 1124–1132, 2007, doi: 10.1016/j.wear.2006.12.024.

[61] S. Chen and S. Ge, "Experimental research on the tactile perception from fingertip skin friction," *Wear*, vol. 376–377, pp. 305–314, 2017, doi: 10.1016/j.wear.2016.11.014.

[62] A. Abdouni, R. Vargiolu, and H. Zahouani, "Impact of finger biophysical properties on touch gestures and tactile perception: Aging and gender effects," *Sci. Rep.*, vol. 8, no. 1, pp. 1–13, 2018, doi: 10.1038/s41598-018-30677-2.

[63] M. S. Kim, I. Y. Kim, Y. K. Park, and Y. Z. Lee, "The friction measurement between finger skin and material surfaces," *Wear*, vol. 301, no. 1–2, pp. 338–342, 2013, doi: 10.1016/j.wear.2012.12.036.

[64] B. Camillieri, M. A. Bueno, M. Fabre, B. Juan, B. Lemaire-Semail, and L. Mouchnino, "From finger friction and induced vibrations to brain activation: Tactile comparison between real and virtual textile fabrics," *Tribol. Int.*, vol. 126, no. March, pp. 283–296, 2018, doi: 10.1016/j.triboint.2018.05.031.

[65] J. S. COMAISH, P. R. H. HARBOROW, and D. A. HOFMAN, "A hand-held friction meter," *Br. J. Dermatol.*, vol. 89, no. 1, pp. 33–35, 1973, doi: 10.1111/j.1365-2133.1973.tb01914.x.

[66] M. Zhang and A. F. T. Mak, "In vivo friction properties of human skin," *Prosthet.*

Orthot. Int., vol. 23, no. 2, pp. 135–141, 1999, doi: 10.3109/03093649909071625.

[67] S. C. Henao, S. Cuartas-Escobar, and J. Ramírez, "Coefficient of Friction Measurements on Transfemoral Amputees," *Biotribology*, vol. 22, no. November 2019, p. 100126, 2020, doi: 10.1016/j.biotri.2020.100126.

[68] C. P. Hendriks and S. E. Franklin, "Influence of surface roughness, material and climate conditions on the friction of human skin," *Tribol. Lett.*, vol. 37, no. 2, pp. 361–373, 2010, doi: 10.1007/s11249-009-9530-7.

[69] A. B. Cua, K. P. Wilhelm, and H. I. Maibach, "Frictional properties of human skin: Relation to age, sex and anatomical region, stratum corneum hydration and transepidermal water loss," *Br. J. Dermatol.*, vol. 123, no. 4, pp. 473–479, 1990, doi: 10.1111/j.1365-2133.1990.tb01452.x.

[70] S. Derler, U. Schrade, and L. C. Gerhardt, "Tribology of human skin and mechanical skin equivalents in contact with textiles," *Wear*, vol. 263, no. 7-12 SPEC. ISS., pp. 1112–1116, 2007, doi: 10.1016/j.wear.2006.11.031.

[71] O. Bobjer, S. E. Johansson, and S. Piguet, "Friction between hand and handle. Effects of oil and lard on textured and non-textured surfaces; perception of discomfort," *Appl. Ergon.*, vol. 24, no. 3, pp. 190–202, 1993, doi: 10.1016/0003-6870(93)90007-V.

[72] M. Klaassen, E. G. de Vries, and M. A. Masen, "Friction in the contact between skin and a soft counter material: Effects of hardness and surface finish," *J. Mech. Behav. Biomed. Mater.*, vol. 92, no. January, pp. 137–143, 2019, doi: 10.1016/j.jmbbm.2019.01.006.

[73] S. Derler, J. Süess, A. Rao, and G. M. Rotaru, "Influence of variations in the pressure distribution on the friction of the finger pad," *Tribol. Int.*, vol. 63, pp. 14–20, 2013, doi: 10.1016/j.triboint.2012.03.001.

[74] O. S. Dinç, C. M. Ettles, S. J. Calabrese, and H. A. Scarton, "Some parameters affecting tactile friction," *J. Tribol.*, vol. 113, no. 3, pp. 512–517, 1991, doi: 10.1115/1.2920653.

[75] M. Srinivasan, J. Biggs, B. Raju, S. De, J. Cysyk, and AC, "Role of skin biomechanics in mechanoreceptor response," 2002.

[76] J. R. Flanagan, M. K. O. Burstedt, and R. S. Johansson, "Control of fingertip forces in multidigit manipulation," *J. Neurophysiol.*, vol. 81, no. 4, pp. 1706–1717, 1999, doi: 10.1152/jn.1999.81.4.1706.

[77] M. J. Adams, R. McKeown, and A. Whall, "A micromechanical model for the confined uni-axial compression of an assembly of elastically deforming spherical particles," *J.*

Phys. D. Appl. Phys., vol. 30, no. 5, pp. 912–920, Mar. 1997, doi: 10.1088/0022-3727/30/5/025.

[78] K. L. Johnson and J. A. Greenwood, "An approximate {JKR} theory for elliptical contacts," *J. Phys. D. Appl. Phys.*, vol. 38, no. 7, pp. 1042–1046, Mar. 2005, doi: 10.1088/0022-3727/38/7/012.

[79] J. van Kuilenburg, *A mechanistic approach to tactile friction*. 2013.

[80] E. W. Rowe, "The Friction and Lubrication of Elastomers. D. F. Moore. Pergamon, Oxford. 1972. 288 pp. Illustrated. £7.50.," *Aeronaut. J.*, vol. 79, no. 769, pp. 45–45, 1975, doi: 10.1017/S0001924000034795.

[81] P. Humbert, F. Ferial, P. Agache, and H. I. Maibach, *Agache ' s Measuring the Skin*. 2004.

[82] N. K. Veijgen, M. A. Masen, and E. Van Der Heide, "A novel approach to measuring the frictional behaviour of human skin in vivo," *Tribol. Int.*, vol. 54, pp. 38–41, 2012, doi: 10.1016/j.triboint.2012.05.022.

[83] M. Kwiatkowska, S. E. Franklin, C. P. Hendriks, and K. Kwiatkowski, "Friction and deformation behaviour of human skin," *Wear*, vol. 267, no. 5–8, pp. 1264–1273, 2009, doi: 10.1016/j.wear.2008.12.030.

[84] T. André, P. Lefèvre, and J. L. Thonnard, "A continuous measure of fingertip friction during precision grip," *J. Neurosci. Methods*, vol. 179, no. 2, pp. 224–229, 2009, doi: 10.1016/j.jneumeth.2009.01.031.

[85] S. E. Tomlinson, R. Lewis, X. Liu, C. Texier, and M. J. Carré, "Understanding the friction mechanisms between the human finger and flat contacting surfaces in moist conditions," *Tribol. Lett.*, vol. 41, no. 1, pp. 283–294, 2011, doi: 10.1007/s11249-010-9709-y.

[86] S. Derler, L. C. Gerhardt, A. Lenz, E. Bertaux, and M. Hadad, "Friction of human skin against smooth and rough glass as a function of the contact pressure," *Tribol. Int.*, vol. 42, no. 11–12, pp. 1565–1574, 2009, doi: 10.1016/j.triboint.2008.11.009.

[87] T. Soneda and K. Nakano, "Investigation of vibrotactile sensation of human fingerpads by observation of contact zones," *Tribol. Int.*, vol. 43, no. 1–2, pp. 210–217, 2010, doi: 10.1016/j.triboint.2009.05.016.

[88] N. K. Veijgen, E. van der Heide, and M. A. Masen, "Skin friction measurement; the development of a new device," *Prod. Acad. Issues*, vol. 2, pp. 28 – 35, 2010.

Chapter - 5
Predictive Modelling and Optimization for Coefficient of Friction

5.1 Introduction

Human skin the largest organ, gets in contact with variety of materials in a day-to-day task of an individual ranging from apparels to handling and gripping of objects. Tactile perception, skin compatibility, touch properties and comfort are the human factors that relate to frictional phenomena at skin-object interface [1]. Experimental studies for the tribological phenomena of human skin have been investigated in variety of applications such as medical [2]–[4] sports [5], [6], and textiles [2], [7]–[9].

In literature [10], a statistical model to predict the coefficient of friction (COF) in a limited range of normal load between 0.2 to 2 N for the parameters affecting the human skin friction is reported. (Discussed in detail in chapters 2 and 3). Till date, no known study has been performed for the optimization or comparison of the experimental investigations making use of available optimization techniques. Hence it is imperative to have a model for the COF prediction for an optimised value of independent variables (attributes affecting human skin friction).

To get coherent range for input variables, statistical tools are the foremost choice to get the most optimum and reliable results. For the predictive model development and optimization research, statistical tool such as response surface methodology (RSM) has been highly adapted in the engineering domain [11]–[14] introduced by box and Wilson [15]. RSM [16] involves three key steps: design of experimental runs, statistical analyses, and optimization of input or the independent variables.

Another technique for the complex decision making and predictive model development, artificial neural network (ANN) is very popular among the research community [17]–[20]. ANN operates very similar to the human nervous system [21]. Modelling by ANN is highly preferable by virtue of its fast-processing time and precision results for the intricate data involved [22]. Various researchers confirm that ANN has higher accuracy and better model predictability than RSM [23]–[26]. ANN's heuristic approach applies the multilayer perceptron to approximate the objective function thereby resolving the optimization problems where Lagrange multipliers are not feasible [27]. Current work reports the predictive models

developed individually through RSM and the ANN technique. Further, the minimization of the COF as a response is performed through the RSM for the optimal values of the input variables.

In section 5.2 predictive model is developed through RSM. Followed by section 5.3 that presents development of predictive model with ANN . In section 5.4, a comparative study of the two predictive model is performed. Section 5.5 presents the optimization of COF as a response variable through RSM. Lastly, section 5.5 summarises chapter 5.

5.2 Predictive Modelling for COF using Response Surface Methodology

RSM optimization technique developed by [28] is a set of mathematical and statistical tools that are employed for the model development and the problem analysis of a response affected by various independent variables. RSM was performed with Minitab software (version 18). Three independent variables were chosen for optimization of the COF values. Normal load (N), sliding velocity (cm/ sec) and skin hydration (Arbitrary units- A.U.) with four levels for normal load and sliding velocity while 3 level for skin hydration as shown in Table 5.1. The quadratic was regarded as a model of the design in a total of 48 run samples. The multiple regression analysis was performed by following the second order polynomial quadratic as in equation 5.1:

$$y = a_0 + a_1 x_i + \sum_{i=1}^{k} a_i x_i^2 + \sum\sum_{i<j<2}^{k} a_{ij} x_i x_j \qquad \textbf{5.1}$$

Where, y is the predicted response, a_0, a_1 a_i, a_{ii}, a_{ij}, x_i, and k are numeric constant, linear coefficient, quadratic coefficient, i^{th} interaction, independent variable, and the error term respectively.

Table 5.1 Experimental runs with corresponding input variables and the response

Experimental run	Input Parameters			Response
	Normal load (N)	Sliding velocity (cm/sec)	Skin hydration (A.U.)	COF
1	4	4.5	34	5.31
2	4	6.5	34	6.72
3	4	8.5	34	4.93
4	4	10.5	34	3.88
5	6	4.5	34	4.53
6	6	6.5	34	4.78
7	6	8.5	34	3.78
8	6	10.5	34	2.26
9	8	4.5	34	3.9

10	8	6.5	34	3.7
11	8	8.5	34	3.24
12	8	10.5	34	2.38
13	10	4.5	34	3.51
14	10	6.5	34	3.4
15	10	8.5	34	2.69
16	10	10.5	34	1.96
17	4	4.5	37	5.69
18	4	6.5	37	5.19
19	4	8.5	37	4.47
20	4	10.5	37	2.67
21	6	4.5	37	5.26
22	6	6.5	37	4.89
23	6	8.5	37	3.37
24	6	10.5	37	2.17
25	8	4.5	37	4.42
26	8	6.5	37	4.59
27	8	8.5	37	3.33
28	8	10.5	37	2.2
29	10	4.5	37	3.28
30	10	6.5	37	4.84
31	10	8.5	37	3.28
32	10	10.5	37	1.94
33	4	4.5	40	4.52
34	4	6.5	40	6.59
35	4	8.5	40	5.96
36	4	10.5	40	3.28
37	6	4.5	40	4.32
38	6	6.5	40	5.36
39	6	8.5	40	4.52
40	6	10.5	40	3.1
41	8	4.5	40	4.17

42	8	6.5	40	4.32
43	8	8.5	40	4.4
44	8	10.5	40	2.33
45	10	4.5	40	3.61
46	10	6.5	40	3.91
47	10	8.5	40	2.53
48	10	10.5	40	1.96

5.2.1 Mathematical model

Experimental values obtained for the coefficient of friction between human finger pad and steel probe measured through the rotary type of human skin tribometer in chapter 4 are tabulated in Table 5.1 that is used for the development of predictive model for the COF at the finger pad interface using equation 5.2.

$$COF = 19.1 - 0.956 * NL + 1.041 * SV - 0.75 * SH + 0.0250\, NL*NL - 0.1153\, SV*SV + 0.0093\, SH*SH + 0.0113\, NL*SV + 0.0060\, NL*SH + 0.0076\, SV*SH \quad \textbf{5.2}$$

Figure 5.1 shows the plot for the experimental and the predicted values of COF obtained through the model using equation 2. Mean square error (MSE) between the experimental and the predicted value of COF is 0.22 which clearly shows the degree of overlapping as per the critical domain of application. Table 5.2 summarises the COF values obtained through the experimental run and the corresponding predicted values.

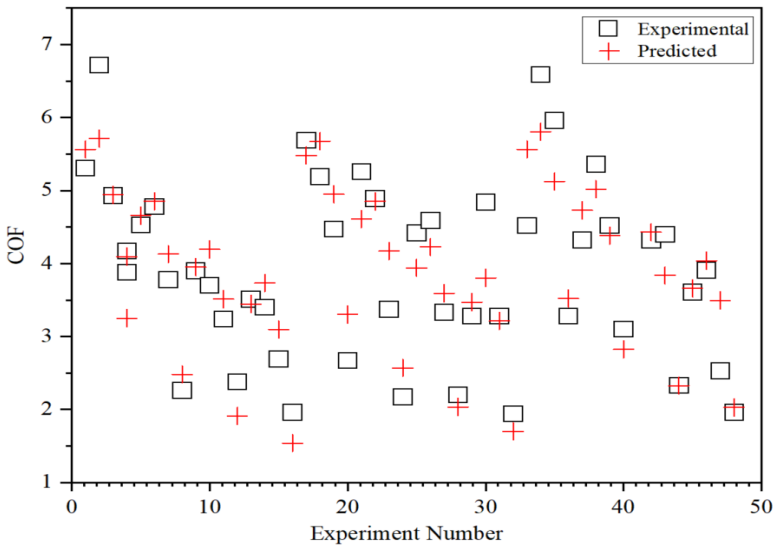

Figure 5.1 Plot for the experimental vs predicted values of COF

Table 5.2 COF value at the finger pad interface obtained through experimentation and the predictive model

Experiment No.	Coefficient of friction	
	Experimental	RSM
1	5.31	5.56
2	6.72	5.71
3	4.93	4.94
4	3.88	3.24
5	4.53	4.65
6	4.78	4.85
7	3.78	4.12
8	2.26	2.48
9	3.9	3.95
10	3.7	4.19
11	3.24	3.51
12	2.38	1.90
13	3.51	3.44
14	3.4	3.73
15	2.69	3.09
16	1.96	1.53
17	5.69	5.47
18	5.19	5.67
19	4.47	4.95
20	2.67	3.30
21	5.26	4.61
22	4.89	4.85
23	3.37	4.17
24	2.17	2.56
25	4.42	3.94
26	4.59	4.22
27	3.33	3.59
28	2.2	2.03
29	3.28	3.47
30	4.84	3.80
31	3.28	3.21
32	1.94	1.69
33	4.52	5.56
34	6.59	5.80
35	5.96	5.12
36	3.28	3.52
37	4.32	4.72
38	5.36	5.01
39	4.52	4.38
40	3.1	2.82
41	4.17	4.09
42	4.32	4.42
43	4.4	3.83
44	2.33	2.32

45	3.61	3.66
46	3.91	4.03
47	2.53	3.49
48	1.96	2.02

5.2.2 Analysis of variance (ANOVA)

ANOVA is a statistical tool or a formula which determines the variances across means for the different groups. Table 5.3 summaries the results of the ANOVA analysis obtained for the development of the predictive model of the COF between steel probe and the finger pad. The model has three independent variables namely normal load (NL), sliding velocity (SV) and the skin hydration (SH). Table 5.3 has the linear terms, square terms, and the interaction terms for the independent variables. Sum of square defines the square of the deviations from the mean. Contribution defines the source of variation for each variable to the total variations in the results. Adjusted sum of squares explains the amount of variation in the response which is explained by an individual term of the developed model. Adjusted mean of squares quantifies the amount of variation the model explains, considering all other terms of the model. F value is the ratio between the variation of means between samples to the variation within the sample. P value or probability value is used to determine the statistical significance of results at a confidence level (95% for the current study). If the p value of a term in the model is more than 0.05, the term is insignificant for the model development and vice-versa.

Table 5.3 Analysis of variance (ANOVA)

Source	DF	Seq SS	Contribution	Adj SS	Adj MS	F-Value	p-Value
Regression	9	59.2458	84.87%	59.2458	6.5829	23.68	0.000
Linear	3	48.1978	69.04%	48.1978	16.0659	57.78	0.000
Normal Load	1	21.7533	31.16%	21.7533	21.7533	78.24	0.000
Sliding Velocity	1	25.9680	37.20%	25.9680	25.9680	93.40	0.000
Skin Hydration	1	0.4765	0.68%	0.4765	0.4765	1.71	0.198
Square	3	10.7610	15.41%	10.7610	3.5870	12.90	0.000
NL*NL	1	0.4790	0.69%	0.4790	0.4790	1.72	0.197
SV*SV	1	10.2075	14.62%	10.2075	10.2075	36.71	0.000
SH*SH	1	0.0745	0.11%	0.0745	0.0745	0.27	0.608
Interaction	3	0.2870	0.41%	0.2870	0.0957	0.34	0.794
NL*SV	1	0.1531	0.22%	0.1531	0.1531	0.55	0.463
NL*SH	1	0.0513	0.07%	0.0513	0.0513	0.18	0.670
SH*SV	1	0.0826	0.12%	0.0826	0.0826	0.30	0.589

Error	38	10.5654	15.13%	10.5654	0.2780
Total	47	69.8112	100.00%		

R^2 = 0.8487 R^2 (adj) = 0.8128 R^2 (pred) = 0.7483

Sliding velocity is found to be the most significant factor affecting the COF with a contribution of 37.20%, followed by normal load contributing 31.16% and square term of sliding velocity contributing 14.62%. Linear term of skin hydration, square terms for normal load and skin hydration including all three interaction terms have p value of more than 0.05 thereby having insignificant role in the development of the model. Coefficient of determination R^2, defined as the ratio of the explained variation to the total variation, signifies how well is the fitness of model. As R^2 tends to the value equal to 1, the fitness of the response model improves. The value of R^2 = 0.8487 indicates that 84.87 % of the total variations are explained by the model. Adjusted R^2 adjusts the R^2 with respect to the variables that are not significant to the model, it considers the number of independent variables used for predicting the response. Adjusted R^2 having value of 0.8128 indicates that model explains variability of 81.28 % when considering the significant terms. Predicted R^2 with value of 0.7483 depicts that the model is expected to explain 74.83 % variability when tested with the new set of data.

5.2.3 Fitness of the model

Model satisfies its appropriacy by the residuals, which is defined as the difference between the experimental(observed) and the predicted value. For model to be adequate, points on the normal probability plots of the residual should form a straight line. Figure 5.2 clearly depicts that all the points approximately lie on a straight line without any special trend and the errors being distributed normally. In residual analysis, 'residual vs fit plot' shown in Figure 5.3 is used to examine outliers, unequal error variances, and the non-linearity.

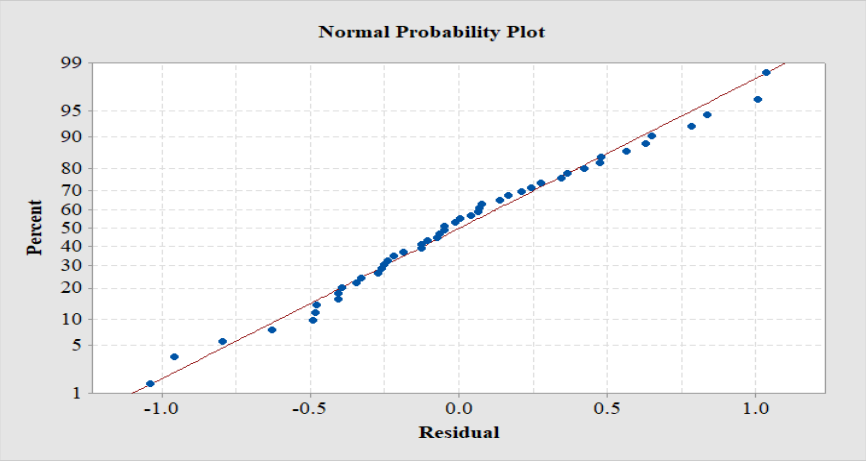

Figure 5.2 Normal probability plot of residual for COF

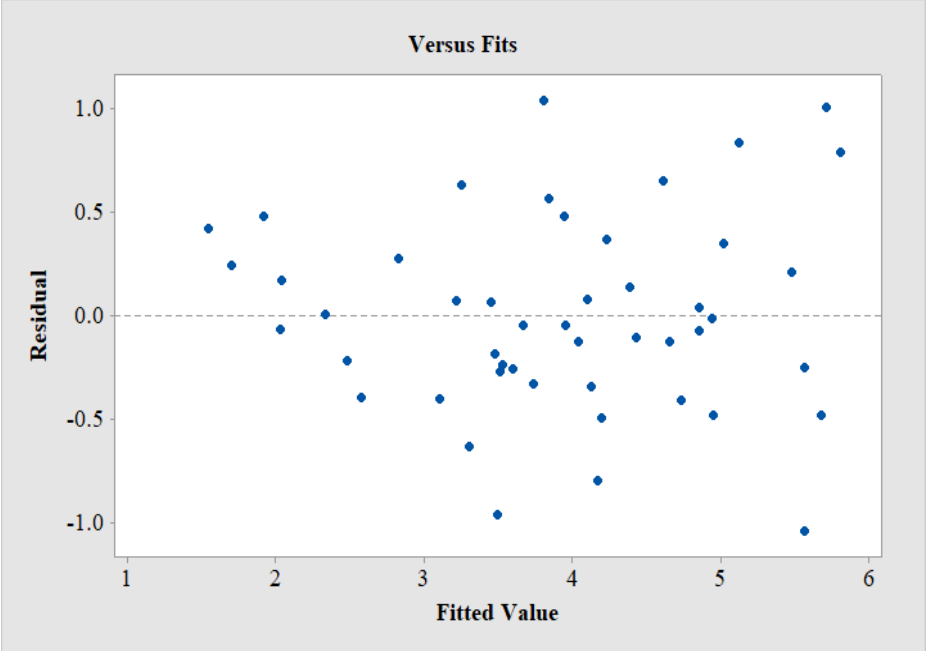

Figure 5.3 Residuals vs fitted value for response (COF)

5.2.4 Parametric influence of input parameters on COF

As discussed in previous chapters, COF at the finger pad interface is affected by multiple macro, micro and intrinsic or extrinsic factors. Since micro factors such as relative humidity, temperature, and surface roughness affecting the human skin friction were not controlled hence are assumed to be similar across the experiments. Only the macro parameters normal load, sliding velocity and skin hydration as an intrinsic attribute of human skin friction measurement are parametrically investigated. Fitted means assess the response differences due to changes in factor levels, it's a good practice to use the fitted means for better and precise results. Figure 5.4 shows the main effect plot, highlight increase in normal load substantially decreases the COF value i.e., normal load being inversely proportional to the COF value. Sliding velocity shows an initial increase and then substantial decrease in the COF that is attributed to the breakage of interfacial bonds at the finger pad in the physical aspects of contact. Effect of skin hydration cannot be concretely defined through these experiments and requires higher number of subjects and datapoints. Main effect plot clearly explains the ANOVA values reported in Table 5.2. Interaction plot in Figure 5.5 illustrates that there is no relation between the interaction of the attributes normal load, sliding velocity and the skin hydration in agreement to the p value obtained in the ANOVA results.

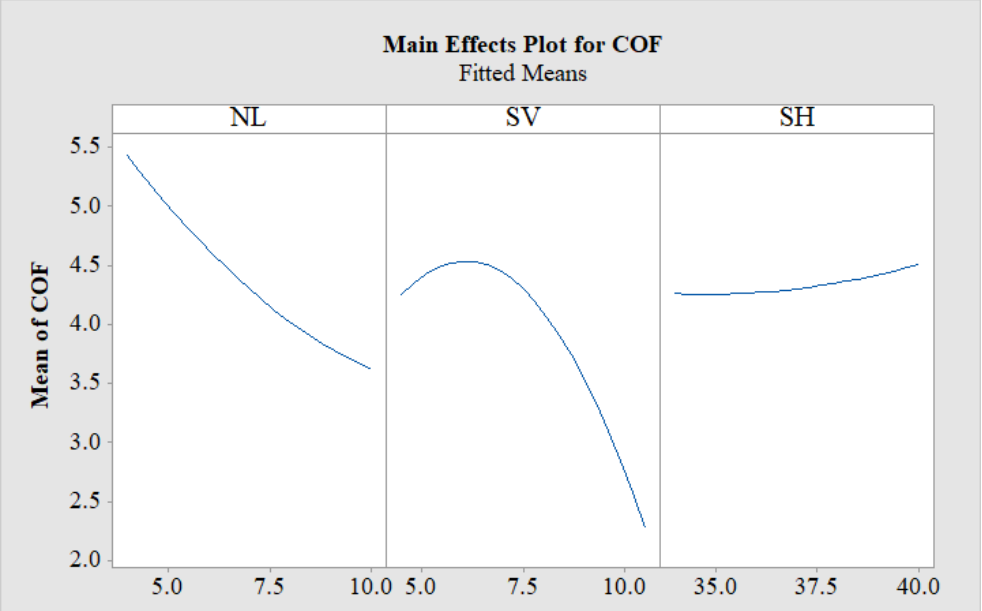

Figure 5.4 Main effects plot for COF

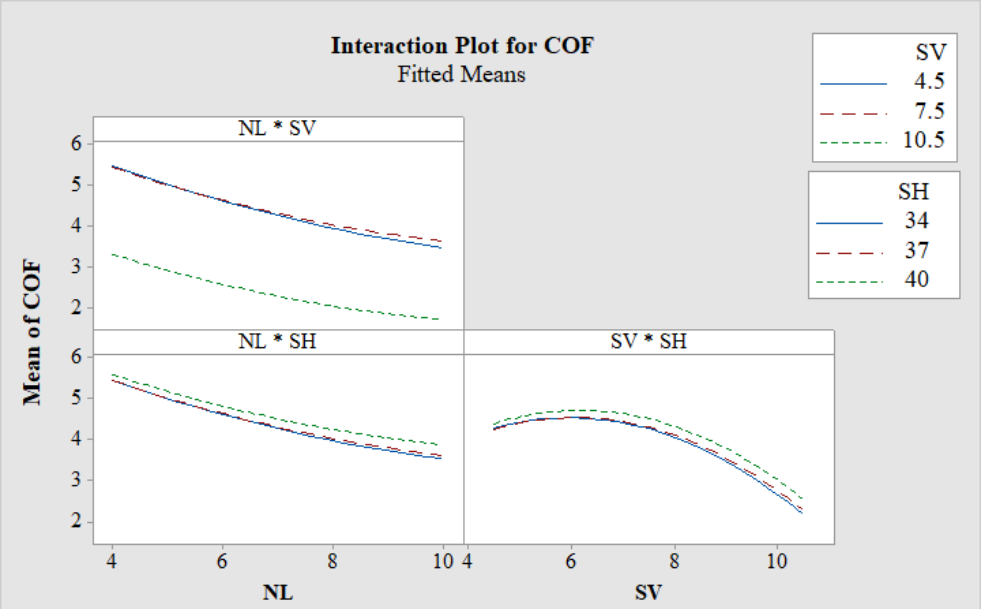

Figure 5.5 Interaction plot for COF

Surface plots and contour plots are shown in Figure 5.6 – Figure 5.8. Figure 5.6 (a) and Figure 5.6 (b) shows the surface plot and contour plot for COF vs sliding velocity and normal load at a constant value of 37 for skin hydration respectively. It is clear from both the plots that COF increases with SV up to approximately 6.5 cm/ sec and decreases beyond it. Although increase in normal load linearly decreases the COF values at the interface.

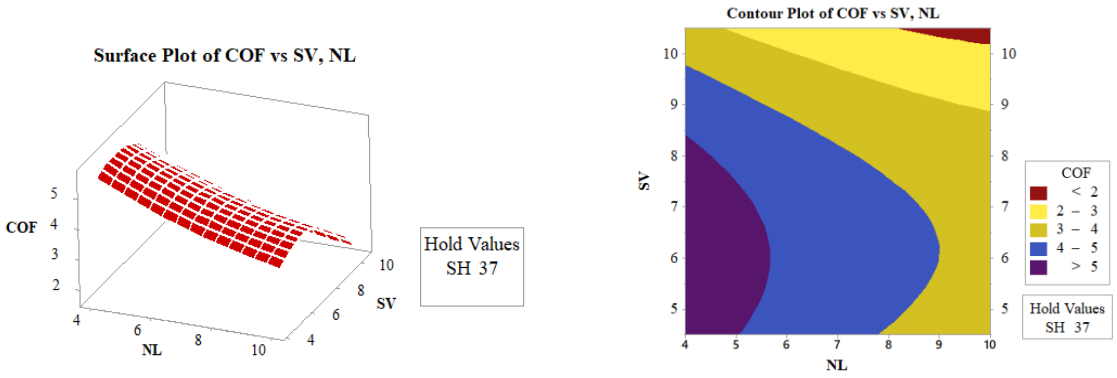

(a) (b)

Figure 5.6 (a) Surface plot and contour Plot for COF vs sliding velocity (SV) and normal load (NL) at skin hydration (SH) of 37

Figure 5.7 (a) and Figure 5.7 (b) shows the surface plot and contour plot for COF vs skin hydration and sliding velocity at a constant value of normal load 7 N respectively. Skin hydration being the insignificant factor as deduced from its p value of more than 0.05 in the ANOVA results, have very small or no effect on the COF values at the finger pad contact.

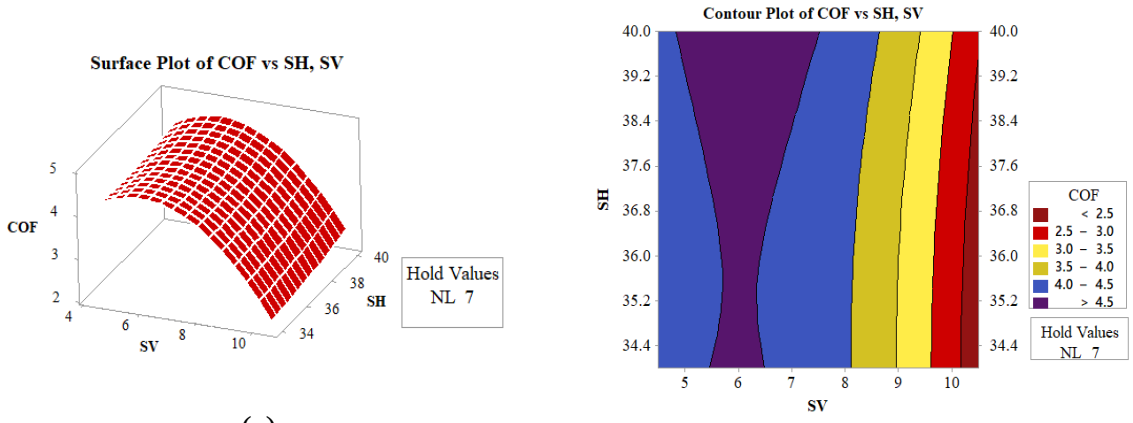

(a) (b)

Figure 5.7 (a) Surface and contour plot for COF vs skin hydration (SH) and sliding velocity (SV) at normal load (NL) of 7N

It is to be observed from Figure 5.8 (a) and Figure 5.8 (b) that only normal load has a pronounced effect on the COF value at a constant sliding velocity. COF forming a ridge at the initial values of normal load, continuously increases the COF value with a decrease in normal load. These 3D plots can be made use of while designing a similar contact device and obtaining a specificized range of the COF keeping the sliding and hydration components in range.

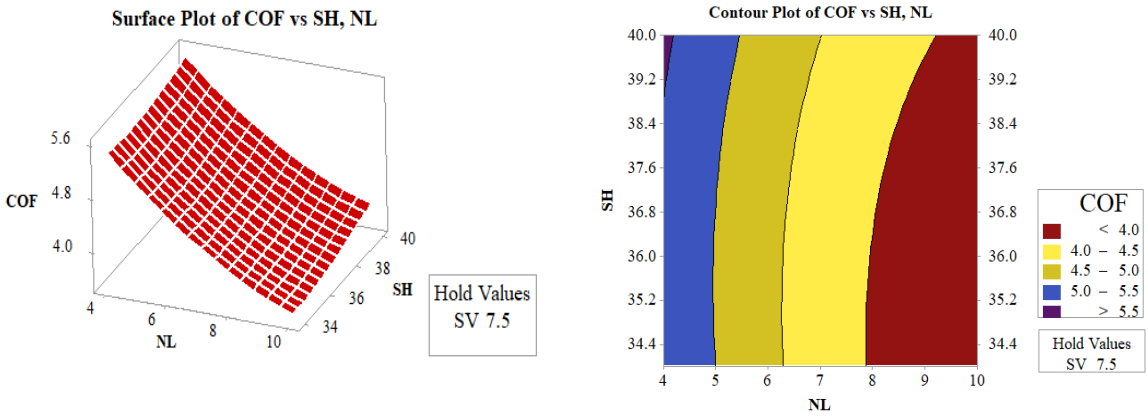

(a) (b)

Figure 5.8 (a) Surface and contour plot for COF vs skin hydration (SH) and normal load (NL) at sliding velocity (SV) of 7.5 cm/ sec

5.3 Predictive Modelling for COF using Artificial Neural Network

Artificial neural network (ANN) is inspired by a real human nervous system. Its basic unit of operation is referred to as neurons. As human brain ANN effectively deals with problems involving large and noisy data. The central framework of the ANN model consists of a neuron which has unidirectional connection such as biological dendrites. Connections carry specific weights that are passed to the hidden layer. Within the hidden layer an activation function (summation unit) is applied along with a bias. Generally, neural network (NN) has three layers viz an input layer to receive signal and information from an environment, an output layer to transmit the information to the environment and in between these lie the hidden layers. NN are structured based on the connection architecture, activation functions, and the learning/ training functions used in the development of network. A multilayer feed forward network is as shown in Figure 5.9 below.

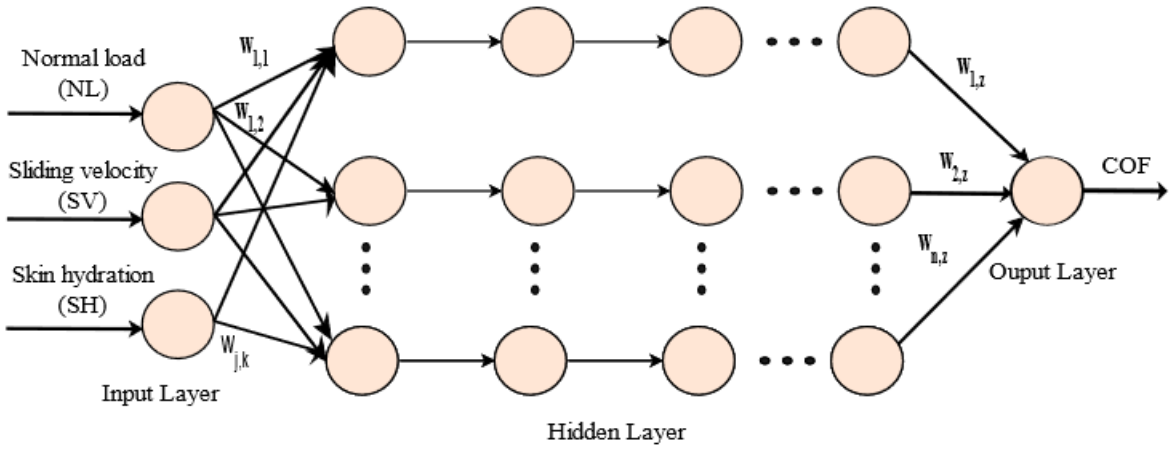

Figure 5.9 Multilayer feed forward network

All layers are interconnected in a way that each neuron of a preceding layer is connected to each neuron of a successive layer. Input layer simply takes value and transmits to its connected neurons. Signals are unidirectional from input to the hidden and finally transmitted by the output layer. All the processing and operations are performed in the hidden or the output layer. NN is further trained to perform a task by adjusting the weights at the connection between the neurons. Error is computed as the difference between the targeted output and the output obtained through the network. An activation function consisting of linear and non-linear equations (to better handle complex non- linearity) is incorporated to determine the output of the neuron. Output layer takes the processed results from activation function and presents the output.

5.3.1 Factors affecting ANN model development

Although not much is reported in the domain of human skin tribology pertaining to ANN, literature highlights that irrespective of application specificity, NN is greatly affected by the following parameters that are common for the development of an efficient predictive model:

Neural network structure

Current predictive model developed through the ANN technique consists of 3 input layers, 10 hidden layers and an output layer.

Dataset

Literature reports that increase in the amount of training data, subsequently enhances the accuracy of the model. Since the current study is human based, in-vivo experiments involving the ethical regulations put limits on the number of experimental runs that could be performed. In other domains of applications such as machining, condition monitoring extraction techniques popularly 27 runs are taken (varies with factors and levels), so having 48 runs seems to be a good fit for training a model involving the associated subjectivities.

Training to testing data ratio

Dataset was divided in the ratio of 70:30, 34 datapoints were taken as training samples while,14 was taken as the testing data sets.

Network type

Feedforward backpropagation is taken for the model development. This technique continuously updates the error to the hidden layer. Backpropagation algorithm used here, is one of the most popular techniques in the engineering domain for the development of predictive models through the ANN.

Transfer function, Adaption learning function and Performance function

The net input to unit 'k' in the hidden layer provided by a multilayer feedforward training network with one hidden layer is given though equation 5.3:

$$Hidden\_net = \sum_{j=1}^{J} W_{j,k} i_j + b_k \qquad \textbf{5.3}$$

Where $w_{j,k}$ is the weight between the input and hidden neurons, i_j is the input value for normal load, sliding velocity and skin hydration in relation to the experimental runs and b_k being the bias on the hidden nodes. The weights and bias between the input and hidden layers used for the model development are tabulated in Table 5.4.

Table 5.4 Weight and bias between input and hidden neurons

$W_{j,k}$ j=3, k=10	W_{1k}	W_{2k}	W_{3k}	b_k
1	3.68	4.84	-0.81	-3.78
2	1.09	-4.83	-3.08	4.65
3	-5.76	1.66	1.496	-2.37
4	-0.10	-0.36	-1.55	0.52
5	3.25	2.05	-0.80	0.75
6	-0.88	3.60	0.83	-0.70
7	-0.53	2.13	-3.45	3.21
8	1.05	-2.81	-2.35	2.57
9	-2.61	3.30	-1.07	-0.31
10	-1.42	1.99	-2.81	-2.86

Net input to the output layer (z) is computed through equation 5.4:

$$Output\_net = \sum_{k=1}^{k} W_{k,z} h_k + b_z \qquad \textbf{5.4}$$

$W_{k,z}$ being the weight between the hidden neurons and the output neuron, h_k is the output through hidden nodes while b_z is the bias attached to the output node. Weights between the hidden and output layer used are shown in Table 5.5. Bias between hidden and output layer is -0.9787.

Table 5.5 Weights between hidden and output neuron

$W_{k,z}$, k=10 z=1	W_{1k}
1	-0.34

2	1.26
3	0.15
4	-1.06
5	-0.24
6	-0.57
7	0.95
8	-0.69
9	-0.09
10	0.42

ANN feed forward back propagation used the Levenberg Marquardt (LM) for training the algorithm with the weights and biases as mentioned in Table 5.4. Mean Squared Error (MSE) is computed for the performance measurement through equation 5.5. Various functions used in the model development are presented in Table 5.6.

$$MSE = \frac{1}{n}\sum_{i=1}^{n}(y_i - \left(y_l\right) \quad \textbf{5.5}$$

Where,

MSE=mean squared error

n = number of sample

y_i = (observed) experimental value

$\widehat{y_l}$ = predicted value

Table 5.6 Summary of parameters used in the developed model

Parameter	Algorithm used
Transfer function	logsig, tansig
Training function	traingdx
Learning function	learngd

5.3.2 Analysis of the results obtained through ANN predictive model

Figure 5.10 shows the plot for MSE and the epoch (iteration number). MSE decreased with each ascending iteration up to 385 and became constant thereon, thus stopping the training algorithm. Further, model was tested with the different set of values not used in the training phase and a plot for the experimental vs ANN – predicted COF values tabulated in Table 5.7 is depicted in Figure 5.11.

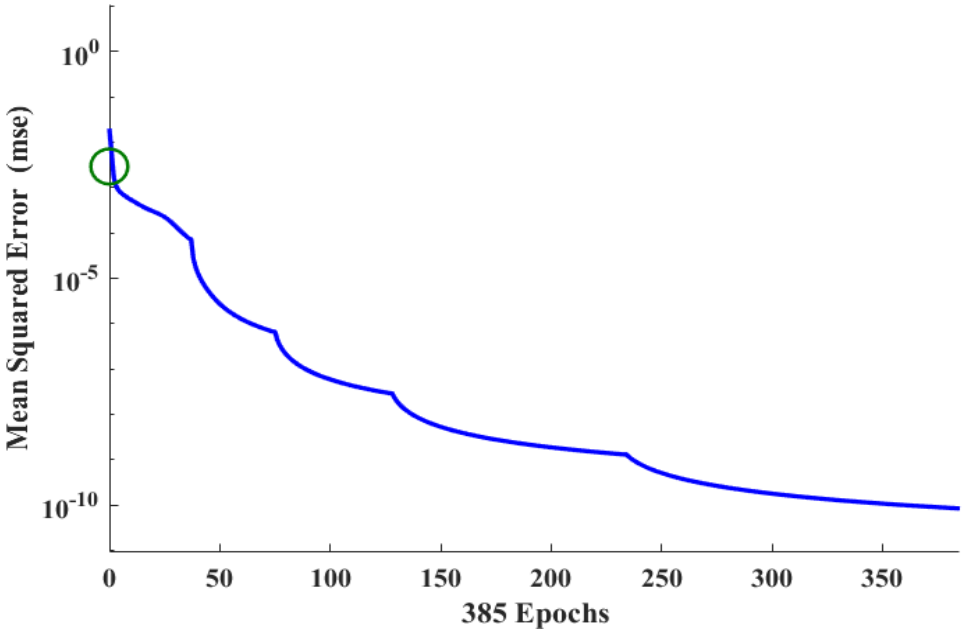

Figure 5.10 Mean square error vs epochs

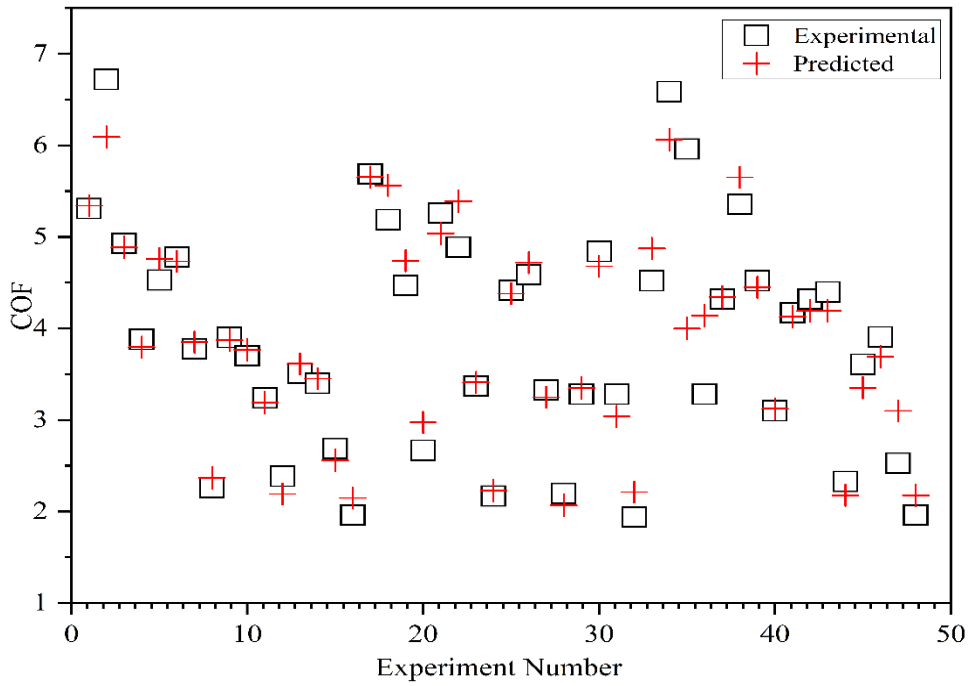

Figure 5.11 Plot for the experimental vs predicted (ANN) values of COF

Table 5.7 Tabulation of experimental and predicted values of COF

Experiment No.	Coefficient of friction	
	Experimental	ANN
1	5.31	5.34
2	6.72	6.09
3	4.93	4.88
4	3.88	3.79
5	4.53	4.76
6	4.78	4.73

7	3.78	3.85
8	2.26	2.36
9	3.90	3.87
10	3.70	3.76
11	3.24	3.19
12	2.38	2.19
13	3.51	3.61
14	3.40	3.45
15	2.69	2.55
16	1.96	2.14
17	5.69	5.65
18	5.19	5.56
19	4.47	4.74
20	2.67	2.97
21	5.26	5.03
22	4.89	5.38
23	3.37	3.41
24	2.17	2.22
25	4.42	4.38
26	4.59	4.72
27	3.33	3.24
28	2.20	2.06
29	3.28	3.35
30	4.84	4.67
31	3.28	3.03
32	1.94	2.21
33	4.52	4.87
34	6.59	6.06
35	5.96	3.99
36	3.28	4.14
37	4.32	4.34
38	5.36	5.65
39	4.52	4.45
40	3.10	3.12
41	4.17	4.12
42	4.32	4.19
43	4.40	4.19
44	2.33	2.17
45	3.61	3.35
46	3.91	3.69
47	2.53	3.09
48	1.96	2.17

5.4 Comparative Analysis of the Developed Predictive Models

Table 5.8 summarises the results obtained through experiment, and the two predictive models developed by RSM and ANN respectively along with the associated relative errors through equation 6 per experimental run. The mean average relative error for RSM is 9.93% while that

for the ANN it is 5.91%. Although ANN model has a lesser relative error in comparison to the predictive model developed by the RSM, considering the nature of subjectivities associated with the domain of application, error < 10% is too in acceptable range. Equation 5.6 calculates the relative error.

$$Relative\ error = \frac{|Experimental - Predicted|}{Experimental} * 100\% \quad \textbf{5.6}$$

Table 5.8 Experimental/ predicted values and relative errors for COF

Experiment No.	Coefficient of friction			Relative error (%)	Relative error (%)
	Experimental	RSM	ANN	RSM	ANN
1	5.31	5.56	5.34	4.76	0.61
2	6.72	5.71	6.09	14.96	9.32
3	4.93	4.94	4.88	0.27	0.88
4	3.88	3.24	3.79	16.23	2.15
5	4.53	4.65	4.76	2.81	5.08
6	4.78	4.85	4.73	1.55	0.95
7	3.78	4.12	3.85	9.21	1.85
8	2.26	2.48	2.36	9.73	4.79
9	3.9	3.95	3.87	1.33	0.71
10	3.70	4.19	3.76	13.33	1.83
11	3.24	3.51	3.19	8.42	1.50
12	2.38	1.90	2.19	19.92	8.08
13	3.51	3.44	3.61	1.82	2.94
14	3.40	3.73	3.45	9.78	1.51
15	2.69	3.09	2.55	15.14	4.83
16	1.96	1.53	2.14	21.45	9.61
17	5.69	5.47	5.65	3.69	0.65
18	5.19	5.67	5.56	9.37	7.18
19	4.47	4.95	4.74	10.75	6.05
20	2.67	3.30	2.97	23.70	11.35
21	5.26	4.61	5.03	12.35	4.21
22	4.89	4.85	5.38	0.77	10.21
23	3.37	4.17	3.41	23.78	1.23
24	2.17	2.56	2.22	18.37	2.66
25	4.42	3.94	4.38	10.85	0.87
26	4.59	4.22	4.72	7.90	2.84
27	3.33	3.59	3.24	7.86	2.40
28	2.2	2.03	2.06	7.52	5.95
29	3.28	3.47	3.35	5.79	2.13
30	4.84	3.80	4.67	21.44	3.34
31	3.28	3.21	3.03	2.06	7.39
32	1.94	1.69	2.21	12.38	14.01
33	4.52	5.56	4.87	23.08	7.87
34	6.59	5.80	6.06	11.90	8.00
35	5.96	5.12	3.99	14.00	32.89

36	3.28	3.52	4.14	7.40	26.27
37	4.32	4.72	4.34	9.48	0.61
38	5.36	5.01	5.65	6.40	5.45
39	4.52	4.38	4.45	3.05	1.51
40	3.10	2.82	3.12	8.88	0.75
41	4.17	4.09	4.12	1.78	1.00
42	4.32	4.42	4.19	2.50	2.95
43	4.4	3.83	4.19	12.76	4.66
44	2.33	2.32	2.17	0.17	6.56
45	3.61	3.66	3.35	1.42	7.12
46	3.91	4.03	3.69	3.29	5.55
47	2.53	3.49	3.09	38.11	22.51
48	1.96	2.02	2.17	3.43	11.12

5.5 Optimization of COF through Response Surface Methodology

Problem formulation

COF optimization formulated through RSM as:

Minimise

*COF = 19.1 - 0.956 * NL + 1.041 * SV - 0.75 * SH + 0.0250 NL*NL - 0.1153 SV*SV+ 0.0093 SH*SH + 0.0113 NL*SV + 0.0060 NL*SH + 0.0076 SV*SH*

Subject to the following constraints:

$$4\ \text{N} \leq \text{NL} \leq 10\ \text{N}$$
$$4.5\ \text{cm/ sec} \leq \text{SV} \leq 10.5\ \text{cm/ sec}$$
$$34 \leq SH \leq 40$$

RSM optimization is based on the desirability function analysis. It works on the principles of reduced gradient algorithm, which starts with multiple solutions and finally obtains the maximum value of the desirability, to determine the most optimal solution. Desirability function is frequently used for the optimization of multi objective responses by converting to a single desirability value [29]–[31]. For the current case of single objective minimization problem, desirability value (d) is calculated using equation 5.7:

$$d = 1\ if\ , y \leq y_{\min}$$

$$d = \left(\frac{y - y_{\min}}{y_{\min} - y_{\max}} \right)^{r}, y_{\min} \leq y \leq y_{\max} \qquad \textbf{5.7}$$

$$d = 0\ if\ , y \geq y_{\max}$$

where,

y is the output during optimization, y_{min} and y_{max} being the lower and upper bounds of the response obtained through experimentation.

Desirability function is scaled in the range of 0 to 1.

The scale of the desirability function ranges between 0 (unacceptable) and 1 (target fit).

Three types of desirability functions are:

- Larger the better
- Smaller the better
- Nominal the better

In the present analysis single response optimization is performed for achieving minimum COF based on the predictive model given in equation 5.2. Optimization results are shown in Figure 5.12. Optimal values for normal load, sliding velocity and skin hydration are 10 N, 10.5 cm/ sec and 34 (A.U.) respectively. The optimum value of COF is 1.5395. Obtained desirability value obtained is 0.770, good with respect to domain of application. In Figure 5.12 individual graphs of COF with normal load, sliding velocity and skin hydration are plotted showing their individual effect on the response which agrees to the main effect plot, interaction plot and the ANOVA results discussed in the previous sections.

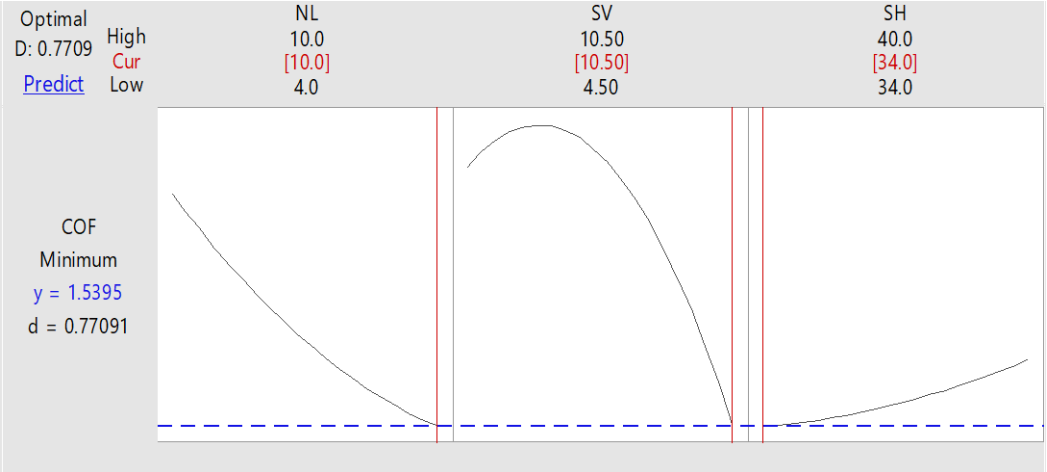

Figure 5.12 Response optimization plot for COF

5.6 Summary

In the current chapter, predictive models have been developed through response surface methodology (RSM) and artificial neural network (ANN). Salient features of the chapter are as mentioned below:

1. Three prominent attribute for the human finger pad friction with a contact interface namely normal load, sliding velocity and skin hydration were taken as independent variables.

2. Total 48 experimental runs were performed for the combination of 4 levels for normal load, sliding velocity and 3 levels for skin hydration.
3. ANOVA results conclude sliding velocity (SV), and normal load (NL) in linear, while SV*SV in quadratic as the most significant terms in the predictive model development through RSM. All interaction terms are insignificant with p value more than 0.05.
4. RSM model is checked through normal probability and residual plots.
5. A 3-10-1 architecture base neural network is designed for the development of predictive model through artificial neural network (ANN).
6. ANN network was validated through different set of data to determine the predictability of the model.
7. Comparative study on the performance of two techniques for the predictive model development with relative error of 9.93% for the RSM while 5.91% that for ANN revealed ANN to be better performing.
8. Parametric optimization performed through RSM resulted desirability value of 0.770 and the optimal values for the normal load, sliding velocity and skin hydration to be 10 N, 10.5 cm/ sec and 34 (A.U.) respectively.

References

[1] S. E. Tomlinson, R. Lewis, and M. J. Carré, "Review of the frictional properties of finger-object contact when gripping," *Proc. Inst. Mech. Eng. Part J J. Eng. Tribol.*, vol. 221, no. 8, pp. 841–850, 2007, doi: 10.1243/13506501JET313.

[2] S. Derler, A. Rao, P. Ballistreri, R. Huber, A. Scheel-Sailer, and R. M. Rossi, "Medical textiles with low friction for decubitus prevention," *Tribol. Int.*, vol. 46, no. 1, pp. 208–214, 2012, doi: 10.1016/j.triboint.2011.03.011.

[3] A. Cavaco, L. Durães, S. Pais, and A. Ramalho, "Friction of prosthetic interfaces used by transtibial amputees," *Biotribology*, vol. 6, pp. 36–41, 2016, doi: 10.1016/j.biotri.2016.04.001.

[4] M. J. Carré, S. K. Tan, P. T. Mylon, and R. Lewis, "Influence of medical gloves on fingerpad friction and feel," *Wear*, vol. 376–377, pp. 324–328, 2017, doi: 10.1016/j.wear.2017.01.077.

[5] R. Lewis, M. J. Carré, and S. E. Tomlinson, "Skin friction at the interface between hands and sports equipment," *Procedia Eng.*, vol. 72, no. December 2014, pp. 611–617, 2014, doi: 10.1016/j.proeng.2014.06.064.

[6] O. Troynikov, E. Ashayeri, and F. K. Fuss, "Tribological evaluation of sportswear with negative fit worn next to skin," *Proc. Inst. Mech. Eng. Part J J. Eng. Tribol.*, vol. 226, no. 7, pp. 588–597, 2012, doi: 10.1177/1350650111425876.

[7] W. Zhong, M. M. Q. Xing, N. Pan, and H. I. Maibach, "Textiles and human skin, microclimate, cutaneous reactions: An overview," *Cutan. Ocul. Toxicol.*, vol. 25, no. 1, pp. 23–39, 2006, doi: 10.1080/15569520500536600.

[8] G. M. Rotaru *et al.*, "Friction between human skin and medical textiles for decubitus prevention," in *Tribology International*, 2013, vol. 65, pp. 91–96, doi: 10.1016/j.triboint.2013.02.005.

[9] L. C. Gerhardt, V. Strässle, A. Lenz, N. D. Spencer, and S. Derler, "Influence of epidermal hydration on the friction of human skin against textiles," *J. R. Soc. Interface*, vol. 5, no. 28, pp. 1317–1328, 2008, doi: 10.1098/rsif.2008.0034.

[10] N. K. Veijgen, E. van der Heide, and M. A. Masen, "A multivariable model for predicting the frictional behaviour and hydration of the human skin," *Ski. Res. Technol.*, vol. 19, no. 3, pp. 330–338, 2013, doi: 10.1111/srt.12053.

[11] N. Mahto and S. R. Chakravarthy, "Response surface methodology for design of gas turbine combustor," *Appl. Therm. Eng.*, vol. 211, p. 118449, 2022, doi:

https://doi.org/10.1016/j.applthermaleng.2022.118449.

[12] L. Velásquez, A. Posada, and E. Chica, “Optimization of the basin and inlet channel of a gravitational water vortex hydraulic turbine using the response surface methodology,” *Renew. Energy*, vol. 187, pp. 508–521, 2022, doi: https://doi.org/10.1016/j.renene.2022.01.113.

[13] A. Shaban and M. A. Shalaby, “Modeling and optimizing of variance amplification in supply chain using response surface methodology,” *Comput. Ind. Eng.*, vol. 120, pp. 392–400, 2018, doi: https://doi.org/10.1016/j.cie.2018.04.057.

[14] P. W. Anggoro, Y. Purharyono, A. A. Anthony, M. Tauviqirrahman, A. P. Bayuseno, and Jamari, “Optimization of cutting parameters of new material orthotic insole using a Taguchi and response surface methodology approach,” *Alexandria Eng. J.*, vol. 61, no. 5, pp. 3613–3632, 2022, doi: https://doi.org/10.1016/j.aej.2021.08.083.

[15] G. E. P. Box and K. B. Wilson, “On the Experimental Attainment of Optimum Conditions,” *J. R. Stat. Soc. Ser. B*, vol. 13, no. 1, pp. 1–38, 1951, doi: 10.1111/j.2517-6161.1951.tb00067.x.

[16] R. H. Myers, D. C. Montgomery, G. Geoffrey Vining, C. M. Borror, and S. M. Kowalski, “Response Surface Methodology: A Retrospective and Literature Survey,” *J. Qual. Technol.*, vol. 36, no. 1, pp. 53–78, 2004, doi: 10.1080/00224065.2004.11980252.

[17] A. F. Yetim, M. Y. Codur, and M. Yazici, “Using of artificial neural network for the prediction of tribological properties of plasma nitrided 316L stainless steel,” *Mater. Lett.*, vol. 158, pp. 170–173, 2015, doi: https://doi.org/10.1016/j.matlet.2015.06.015.

[18] I. I. Argatov and Y. S. Chai, “An artificial neural network supported regression model for wear rate,” *Tribol. Int.*, vol. 138, pp. 211–214, 2019, doi: https://doi.org/10.1016/j.triboint.2019.05.040.

[19] V. W. Y. Tam, A. Butera, K. N. Le, L. C. F. Da Silva, and A. C. J. Evangelista, “A prediction model for compressive strength of CO2 concrete using regression analysis and artificial neural networks,” *Constr. Build. Mater.*, vol. 324, p. 126689, 2022, doi: https://doi.org/10.1016/j.conbuildmat.2022.126689.

[20] R. Masoudi Nejad, N. Sina, D. Ghahremani Moghadam, R. Branco, W. Macek, and F. Berto, “Artificial neural network based fatigue life assessment of friction stir welding AA2024-T351 aluminum alloy and multi-objective optimization of welding parameters,” *Int. J. Fatigue*, vol. 160, p. 106840, 2022, doi: https://doi.org/10.1016/j.ijfatigue.2022.106840.

[21] M. S. Mhatre, D. Siddiqui, M. Dongre, and P. Thakur, “A Review paper on Artificial

Neural Networks: A Prediction Technique," *Int. J. Sci. Eng. Res.*, vol. 8, no. 3, pp. 1–3, 2017, [Online]. Available: http://www.ijser.org.

[22] M. R. G. Meireles, P. E. M. Almeida, and M. G. Simões, "A comprehensive review for industrial applicability of artificial neural networks," *IEEE Trans. Ind. Electron.*, vol. 50, no. 3, pp. 585–601, 2003, doi: 10.1109/TIE.2003.812470.

[23] K. A. Patel and P. K. Brahmbhatt, "A Comparative Study of the RSM and ANN Models for Predicting Surface Roughness in Roller Burnishing," *Procedia Technol.*, vol. 23, pp. 391–397, 2016, doi: 10.1016/j.protcy.2016.03.042.

[24] N. S. R. Talib, M. I. E. Halmi, S. S. A. Ghani, U. H. Zaidan, and M. Y. A. Shukor, "Artificial Neural Networks (ANNs) and Response Surface Methodology (RSM) Approach for Modelling the Optimization of Chromium (VI) Reduction by Newly Isolated Acinetobacter radioresistens Strain NS-MIE from Agricultural Soil," *Biomed Res. Int.*, vol. 2019, 2019, doi: 10.1155/2019/5785387.

[25] A. Ciric, B. Krajnc, D. Heath, and N. Ogrinc, "Response surface methodology and artificial neural network approach for the optimization of ultrasound-assisted extraction of polyphenols from garlic," *Food Chem. Toxicol.*, vol. 135, no. November 2019, p. 110976, 2020, doi: 10.1016/j.fct.2019.110976.

[26] C. E. Onu, J. T. Nwabanne, P. E. Ohale, and C. O. Asadu, "Comparative analysis of RSM, ANN and ANFIS and the mechanistic modeling in eriochrome black-T dye adsorption using modified clay," *South African J. Chem. Eng.*, vol. 36, no. July 2020, pp. 24–42, 2021, doi: 10.1016/j.sajce.2020.12.003.

[27] G. Villarrubia, J. F. De Paz, P. Chamoso, and F. De la Prieta, "Artificial neural networks used in optimization problems," *Neurocomputing*, vol. 272, pp. 10–16, 2018, doi: 10.1016/j.neucom.2017.04.075.

[28] G. E. P. Box and N. R. Draper, *Empirical Model-Building and Response Surface*. USA: John Wiley & Sons, Inc., 1986.

[29] D. Scaramozzino, B. Albitos, G. Lacidogna, and A. Carpinteri, "Selection of the optimal diagrid patterns in tall buildings within a multi-response framework: Application of the desirability function," *J. Build. Eng.*, vol. 54, p. 104645, 2022, doi: https://doi.org/10.1016/j.jobe.2022.104645.

[30] R. Manimaran, T. Mohanraj, M. Venkatesan, R. Ganesan, and D. Balasubramanian, "A computational technique for prediction and optimization of VCR engine performance and emission parameters fuelled with Trichosanthes cucumerina biodiesel using RSM with desirability function approach," *Energy*, vol. 254, p. 124293, 2022, doi:

https://doi.org/10.1016/j.energy.2022.124293.

[31] E. Barreno-Avila, E. Moya-Moya, and C. Pérez-Salinas, “Rice-husk fiber reinforced composite (RFRC) drilling parameters optimization using RSM based desirability function approach,” *Mater. Today Proc.*, vol. 49, pp. 167–174, 2022, doi: https://doi.org/10.1016/j.matpr.2021.07.498.

Chapter - 6
Conclusions and Future Scope of Work

6.1 Conclusions

Concepts of human skin tribology have direct influence on the day-to-day tasks of an individual. Ranging from picking an object, writing, typing to its feel or perception and classification, tactile properties play a vital role. Although tribological properties of skin depend on multiple factors that are intricately related to one another, this study examines the effect of normal load, sliding velocity and skin hydration on the human skin tribological aspects in Indian context. The thesis addresses the need of a skin friction measurement device with development of human skin tribometers, and its performance is evaluated via experimental investigations. Further, a predictive model for the determination of COF at the finger pad interface is developed.

A bibliometric study is performed by exploring 3956 from scopus and 190 documents through web of science database and is presented in **Chapter 2**. Bibliometric analysis is performed to identify influential authors, organizations, highly cited research articles, and collaborations. Co- citation analysis performed provides the insights on the simultaneous citations of an author to different articles. Collaboration network highlights the collaborations from domain experts on the global scale. Three field plot presents the most influential country, authors, and the keywords with respect to documented research in human skin tribology. Later sections of this chapter provide a scoping review using "Preferred reporting items for systematic reviews and meta-analyses" (PRISMA) technique. Sixty-three articles were selected post year 2000 focussing exclusively on, *in-vivo* experimental investigations. Further, for the theme of current work, these studies were classified in four anatomical regions highlighting their measurement techniques, scope, parameters, range of coefficient of friction (COF) and the contact material.

Chapter 3 dealt with the development of two tribometers first rotary type and second reciprocating type for the measurement of human skin friction. In this chapter the design and development of the rotary type tribometer having the round test probes is presented with its validation through gage repeatability and reproducibility tests. Rotary type tribometer is highly portable with versatile applications over forearm, lower limbs, and tactile friction measurements. Further, development of sliding type human skin tribometer is presented. Sliding tribometer design measures COF at higher range of normal loads and velocity taking flat test samples as the countersurface with the human skin.

Experimental investigations and their analysis in relation to the tribological aspects of the finger pad contact with test samples is reported in **Chapter 4**. For the selection of optimum experimentation conditions, mean temperature and relative humidity were computed to replicate the major atmospheric conditions of six climatic divisions of India. Average atmospheric conditions obtained are 23.9 °C temperature and relative humidity of 66.6 %. A response-based survey conducted for the test samples received maximum responses for rubber followed by plastic, wood, enamel coated wood and steel for the grip material selection. An expert survey with the operators on the shop floor, rated steel and brass for the hand tool material as the first preference followed by copper and aluminium.

Variation of COF values at four discrete normal load values at varying sliding velocities is investigated in both dry and wet state. Wet state shows higher COF values at the comparable values of normal load and sliding velocities. Same phenomenon of higher COF values in wet compared to that in dry state is observed for the sliding tribometer. Rotary experiments were performed with textile, rubber, acrylic, metals included aluminium, brass, copper, and steel. Test materials used in sliding tribometer included acrylic, wood, and metals (aluminium , brass, copper, and steel).

Chapter 5 presents the predictive model for COF between finger pad and steel probe based on the three input variables namely normal load, sliding velocity and the skin hydration. Two separate models are developed, and a comparison is made between the two through the experimental results obtained by rotary type tribometer. First model is developed by analysing the experimental design through response surface methodology (RSM) while the other model is developed through artificial neural network (ANN) technique. Although both the models have good predictability considering the subjectivities involved in the tactile friction measurements. When compared ANN model shows better performance with relative error of 5.91% over that of 9.93 % for RSM model. The developed model is useful for the manufacturers to design customised products such as hand tools, gripping objects, assistive devices for the disabled and sports equipment design as per the required precision or the power in grip.

6.2 Future Scope of Work

Following are the proposed future directions to further explore the field of *in-vivo* human skin tribological investigations:

1. Developed tribometers can further be modified in structure to make it more portable and handier to operate on other anatomical regions of the human body.

2. Environmental controlled investigations can be performed to better understand its effect over the human skin tribological phenomenon.
3. More experiments with sufficiently greater number of subjects with varying range of age and gender are needed to generalise the frictional behaviour.
4. Test samples with surface modifications in terms of roughness, textures and surface finish be tested, to parametrically analyse its tactile frictional behaviour.
5. Tests with on bed patients to prevent the development of pressure ulcers by monitoring the generation of shear forces and continuous repositioning.
6. Higher number of experiments shall be conducted with variety of materials to increase the predictability of model by including only the significant factors.

Questionnaire for the Test Material Selection Survey

Question 1:

Fabric preferences at the workplace?

Question 2:

Choice of material for grip development.

Question 3:

Most preferred material for the development of cell phone cases?

RESEARCH PUBLICATIONS

A. International Journals (Peer reviewed)

1. **A K Srivastava**, J S Rathore and S Shrivastava "Multidimensional Outline of Experimental Techniques for Human Skin Tribology: A Scoping Review" **[ACCEPTED]**
2. **A K Srivastava**, J S Rathore and S Shrivastava "Tribological investigations of metal-fin ger pad interface" **[Under Review]**
3. **A K Srivastava**, J S Rathore and S Shrivastava "Experimental investigations of human pad through sliding type tribometers in dry and wet state" **[Under Review]**
4. **A K Srivastava**, J S Rathore and S Shrivastava "Human Skin Tribology: A Bibliometric Analysis" **[To be submitted]**
5. **A K Srivastava**, J S Rathore and S Shrivastava. "Predictive modelling and optimization of COF at human skin contact" **[To be submitted]**

B. International Conferences

1. P Jain, **A K Srivastava**, J S Rathore and S Shrivastava. "An evaluation of tactile frictional behaviour of the wooden material", NFEST Conference, 18th - 22nd February 2019, NIT Kurukshetra
2. **A K Srivastava**, J S Rathore and S Shrivastava. "Optimum range selection for macro parameters to minimize the friction coefficient between materials in contact: A case study on human skin", 20th ISME Conference on Advances in Mechanical Engineering, 19th – 21st May 2022, IIT Ropar
3. **A K Srivastava**, J S Rathore and S Shrivastava. "Efficacy of ANN and ANFIS as an AI technique for the prediction of COF at finger pad interface in manipulative tasks", International Conference on Recent Advances in Materials, Manufacturing and Thermal Engineering (RAMMTE- 2022), 8th - 9th July 2022, DTU, New Delhi
4. **A K Srivastava**, J S Rathore and S Shrivastava. "Development and Validation of Parallel-Rotary Type Human Skin Tribometer**"** IndiaTrib-2022, 11th International Conference on Industrial Tribology 12th - 14th December 2022, IIT Delhi, New Delhi

Prof. Jitendra Singh Rathore received his B.E. degree in Mechanical Engineering from M.B.M. Engineering College, Jodhpur (Rajasthan) in 2000, M.Tech. degree in Machine Design Engineering from Indian Institute of Technology (IIT), Roorkee in 2005, and Ph.D. from Birla Institute of Technology and Science (BITS), Pilani in 2014. His Ph.D. research was on "Investigations on the Dynamics and Design of Uniflagellated Nanoswimmers using Resistive Force Theory". After working for four years in Indian Ordnance Factories Organization, he joined the Mechanical Engineering Department, BITS, Pilani, India, in December 2006. Currently, He is a faculty in Mechanical Engineering Department, BITS, Pilani for over 17 years and serving as an Associate Professor. He has more than 30 international and national publications. His area of research includes

- Nanorobotics and low Reynolds number hydrodynamics
- Human skin tribology and biomaterials
- Carbon nanotube (CNT) reinforced metal matrix composites.

He has 18+ years teaching expertise on Theory of Elasticity and Plasticity, Advance Mechanics of Solids, Thermodynamics, Mechanisms and Machines, Fluid Mechanics and Mechanics of Materials. He has supervised several Ph.D., Master and Undergraduate students for thesis and project work.

Prof. Sharad Shrivastava holds a Ph.D. degree from BITS-Pilani, Pilani Campus, India and a master's degree from Indian Institute of Technology (IIT) Kharagpur. His Ph.D. was in the field of application of non-destructive testing in Biomedical engineering. He has more than 18 years of teaching and research experience. He is presently Associate Professor, Mechanical Engineering Department, BITS-Pilani, Pilani Campus, India. He has more than 20 research publications in the field of Materials, Non-destructive techniques, coating technology and Biomedical engineering. He is member of a number of professional societies and has delivered number of invited lectures both in India and abroad. He has successfully handled a sponsored project (73lakhs) from GAIL India Limited on condition monitoring on underground pipelines.

His area of research is on

- Biomedical engineering, biomaterials for flame retardant applications, coatings by thermal spray HVOF process, hybrid composite materials, fracture mechanics, non-destructive testing,
- Specializes in non-destructive testing techniques mainly acoustic emission and acousto-ultrasonic technique, biomaterials.
- Involved in teaching and research of subjects related to NDT, materials, fracture mechanics and theory of elasticity and plasticity, mechanics of solids.

He has 15+ years teaching expertise on Non-destructive testing, composite materials, biomedical engineering, thermal spray coatings, fracture mechanics, mechanics of materials. He has supervised several Ph.D., master and undergraduate students for thesis and project work.

Prof. Sharad Shrivastava has served as Principal Investigator and Co-Principal Investigatorin many projects based on Biomedical engineering, biomaterials for flame retardant applications, coatings by thermal spray HVOF process, hybrid composite materials, fracture mechanics, non-destructive testing.

Ashish Kr. Srivastava has received the Bachelor of Technology (B.Tech) in Mechanical and Industrial Engineering from Dr. A .P. J. Abdul Kalam University , Uttar Pradesh, India in 2013. In 2017 He was awarded with a Master's in Technology (M.Tech) in Design Engineering from Gautam Budhdha University ,Gautam Buddha Nagar, Uttar Pradesh. He joined the department of mechanical engineering, BITS Pilani, Pilani campus as a research scholar in August 2017. His research interest lies in bio tribology, contact mechanics, and biomedical instrumentation.